

Old Dominion University

## ODU Digital Commons

---

Civil & Environmental Engineering Theses & Dissertations

Civil & Environmental Engineering

---

Summer 2015

# Hydrothermal Catalytic Liquefaction and Deoxygenation of Biomass for Renewable Fuel Production

Sergiy Popov  
*Old Dominion University*

Follow this and additional works at: [https://digitalcommons.odu.edu/cee\\_etds](https://digitalcommons.odu.edu/cee_etds)



Part of the [Chemical Engineering Commons](#), and the [Environmental Engineering Commons](#)

---

### Recommended Citation

Popov, Sergiy. "Hydrothermal Catalytic Liquefaction and Deoxygenation of Biomass for Renewable Fuel Production" (2015). Doctor of Philosophy (PhD), Dissertation, Civil & Environmental Engineering, Old Dominion University, DOI: 10.25777/jtma-a081  
[https://digitalcommons.odu.edu/cee\\_etds/62](https://digitalcommons.odu.edu/cee_etds/62)

This Dissertation is brought to you for free and open access by the Civil & Environmental Engineering at ODU Digital Commons. It has been accepted for inclusion in Civil & Environmental Engineering Theses & Dissertations by an authorized administrator of ODU Digital Commons. For more information, please contact [digitalcommons@odu.edu](mailto:digitalcommons@odu.edu).

**HYDROTHERMAL CATALYTIC LIQUEFACTION AND DEOXYGENATION OF  
BIOMASS FOR RENEWABLE FUEL PRODUCTION**

by

Sergiy Popov

B.S. June 1981, South-Russian State Technical University, Russia

A Dissertation Submitted to the Faculty of  
Old Dominion University in Partial Fulfillment of the  
Requirements for the Degree of

DOCTOR OF PHILOSOPHY

CIVIL AND ENVIRONMENTAL ENGINEERING

OLD DOMINION UNIVERSITY

August 2015

Approved by:

\_\_\_\_\_  
Sandep Kumar (Director)

\_\_\_\_\_  
Gary Schafran (Member)

\_\_\_\_\_  
Mujde Erten-Unal (Member)

\_\_\_\_\_  
James W. Lee (Member)

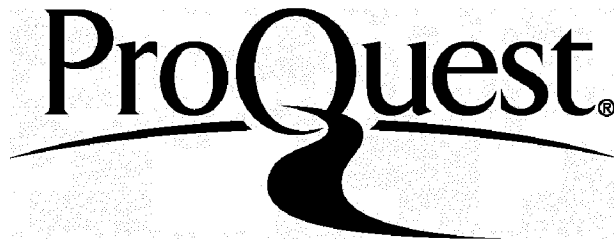
ProQuest Number: 3664135

All rights reserved

INFORMATION TO ALL USERS

The quality of this reproduction is dependent upon the quality of the copy submitted.

In the unlikely event that the author did not send a complete manuscript and there are missing pages, these will be noted. Also, if material had to be removed, a note will indicate the deletion.



ProQuest 3664135

Published by ProQuest LLC(2015). Copyright of the Dissertation is held by the Author.

All rights reserved.

This work is protected against unauthorized copying under Title 17, United States Code.  
Microform Edition © ProQuest LLC.

ProQuest LLC  
789 East Eisenhower Parkway  
P.O. Box 1346  
Ann Arbor, MI 48106-1346

## ABSTRACT

### HYDROTHERMAL CATALYTIC LIQUEFACTION AND DEOXYGENATION OF BIOMASS FOR RENEWABLE FUEL PRODUCTION

Sergiy Popov

Old Dominion University, 2015

Director: Sandeep Kumar

In recent years, sub- and supercritical water technologies received an increasing attention because of the numerous advantages they offer for biomass converting into biofuels. Water at elevated temperatures and pressures provides an ideal medium for chemical transformations. It serves as a reactant, reaction medium, and catalyst that helps biomass compounds undergo hydrolysis, depolymerization, dehydration, decarboxylation, and condensation/repolymerization reactions. Biomass is the fourth largest source of energy in the world after coal, oil, and natural gas that has the potential to provide the large scale substitution of hydrocarbon-based liquid transportation fuels and minimize the environmental issues. Biomass typically contains 40-60% oxygen. Maximal removal of oxygen from biomass is the main objective of biofuel production. In this work, several hydrothermal technologies of processing biomass to biofuels and valuable byproducts were investigated.

In Chapter 2, the reaction pathways of conversion of triacylglycerols into alkanes, influence on temperature, pressure, catalysts, and hydrogen on the hydrodeoxygenation process was reviewed in details.

In Chapter 3, the effects of reaction temperatures and catalysts on the degree of liquefaction, bio-oil yield, energy conversion ratio, and bio-oil composition were studied and the overall mass balance of the process was developed.



In Chapter 4, it was shown that the integrated process provides several major advantages over conventional processes: better extractability of oil, shorter extraction time, tolerance to high moisture content of the feedstock, avoiding preparation stages, and utilization of the extracted seedcake for biochar production.

In Chapter 5, it was demonstrated that the integration of hydrothermal liquefaction of algal biomass, extraction of bio-oil from the liquid phase, and gasification of the extracted aqueous phase can provide additional energy and a potential source of nutrients for fresh algae cultivation.

In Chapter 6, a novel approach to converting fatty acids into *n*-alkanes was investigated. Fuel range hydrocarbons were obtained in a continuous flow process within a short residence time from oleic acid using near- and supercritical water as reaction medium, granulated activated carbon as a catalyst, and  $\leq 1\%$  v/v formic acid as an in situ source of hydrogen.

Copyright, 2015, by Sergiy Popov, All Rights Reserved.

This dissertation is dedicated to my family in Ukraine.

## ACKNOWLEDGMENTS

I would like express my sincere gratitude to my advisor Dr. Sandeep Kumar for his continued guidance, invaluable advice, discussions, and support during my dissertation research.

I appreciate my dissertation committee members Dr. Gary C. Schafran, Dr. Mujde Erten-Unal, and Dr. James W. Lee for their valuable comments and suggestions.

I would like to acknowledge Dr. Isao Ishibashi, the Department of Civil and Environmental Engineering, and the Batten College of Engineering and Technology for the financial and institutional support.

I thank the members of my research group who helped me along the way. My special thanks is to Dr. Jose Garcia for his friendship, help, advise, discussions, and looking for solutions of the problems together.

I would like to thank Dr. Patrick G. Hatcher and his research group at the Department of Chemistry and Biochemistry for their help with sample analysis and collaborative research. My special thanks are to Isaiah Ruhl for his help, advice, and friendship.

I wish to thank my mother, sons, and wife for their love, encouragement, and support during all the years of my dissertation work.

**NOMENCLATURE**

<i>ACS</i>	Ammonia-pretreated corn stover
<i>AFEX</i>	Ammonia Fiber Expansion
<i>DOE</i>	Department of Energy
<i>ECR</i>	Energy conversion ratio
<i>EDS</i>	Energy dispersive spectroscopy
<i>EISA</i>	Energy Independence and Security Act
<i>EPA</i>	Environmental Protection Agency
<i>FFA</i>	Free fatty acid
<i>FTIR</i>	Fourier transform infrared spectroscopy
<i>GC</i>	Gas chromatograph
<i>GC-FID</i>	Gas chromatograph with flame ionization detector
<i>GC-TCD</i>	Gas chromatograph with thermal conductivity detector
<i>GC-MS</i>	Gas chromatograph with mass spectrometer
<i>HBO</i>	Heavy bio-oil
<i>HDO</i>	Hydrodeoxygenation
<i>HHV</i>	Higher heating value
<i>HPLC</i>	High performance liquid chromatograph
<i>HPOE</i>	Hydrothermal pretreatment – oil extraction
<i>HTC</i>	Hydrothermal carbonization
<i>HTG</i>	Hydrothermal gasification
<i>HTL</i>	Hydrothermal liquefaction

<i>IR</i>	Infrared
<i>LBO</i>	Light bio-oil
<i>NMR</i>	Nuclear magnetic resonance spectroscopy
<i>NREL</i>	National Renewable Energy Laboratory
<i>PUFA</i>	Polyunsaturated fatty acid
<i>RSD</i>	Relative standard deviation
<i>SEM</i>	Scanning electron microscope
<i>TAG</i>	Triacylglycerol
<i>TC</i>	Total carbon
<i>TGA</i>	Thermogravimetric analysis
<i>TN</i>	Total nitrogen
<i>TOC</i>	Total organic carbon
<i>XRD</i>	X-ray diffraction
<i>UHS</i>	Unhydrolyzed solids
<i>WSP</i>	Water-soluble products

## TABLE OF CONTENTS

Chapter	Page
TABLE OF CONTENTS .....	X
LIST OF TABLES .....	XIV
LIST OF FIGURES .....	XVII
1. INTRODUCTION.....	1
1.1.  HYDROTHERMAL MEDIUM .....	1
1.2.  BIOMASS POTENTIAL .....	5
1.3.  MAJOR HYDROTHERMAL PROCESSES FOR BIOMASS CONVERSION.....	10
1.4.  MOTIVATION AND SCOPE OF THE STUDY .....	23
2. RENEWABLE FUELS VIA CATALYTIC HYDRODEOXYGENATION OF LIPID- BASED FEEDSTOCKS (REVIEW).....	29
2.1.  INTRODUCTION.....	30
2.2.  FUEL COMPOSITION AND PROPERTIES .....	40
2.3.  HDO OF LIPID-BASED FEEDSTOCKS .....	43
2.4.  DEOXYGENATION IN HYDROTHERMAL MEDIA .....	71
2.5.  FUTURE PERSPECTIVE AND POTENTIAL RESEARCH AREAS.....	75
2.6.  EXECUTIVE SUMMARY .....	78
2.7.  ACKNOWLEDGMENTS .....	79
3. HYDROTHERMAL CATALYTIC LIQUEFACTION OF UNHYDROLYZED SOLIDS ....	80

Chapter	Page
3.1. INTRODUCTION.....	81
3.2. EXPERIMENTAL PART.....	86
3.3. RESULTS AND DISCUSSION .....	94
3.4. HTL MECHANISM .....	110
3.5. OVERALL MASS BALANCE FOR A CONCEPTUAL BIOREFINERY.....	112
3.6. FUTURE PERSPECTIVE AND POTENTIAL RESEARCH AREAS.....	115
3.7. EXECUTIVE SUMMARY .....	117
3.8. ACKNOWLEDGMENTS .....	118
4. HYDROTHERMAL TREATMENT FOR ENHANCING OIL EXTRACTION AND BIOCHAR PRODUCTION FROM OILSEEDS .....	119
4.1. INTRODUCTION.....	120
4.2. MATERIALS AND METHODS .....	124
4.3. RESULTS AND DISCUSSION .....	133
4.4. OVERALL MASS BALANCE AND ENERGY REQUIREMENTS FOR HPOE PROCESS.....	154
4.5. CONCLUSIONS .....	155
4.6. ACKNOWLEDGMENTS .....	156
5. HYDROTHERMAL LIQUEFACTION OF <i>SCENEDESMUS SP.</i> AND CATALYTIC GASIFICATION OF THE AQUEOUS PHASE IN NEAR- AND SUPERCRITICAL WATER.....	157



Chapter	Page
5.1. INTRODUCTION.....	158
5.2. EXPERIMENTAL SECTION.....	166
5.3. RESULTS AND DISCUSSION .....	172
5.4. OVERALL MASS BALANCE.....	184
5.5. CONCLUSIONS .....	185
5.6. ACKNOWLEDGMENTS .....	186
6. RAPID HYDROTHERMAL DEOXYGENATION OF OLEIC ACID IN A CONTINUOUS FLOW PROCESS.....	187
6.1. INTRODUCTION.....	188
6.2. EXPERIMENTAL SECTION.....	191
6.3. RESULTS AND DISCUSSION .....	197
6.4. CONCLUSIONS .....	213
6.5. ACKNOWLEDGMENTS .....	214
7. CONCLUSIONS AND RECOMMENDATIONS .....	219
REFERENCES .....	228
APPENDICES	
A. ENVIRONMENTAL PROTECTION AGENCY (EPA) P3 (PEOPLE, PROSPERITY AND THE PLANET) COMPETITION, PHASE I AND II.....	261
B. 1. STANDARD OPERATION PROCEDURES FOR SRI 8610C GAS CHROMATOGRAPH.....	263

Chapter	Page
B. 2. ANALYSIS OF GAS SAMPLES USING SRI 8610C GAS CHROMATOGRAPH WITH THE THERMAL CONDUCTIVITY DETECTOR (TCD).....	264
B. 3. ANALYSIS OF LIQUID SAMPLES USING SRI 8610C GAS CHROMATOGRAPH WITH THE FLAME IONIZATION DETECTOR (FID).....	268
VITA .....	273

## LIST OF TABLES

Table	Page
1. Comparison of physicochemical properties of ambient and supercritical water .....	4
2. General composition of different algae (% of dry matter) .....	9
3. Typical biomass feedstock compounds used for hydrothermal processing .....	10
4. Comparison of biomass and biochar as solid fuels .....	16
5. Typical operating conditions for HDO of bio-oils.....	19
6. Comparison of different diesel fuels .....	34
7. Typical operating conditions for HDO of bio-oils.....	37
8. Summary of (heterogeneous) catalysts for HDO of lipid-based feedstocks and model compounds.....	54
9. Process yields and hydrogen requirements for a range of different feedstocks and diesel cloud point targets.....	68
10. Composition, elemental analysis, and HHV of ACS-UHS .....	90
11. Experimental conditions used in the study .....	91
12. Composition of gaseous products obtained after catalytic runs at 350 °C .....	96
13. HTL products obtained under different experimental conditions.....	97
14. Elemental analysis, H/C and O/C ratios, and HHV of bio-oils and biochar .....	100
15. Identification of compounds in LBO from runs 6 (350 °C, Na <sub>2</sub> CO <sub>3</sub> ) and run 9 (350 °C, CoMo/Al <sub>2</sub> O <sub>3</sub> ) by GC-MS .....	105

Table	Page
16. Weights of oilseeds after hydrothermal pretreatment .....	134
17. Fatty acid compositions of oils extracted from raw and hydrothermally pretreated canola and jatropha seeds .....	139
18. Evaluation of FTIR spectra of jatropha oils .....	142
19. Unsaponifiable matter in crude oils extracted from raw and pretreated at 210 °C seeds.....	144
20. Crude oil yield from ground raw and hydrothermally pretreated at 210 °C canola seeds at different number of extraction cycles.....	145
21. BET surface area and pore size/volume analysis results for raw and pretreated canola and jatropha seeds .....	148
22. Elemental and ash analyses of raw, pretreated, extracted, and hydrothermally carbonized canola and jatropha seeds .....	151
23. Mass and energy distribution of the products obtained during HPOE processing and carbonization of canola and jatropha seeds .....	153
24. Composition and amount of the gas produced during HTL of algae .....	172
25. Elemental analyses of microalgae, solid phase, bio-oil, and gaseous products after HTL at 300 °C .....	174
26. Composition of gaseous products from the catalytic and non-catalytic runs .....	178
27. Elemental compositions and HHV gaseous products from the catalytic and non-catalytic runs .....	180

Table	Page
<b>28.</b> Gasification efficiencies, unreacted aqueous carbon, and carbon balance closure.....	182
<b>29.</b> Products from hydrothermal deoxygenation of oleic acid at 350 °C without formic acid added .....	200
<b>30.</b> Conversion, deoxygenation product yield, and selectivity to heptadecane at different reaction temperatures .....	202
<b>31.</b> Products from hydrothermal deoxygenation of oleic acid over activated carbon at different reaction temperatures .....	205
<b>32.</b> Product distribution of liquid and gaseous products from hydrothermal deoxygenation of oleic acid at different temperatures.....	206
<b>33.</b> Yields of gaseous products from hydrothermal deoxygenation of oleic acid at 380 °C.....	207
<b>34.</b> Effect of temperature on the stearic acid conversion and the rate of its deoxygenation.....	211

## LIST OF FIGURES

Figure	Page
1. Dielectric constant ( $\epsilon$ ) and ion dissociation constant ( $K_w$ ) of water as a function of temperature .....	3
2. Hydrothermal processing regions referenced to the pressure-temperature phase diagram of water .....	5
3. Typical composition of lignocellulosic biomass.....	7
4. Fatty acids deoxygenation pathways over Pd/C catalyst.....	21
5. Properties of different types of diesel fuels. ....	40
6. The effect of the HDO reaction temperature on the yields of buriti oil products.....	47
7. Different lipid molecules: triacylglycerols on the left, phospholipids in the middle, and glycolipids on the right.....	61
8. Compositions of lipids extracted from <i>Nannochloropsis oculata</i> during logarithmic and stationary phases .....	61
9. Fatty acid composition of lipid extracted from species <i>Tetraselmis suecica</i> at the end of logarithmic phase .....	63
10. Simplified Ecofining process flow diagram .....	67
11. Fatty acids deoxygenation pathways over Pd/C catalyst.....	70
12. (a) The solubility of saturated fatty acids in water at 15 MPa; (b) The solubility of water in fatty acids at the vapor pressure of the system .....	72

Figure	Page
<b>13.</b> Products separation procedure that was followed to produce light bio-oil (LBO), heavy bio-oil (HBO), biochar, and aqueous-soluble products from ACS-UHS.....	93
<b>14. (a)</b> pH and <b>(b)</b> TOC of the aqueous phase as functions of temperature.....	94
<b>15.</b> Bio-oil yields for all the HTL experiments.....	97
<b>16. (a)</b> Energy (HHV) distribution of the products from runs 6 (350 °C with K <sub>2</sub> CO <sub>3</sub> ) and <b>(b)</b> – from run 9 (350 °C with CoMo/Al <sub>2</sub> O <sub>3</sub> ).....	102
<b>17.</b> Energy conversion ratios for all the HTL experiments .....	103
<b>18.</b> 1D <sup>1</sup> H NMR spectra of LBO and HBO from runs 6 and 9 in CDCl <sub>3</sub> .....	108
<b>19.</b> The overall mass balance for four different unit operations of a conceptual biorefinery to produce bioethanol and bio-oil from ACS-UHS .....	113
<b>20.</b> Schematic of the integrated HPOE process .....	123
<b>21. (a)</b> Distribution of products' pH in aqueous phase; <b>(b)</b> distribution of TOC in aqueous phase.....	134
<b>22.</b> Crude oil yields from raw and hydrothermally pretreated at different temperatures oilseeds .....	136
<b>23.</b> Crude oil yields from raw and hydrothermally pretreated at different temperatures seeds on a raw seed basis.....	137
<b>24.</b> FFA concentrations in crude oils extracted from raw and pretreated at different temperatures canola and jatropha seeds .....	138
<b>25.</b> FTIR spectra of oils extracted from <b>(a)</b> raw and <b>(b)</b> pretreated at 210 °C jatropha seeds ....	141

Figure	Page
26. Progress of oil extraction from ground raw and hydrothermally pretreated canola seeds ....	146
27. SEM images of raw <b>(a)</b> and hydrothermally pretreated <b>(b)</b> jatropha seeds.....	150
28. Overall mass balance for three different unit operations of HPOE process to produce oil and biochar from canola and jatropha seeds.....	154
29. Schematic of HTL of microalgae followed by HTG of the extracted aqueous phase .....	165
30. Experimental setup for hydrothermal gasification of the aqueous phase.....	167
31. <b>(a)</b> Products and <b>(b)</b> energy (HHV) distribution from HTL of algae at 300 °C .....	174
32. Product gas yields for <b>(a)</b> catalytic and <b>(b)</b> non-catalytic runs.....	179
33. Gasification efficiencies for catalytic and non-catalytic HTG of the aqueous phase .....	181
34. <b>(a)</b> Products and <b>(b)</b> energies (HHV) distribution from the HTL and catalytic HTG at 400 °C.....	183
35. Overall mass balance for HTL of microalgae followed by HTG of the extracted aqueous phase.....	185
36. Experimental setup for rapid hydrothermal deoxygenation of oleic acid .....	192
37. Conversion of stearic acid, heptadecane yield, and selectivity to heptadecane at different reaction temperatures .....	203
38. GC-FID of the products from hydrothermal deoxygenation of oleic acid at: <b>(a)</b> 360 °C, <b>(b)</b> 370°C, and <b>(c)</b> 380 °C .....	204



Figure	Page
<b>39.</b> Effect of temperature on the rate of stearic acid disappearance in Arrhenius form.....	212
<b>40.</b> Sample chromatogram of a gas mixture analyzed with GC-TCD. ....	267
<b>41.</b> Sample chromatogram of a FAME mixture analyzed with GC-FID. ....	272

## CHAPTER 1

### INTRODUCTION

#### 1.1. Hydrothermal medium

In recent years, sub- and supercritical water technologies received an increasing attention because of the numerous advantages they offer for biomass converting into biofuels, including (Peterson, Vogel et al. 2008):

- Non-toxic, environmentally benign, inexpensive, and tunable reaction medium;
- Ability to serve as a reactant, reaction medium, and catalyst for ionic/free radical reactions;
- Ability to process wet biomass;
- High throughputs;
- High energy and separation efficiency;
- Lower energy requirements because of avoiding the phase change;
- Ability to use mixed feedstocks;
- Ability to produce the direct replacements for petroleum-derived fuels;
- Can be used as a pretreatment step in coordination with other biofuel production methods;
- Can be used as a post-fermentation for processing solid residues;
- Versatility of chemistry (can produce liquid, gaseous, and solid fuels);
- No need to maintain specialized microbial cultures//enzymes;
- Reduced mass transfer resistance;
- Increased selectivity for the desired products/chemicals (hydrogen, methane, biocrude, carbohydrates, organic acids, etc.);

- Possibility of efficient energy recovery;
- Complete sterilization of the products.

Sub- and supercritical water, which is also defined as hydrothermal media, is a water-rich phase above 200 °C that is kept in a liquid or supercritical state by applying a sufficient pressure. A critical point of water is 374 °C and 22.1 MPa. Above this point, water has a liquid-like density and gas-like transport properties and forms a single-phase medium with the properties very different from those of ambient water. Supercritical water is non-polar and is fully miscible with most organic compounds and gases (oxygen, nitrogen, hydrogen, carbon dioxide, methane) while polar compounds (e.g., inorganic salts) are not soluble under supercritical conditions (Peterson, Vogel et al. 2008). The single-phase mixture formed under supercritical conditions does not have many of the transport limitations inherent to most of the multi-phase reactor systems. Supercritical water has lower viscosity, lower dielectric constant, higher diffusivity, and higher ionization constant than ambient water, which significantly increases the rates of chemical reactions. Physicochemical properties of supercritical water are shown in Fig. 1 and Table 1.

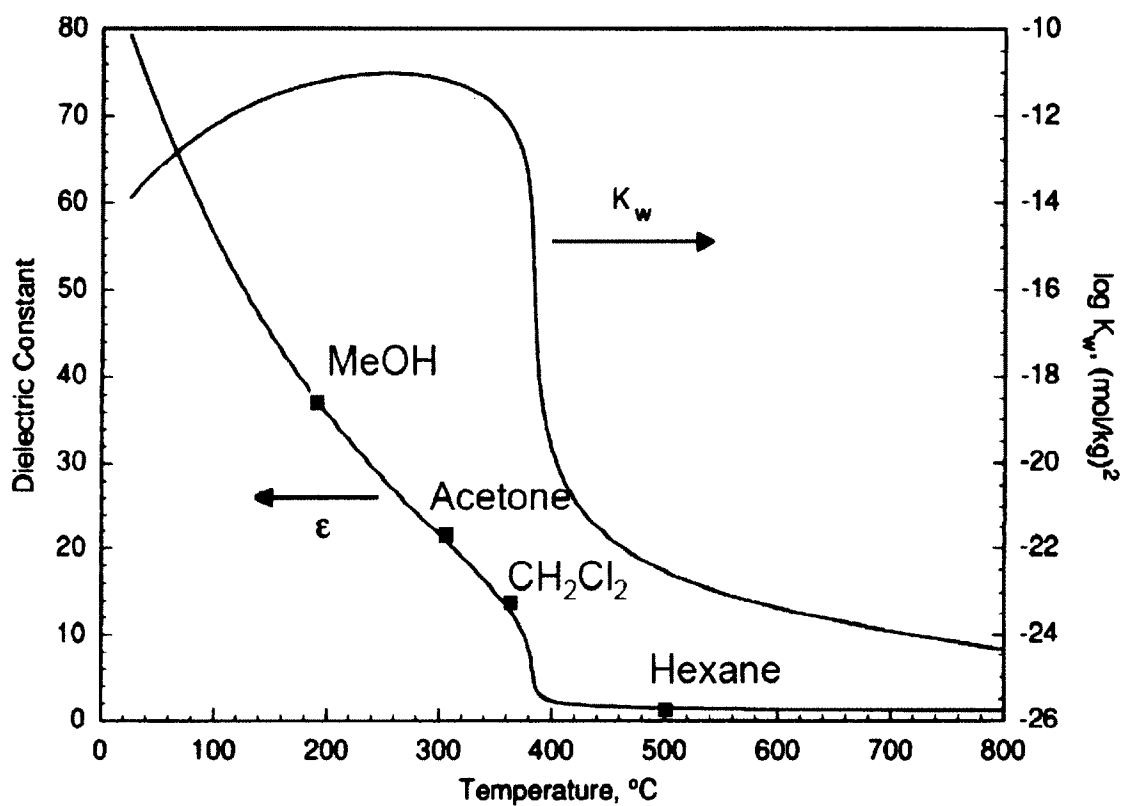


**Figure 1.** Dielectric constant ( $\epsilon$ ) and ion dissociation constant ( $K_w$ ) of water as a function of temperature (Kritzer and Dinjus 2001).

As we can see from Fig. 1, the dielectric constant of water drops with temperature and at supercritical conditions approaches that of non-polar solvents at ambient conditions.

**Table 1.** Comparison of physicochemical properties of ambient and supercritical water (Kumar 2013)

	Ambient water	Supercritical water
<b>Dielectric constant</b>	78	< 5
<b>Solubility of organic compounds</b>	Very low	Fully miscible
<b>Solubility of oxygen</b>	6 ppm	Fully miscible
<b>Solubility of inorganic compounds</b>	Very high	~ 0
<b>Diffusivity, cm<sup>2</sup>/s</b>	10 <sup>-5</sup>	10 <sup>-3</sup>
<b>Viscosity, g × cm/s</b>	10 <sup>-2</sup>	10 <sup>-4</sup>
<b>Density, g/cm<sup>3</sup></b>	1	0.2-0.5

Hydrothermal processing of biomass can be divided into three main regions, which are liquefaction (biocrude, bio-oil production), catalytic gasification (hydrogen, methane production), and high-temperature gasification (syngas production), depending on the reaction temperature and pressure as shown in Fig. 2. Subcritical conditions (150-250 °C) can be used for pretreatment, hydrolysis, or extraction of carbohydrates and proteins from biomass feedstocks. Higher reaction temperatures (200-370 °C) facilitate liquefaction of biomass. The temperatures between 400 and 500 °C provide effective reforming and gasification of biomass feedstock. In order to enhance gasification reactions efficiency and achieve good reaction rates and selectivity, a catalyst is typically required. At the temperatures above 500 °C, homogeneous gasification and thermolysis occur.

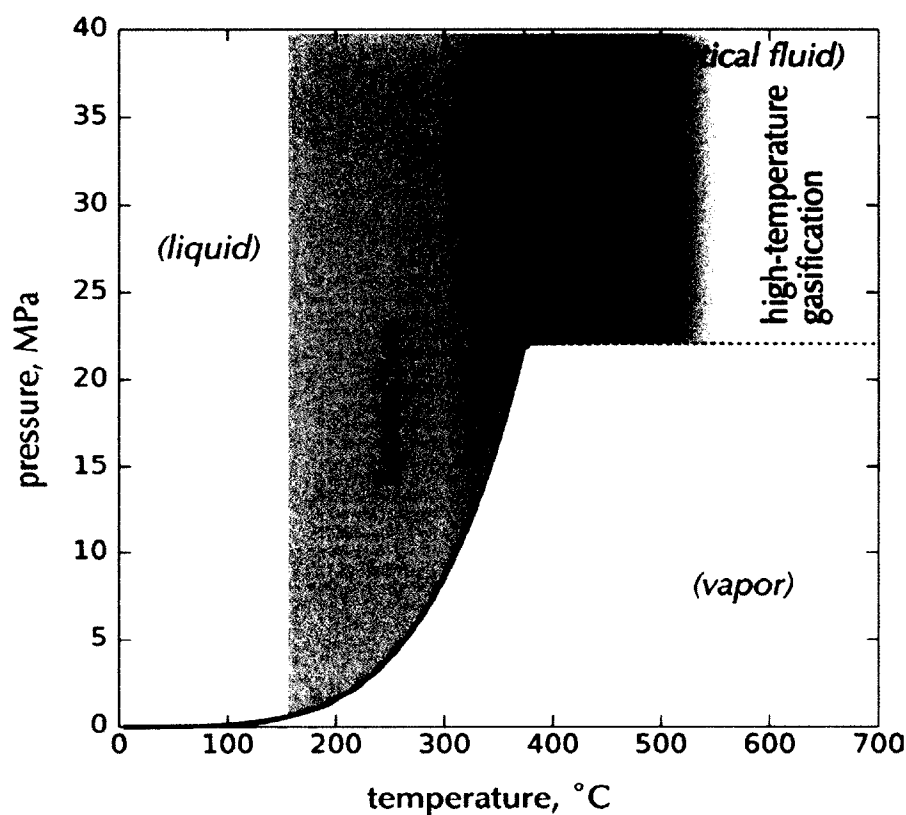


**Figure 2.** Hydrothermal processing regions referenced to the pressure-temperature phase diagram of water (Peterson, Vogel et al. 2008).

## 1.2. Biomass potential

In recent years, there is an increasing interest to renewable fuels production from a variety of biomass feedstocks. Renewable and nuclear energy are considered by many as long term solutions that can solve the problems of energy security, sustainability, and climate change. However, only biomass has the potential to provide the large scale substitution of hydrocarbon-based liquid transportation fuels and minimize the environmental issues (Farrell, Plevin et al. 2006). Biomass is the fourth largest source of energy in the world after coal, oil, and natural gas that possesses the following advantages (Kumar 2013):

- It has a significant economic potential taking into account the depleting fossil resources and growing prices of the fossil fuels;
- It provides energy security since the biomass resources are distributed all over the world;
- It is an environmentally benign and carbon-neutral resource that does not increase the greenhouse gas emissions and reduces the amounts of  $\text{NO}_x$  and  $\text{SO}_x$  in the atmosphere.

Two major biofuel production pathways have been commercialized up to day. They are fermentation of starches obtained from corn grains or sugar cane to produce ethanol and transesterification of oils obtained from canola, soy, and other oil crops to produce biodiesel. In both cases, biofuel production raises the issue “food versus fuel” and therefore has a limited potential. Since the biofuels production from food feedstock has the limitations, much research and development efforts are currently focused on using non-food feedstocks (lignocellulosic biomass and microalgae). The main compounds of lignocellulosic biomass are cellulose, hemicellulose, and lignin. Cellulose and hemicellulose are an excellent feedstock for ethanol production via enzymatic hydrolysis and fermentation. Lignin can be used for energy-rich bio-oil production that can be upgraded to renewable hydrocarbons by removal of oxygen. The typical composition of lignocellulosic biomass is presented in Fig. 3.

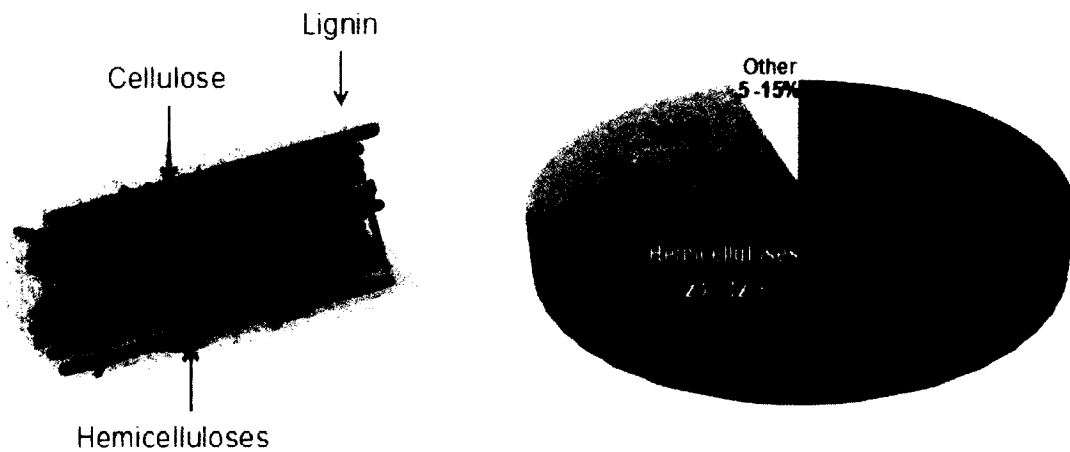


**Figure 3.** Typical composition of lignocellulosic biomass (Kumar 2013).

Terrestrial crops are not very efficient in utilizing the solar energy and can convert only up to  $1 \text{ W/m}^2$  per year (Li 2008). Microalgae are generally more efficient in capturing the solar energy and converting it into biomass. The productivity of microalgae can be 50 times greater than that of switchgrass (Demirbas 2006). The Department of Energy, USA, conducted a comprehensive analysis of the potential of microalgae as a feedstock for biofuel production and reported that land is not a limitation for sustainable algae cultivation (DOE 2010).

Microalgae can be used for production of a wide range of advanced biofuels and bioproducts (Schenk, Thomas-Hall et al. 2008, Huesemann and Benemann 2009). Biofuels derived from microalgae are currently considered to be the most economical and technically viable route that is able to compete with petroleum-derived fuels (Chisti 2010). This is due to a number of potential advantages the algae have in comparison with terrestrial crops:



- Higher annual growth rates, e.g., rates of up to 37 tons per ha per annum have been recorded, primarily due to the higher photosynthetic efficiencies (up to 10% of the solar energy) when compared with terrestrial plants (Weissman and Tillett 1992);
- Higher lipid productivity (up to 75% dry weight for some algae species), with higher proportion of triacylglycerols (TAG) that are essential for efficient biodiesel production (Schenk, Thomas-Hall et al. 2008);
- Microalgae production can effect biofixation of CO<sub>2</sub> (production utilizes about 1.83 kg of CO<sub>2</sub> per kg of dry algal biomass yield) thus making a contribution to air quality improvement (Chisti 2008);
- Capability of growing in wastewater, which offers the potential for integrating the treatment of organic effluent with biofuel production (Cantrell, Ducey et al. 2008);
- Capability to thrive in saline/brackish water/coastal seawater and tolerate marginal lands (e.g. desert, arid- and semiarid lands) that are not suitable for conventional agriculture;
- Inherent yield of valuable co-products such as proteins, polyunsaturated fatty acids (PUFAs), pigments, biopolymers may be used to enhance the economics of production systems (Spolaore, Joannis-Cassan et al. 2006).

Microalgae mainly comprise of proteins, carbohydrates, and lipids. The amounts of each compound depend on the species. Table 2 shows the general composition of different microalgae.

**Table 2.** General composition of different algae (% of dry matter) (Becker 2007)

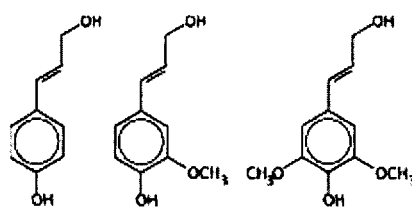
<b>Alga</b>	<b>Protein</b>	<b>Carbohydrates</b>	<b>Lipids</b>
<i>Anabaena cylindrica</i>	43-56	25-30	4-7
<i>Aphanizomenon flos-aquae</i>	62	23	3
<i>Chlamydomonas reinhardtii</i>	48	17	21
<i>Chlorella pyrenoidosa</i>	57	26	2
<i>Chlorella vulgaris</i>	51-58	12-17	14-22
<i>Dunaliella salina</i>	57	32	6
<i>Euglena gracilis</i>	39-61	14-18	14-20
<i>Porphyridium cruentum</i>	28-39	40-57	9-14
<i>Scenedesmus obliquus</i>	50-56	10-17	12-14
<i>Spirogyra sp.</i>	6-20	33-64	11-21
<i>Arthrospira maxima</i>	60-71	13-16	6-7
<i>Spirulina platensis</i>	46-63	8-14	4-9
<i>Synechococcus sp.</i>	63	15	11

As we can see from Table 2, many species of algae have high lipid content, which makes them an excellent feedstock for renewable fuel production. Carbohydrate fraction

can be used for ethanol production. Proteins are a valuable co-product that can be used as an animal feed, as a feedstock for bioplastic production (Kumar, Hablot et al. 2014), or as a fertilizer for growing fresh algae that reduces the cost of converting the algae to fuels (Jena, Vaidyanathan et al. 2011).

Table 3 provides the composition of the main compounds of lignocellulosic and microalgal biomass.

**Table 3.** Typical biomass feedstock compounds used for hydrothermal processing. Adapted from (Peterson, Vogel et al. 2008).

Compound	Chemical formula	Structural information
Cellulose	$[C_6H_{10}O_5]_n$	$n \approx 500 - 10\,000$ ; $\beta \rightarrow (1/4)$ linkages between glucose residues
Hemicellulose	Typical monomers: $[C_5H_8O_4]$ , $[C_6H_{10}O_5]$	Branched with variable monosaccharide residues; degree of polymerization $\approx 500 - 3000$
Lignin	Typical monomers: 	Polymer of aromatic subunits in random structure; molecular weight: $>10\,000$

---

Triacylglycerides (oils)	$\text{RCOO-CH}_2\text{CH(R'COO)CH}_2\text{-}$ $(\text{R''COO})$	RCOO, R'COO, R''COO are fatty acids with ester linkages to the glycerol backbone
Proteins	$[\text{NHCH(R)C(O)}]_n$	Monomer is amino acid residue with various side (R) groups; $n \approx 50\text{--}2000$

---

### 1.3. Major hydrothermal processes for biomass conversion

#### 1.3.1. Hydrothermal liquefaction

Biomass feedstocks often contain 50-60 wt% oxygen and have low higher heating values (HHV) of 10-20 MJ/kg. Therefore, one of the main objectives in producing fuels from biomass is removal of oxygen. Oxygen heteroatoms can be removed by dehydration (removal of oxygen in form of water), decarboxylation (removal of oxygen in form of carbon dioxide), and decarbonylation (removal of oxygen in form of carbon monoxide). Hydrothermal liquefaction (HTL) is an important process in biofuel production that allows obtaining a liquid product (often called biocrude) with a HHV of 30-36 MJ/kg and oxygen content of 10-20 wt%. Biocrude can be further upgraded to hydrocarbons by removal of oxygen heteroatoms by the above methods or converted to hydrogen gas or chemicals.

Biocrude can be produced by either HTL or fast pyrolysis of biomass. However, biocrude from HTL has more desirable qualities than oils from fast pyrolysis and can be produced with higher energetic efficiency due to avoiding evaporating of water. Oils

from fast pyrolysis have more oxygen and moisture content, a large amount (75-80 wt%) of polar organic compounds, and lower heating content (Bridgwater and Peacocke 2000).

In general, HTL is conducted under the following conditions: reaction temperatures from 280 to 380 °C, pressures from 7 to 30 MPa, time from 10 to 60 min, often with a catalyst present, which is generally alkaline, and sometimes with reducing gases (H<sub>2</sub> and CO) present (Elliott, Beckman et al. 1991).

HTL of lignocellulosic biomass proceeds through a series of structural and chemical transformations (Chornet and Overend 1985, Demirbas 2000, Akhtar and Amin 2011):

- Hydrolysis of biomass resulting in micellar-like structure;
- Depolymerization of the cellulose, hemicellulose, and lignin (the bonds of biomass materials are broken at heteroatom sites);
- Hydrolysis of the fragments produced;
- Chemical and thermal decomposition of the fragments to smaller molecules;
- Dehydration and decarboxylation of the resulting molecules.

In case of microalgal biomass, the three major components, which are carbohydrates, lipids, and proteins, also undergo hydrolysis, depolymerization, decomposition, and deoxygenation. Carbohydrates are rapidly hydrolyzed at 200 °C to produce glucose, fructose, maltose, and 5-hydroxymethylfurfural that are further degraded depending on the reaction temperature and time (Nagamori and Funazukuri 2004). Lipids under HTL conditions become miscible with water and at higher temperatures (330 to 340 °C) and water-to-oil ratios 2.5 to 5: 1, TAGs are hydrolyzed to

produce free fatty acids (FFAs) (King, Holliday et al. 1999). At higher temperatures (400 °C), fatty acids are subjected to deoxygenation to produce alkanes and alkenes, especially in the presence of a catalyst (Watanabe, Iida et al. 2006) Proteins comprised of amino acids linked by peptide bonds between carboxyl and amine groups undergo slow hydrolysis and depolymerization that start occurring below 230 °C to produce amino acids and peptides (Toor, Reddy et al. 2013).

### **1.3.2. Hydrothermal gasification**

Hydrothermal gasification (HTG) is a relatively novel process that leads to biomass degradation and gas formation above the critical point of water. The main advantages of HTG are (Kumar 2013):

- can utilize wet biomass;
- high gasification efficiency at relatively low reaction temperatures (400-700 °C);
- homogeneous reaction medium with reduced transport limitations and a mass transfer resistance;
- easier separation of gaseous products;
- does not depend on type of biomass.

Biomass in supercritical water undergoes fast hydrolysis, which leads to fast degradation of its polymeric structure. Supercritical water that has a low density and favors free radical reactions promotes the formation of H<sub>2</sub>, CH<sub>4</sub>, CO, CO<sub>2</sub>, and light hydrocarbons (Kruse and Gawlik 2003).

There are two types of HTG processes:

- (1) low-temperature (350-500 °C) HTG with metal catalysts leading to formation of methane-rich gas;
- (2) high-temperature (500-750 °C) HTG without catalysts or with non-metal catalysts leading to formation of hydrogen-rich gas (Matsumura, Minowa et al. 2005).

In near- or supercritical water (350-400 °C), biomass can be gasified mainly to methane and carbon dioxide in the presence of a heterogeneous catalyst. At higher reaction temperatures, biomass is converted into hydrogen-rich gas mixture without a catalyst or in the presence of a non-metal catalyst (Elliott 2008). Hydrogen is an especially attractive source of energy that can be used in a number of applications. For production of hydrogen from biomass, Watanabe et al. used  $ZrO_2$  as a catalyst (Watanabe, Inomata et al. 2003), Elliott et al. and Byrd et al. used Ru, Rh, and Ni on different supports that demonstrated high catalytic activity (Elliott, Sealock et al. 1993, Byrd, Kumar et al. 2011).

HTG of lignocellulosic biomass involves rapid hydrolysis of lignin and hemicellulose at lower temperatures and hydrothermolysis of remaining compounds at higher temperatures. Biomass subsequently undergoes a number of chemical transformations including isomerization, dehydration, fragmentation, and condensation that lead to formation of gas (Matsumura, Minowa et al. 2005). The homogeneous supercritical reaction medium that has minimal transport limitation and a mass transfer resistance favors decomposition of organic compounds into gases while suppresses the formation of tars and chars (Calzavara, Jousot-Dubien et al. 2005).

In case of HTG of algal biomass, the presence of sulfur and nitrogen in the protein fraction of the feedstock can cause impurities in the resulting gas. Sulfur content of microalgae are low (< 0.1 wt%) and can hardly be a matter of concern. However, nitrogen content of algae is high and leads to formation of NH<sub>3</sub>, NO<sub>x</sub>, and HCN that have to be removed from the gas mixture before further processing. Unlike lignocellulosic biomass, microalgae do not contain recalcitrant fibers and can be easily gasified under supercritical water conditions. It was reported that more than 80 wt% of microalgal biomass (*Chlorella vulgaris*) was gasified in supercritical water at 400-700 °C for 1-15 min with a Ni catalyst. The produced gas mainly contained CO<sub>2</sub>, CO, CH<sub>4</sub>, H<sub>2</sub>, and some light (C<sub>2</sub>-C<sub>3</sub>) hydrocarbons (Chakinala, Brilman et al. 2010).

### **1.3.3. Hydrothermal carbonization**

Hydrothermal carbonization (HTC) is a process for production of biochar from biomass feedstock. Biochar is a carbon-rich product with a high energy density comparable to that of bituminous coal. It can be produced from any solid organic feedstock such as wood wastes, agricultural residues, paper sludge, etc. The friable structure and high calorific value of biochar make it an excellent solid fuel. Resistance to decomposition and porous structure makes biochar an excellent means for soil amendment (Bruun and Luxhoi 2008). Table 4 compares some qualities of biomass and biochar as solid fuel.



**Table 4.** Comparison of biomass and biochar as solid fuels (Kumar 2013)

<b>Biomass</b>	<b>Biochar</b>
High moisture content	Low moisture content, easily dried
Low heating value, high transportation cost	High heating value, less transportation cost, \$/MJ
Perishable during storage	Non-perishable
Fibrous structure, difficult to handle	Friable structure, easier to compact and handle
Poor compatibility with coal for co-firing	Good compatibility with coal for co-firing

In the nature, coal is formed from plant material under high temperature and pressure for millions of years. The acceleration of this process by a factor of  $10^6$ - $10^9$  in hydrothermal medium under milder reaction conditions can be a technically feasible and attractive alternative to the natural process (Titirici, Thomas et al. 2007).

Biomass typically contains 40-60% oxygen. Maximal removal of oxygen from biomass is the main objective for biochar production. This can be done by dehydration (removal of oxygen in form of water) and/or decarboxylation/decarbonylation (removal of oxygen in form of  $\text{CO}_2/\text{CO}$ ). Subcritical water provides an ideal medium for those kinds of chemical reactions. It serves as a reactant, reaction medium, and catalyst that helps biomass compounds undergo hydrolysis, depolymerization, dehydration, decarboxylation, and condensation/repolymerization reactions. Several chemical mechanisms play an important role in biomass conversion in hydrothermal medium:

proton-catalyzed mechanism, direct nucleophilic attack, hydroxide ion catalyzed mechanism, and the radical mechanism (Savage 1999, Masaru, Takafumi et al. 2004).

Subcritical water at 180-250 °C is an efficient reaction medium for biochar production (Kumar 2010). Several hours is typically required to remove most of oxygen from biomass by dehydration and to change the fibrous structure of biomass. Dehydration of biomass can be accelerated by the addition of a small amount of acid to the reaction medium. The oxygen content of the obtained biochar can be reduced to 10-30 wt% depending on the reaction temperature and time (Kalderis, Kotti et al. 2014).

Biochar is traditionally produced by slow pyrolysis at the temperatures of 500 to 800 °C. HTC, which is conducted in subcritical water below 300 °C, can be an economically preferable option for biochar production.

#### **1.3.4. Catalytic hydrodeoxygenation**

Biomass with high lipid content is an attractive feedstock for producing renewable fuels. Biomass-derived oils that primarily consist of TAGs and FFAs can be readily converted into biodiesel via the well-studied transesterification process (Mittelbach and Remschmidt 2004, Knothe, Krahl et al. 2005). However, due to some oxygen content, biodiesel cannot serve as a fully-fledged replacement for conventional petrodiesel. In this respect, renewable diesel obtained via catalytic hydrodeoxygenation (HDO) of lipid-based feedstocks is a more attractive and fungible option. This process makes it possible to produce fuels with the chemical composition indistinguishable from that of petroleum-derived products. Since all kinds of biomass have high oxygen content, research of the catalytic HDO process attracts much attention. In the research by Corma

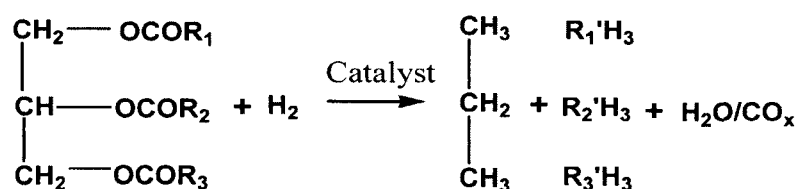
(Corma, Iborra et al. 2007), Huber (Huber, Iborra et al. 2006), Kamm (Kamm, Gruber et al. 2000), and Centi (Centi and Santen 2007) with co-workers, different chemical routes for the transformation and upgrading of this category of biomass into chemicals and fuels have been investigated.

HDO is a hydrogenolysis process for removing oxygen from various compounds that is conducted under high hydrogen pressure and at high temperatures in the presence of a specific heterogeneous catalyst. HDO is an efficient technology for the production of fuels from renewable feedstocks as discussed in the studies by Marinangeli et al. (Marinangeli, Marker et al. 2005) and Choudhary and Phillips (Choudhary and Phillips 2011).

Transesterification is an important process for producing biofuels from lipid-based feedstocks. This conventional process can be typically performed by transesterification of TAGs with an alcohol in the presence of an alkali catalyst to form FAMEs.

Biofuels can be also produced from TAGs by removing oxygen and saturating double bonds of fatty acid chains with hydrogen via catalytic HDO. In this case, renewable diesel that consists of straight-chain hydrocarbons and propane are formed (R' represents saturated alkyl groups, R – unsaturated alkyl groups):

During HDO, hydrocarbons with lower oxygen content are produced:



Bio-oils produced from lignocellulosic biomass can be upgraded via HDO process to obtain saturated hydrocarbons in a similar way (Elliott 2007, Bu 2012). Table 5 summarizes the typical operation conditions for renewable fuel production via HDO of oils/bio-oils.

**Table 5.** Typical operating conditions for HDO of bio-oils (Elliott 2007)

<b>Temperature, °C</b>	250-400
<b>Pressure, MPa</b>	10-22
<b>Liquid hourly space velocity, (vol. oil)/(vol. catalyst)/h</b>	0.1-0.8
<b>H<sub>2</sub> feed rate, (L H<sub>2</sub>)/(L bio-oil)</b>	100-700
<b>Catalyst active metals</b>	CoO/MoO <sub>3</sub> , NiO/MoO <sub>3</sub> , NiO/WO <sub>2</sub> , Ni, Pt
<b>Catalyst support</b>	Al <sub>2</sub> O <sub>3</sub> , $\gamma$ -Al <sub>2</sub> O <sub>3</sub> , silica-alumina, Y-zeolite/Al <sub>2</sub> O <sub>3</sub>

The structure of resulting renewable diesel molecules is indistinguishable from that of petrodiesel molecules. In this respect, Holmgren et al. (Holmgren, Gosling et al. 2007) found it especially attractive that HDO of biomass-derived feedstocks can be performed at the existing refineries. This can significantly minimize capital costs required for the industrial application of the process, thus making it one of the most important advantages of the HDO route.

During the catalytic HDO of lipid-based feedstocks, several types of reactions take place. They can be divided into four main categories:

- Hydrogenation of the double bonds of the fatty acids chains (Benedict and Daubert 1950);
- Thermal decomposition/degradation of TAGs (Vonghia, Boocock et al. 1995);
- Decarbonylation, decarboxylation, and hydrodeoxygenation of those degradation products (FFAs and fatty alcohols, mono- and diacylglycerols, glycerol, etc.) to produce straight-chain alkanes (Leung, Boocock et al. 1995, Snåre, Kubičková et al. 2008, Krar, Kovács et al. 2010);
- Isomerization and cracking of those alkanes (Huber, O'Connor et al. 2007).

Complete reaction pathways of the catalytic HDO of vegetable oils were studied in details and illustrated by Huber and co-workers (Huber, O'Connor et al. 2007) and by Kubicka and Kaluza (Kubicka and Kaluza 2010). It was stated that in the presence of hydrogen and conventional hydrotreating catalysts at elevated temperatures (300-450 °C), fatty acids chains get saturated, TAGs decompose into FFAs and other intermediates, and those intermediates undergo decarbonylation, decarboxylation, and hydrogenolysis to produce renewable diesel. During hydrogenolysis, fatty acid esters are reduced to fatty alcohols directly or via dehydration-hydrogenation steps and fatty alcohols are reduced to alkanes (Yakovlev, Khromova et al. 2009). The reaction pathways of conversion of TAGs into alkanes, influence on temperature, pressure, catalysts, and hydrogen on the

process will be reviewed in details in Chapter 2. The overall reaction network is provided in Fig. 4.

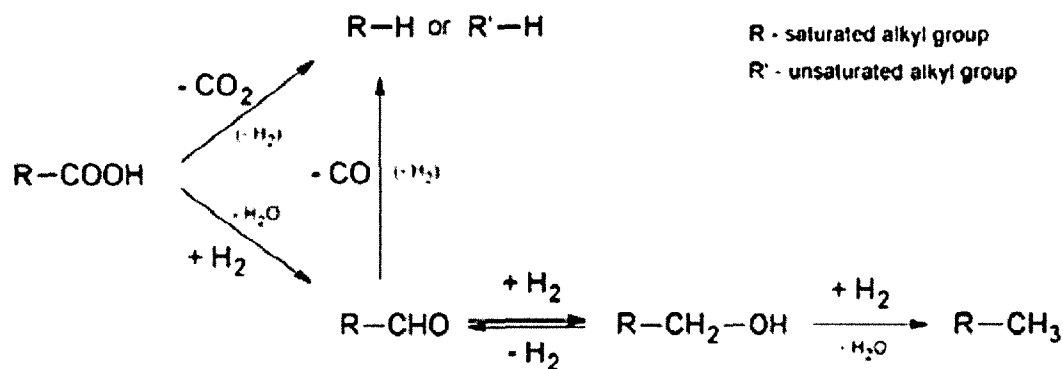


**Figure 4.** Fatty acids deoxygenation pathways over Pd/C catalyst (Davis and Barteau 1990).

Sub- and supercritical water can be an attractive reaction medium for hydrolysis of TAGs and deoxygenation of resulted FFAs to produce liquid fuels. It is now commonly accepted that the rates of chemical reactions can be substantially increased due to reduction of interphase mass transfer resistances and the ability of supercritical water to maintain both ionic and free-radical reactions (Antal, Brittain et al. 1987).

TAGs can be readily split to form FFAs and glycerol via Colgate-Emery process (Barneby and Brown 1948). King and co-workers found that fast hydrolysis of TAGs can be conducted at the temperatures of 330 to 340 °C and oil-to-water ratios of 1:2.5 to 5.0. At these conditions, the yield of FFAs can be 90 to 100% (King, Holliday et al. 1999). It was observed that the phase behavior of components is crucial for the process and determined that the reaction quickly went to completion with almost 100% yield of FFAs when the mixture became a single phase at 339 °C.

No research has been conducted on catalytic HDO of lipid-based feedstocks in hydrothermal medium yet. However, in recent years, a few studies on fatty acid decarboxylation in hydrothermal media without adding hydrogen were carried out. The advantage of hydrothermal medium is not only the use of water as an environmentally benign solvent but also the avoidance of a separation step after TAGs hydrolysis and generation of FFAs (Idem, Katikaneni et al. 1996, Huber and Dumesic 2006). FFAs have been shown to degrade in hydrothermal media producing long-chain hydrocarbons. Watanabe and co-workers investigated the decomposition of stearic acid ( $C_{17}H_{35}COOH$ ) in a fixed bed batch reactor to the maximum temperature of 400 °C (Watanabe, Iida et al. 2006). Two major products,  $C_{17}H_{36}$  and  $C_{16}H_{32}$ , were found in the reaction products. The authors compared this process to the stearic acid pyrolysis and found that stearic acid decomposition under hydrothermal conditions was suppressed and resulted in prevailing alkenes over alkanes. The formation of shorter-chain hydrocarbons was also suppressed under the hydrothermal conditions. However, when NaOH or KOH was added, decomposition of stearic acid enhanced significantly producing more alkanes than alkenes.

Fu et al. conducted a series of research projects on hydrothermal deoxygenation of fatty acids. It was reported that Pd/C and Pt/C catalysts possess catalytic activity in near critical water at 370 °C for decarboxylation of a saturated fatty acid (palmitic acid) with 76% molar yield of pentadecane (Fu, Lu et al. 2010). It was found that Pt/C catalyst is more active in water than Pd/C catalyst. However, the catalyst metal dispersion exhibited a significant reduction (from 38.9% to 0.8% for Pt and from 21.1 to 1.5% for Pd) after the reaction for 1-3 h.

Fu et al. (Fu, Lu et al. 2011) studied the effect of degree of fatty acid unsaturation on the decarboxylation over Pt/C catalyst in subcritical water at 330 °C. It was reported that unsaturated fatty acids provided much lower heptadecane yield (< 20%) and selectivity than saturated fatty acids (> 80%) after the reaction for 2.5 h.

Fu et al. also demonstrated that activated carbon itself possesses catalytic activity for decarboxylation of both saturated and unsaturated fatty acids, which can be a low-cost alternative to the expensive noble metal catalysts (Fu, Shi et al. 2011). However, the major product from oleic acid conversion was stearic acid with 24% molar yield. The desired decarboxylation product (heptadecane) molar yield was only 6% after the reaction at 370 °C for 3 h. In all cases, complete hydrogenation was not observed, and the reaction products included both alkanes and alkenes.

Further research is required in order to increase hydrogenation and deoxygenation efficiency of the hydrothermal process, increase conversion of fatty acids, molar yield of alkanes, and selectivity for the respective products.

#### **1.4. Motivation and scope of the study**

Biomass is the fourth largest source of energy in the world after coal, oil, and natural gas. From all available sources of renewable energy, only biomass has the potential to provide the large scale substitution of hydrocarbon-based liquid transportation fuels and minimize the environmental issues (Farrell, Plevin et al. 2006).

In recent years, biomass-derived fuels received increasing attention as one of the solutions to the U.S.' growing dependence on imported oil, which exposes the country to



the risk of critical disruptions in the fuel supply, creates economic and social uncertainties for businesses and individuals, and impacts the national security (DOE 2010). The Energy Independence and Security Act of 2007 (EISA 2007) established a mandatory Renewable Fuel Standard (RFS) requiring the transportation fuel sold in the U.S. to contain a minimum of 36 billion gallons per year of renewable fuel, including advanced cellulosic and biomass-based diesel, by 2022.

In order to develop a sustainable and efficient way of biomass processing in hydrothermal media, maximize yields of biofuels, useful intermediates and byproducts, maximize energy yields, minimize the costs of processing, and contribute to the development of biomass-based biorefinery concept, different novel approaches to biomass conversion were investigated in this work.

Biomass with high lipid content is an attractive feedstock for renewable fuels production. Biomass-derived oils can be readily converted into biodiesel via the well-studied transesterification process. However, due to some oxygen content, it cannot serve as a fully-fledged replacement for conventional petrodiesel. In this respect, renewable diesel obtained via catalytic hydrodeoxygenation of lipid-based feedstocks is a more attractive and fungible option. This process makes it possible to produce fuels with the chemical composition indistinguishable from that of petroleum-derived products. Since all kinds of biomass have high oxygen content, comprehensive research of the catalytic HDO process attracts a great interest. Chapter 2 provides a comprehensive review of the state-of-the-art studies related to the catalytic HDO of lipid-based feedstocks including microalgae for the last decade with an analysis of the possible advantages of this process.

Lignocellulosic biomass is currently widely used for ethanol production using a biochemical route. It involved enzymatic hydrolysis followed by microbial fermentation. The process is able to utilize only cellulose and hemicellulose contained in the biomass and therefore leaves behind from 30 to 40% of unhydrolyzed solids (UHS) containing mostly lignin. The efficient conversion of UHS into bio-oil would increase the overall conversion efficiency of ethanol production and has the potential to reduce the cost of biofuel production from lignocellulosic biomass. In Chapter 3, bio-oil production from the lignin waste via hydrothermal liquefaction was investigated. The effects of reaction temperatures (280-350 °C) and catalysts (homogeneous  $K_2CO_3$  and heterogeneous  $CoMo/Al_2O_3$ ) on the degree of liquefaction, bio-oil yield, energy conversion ratio, and bio-oil composition were studied and the overall mass balance of the process was developed. The results of the study can contribute to the development of the integrated process that includes ethanol and bio-oil production from lignocellulosic biomass and upgrading the bio-oil to liquid hydrocarbons.

A novel integrated oil extraction process that includes hydrothermal pretreatment and oil extraction (HPOE) from the whole oilseeds followed by hydrothermal carbonization of the extracted seedcake to biochar was developed and reported in Chapter 4. Five different types of oilseeds including cotton-, flax-, mustard-, canola-, and jatropha seeds were used in the study. The seeds were subjected to hydrothermal pretreatment in the range of temperatures from 120 to 210°C for 30 min. Oils were extracted from the pretreated seeds using *n*-hexane in a Soxhlet apparatus for 120 min. The crude oil yields from the pretreated seeds at 180 °C and 210 °C were significantly higher than those from the respective untreated ground seeds. The seedcake after oil extraction was subjected to

HTC at 300 °C with the recycled aqueous phase collected from the pretreatment step. The kinetics study showed that HPOE method provided better extractability of oil and shorter extraction time. Analyses of the crude oil did not show significant signs of degradation after the hydrothermal pretreatment of oilseeds. The mass and energy balances of the process were developed. The study is the first of its kind where integrated oil extraction and biochar production from oilseeds have been studied with the objective of minimizing feedstock preparation and maximizing oil extraction and overall energy conversion using environmentally benign hydrothermal processes. The extracted oil can be used for the renewable fuel production.

In Chapter 5, the results of hydrothermal liquefaction of microalga *Scenedesmus sp.* with following catalytic gasification of the aqueous phase in near- and supercritical water were reported. In this study, we attempted to maximize the overall energy yield by producing gas from the extracted aqueous phase. *Scenedesmus sp.* was liquefied in a batch reactor at 300 °C for 30 min. The liquid phase consisting mainly of partially hydrolyzed carbohydrates and proteins were rich in nutrients required for growing the fresh algae that can be recycled. However, the direct use of the liquid phase as a source of nutrients poses challenges due to the presence of some inhibitors that can suppress the algae growth. The liquid phase was extracted with dichloromethane yielding energy-dense bio-oil. After that, the extracted aqueous phase was subjected to gasification in a continuous flow reactor over an activated carbon catalyst at the temperatures from 350 to 400 °C with a weight hourly space velocity (WHSV) of 3.3 h<sup>-1</sup>. The produced gas contained mostly H<sub>2</sub>, light hydrocarbons, and CO<sub>2</sub>. The results of the study show that considerable amount of H<sub>2</sub> and gaseous hydrocarbons can be produced at relatively low

temperature of 400 °C using a low-cost activated carbon as a catalyst. The processed aqueous phase was intended to be used as a source of nutrients for microalgae growth in the followed up research. It was reported that that some strains of microalgae (i.e., *Chlorella vulgaris* and *Nannochloropsis gaditana*) can grow as well as in the standard medium even when 75% of the nutrients were substituted by the addition of the aqueous phase after HTG (López Barreiro, Bauer et al. 2015). The integration of HTL and HTG of the algal biomass with the following nutrient recycling could be an important approach to the biorefinery concept in terms of maximizing the carbon utilization in an economically viable way.

One of the main goals of this work was to find an efficient way of the renewable fuel production from algal oil, which mainly contains unsaturated fatty acids. Therefore, oleic acid was employed as a model compound in the study. In this research project, a novel approach to converting fatty acids into *n*-alkanes was investigated (Chapter 6). Fuel range hydrocarbons were obtained in a continuous flow process from oleic acid using near- and supercritical water as reaction medium, granulated activated carbon as a catalyst, and  $\leq 1\%$  v/v formic acid as an in situ source of hydrogen. Formic acid in low concentrations can serve as an active donor of free-radical hydrogen and provide the complete hydrogenation of unsaturated fatty acids/hydrocarbons within a short residence time. No supplying of gaseous H<sub>2</sub> with high feed rates and no noble metals are required. The study shows that activated carbon can be a promising and inexpensive alternative to the costly noble metal catalysts for renewable fuel production in hydrothermal medium. The experimental part was carried out in a packed-bed tubular reactor with the weight hourly space velocity of 4 h<sup>-1</sup> at the temperatures from 350 to 400 °C and pressure 3500

psi (24.1 MPa). The oil to water to formic acid ratio was 1:5:0.05 by volume. The main reaction pathways were hydrogenation of oleic acid and decarboxylation/decarbonylation of the resulted stearic acid to form heptadecane. The results of the study show that the efficient hydrothermal deoxygenation of fatty acids can be achieved with activated carbon as a catalyst and formic acid as an in situ source of hydrogen within minutes. The analyses of the obtained renewable diesel and kinetics study of the process were carried out and showed the high efficiency of the process. The proposed process is readily scalable and offers a green approach to the renewable fuel production.

## CHAPTER 2

### RENEWABLE FUELS VIA CATALYTIC HYDRODEOXYGENATION OF LIPID-BASED FEEDSTOCKS (REVIEW)

*Note: the contents of this chapter have been published in Biofuels. Popov, S., Kumar, S. Renewable fuels via catalytic hydrodeoxygenation of lipid-based feedstocks. Biofuels, 4 (2), 219-239 (2013). DOI:10.4155/bfs.12.89.*

Energy security concerns have led to the search for alternative and renewable energy resources. Biomass with high lipid content is an attractive feedstock for producing renewable fuels. Biomass-derived fats and oils can be readily converted into biodiesel via the well-studied transesterification process. However, due to some oxygen content, it cannot serve as a fully-fledged replacement for conventional petrodiesel. In this respect, renewable diesel obtained via catalytic hydrodeoxygenation (HDO) of lipid-based feedstocks is a more attractive and fungible option. This process makes it possible to produce fuels with the chemical composition indistinguishable from that of petroleum-derived products. Since all kinds of biomass have high oxygen content, comprehensive research of the catalytic HDO process arouses a great interest. The paper aims to review the state-of-the-art studies related to the catalytic HDO of lipid-based feedstocks for the last decade. The suitability of microalgae as a feedstock for renewable fuel production as well as the possible advantages of processing lipid-based feedstocks using aqueous HDO is also addressed in this review.

## **2.1. Introduction**

In recent years, biomass-derived fuels have received increasing attention as one solution to the U.S.' continued and growing dependence on imported oil, which exposes the country to the risk of critical disruptions in fuel supply, creates economic and social uncertainties for businesses and individuals, and impacts the national security (DOE 2010). The Energy Independence and Security Act of 2007 (EISA 2007) established a mandatory Renewable Fuel Standard (RFS) requiring transportation fuel sold in the U.S. to contain a minimum of 36 billion gallons of renewable fuel, including advanced cellulosic and biomass-based diesel, by 2022.

Renewable fuel can be defined as fuels produced from biological sources such as biomass to reduce the amount of fossil fuel used in transportation system. There are many biofuel production technologies that are capable of producing liquid transportation fuels via processing and upgrading different kinds of biomass and municipal waste feedstocks. Biofuels are classified based on the type of feedstocks and technologies used to produce them (Naik, Goud et al. 2010). First-generation biofuels are biofuels made from edible feedstocks such as sugar, starch, and vegetable oil and usually employ enzymatic fermentation or transesterification processes of the above feedstocks to produce biofuels. Second generation biofuels are produced from sustainable feedstocks such as lignocellulosic biomass, municipal wastes, inedible oils and greases, etc. via pyrolysis, gasification followed by Fischer-Tropsch synthesis, or hydrothermal liquefaction technologies. Third generation biofuels that are currently in an active research and development stage are derived from microalgae and other aquatic species with high biomass yield. The International Energy Agency (IEA) categorizes different generation

biofuels as conventional and advanced biofuels. According to the IEA, ethanol from sugar and starch crops, biodiesel via transesterification, and biogas via anaerobic digestion are considered as conventional biofuels whereas other biofuels produced mainly from non-food biomass are considered as advanced biofuels.

Biomass feedstocks can also be classified into three categories, which are carbohydrates, lignin, and fats/oils. Carbohydrates mainly include the fractions containing sugars, celluloses, and hemicelluloses. Lignin is one of the main components of wood, agriculture residues, and so-called energy crops. Fats and oils primarily consist of triacylglycerols (TAG) and fatty acids. The last category is of primary interest of this paper that aims to review the studies related to catalytic HDO of the real feedstocks in the last decade. In the research by Corma (Corma, Iborra et al. 2007), Huber (Huber, Iborra et al. 2006), Kamm (Kamm, Gruber et al. 2000), and Centi (Centi and Santen 2007) with co-workers, different chemical routes for the transformation and upgrading of this category of biomass feedstocks into chemicals and fuels have been investigated.

Fuels derived from non-food based lipid biomass such as fats and oils are being viewed as one of the important options of producing drop-in liquid fuels. Different processes can be employed for producing biofuels from biomass-derived fats and oils. Depending on the technology utilized, biofuels with different composition and properties can be obtained. Among them, biodiesel (Mittelbach and Remschmidt 2004, Knothe, Krahl et al. 2005), which is a mixture of mono-alkyl esters of fatty acids, is the most studied up to date. It can be typically produced via the reaction of transesterification of the TAGs with an alcohol in the presence of a base catalyst (Knothe, Krahl et al. 2005).



Compared to traditional diesel fuel, biodiesel has the advantages of reducing particulate exhaust emissions, biodegradability, higher flash point, and can be produced locally near the feedstock source (Knothe, Krahl et al. 2005). However, biodiesel has a number of shortcomings, namely: low energy density resulting from high oxygen content, poor cold flow properties, relatively high production costs due to costly feedstock production/oil extraction, higher NO<sub>x</sub> exhaust emissions, corrosion properties, and generally limited to relatively high quality (e.g., low free fatty acid (FFA) content) feedstock. With these difficulties that are mainly conditioned by unsaturated chemical bonds, unreacted FFA, presence of carboxyl and other oxygen functional groups, efforts are underway to develop alternative production process to produce drop-in biofuels to replace petroleum-derived fuels.

### **2.1.1. Terminology for fuels**

Terminology is important for the correct definition of different kinds of fuels that are the subject of our discussion. Reviewing the present literature, we can see that sometimes one term is used for different fuels and different terms are used for the same fuel derived from lipid-based feedstocks. Therefore, we need to correctly define the fuel categories that will be discussed and compared in the paper.

*Petrodiesel* is the diesel fuel derived from petroleum that meets the requirements of the standards ASTM D 975 in the United States and EN 590 in Europe.

*Biodiesel*: According to the US standard specification for biodiesel fuel blend stock (B100) for middle distillate fuels ASTM D 6751, biodiesel is a “fuel comprised of mono-alkyl esters of long-chain fatty acids derived from animal fats or vegetable oil”. European

Committee for Standardization in the standard EN 14214 defines biodiesel as fatty acid methyl esters (FAME).

*Renewable diesel* is the most contradictory term that is used for definition of petroleum-like diesel produced from renewable biological resources. The term “green diesel” is also used for defining the same fuel. Even though this term may attribute to the origin of the fuel, the resulting diesel has the same nature as petrodiesel. Therefore, in order to avoid confusion, the best term for the fuel derived from a renewable resource has to be “renewable diesel” (Knothe 2010).

*F-T Diesel/Syndiesel*: The term “synthetic diesel” (syndiesel) defines liquid hydrocarbons produced from syngas (CO and H<sub>2</sub>) using Fisher-Tropsch (F-T) synthesis process. This gas-to-liquids technology can be employed to produce syndiesel from the products of gasification of natural gas, coal, and almost any kind of biomass. Syndiesel has greater cetane number and little or no aromatics and sulfur content in comparison with petrodiesel.

The main properties of the different kind of fuels discussed above were studied by Kalnes (Kalnes, Marker et al. 2007), Kuronen (Kuronen, Mikkonen et al. 2007), and Rantanen (Rantanen, Linnaila et al. 2005) with co-workers. The comparison of different diesel fuels properties are shown in Table 6.

**Table 6.** Comparison of different diesel fuels (EN 590 , ASTM D 6751 , EN 14112 , EN 14214 , Leckel and Liwanga-Ehumbu 2006, Lamprecht 2007, Kalnes, Marker et al. 2008, Oja 2008)

<b>Fuel properties</b>	<b>Petrodiesel</b>	<b>Biodiesel</b>	<b>Renewable Diesel</b>	<b>Syndiesel</b>
<b>Oxygen, %</b>	0	11	0	0
<b>Specific gravity</b>	0.84	0.88	0.78	0.77
<b>Sulfur, ppm</b>	<10	<1	<1	<1
<b>Heating value, MJ/kg</b>	43	38	44	44
<b>Cloud point, °C</b>	-23 to +4	-5 to- +15	-30 to -5	- 18 to +2
<b>Cetane No.</b>	40-55	46-52* 56-60**	70-90	>75
<b>Oxidative stability, h (Rancimat method)</b>	22-33	3-6	N/A	N/A

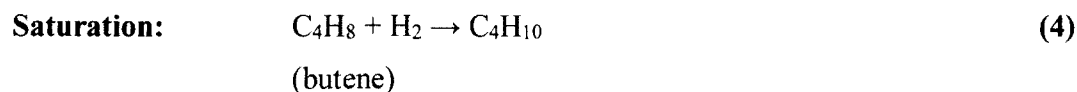
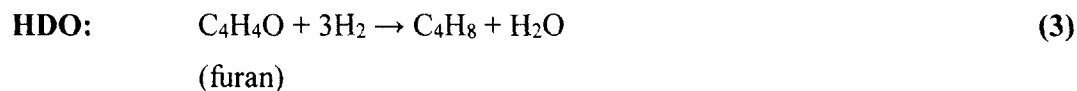
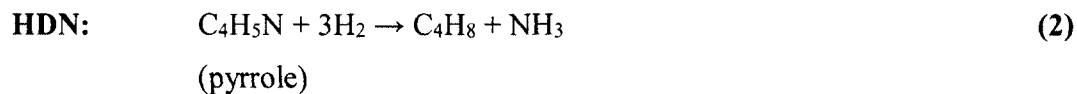
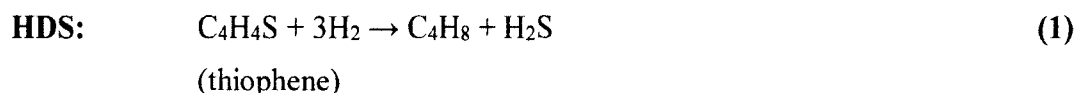
\*For biodiesels produced from vegetable oils

\*\*For biodiesels produced from animal fats

No report on oxidative stability of renewable diesel and syndiesel being tested according to the petrodiesel standards ASTM D 975 or EN 590 seems to be available yet (Knothe 2010). However, taking into account other available properties of those fuels, it appears likely they would exhibit oxidative stability comparable to petrodiesel.

### 2.1.2. HDO process

HDO is a hydrogenolysis process for removing oxygen from various compounds that is conducted under high hydrogen pressure and at high temperatures in the presence of a specific heterogeneous catalyst. During HDO, hydrocarbons with lower oxygen content are produced. HDO is an efficient technology for the production of fuels from renewable feedstocks as discussed in the studies by Marinangeli (Marinangeli, Marker et al. 2005) et al. and Choudhary et al. (Choudhary and Phillips 2011). HDO takes place during hydroprocessing of petroleum along with hydrodesulfurization (HDS), hydrodenitrogenation (HDN), hydrodemetallization (HDM), and saturation of olefins/aromatic compounds (Leliveld and Eijsbouts 2008). The examples of the reactions are as follows:

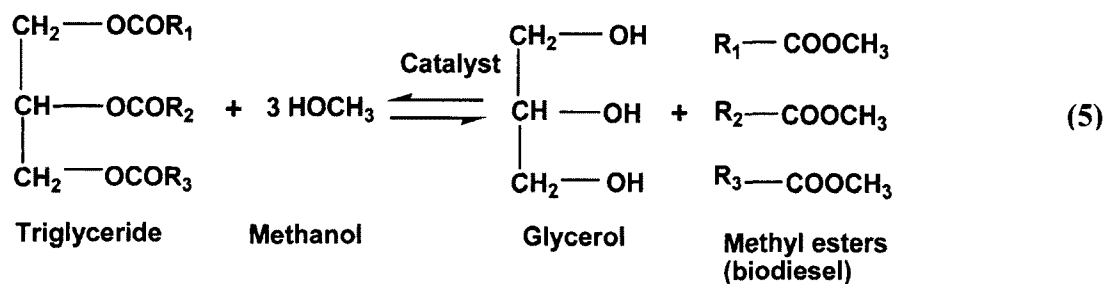


The purpose of conventional hydroprocessing reactions in petroleum refineries is to remove sulfur, nitrogen, and oxygen heteroatoms from petroleum. In these processes, more attention is paid to HDS and HDN because oxygen content of the feedstock is low, typically less than 0.3 wt%. However, since biomass feedstocks contain a large amount of oxygen, HDO is more focused on oxygen removal and molecular-weight reduction of biofuels. HDO technologies are similar to those for converting crude oil to fuels and play rather a crucial role in biofuel upgrading, which largely determines the biofuel properties. The oxygen content of biomass varies with the type of biomass and may approach 50 wt% (Thigpen and Berry 1982, Elliott, Beckman et al. 1991, Bridgwater and Peacocke 2000). In the comprehensive reviews by Furimsky (Furimsky 2000) and Elliott (Elliott 2007), HDO of different biomass-derived products has been thoroughly analyzed. The review by Furimsky mainly focuses on the chemistry of HDO for a number of oxygen-containing compounds in petroleum and bio-oils obtained via biomass pyrolysis. Elliott reviews different HDO technologies and processes employed in upgrading of bio-oils. HDO of lignin-derived phenols was recently reviewed by Bu et al. (Bu 2012) This work reviewed the reaction mechanisms and kinetics of HDO for different lignin-derived compounds as well as the catalysts that can be applied for HDO of lignin-derived phenols. Table 7 summarizes typical operating conditions for HDO of bio-oils.

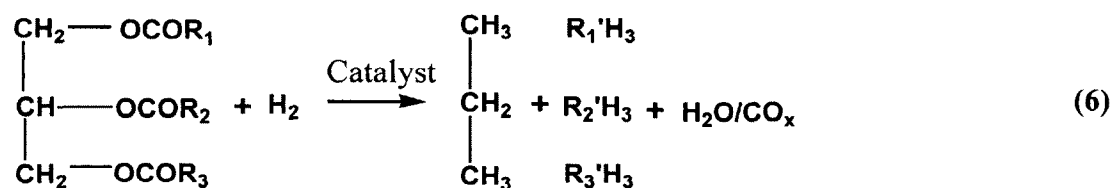
**Table 7.** Typical operating conditions for HDO of bio-oils. Reproduced from (Elliott 2007).

<b>Temperature, °C</b>	250-400
<b>Pressure, MPa</b>	10-18 22
<b>Liquid hourly space velocity, (vol. bio-oil)/(vol. catalyst)/h</b>	0.1-0.8
<b>H<sub>2</sub> feed rate, (L H<sub>2</sub>)/(L bio-oil)</b>	100-700
<b>Catalyst active metals</b>	CoO/MoO <sub>3</sub> , NiO/MoO <sub>3</sub> , NiO/WO <sub>2</sub> , Ni, Pt
<b>Catalyst support</b>	Al <sub>2</sub> O <sub>3</sub> , $\gamma$ -Al <sub>2</sub> O <sub>3</sub> , silica-alumina, Y-zeolite/Al <sub>2</sub> O <sub>3</sub>

Transesterification is an important process for producing biofuels from lipid-based feedstocks such as animal fats and vegetable oils. This conventional reaction can be typically performed by esterification of TAGs with methanol in the presence of alkali catalyst to form FAME. The FAME molecules consist of the fatty hydrocarbon tails R<sub>1</sub>, R<sub>2</sub>, or R<sub>3</sub> that vary in the length of carbon chains and in the number of unsaturated bonds and two oxygen atoms (Meher, Vidya Sagar et al. 2006):



Biofuels can be also produced from TAGs by removing oxygen and saturating double bonds of fatty acid chains with hydrogen (e.g., via catalytic HDO). In this case, renewable diesel that consists of straight-chain hydrocarbons and propane are formed (R' represents saturated alkyl groups, R – unsaturated alkyl groups):



The structure of resulting renewable diesel molecules is indistinguishable from that of petrodiesel molecules. In this respect, Holmgren (Holmgren, Gosling et al. 2007) finds it especially attractive that HDO of biomass-derived feedstocks can be performed at the existing refineries. This can significantly minimize capital costs required for the industrial application of the process, thus making it one of the most important advantages of the HDO route.

A number of research projects were conducted for understanding the HDO process chemistry in the recent years. In most of the research, model fats and oils represented by different TAGs, fatty acids, and fatty acid alkyl esters were used. Tristearate, stearic acid, and methyl stearate were commonly used in those studies. A significant contribution to understanding of the HDO reaction pathways in the last decade

was made by Krause and co-workers (Viljava, Komulainen et al. 2000, Viljava, Saari et al. 2001, Şenol, Viljava et al. 2005, Şenol, Viljava et al. 2005, Senol, Ryymin et al. 2007, Şenol, Ryymin et al. 2007, Şenol, Viljava et al. 2007). The studies of model feedstocks are important for understanding the reaction kinetics and assessing catalyst activities and selectivities for HDO. However, this paper aims to review the recent progress in the catalytic HDO of real feedstocks, namely animal fats, vegetable oils, algae lipid-rich residue, etc.

The paper focuses mainly on the effect of process parameters, feedstock, hydrogen, and types of heterogeneous catalyst on HDO process. Among the several renewable energy options available, biomass is the only renewable source that is capable of producing petroleum-compatible products (Perlack, Wright et al. 2005). The major focus is on non-food biomass resources. In general, higher land plants are not very efficient in capturing the solar energy. The biomass productivity of microalgae can be 50 times greater than that of biomass such as switchgrass (Demirbaş 2006). Despite the several advantages of microalgae over other biomass feedstocks for liquid fuels production, the high moisture content/ dewatering is a major challenge in utilizing microalgae cost-efficiently. Conversion processes that can process wet biomass are highly desirable for reducing the energy intensive dewatering cost. Hydrothermal media, which can be broadly defined as water-rich phase above 200 °C (sub- and supercritical water) offers several advantages over other biofuel production methods (Peterson, Vogel et al. 2008). The present paper reviews the application of hydrothermal media for HDO (aqueous HDO) process, when vegetable oils or microalgae are used as a feedstock.



## 2.2. Fuel composition and properties

The fuel properties are largely influenced by its composition (Fig. 5). As it was mentioned above, biodiesel or FAME represents alkyl esters of fatty acids derived from the TAGs, which, in their turn, are the main constituent of animal fats and vegetable oils. The structure of the fatty acids that are typically unsaturated straight-chain molecules with 16 or 18 carbon atoms, determines the structure of biodiesel molecules. Biodiesel fuels also contain residual mono-, di, and triglycerols, FFAs, methanol, sterols, glucosides, and glycerol. These impurities have been limited by the biodiesel standards ASTM D 6751 and EN 14214.

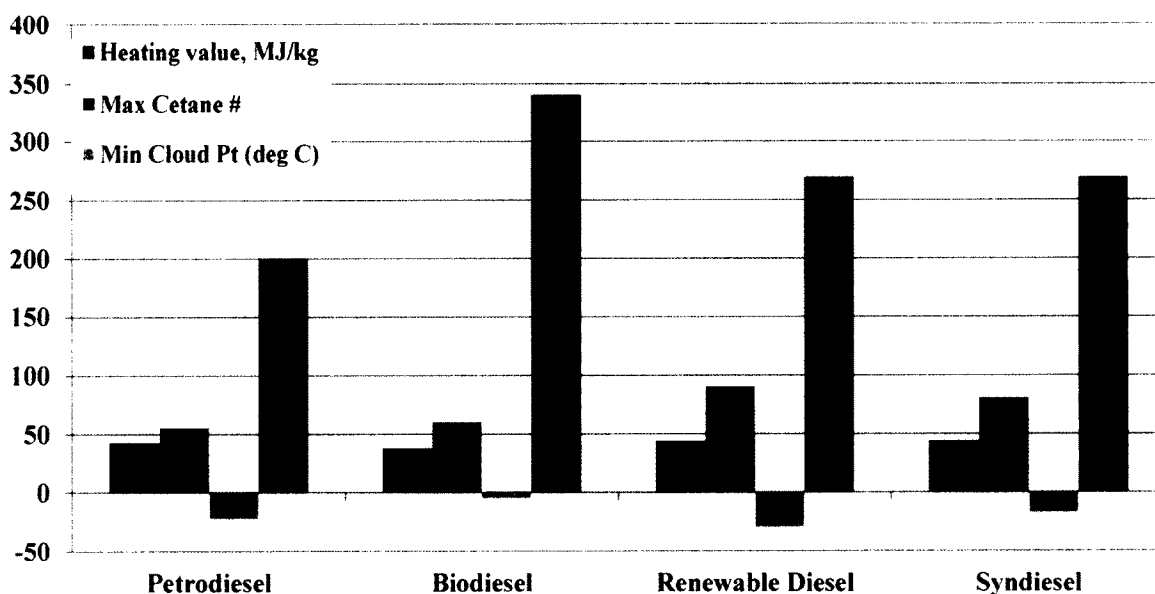


**Figure 5.** Properties of different types of diesel fuels.

Cetane number is a measurement of the combustion quality of diesel fuel during compression ignition and is an important characteristic of its overall quality. The higher is the cetane number, the easier the fuel combusts in a compression setting such as a diesel engine. The cetane number of biodiesel depends on the chain length and the degree of unsaturation of fatty esters. Biodiesel from vegetable oil sources have been recorded as having a cetane number range of 46 to 52, and animal-fat based biodiesels cetane numbers range from 56 to 60. Higher amounts of saturated fatty esters increase the cetane number but contribute to the cold flow problems. On the other hand, higher amounts of unsaturated fatty esters cause the oxidative stability problems. Therefore, a compromise has to be found in order to obtain biodiesel with optimal overall properties. Optimization of fatty ester composition for best biodiesel performance is a subject of current research (Knothe 2009, Pinzi, Garcia et al. 2009).

Petrodiesel is a complex mixture of straight-chain alkanes, branched alkanes, and aromatic compounds. Hexadecane (also called cetane) is an ideal compound of petrodiesel. However, since there are hundreds of components in diesel fuel, with each having a different cetane quality, the overall cetane number of the diesel is the average cetane quality of all the components.

Typically, petrodiesel produced in the US has cetane numbers from 40 to 55 according to ASTM D 975, with typical values in the 42-45 range. The current standard for diesel sold in European Union, Iceland, Norway, and Switzerland is set in EN 590, with a minimum cetane number of 51. The EU premium diesel fuel can have a cetane number as high as 60.

Branched alkanes and aromatic compounds (alkylaromatics and alkylcycloalkanes) possess lower cetane numbers in comparison with straight-chain alkanes, which increase with increasing the side chain lengths (Clothier, Aguda et al. 1993). Those compounds, however, have lower melting points, which improves the overall performance of petrodiesel. Another issue associated with petrodiesel is HDS process that removes not only sulfur-containing compounds from the diesel fuel but also removes compounds containing oxygen and nitrogen. Those compounds are known to be responsible for the petrodiesel lubricity (Barbour, Rickeard et al. 2000) along with aromatics and other cyclic hydrocarbons. Therefore, ultra-low sulfur diesel exhibits poor lubricity and requires adding at least 2% of biodiesel or other aromatic/cyclic additive to improve lubricity.

As it was mentioned above, renewable diesel simulates petrodiesel. The main components of renewable diesel are long-chain alkanes that are ideal components of petrodiesel. The high content of long-chain alkanes determines high cetane numbers of renewable diesel that is typically  $> 75$  (Rantanen, Linnaila et al. 2005, Holmgren, Gosling et al. 2007, Kuronen, Mikkonen et al. 2007, Aatola, Larmi et al. 2009, Murtonen, Aakko-Saksa et al. 2010). Shorter-chain alkanes and isomerized compounds that are also present in renewable diesel make the cetane number lower. However, those species improve low-temperature properties of the fuel and so are desirable compounds of renewable diesel. The cloud point of renewable diesel depends on the production process conditions that determine the product composition. It is usually stated to be between  $-30$  and  $-5$  °C (Rantanen, Linnaila et al. 2005, Holmgren, Gosling et al. 2007, Kuronen, Mikkonen et al. 2007, Aatola, Larmi et al. 2009, Murtonen, Aakko-Saksa et al. 2010, Oja

2008). No report on renewable diesel being tested according to the petrodiesel standards ASTM D 975, EN 590, or the jet fuel standard specification ASTM D 1655 (1655) seems to be available up to date. Neste Oil Corporation claims that their renewable diesel NExBTL meets EN 590 requirements and takes an active part in its standardization (Oja 2008).

According to the new revised standard specification for aviation turbine fuel containing synthesized hydrocarbons ASTM 7566-11, up to 50 percent bioderived synthetic blending components can be added to conventional jet fuel. These renewable fuel components, called in the standard hydroprocessed esters and fatty acids (HEFA) come from vegetable oil-containing feedstock. Since the properties of syndiesel are very similar to the ones of renewable diesel, the standard also has criteria for fuel produced from biomass, coal, or natural gas using Fischer-Tropsch synthesis (7566-11a).

### **2.3. HDO of lipid-based feedstocks**

HDO is a hydrogenolysis process for removing oxygen heteroatoms from feedstock compounds. The process is generally results in saturation of the double bonds and release of oxygen in the forms of carbon oxides and water with producing oxygen-free hydrocarbons. The main advantage of HDO is the ability to convert lipid-based feedstocks to high quality renewable diesel that is fully compatible with conventional petrodiesel (Stumborg, Wong et al. 1996, Sebos, Matsoukas et al. 2009, Bezergianni, Voutetakis et al. 2009). Studies on hydrogenation of lipid-based feedstocks have been conducted both in the food and fuel industries. In the food industry, the primary effort is

to saturate vegetable oils through the hydrogenation reaction (Veldsink, Bouma et al. 1997, Singh, Rezac et al. 2010):

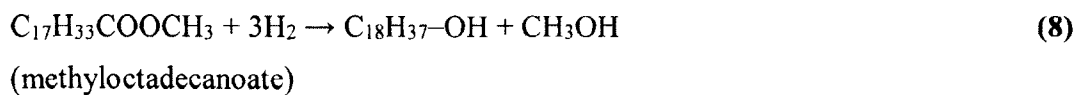


In fuel industry, HDO studies are focused on complete conversion of animal fats and vegetable oils to alkanes. In recent years, optimization of HDO process for production of renewable fuels has received increasing attention. A number of studies related to optimization of the process conditions and investigation of efficient HDO catalysts have been done. These two main areas of HDO studies are reviewed below.

### **2.3.1. Influence of temperature and pressure**

During the catalytic HDO of lipid-based feedstocks, several types of reactions take place. They can be divided into four main categories: (1) hydrogenation of the double bonds of the fatty acids chains (Benedict and Daubert 1950), (2) thermal decomposition/degradation of TAGs (Vonghia, Boocock et al. 1995), (3) decarbonylation, decarboxylation, and hydrodeoxygenation of those degradation products (FFAs and fatty alcohols, mono- and diacylglycerols, glycerol, etc.) to produce straight-chain alkanes (Leung, Boocock et al. 1995, Snåre, Kubičková et al. 2008, Krar, Kovács et al. 2010), (4) isomerization and cracking of those alkanes (Huber, O'Connor et al. 2007). Complete reaction pathways of the catalytic HDO of vegetable oils were studied in details and illustrated by Huber and co-workers (Huber, O'Connor et al. 2007) and by Kubicka and Kaluza (Kubicka and Kaluza 2010). It was stated that in the presence of hydrogen and conventional hydrotreating catalysts at elevated temperatures (300-450 °C),

fatty acids chains get saturated, TAGs decompose into FFAs and other intermediates, and those intermediates undergo decarbonylation, decarboxylation, and hydrogenolysis to produce renewable diesel. During hydrogenolysis, fatty esters are reduced to fatty alcohols directly or via dehydration-hydrogenation steps and fatty alcohols are reduced to alkanes (Yakovlev, Khromova et al. 2009):

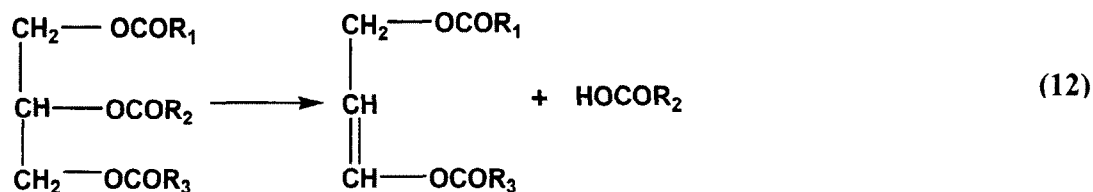


The reaction of decarbonylation of TAGs releases carbon monoxide and water to produce long-chain alkanes and alkenes (depending on the degree on hydrogenation).

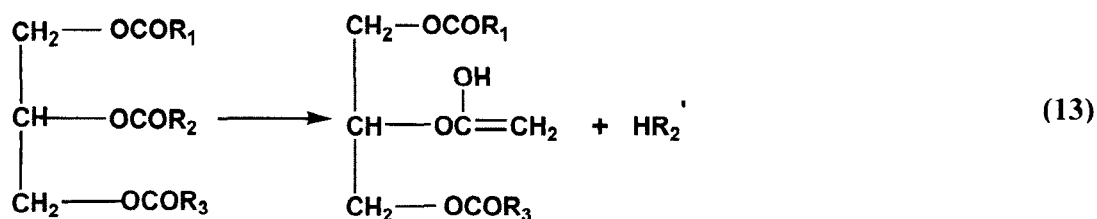
Accordingly, the reaction of decarboxylation releases carbon dioxide:



Vonghia with co-workers studied the functional group pathways during the conversion of model compounds of triglycerides to aliphatic hydrocarbons over activated alumina at 450 °C (Vonghia, Boocock et al. 1995). It was determined that TAGs can be decomposed either through  $\beta$ -elimination of carboxylic acids to produce unsaturated diacylglycerols and FFAs:



or through  $\gamma$ -hydrogen transfer within the acyl group to produce monoalkenes (in this case, R' has one carbon atom less than R):



The study has shown that hydrogen plays an important role in the reaction pathways. In the absence of hydrogen, both pathways take place but only one  $\beta$ -elimination of a TAG molecule occurred. In the presence of hydrogen and a hydroprocessing catalyst, monoalkenes are readily saturated, which results in more  $\beta$ -eliminations of the TAG backbone.

Another major factor that contributes significantly to the final product composition is the HDO reaction temperature. Da Rocha Filho with co-workers investigated the influence of the reaction temperatures in the range of 360-430 °C on the yields of alkanes, cycloalkanes, alkylbenzenes, and light gases during the catalytic HDO of buriti oil over a sulfided NiMo catalyst and in the presence of hydrogen at the pressure of 14 MPa (Filho, Brodzki et al. 1993). As shown in Fig. 6, the yield of alkanes tends to decrease with increasing the reaction temperature while the yields of cycloalkanes, alkylbenzenes, and gases tend to increase.

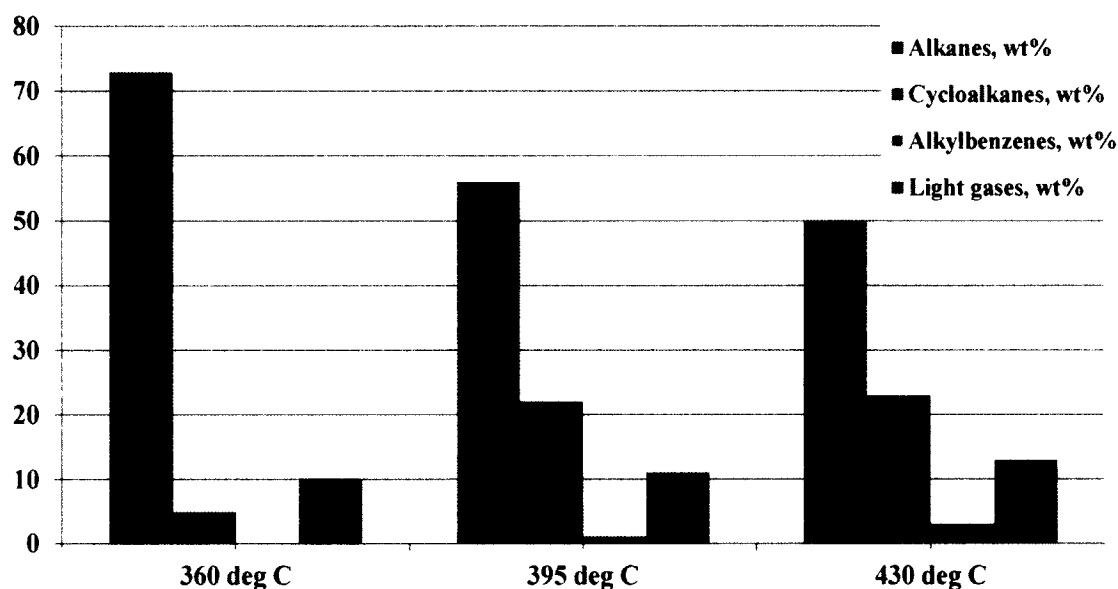


**Figure 6.** The effect of the HDO reaction temperature on the yields of buriti oil products.

Adapted from (Filho, Brodzki et al. 1993).

Simacek and co-workers (Simacek, Kubicka et al. 2010) studied the effect of temperature on the properties of hydroprocessed rapeseed oil over NiMo catalyst and found that the resulting product had a high cetane number but its cold flow properties such as cloud point and pour point were poor. At the temperatures above 310 °C and pressure of 7 MPa, the main products were alkanes with 17 and 18 carbon atoms in the chain. At 310 °C, they observed small amounts of unreacted oil and intermediate products while at 360 °C those compounds were absent in the resulting product. It was found that formation of *n*-heptadecane and iso-alkanes increased with increasing the temperature while formation of *n*-octadecane decreased. Also, the cold flow properties of the renewable diesel improved with increasing the temperature, which can be explained by the increased isomerization of the alkanes. These studies suggested that formation of alkanes with one carbon atom in the chain less than the respective fatty acids was due to



the decarboxylation reaction that is favored at elevated temperatures (360 °C). Similar results were obtained at both hydrogen pressures studied (7 MPa and 15 MPa). Different NiMo catalysts demonstrated similar temperature effects on the product yields (Simacek, Kubicka et al. 2009). Investigations of Co-Mo catalysts with different supports demonstrated that selectivity of oxygenated intermediates decreased with increasing the reaction temperature regardless of the support (Kubicka, Simacek et al. 2009).

Studies of the effect of pressure on hydroprocessing of vegetable oil and model compounds showed that higher pressures were favorable for the process (Gusmao, Brodzki et al. 1989, Guzman, Torres et al. 2010). The concentration of unreacted fatty acids was higher while the concentration of alkanes was lower at the lowest pressure studied (7 MPa). At the same time, at the highest pressure studied (14 MPa) the concentration of unreacted fatty acids was negligible while the concentration of alkanes was significantly higher. It was also found that the amount of alkanes increased in the range of pressures from 7 to 10 MPa while it remained almost constant in the range of pressures from 10 to 14 MPa. The gaseous products yield was observed to increase almost linearly with increase of pressure.

### **2.3.2. Influence of feedstocks and catalysts**

HDO studies have shown that hydroprocessing of lipid-based feedstocks can result either in producing hydrocarbons with the same number of carbon atoms in the chain or one atom less than the corresponding fatty acids. This observation makes it possible to estimate the composition of renewable diesel based on the fatty acid profile of the feedstock. However, it was found that the ratio of the resulting compounds can be

different depending on the chain length and degree of saturation of the parent fatty acids (Vonghia, Boocock et al. 1995). The increase of degree of saturation of fatty acids results in increase of the alkane and decrease of the cycloalkane yields. Saturated fatty acids with shorter chain lengths favor gas formation. It was also observed that water formed during the HDO process may decrease activity of the reactions (Şenol, Viljava et al. 2005, Huber, O'Connor et al. 2007). However, this effect was stated to be weak (Laurent and Delmon 1994).

A number of various catalytic systems have been studied over the last decade. The main trend was adaptation of the conventional hydroprocessing catalysts for different HDO processes and feedstocks. The most commonly used catalysts were NiMo/ $\gamma$ -Al<sub>2</sub>O<sub>3</sub> and CoMo/ $\gamma$ -Al<sub>2</sub>O<sub>3</sub> (Gusmao, Brodzki et al. 1989, Filho, Brodzki et al. 1993, Laurent and Delmon 1994, Laurent and Delmon 1994, Centeno, Laurent et al. 1995, Şenol, Viljava et al. 2005, Şenol, Viljava et al. 2005, Huber, O'Connor et al. 2007, Senol, Ryymin et al. 2007, Şenol, Ryymin et al. 2007, Şenol, Viljava et al. 2007, Bezergianni, Kalogianni et al. 2009, Sebos, Matsoukas et al. 2009, Simacek, Kubicka et al. 2009). However, other catalysts such as CoMo/C (Maier, Roth et al. 1982, Centeno, Laurent et al. 1995, Ferrari, Bosmans et al. 2001), CoMo/Si (Centeno, Laurent et al. 1995) Rh/Al<sub>2</sub>O<sub>3</sub> (Nunes, Brodzki et al. 1986, Ferrari, Maggi et al. 2001), Pd/SiO<sub>2</sub> (Maier, Roth et al. 1982), reduced Ni/SiO<sub>2</sub> (Gusmao, Brodzki et al. 1989), Pd/C (Kubickova, Snare et al. 2005, Mäki-Arvela, Kubickova et al. 2006, Snåre, Kubičková et al. 2008), Pt/C (Nunes, Brodzki et al. 1986) have also been investigated. NiMo, CoMo, Ni, etc. refer to respective metal oxides (NiO, CoO, MoO<sub>3</sub>) while  $\gamma$ -Al<sub>2</sub>O<sub>3</sub>, C, SiO<sub>2</sub>, etc. indicated the catalyst support. In order to increase the activity of the catalysts, they were typically sulfided with elemental sulfur or

H<sub>2</sub>S to form metal sulfides (Şenol, Viljava et al. 2005). The sulfiding of the catalysts along with a small partial pressure of H<sub>2</sub>S during the HDO process preserves the catalytic sites, thus making them more active and tolerant to poisoning by feedstock impurities. Dimethyl disulfide has also been reported as an effective means to preserve the catalytic sites during HDO of different vegetable oils (Bezergianni, Kalogianni et al. 2009, Sebos, Matsoukas et al. 2009, Simacek, Kubicka et al. 2010).

Few studies were previously carried out in order to investigate the whole algae liquefaction efficiency in the hydrothermal medium in the presence of a potential solid catalyst (Jena and Das 2009, Duan and Savage 2011). Duan and Savage (Duan and Savage 2011) studied the influence of several different heterogeneous catalysts on the efficiency of hydrothermal liquefaction of *Nannochloropsis sp.* at 350°C under inert (helium) and high-pressure hydrogen conditions. The microalga contained 52% of protein, 12% of carbohydrates, and 28% of lipids. The following catalysts were used in the study: Pd/C, Pt/C, Ru/C, sulfidied CoMo/ $\gamma$ -Al<sub>2</sub>O<sub>3</sub>, Ni/SiO<sub>2</sub>-Al<sub>2</sub>O<sub>3</sub>, and zeolite (aluminum silicate) catalyst.

The crude bio-oil yield ranged from a low of 35% from uncatalyzed liquefaction without H<sub>2</sub> to a high of 57% from Pd/C catalyzed liquefaction without H<sub>2</sub>. The carbon and hydrogen contents of the bio-oil always were higher than those of the biomass. The oxygen content was reduced to 8.3-9.6 wt% (from 26 wt% in the feedstock). As a result, the bio-oil obtained in this process had a much higher heating value than the dry biomass feedstock (38-40 MJ/kg). This is higher than the heating value of bio-oil obtained from pyrolysis of microalgal biomass and close to that of petroleum-derived fuels (~ 42 MJ/kg). The use of noble metal catalysts (Pd/C, Pt/C, Ru/C) increased the H/C ration

even in the absence of added H<sub>2</sub>. The presence of Pt, Ni, and CoMo catalysts allowed obtaining bio-oils with lower O/C ratios than of those produces in the absence of catalysts. These findings indicate that HDO takes place during hydrothermal liquefaction of microalgae and that there may be an opportunity for a single-step catalytic process to obtain a high quality bio-oil.

### 2.3.3. Bimetallic versus monometallic catalysts

The catalysts used for HDO of lipid-based feedstocks have different activities that depend on the active component, support used, and the feedstock properties (Senol, Ryymin et al. 2007). Bimetallic catalysts such as NiMo/Al<sub>2</sub>O<sub>3</sub> were found to be more active than monometallic ones such as Ni/Al<sub>2</sub>O<sub>3</sub> or Mo/Al<sub>2</sub>O<sub>3</sub> (Kubicka and Kaluza 2010). The selectivity of bimetallic catalysts to hydrocarbons was also much higher in comparison with monometallic catalysts. The increased activity of bimetallic catalysts was attributed to the effect of synergy when two or more compounds functioning together provide an effect not independently obtainable. It was also found that NiMo/ $\gamma$ -Al<sub>2</sub>O<sub>3</sub> catalyst is more active for decarboxylation than CoMo/ $\gamma$ -Al<sub>2</sub>O<sub>3</sub> at the reaction temperatures about 300 °C (Laurent and Delmon 1994). Pd/C has been shown to have the optimum performance for decarboxylation (Snåre, Kubičková et al. 2006). Also, Pt/Al<sub>2</sub>O<sub>3</sub> showed the highest activity for deoxygenation of bio-oils decreasing the oxygen content from 41.4 wt% to 5.8 wt% (Fisk, Morgan et al. 2009).

The studies by Yakovlev and co-workers showed that the bimetallic NiCu/CeO<sub>2</sub> catalyst had a better performance for upgrading biodiesel via HDO than the monometallic

Ni/CeO<sub>2</sub> (Yakovlev, Khromova et al. 2009). This research has made it possible to understand the reaction pathways occurring during the biodiesel deoxygenation. It was found that decarboxylation was the primary pathway over NiCu/CeO<sub>2</sub> while C-O bond hydrogenolysis (breaking C-O bonds with adding hydrogen) prevailed over Ni/CeO<sub>2</sub>. The effect of synergy for bimetallic catalytic systems (Re-modified Pt/HZSM-5) was also observed by Murata et al. for hydrotreating of jatropha oil (Murata, Liu et al. 2010).

The media supporting active metals/oxides of catalysts also play an important role in the reactions routes and overall catalyst performance. Alumina-supported catalysts were found to be more active for decarboxylation and de-esterification than catalysts supported on silica and carbon (Laurent and Delmon 1994). It was also found that acidity of the support contributes to decarboxylation and hydrogenation of carboxyl groups due to the formation of active acid sites on the catalyst (Centeno, Laurent et al. 1995). On the other hand, it was observed that alkaline components such as ammonia depress the activity of NiMo and CoMo catalysts for the conversion of carboxylic and methoxy groups but not ketones (Laurent and Delmon 1994). In the case of ketones, H<sub>2</sub>S depresses the activity of NiMo but not CoMo catalysts. H<sub>2</sub>S also increases the conversion of ester groups (Laurent and Delmon 1994, Şenol, Ryymin et al. 2007) and, for this purpose, is more active than CS<sub>2</sub> (Şenol, Viljava et al. 2007). The above finding suggests that NH<sub>3</sub> and H<sub>2</sub>S can be used to control hydrotreating processes.

Some research has also been carried out to understand the effect of others than alumina active component supports (Mäki-Arvela, Kubickova et al. 2006, Maher, Kirkwood et al. 2008, Yakovlev, Khromova et al. 2009, Immer, Kelly et al. 2010, Murata, Liu et al. 2010). The studies by Kubicka and co-workers on the deoxygenation of

rapeseed oil over Co and Mo sulfided catalysts supported on MCM-41 showed that the overall performance of the MCM-41-supported catalysts was inferior to the alumina-supported catalysts (Kubicka, Bejblova et al. 2010). Nava and co-workers investigated the effect of CoMo catalysts with other mesoporous silicate supports (SBA-15, SBA-16, HMS, DMS-1) on the hydroprocessing of olive oil by-products (Nava, Pawelec et al. 2009). It was found that the selectivity of these catalysts for alkanes decreased in the following order: CoMo/SBA-15 > CoMo/HMS > CoMo/SBA-16 >> CoMo/DMS-1.

Nanomaterials have attracted a great interest in catalyst application as they help catalysts to become active, efficient, reusable, stable, and pollutant-free. The nanocatalysts have improved mass transfer, product separation, and recovery properties. The higher catalytic activity of metal nanoparticles has been attributed to their higher surface area; therefore, more catalytic reactions can occur at the same time. No research has been reported on nanocatalytic HDO of lipid-based feedstocks up to date. The utilization of nanomaterials as catalysts in biofuel production is mainly in 1) feedstock pretreatment and hydrolysis, 2) storage of products (biogasoline, bioethanol, biogas, biobutanol, biodiesel, and hydrogen), and 3) catalytic conversion of animal fat, vegetable oils and microbial lipids into biodiesel. Applications of nanocatalysts and nanotechnologies can reduce the cost of transportation of raw feedstock and enhance the feedstock utilization as well as biofuel production rates. However, nanotechnology application in biofuel production is still at the infant stage. Therefore, further research on new materials, processes, and devices with nanotechnologies is needed to overcome the challenges.

Peterson and co-workers provided a comprehensive summary of catalysts for conversion of different types of biomass and model compounds at hydrothermal conditions (Peterson, Vogel et al. 2008). Here, we provide a summary of heterogeneous catalysts for HDO of lipid-based feedstocks and model compounds (Table 8). The products are mainly the mixture of deoxygenated and cracked hydrocarbons depending on the feedstock used.

**Table 8.** Summary of (heterogeneous) catalysts for HDO of lipid-based feedstocks and model compounds (N.R.: not reported).

Feedstock	Catalyst	T, °C	P, MPa	Reactor	Reference
Phenol, aliphatic oxygenates (methyl heptanoate, ethyl heptanoate, heptanol, heptanoic acid), anisole, mercaptoanisole, mercaptobenzene	Sulphided NiMo/ $\gamma$ -Al <sub>2</sub> O <sub>3</sub> , CoMo/ $\gamma$ -Al <sub>2</sub> O <sub>3</sub>	250	1.5, 7.5	Batch, fixed-bed flow	(Viljava, Komulainen et al. 2000, Viljava, Saari et al. 2001, Şenol, Viljava et al. 2005, Şenol, Viljava et al. 2005, Senol, Ryymin et al. 2007, Şenol, Ryymin et al. 2007, Şenol, Viljava et al. 2007)
10% cottonseed oil in desulphurized diesel	CoMo/Al <sub>2</sub> O <sub>3</sub>	305-345	3	N.R.	(Sebos, Matsoukas et al. 2009)

Oleic acid, linoleic acid, methyl oleate	Pd/C	300-360	1.5-2.7	Semi-batch	(Snåre, Kubičková et al. 2008)
Sunflower oil, heavy vacuum oil (HVO) mixtures	Sulfided NiMo/Al <sub>2</sub> O <sub>3</sub>	300-450	5	MAT	(Huber, O'Connor et al. 2007)
Rapeseed oil	Sulfided Ni, Mo, NiMo/Al <sub>2</sub> O <sub>3</sub>	260-280	3.5	Fixed-bed	(Kubicka and Kaluza 2010)
Biodiesel	Ni, NiCu/CeO <sub>2</sub> , ZrO <sub>2</sub>	240-400	1	Autoclave	(Yakovlev, Khromova et al. 2009)
Vegetable oils: Passiflora edulis (maracuja), Astrocaryum vulgare (tucuma), Mauritia flexuosa (buriti), Orbygnya martiana (babassu), soybean	Sulfided NiMo/ $\gamma$ -Al <sub>2</sub> O <sub>3</sub>	360-430	14	Batch	(Filho, Brodzki et al. 1993)
Rapeseed oil	Sulfided NiMo, CoMo/mesoporous Al <sub>2</sub> O <sub>3</sub> , MCM-41	260-360	7-15	Continuous flow	(Kubicka, Simacek et al. 2009, Simacek, Kubicka et al. 2009, Simacek, Kubicka et al. 2010)
Vegetable oil	Reduced Ni/SiO <sub>2</sub> , sulfided NiMo/ $\gamma$ -Al <sub>2</sub> O <sub>3</sub>	350-400	1-20	Batch	(Gusmao, Brodzki et al. 1989, Guzman, Torres et al. 2010)



Pyrolysis oils	Sulfided CoMo/ $\gamma$ - Al <sub>2</sub> O <sub>3</sub> , NiMo/ $\gamma$ -Al <sub>2</sub> O <sub>3</sub> , Co-Mo/C, Co- Mo/SiO <sub>2</sub>	200-300	N.R.	Batch	(Laurent and Delmon 1994, Laurent and Delmon 1994, Centeno, Laurent et al. 1995)
Vacuum gas oil (vegetable oil mixtures)	CoMo/Al <sub>2</sub> O <sub>3</sub> , NiMo/Al <sub>2</sub> O <sub>3</sub>	350	7-14	N.R.	(Bezergianni, Kalogianni et al. 2009)
Guaiacol, ethyldecanoate, 4- methylacetophenone	CoMo/C	200, 270	7	N.R.	(Ferrari, Bosmans et al. 2001, Ferrari, Maggi et al. 2001)
Soybean oil	Rh/ANOi	420	4	N.R.	(Laurent and Delmon 1994)
Stearic acid, ethyl stearate, tristearine	Pd/C	300	0.6	Semi- batch	(Centeno, Laurent et al. 1995, Ferrari, Maggi et al. 2001)
Oleic acid, linoleic acid, methyl oleate	Pd/C	300-360	1.5-2.7	Semi- batch	(Mäki-Arvela, Kubickova et al. 2006)
Jatropha oil	Pt/H-ZSM-5	270-300	N.R.	N.R.	(Murata, Liu et al. 2010)
Stearic acid, oleic acid	5%Pt/C, Pd/C, Pd/Al <sub>2</sub> O <sub>3</sub> , Pd/SiO <sub>2</sub>	300	1.5	Stirred autoclave	(Immer, Kelly et al. 2010)
Rapeseed oil	Sulfided CoMo/mesopo rous MCM-41	300-320	2-11	Continuou s flows	(Kubicka, Bejblova et al. 2010)

Olive oil by-products	Sulfided CoMo/DMS-1, SBA-15, SBA-16, HMS	250	3	Down-flow fixed-bed	(Nava, Pawelec et al. 2009)
Lauric acid, lauric aldehyde, lauric alcohol	5%Pd/C (Subinit)	300	2	Semi-batch	(Rozmyslowicz, Mäki-Arvela et al. 2011)
Stearic acid	5%Pd/C	300	1.5	Stirred autoclave	(Immer 2010 )
Canola oil	5%Pd/C (E117)	300	1.9	Continuous flow, hydrothermal, stirred fed-batch	(Wang, Thapaliya et al. 2012)
Bio-oil (methanol, acetaldehyde, acetic acid, glyoxal, acetol, glucose, guaiacol, furfural, vanillin)	1%Pt/ $\gamma$ -Al <sub>2</sub> O <sub>3</sub> , TiO <sub>2</sub> , ZrO <sub>2</sub> , SiO <sub>2</sub> -Al <sub>2</sub> O <sub>3</sub> , CeO <sub>2</sub> , Ce <sub>0.7</sub> Zr <sub>0.3</sub> O <sub>2</sub>	350	0.7	Stirred autoclave	(Fisk, Morgan et al. 2009)
Stearic acid	CeO <sub>2</sub> , Y <sub>2</sub> O <sub>3</sub> , ZrO <sub>2</sub>	400	25	Unstirred batch, hydrothermal medium	(Watanabe, Iida et al. 2006)
Microalga ( <i>Spirulina platensis</i> )	Na <sub>2</sub> CO <sub>3</sub> , Ca <sub>3</sub> (PO <sub>4</sub> ) <sub>2</sub> , NiO	200-380 (350)	2	Batch, hydrothermal medium	(Jena and Das 2009)

Microalga ( <i>Nannochloropsis</i> sp.)	Pd/C, Pt/C, Ru/C, Ni/SiO <sub>2</sub> - Al <sub>2</sub> O <sub>3</sub> , sulfided CoMo/ $\gamma$ - Al <sub>2</sub> O <sub>3</sub> , zeolite	350	0.07- 3.5	Batch, hydrother mal medium	(Duan and Savage 2011)
Microalga ( <i>Chlorella</i> <i>vulgaris</i> )	50%Ni/SiO <sub>2</sub> - Al <sub>2</sub> O <sub>3</sub>	350	18	Stirred autoclave, hydrother mal medium	(Minowa and Sawayama 1999)
Phenol, cyclohexanone, cyclohexanol, cyclohexene	Pd/C, Ru/C, Pt/C, Rh/C	150, 200, 250	5	Batch, hydrother mal medium	(Zhao, Kou et al. 2009, Zhao, He et al. 2011)
Phenol, guaiacol, eugenol	Ru/SBA-15	120	4	Batch, hydrother mal medium	(Guo, Ruan et al. 2012)

#### 2.3.4. Algal lipids

Microalgae are now considered to be one of the most prospective sources of biomass for biofuel production (John Sheehan 1998). Investigations carried out to determine the suitability of microalgal biomass for bio-oil production demonstrated that, in general, microalgae bio-oils are of higher quality than bio-oil from wood (Demirbas 2006). Biofuels derived from microalgae are currently considered to be the most economical and technically viable route able to compete with petroleum-derived fuels (Chisti 2010). This is due to a number of important advantages they have in comparison with biofuels derived from land-based energy crops:

1. Higher annual growth rates, e.g., rates of up to 37 tones ha<sup>-1</sup> per annum have been recorded, primarily due to higher photosynthetic efficiencies (up to 10% of the solar energy) when compared with terrestrial plants (Weissman and Tillett 1992).
2. Higher lipid productivity (up to 75% dry weight for some algae species), with higher proportion of TAGs that is essential for efficient biodiesel production (Schenk, Thomas-Hall et al. 2008).
3. Microalgae production can effect biofixation of CO<sub>2</sub> (production utilizes about 1.83 kg of CO<sub>2</sub> per kg of dry algal biomass yield), thus making a contribution to air quality improvement (Chisti 2008).
4. Capability of growing in wastewater, which offers the potential for integrating the treatment of organic effluent with biofuel production (Cantrell, Ducey et al. 2008).
5. Inherent yield of valuable co-products such as proteins and polyunsaturated fatty acids may be used to enhance the economics of production systems (Spolaore, Joannis-Cassan et al. 2006).
6. Microalgae do not require arable land and, therefore, do not compete with food crops (Widjaja, Chien et al. 2009).

Since microalgae has been cultivated in the mariculture and used as the food supplement, their biochemical composition has been thoroughly investigated (Dunstan, Volkman et al. 1993, Brown, Jeffrey et al. 1997, De Angelis, Risé et al. 2005, Herrero, Cifuentes et al. 2006, Sajilata, Singhal et al. 2008). Despite the wide variety of classes and species, microalgae and cyanobacteria generally consist of 4-64 wt% of carbohydrates, 6-71 wt% protein, and 2-40 wt% lipids (up to 75 wt% for some algae

species) on the dry biomass basis (Brown, Jeffrey et al. 1997, Ramadan, Asker et al. 2008). The high lipid content facilitates its potential use as a biodiesel feedstock because the lipids can be readily extracted and converted into biodiesel.

Algal lipids can be classified based on the polarity of their head groups (Becker 1994): (1) neutral lipids that include triacylglycerols, diacylglycerols, monoacylglycerols, hydrocarbons, sterols, ketones, FFAs and (2) polar lipids that comprise of phospholipids and glycolipids (Fig. 7). Fatty acids are the main constituent of lipid molecules, both neutral and polar. They are carboxylic molecules with unbranched aliphatic tails range from 12 to 22 carbons in length that can be saturated with no double bonds and unsaturated with up to 6 double bonds in the chain (Medina, Grima et al. 1998).

TAGs are the main constituent of lipids and comprise of three fatty acids ester-boned to glycerol backbones. The composition and the fatty acid profile of microalgal lipids vary with the species, its life cycle, and its cultivation conditions. As shown in Fig. 8, microalgal cells harvested during stationary phase have higher acylglycerol contents and lower polar lipid contents than those harvested during logarithmic phase (Dunstan, Volkman et al. 1993). It should be taken into consideration that acylglycerols are the only lipid fractions that can be used for transesterification at the current industrial-scale refineries. Also, microalgal fractions that contain high levels of polar lipids and non-acylglycerol neutral impurities have to be purified before converting into usable biodiesel (Halim, Harun et al. 2013).

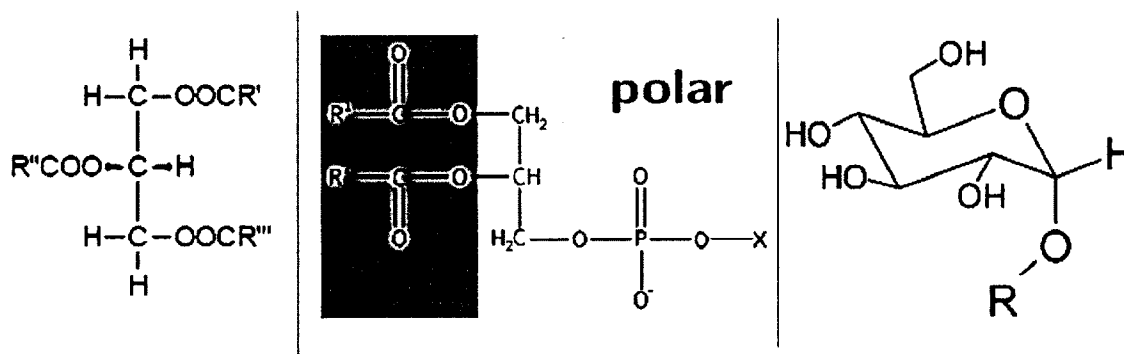


**Figure 7.** Different lipid molecules: triacylglycerols on the left, phospholipids in the middle, and glycolipids on the right. R in each molecule represents a fatty acid chain. Reproduced from (Halim, Harun et al. 2013)

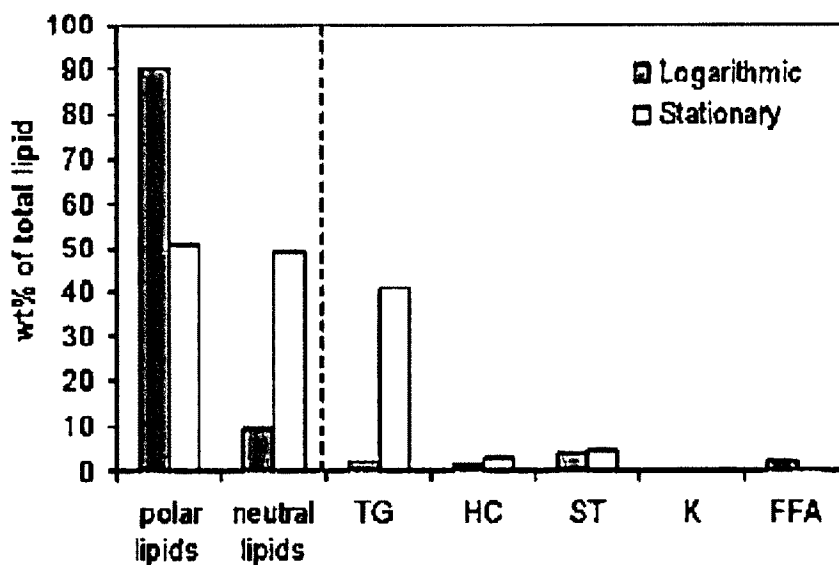


**Figure 8.** Compositions of lipids extracted from *Nannochloropsis oculata* during logarithmic and stationary phases (TG: triacylglycerols, HC: hydrocarbons, ST: sterols, K: ketones, FFA: free fatty acids. Reproduced from (Dunstan, Volkman et al. 1993).

A fatty acid profile of the lipids extracted from a common green microalgal species (*Tetraselmis suecica*) during the stationary phase was examined for biodiesel production (Volkman, Jeffrey et al. 1989). The principal fatty acids identified in this study had C16:0, C18:1, and C18:2 profiles, which are very favorable for production of high-quality biodiesel. A large amount of saturated fatty acids can cause flow cold problems in the resulting fuel. Therefore, the relatively low amount of saturated fatty acids (25.5 wt%) in the algal biomass is desirable for production of biodiesel with good flow cold properties (Lang, Dalai et al. 2001, Chisti 2007). The relatively low portion of polyunsaturated fatty acids with 4 or more double bonds (C16:4 being the highest at 7.9 wt%) in the lipid is also desirable because these acids are known to produce biodiesel with low oxidation stability (Lang, Dalai et al. 2001). The results of this study is provided in Fig. 9.

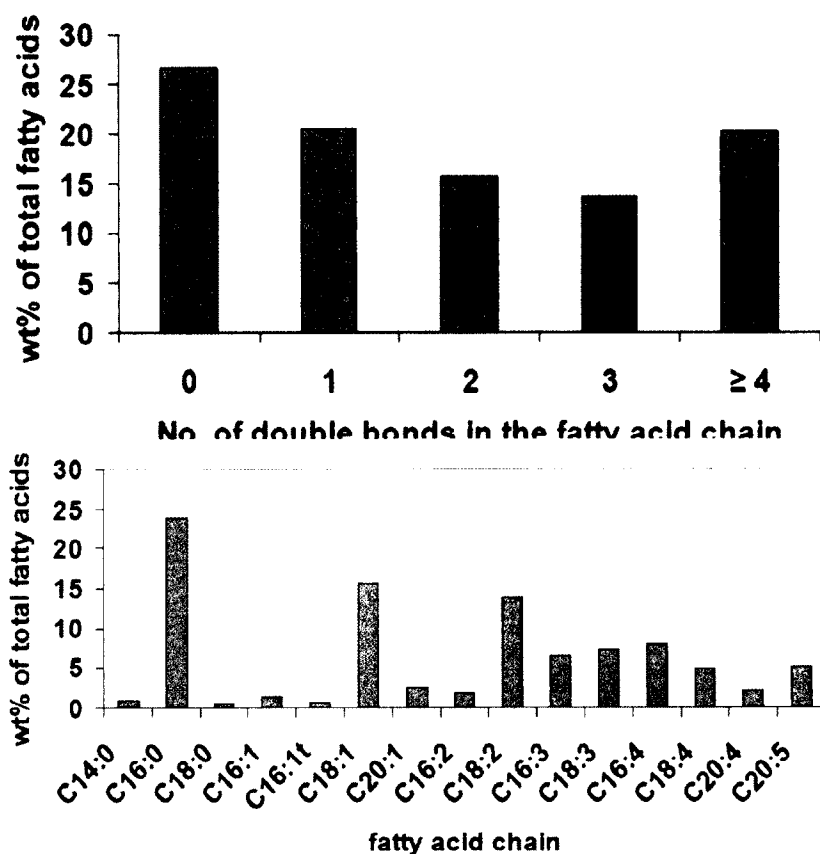


**Figure 9.** Fatty acid composition of lipid extracted from species *Tetraselmis suecica* at the end of logarithmic phase (beginning of stationary phase): (top) in terms of fatty acid chain. (bottom) in terms of number of double bonds in the fatty acid chain. Reproduced from (Volkman, Jeffrey et al. 1989).

The suitability of microalgal biomass for biodiesel production has to be examined on a case-by-case basis. In order to achieve the highest possible production rate, oil content has to be balanced against growth kinetics. Furthermore, there are many advantages in having a robust species of alga since the system will be less sensitive to variations in parameters like temperature, pH, and salinity. As it was said above, oil composition and size are also important in order to achieve a simple separation and post



processing. Last but not least, it is important that an alga strain is well known and sufficient research and information about it is available.

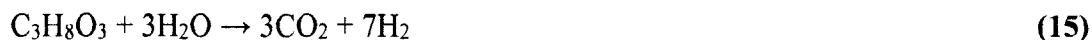
Unlike biodiesel production, where fuel properties depend on feedstock composition and process configuration, renewable diesel production is less dependent on feedstock origin and allows utilizing any feedstock containing TAGs and fatty acids to produce the fully deoxygenated fuel readily blended with conventional diesel. Algal lipids can be processed by hydrothermal HDO into renewable fuels by converting the carboxylic acid moiety to a mixture of hydrocarbons, water, and carbon dioxide and converting glycerol to propane.

However, since algal crude algal oils may contain high levels of phosphorus from phospholipids, nitrogen from extracted proteins, and metals (especially magnesium) from chlorophyll, it is necessary to optimize both the level of lipids purification and the tolerance of the catalysts for the contaminants in order to develop the most cost-effective process. The primary barrier to utilizing algae oils to make renewable fuels is catalyst development, and, to our knowledge, no research was carried out in this area up to date. Most researchers use catalysts that have been optimized for petroleum-based feedstocks, and therefore, it would be desirable to develop catalysts that are able to minimize CO<sub>2</sub> and CO lost, the amount of H<sub>2</sub> used, withstand the hydrothermal media conditions as well as the specific for algal lipids contaminants/poisons.

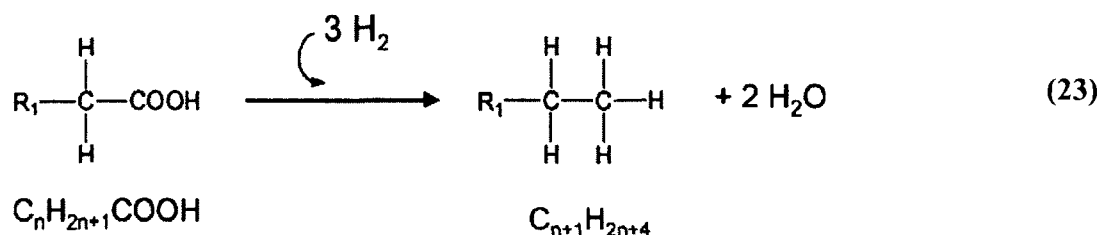
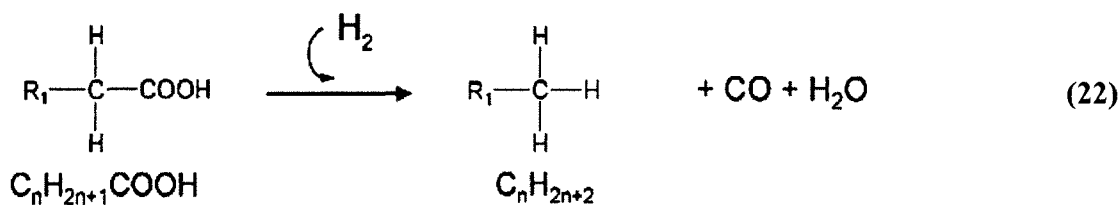
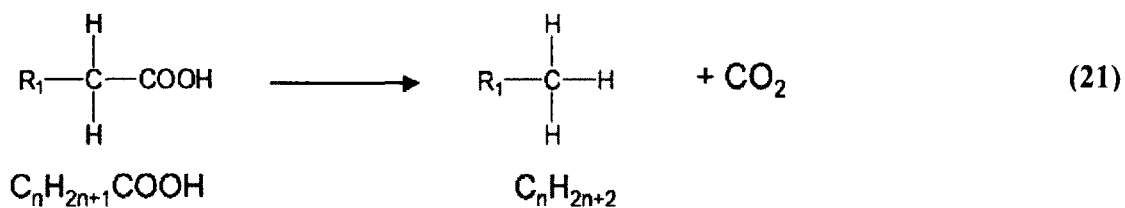
### **2.3.5. Influence of hydrogen on HDO**

Hydrogen has been extensively utilized in the deoxygenation processes. However, it is desirable to minimize the amount of hydrogen required for renewable diesel

production, especially if it is derived from petroleum-based feedstocks. Hydrogen can be produced from biomass via gasification combined with the water-gas shift reaction, via aqueous phase reforming of oxygenates such as polyols (e.g. low quality glycerol that is a by-product of the transesterification reaction) (Cortright, Davda et al. 2002, Davda and Dumesic 2003, Davda and Dumesic 2004), or via anaerobic digestion of biomass residue followed by steam methane reforming or autothermal reforming:



Many biomass conversion reactions do not consume hydrogen. These reactions (e.g. ketonization (coupling) of carboxylic acids, conversion of alcohols into alkenes, oligomerization of alkenes) proceed via dehydration and decarboxylation routes without hydrogen input. However, production of *n*-alkanes from TAGs requires relatively large amounts of hydrogen (10-15 moles H<sub>2</sub>) for each equivalent of TAG (Huber, O'Connor et al. 2007). This process achieves HDO by decarboxylation (21), decarbonylation (22), and hydrodeoxygenation (23) routes:



The UOP/Eni Ecofining technology described by Kalnes et al. (Kalnes, Marker et al. 2007) is based on HDO of vegetable oils and developed for existing refinery infrastructure. The feedstock is typical plant oil that consists primarily of TAGs with 10-12 wt% oxygen and 1-2 wt% FFA content. Other low cost feedstocks such as tail oil, tallow oil, fish oil, and waste greases can also be used for the above process.

A simplified block flow diagram of the process is shown in Fig. 10. Feedstock is directed to the catalytic reactor where it is combined with hydrogen, brought to the reaction temperature, and then converted by a series of HDO and hydroisomerization reactions to branched paraffin rich diesel fuel. Water and CO<sub>2</sub> formed by HDO reactions are separated from the deoxygenated product. The mixture of the hydrocarbons is then fractionated to remove the small amount of light fuel by-products. Hydrogen is recovered

and recycled back to the reactor to maintain the required partial pressure. Make-up hydrogen is added to compensate losses.

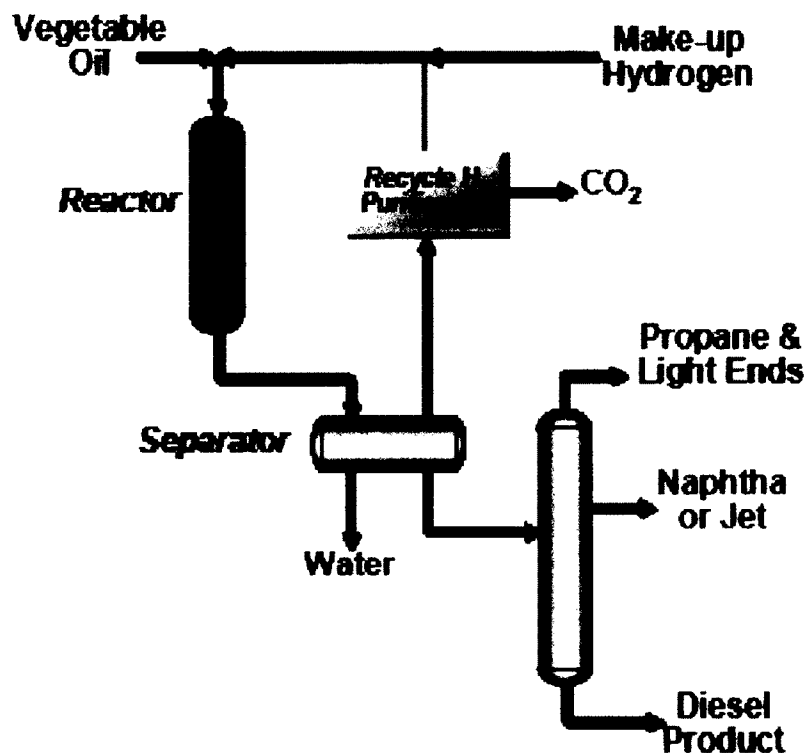


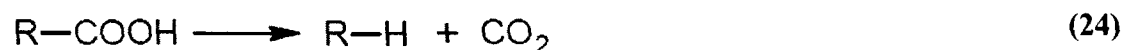
**Figure 10.** Simplified Ecofining process flow diagram. Reproduced from (Kalnes, Marker et al. 2007).

The process hydrogen requirements and product yields are provided in Table 9. The primary product is paraffinic diesel and co-products include propane and naphtha. Product carbon number distribution and selectivity of HDO to H<sub>2</sub>O and CO<sub>x</sub> is controlled by reaction conditions and choice of catalyst. Diesel yield depends both on feedstock type and operating conditions and varies from 88 vol% to 99 vol% depending on the level of hydroisomerization required to achieve the product cloud point specification.

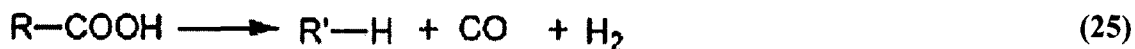
**Table 9.** Process yields and hydrogen requirements for a range of different feedstocks and diesel cloud point targets. Adapted from (Kalnes, Marker et al. 2007).

<b>Feeds</b>	<b>wt%</b>
Vegetable oil	100
Hydrogen	1.5-3.8
<b>Products</b>	<b>vol%</b>
Propane	8-9
Naphtha/Kerosene	1-10
Renewable diesel	88-99

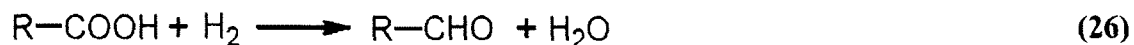
In the recent studies, the influence of hydrogen on the catalytic deoxygenation of fatty acids over a mesoporous Pd/C catalyst has been investigated (Maher, Kirkwood et al. 2008). It was determined that depending on the hydrogen content in the reaction medium, different routes of HDO can dominate. Under inert atmosphere, hydrocarbon formation occurs via decarboxylation of fatty acids (Snåre, Kubičková et al. 2008, Bernas, Eränen et al. 2010):



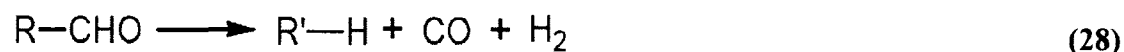
Also, under inert condition, minor generation of hydrogen can take place, which leads to decarbonylation of fatty acids with generation of CO:



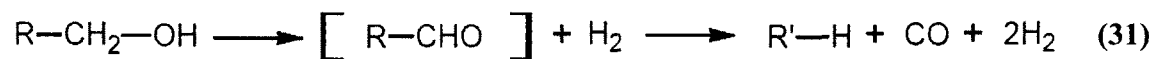
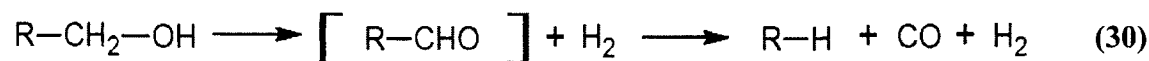
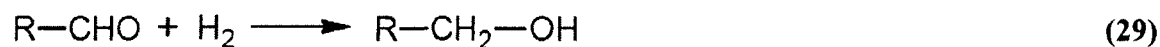
Deoxygenation of fatty acids under hydrogen rich conditions has a more complex reaction pathway. First, hydrogenation of carboxylic groups occurs, forming aldehydes as an intermediate product:



Then the aldehydes decompose via decarbonylation reaction producing hydrocarbons and CO:



Some of the aldehydes can further be hydrogenated to alcohols (29), which decompose via dehydrogenation to aldehydes. After that, the aldehydes are subject to decarbonylation over Pd/C catalyst (Cortright, Davda et al. 2002) and form hydrocarbons (30, 31):



The overall reaction network is provided in Fig. 11. In this study, a higher yield of hydrocarbons (59 mol%) was obtained in the HDO of the fatty acids under hydrogen pressure compared to the process under argon pressure where the yield of hydrocarbons reached 39 mol%.

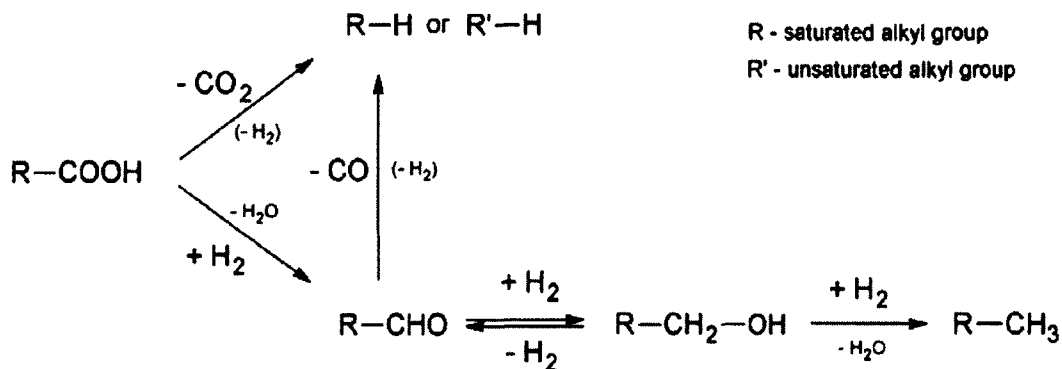


**Figure 11.** Fatty acids deoxygenation pathways over Pd/C catalyst. Reproduced from (Davis and Barteau 1990).

In the studies by Immer et al., Pd/C catalyst along with hydrogen and helium as carrier gases was used for HDO of lipid-based feedstock (Immer, Kelly et al. 2010). Hydrogen prevents Pd from deactivating, helps organic species desorb from the surface of the metal, and saturates the double bonds of the unsaturated FFA (Wang, Thapaliya et al. 2012). Compared with the reaction in the inert atmosphere, the conversion of unsaturated FFAs improved in the presence of hydrogen (Snåre, Kubičková et al. 2008). Nevertheless, the increase of H<sub>2</sub> partial pressure reduces the rates of decarboxylation and results in lower CO<sub>2</sub> selectivity (Immer 2010). An increased H<sub>2</sub> partial pressure pushed the reaction pathway toward decarbonylation and increased the concentration of CO in the gaseous product, respectively (Immer, Kelly et al. 2010).

#### 2.4. Deoxygenation in hydrothermal media

Most of biomass feedstocks contain large amounts of water. In order to make the feedstock applicable for biofuel production, the water has to be removed. This can be typically done by thermal separation. The separation processes consume a great deal of biomass energy content, thus making the biofuel production less advantageous. However, the separation steps can be avoided by performing the thermochemical reactions in hydrothermal media near or above the critical point of water (374 °C, 22.1 MPa). In this case, the water phase change is avoided, which provides possible energy advantages in the thermochemical processing of the biomass. The hydrothermal processing of lipid-rich feedstocks allows producing a wide range of liquid and gaseous fuels that can be further upgraded in existing commercial infrastructures (Peterson, Vogel et al. 2008).

Density and dielectric constant of the water medium play a major role in solubilizing different compounds. Ambient water at 25 °C and 0.1 MPa is a good solvent for electrolytes because of the high dielectric constant (78.5), but most organic matters are poorly soluble in water at this condition. When water is heated, H-bonds start weakening and this allows dissociation of water into acidic hydronium ions ( $\text{H}_3\text{O}^+$ ) and basic hydroxide ions ( $\text{OH}^-$ ). Near the critical point, structure of water changes significantly because of the breakage of hydrogen bonds network. At this condition, water exists as separate clusters with a chain structure (Kalinichev and Churakov 1999), its dielectric constant decreases, which causes a change in the dynamic viscosity and also increases self-diffusion coefficient (Marcus 1999).

By operating at sub- or supercritical conditions, interphase mass transfer resistances can be significantly reduced or eliminated. Supercritical water has liquid-like



density and gas-like transport properties and is highly non-polar media that permits complete solubility of oxygen and most organic compounds including FFAs (Fig. 12). However, the polar species, such as inorganic salts, are no longer soluble at this condition and start precipitating. The physiochemical properties of water in the supercritical region, such as viscosity, density, and heat capacity, also change dramatically with only a small change in the temperature or pressure, which results in substantial increase in the rates of chemical reactions. In addition to the unusual dielectric behavior, transport properties of supercritical water are also significantly different from those of ambient water.

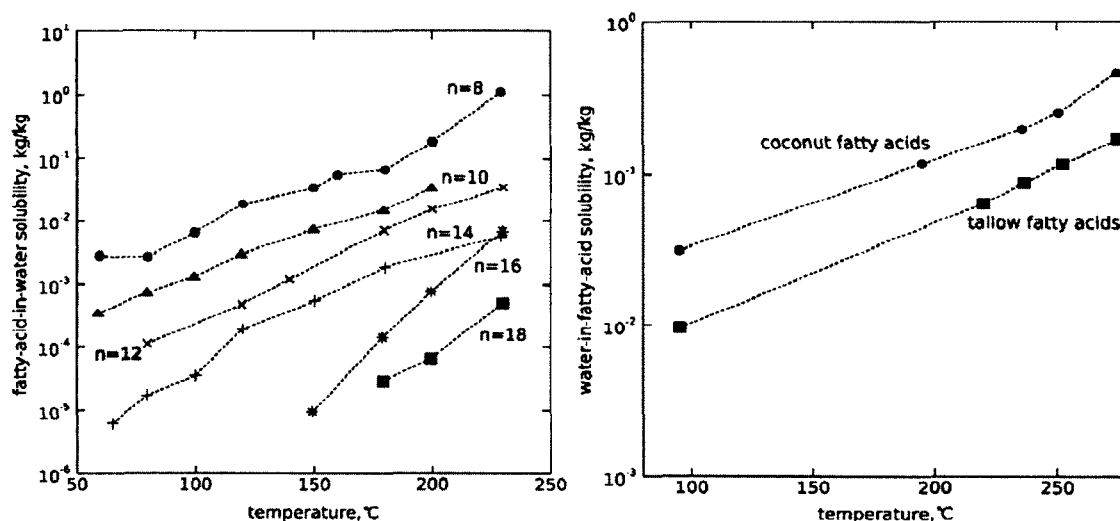


**Figure 12.** (a) The solubility of saturated fatty acids in water at 15 MPa. n is the carbon number of each fatty acid. Adapted from (Khuwijtjaru, Adachi et al. 2002). (b) The solubility of water in fatty acids at the vapor pressure of the system. Reproduced from (Mills and McClain 1949).

The use of sub- and supercritical water media has advantages over other biofuel production methods (Peterson, Vogel et al. 2008) and is an attractive thermochemical process for biomass conversion for the following reasons:

1. The water contents of the biomass feedstock. Since the process is conducted in water phase, it is not necessary to separate water from biomass, which increases the overall efficiency of the conversion process.
2. Versatility of chemistry. The hydrothermal technology can be applied to produce a variety of solid, liquid, and gaseous fuels from different types of biomass. The product pathways depend on the density of hydrothermal media, which is a key parameter in deciding the product pathways.
3. Increased reaction rates and easier separations. The mass transfer resistances between phases are reduced or eliminated in the hydrothermal media, which results in significant increase in the rates of chemical reactions. The final products can be easily separated at lower temperatures.

No research has been conducted on catalytic HDO of lipid-based feedstocks in hydrothermal media yet. This can be attributed to the lack of knowledge about the reactions pathways, kinetics, and interactions between the biomass components as well as the absence of efficient catalysts that are resistant to hydrothermal media. However, the chemistry behind reactions of TAGs in hydrothermal media is investigated well enough (Peterson, Vogel et al. 2008). It is now commonly accepted that rates of chemical reactions can be substantially increased due to reduction of interphase mass transfer resistances and the ability of supercritical water to maintain both ionic and free-radical reactions (Antal, Brittain et al. 1987).

The kinetics of the catalytic HDO of phenolic bio-oils in hydrothermal media has also been investigated (Zhao, Kou et al. 2009, Zhao, He et al. 2011). The dual-functional catalytic system (Pd/C and H<sub>3</sub>PO<sub>4</sub>) has been proven to efficiently convert phenol-based bio-oils to the mixture of cyclic alcohols or alkanes depending on the chosen reaction conditions.

In producing renewable fuels from lipid-based feedstocks in hydrothermal media, the main objective is to remove oxygen, which can be readily performed by dehydration and decarboxylation. Despite the presence of a large amount of water, dehydration is a typical thermochemical reaction that occurs in hydrothermal media at elevated temperatures and pressures in the presence of an Arrhenius acid such as H<sub>2</sub>SO<sub>4</sub>. Decarboxylation is another major route of oxygen removal, which is more attractive because it also increases H/C ratio. The latter allows producing biofuels with increased higher heating values.

TAGs can be readily split to form FFAs and glycerol via Colgate-Emery process (Barneby and Brown 1948). The process has been conducted at the conditions similar to that of hydrothermal processing (250 °C and 5 MPa) without a catalyst and with oil-to-water ratio of 2:1. These conditions make the process more steam-based hydrolysis than subcritical one. King and co-workers found that fast hydrolysis of TAGs can be conducted at the temperatures of 330 to 340 °C and oil-to-water ratios of 1:2.5 to 5.0. At these conditions, the yield of FFAs can be 90 to 100% (King, Holliday et al. 1999). It was observed that the phase behavior of components is crucial for the process and determined that the reaction quickly went to completion with almost 100% yield of FFAs when the mixture became a single phase at 339 °C.

FFAs have been shown to degrade in hydrothermal media producing long-chain hydrocarbons. Watanabe and co-workers investigated the decomposition of stearic acid ( $C_{17}H_{35}COOH$ ) in a fixed bed batch reactor to the maximum temperature of 400 °C (Guo, Ruan et al. 2012). Two major products,  $C_{17}H_{36}$  and  $C_{16}H_{32}$ , were found in the reaction products. The authors compared this process to the stearic acid pyrolysis and found that stearic acid decomposition under hydrothermal conditions was suppressed and resulted in prevailing alkenes over alkanes. The formation of shorter-chain hydrocarbons was also suppressed under the hydrothermal conditions. However, when NaOH or KOH was added, decomposition of stearic acid enhanced significantly producing more alkanes than alkenes.

The studies of decarboxylation of formic (Maiella and Brill 1998, Yu and Savage 1998) and acetic acids in hydrothermal media (Bell, Palmer et al. 1994, Meyer, Marrone et al. 1995) have shown that the reaction is greatly influenced by catalytic effects of the reactor wall (stainless steel) surfaces. The studies of acetic acid and sodium acetate decomposition in hydrothermal media at 335 °C and 13.7 MPa by Bell and co-workers (Bell, Palmer et al. 1994) showed that numerous mineral surfaces enhanced the reaction rates by two orders of magnitude. These findings suggest that investigation of heterogeneous catalysts effects on HDO of lipid-based feedstocks is needed.

## **2.5. Future perspective and potential research areas**

The HDO studies on lipid-based feedstocks reviewed in this paper revealed a considerable amount of information on different aspects of the process. However, as a matter of fact, HDO technologies have not been widely commercialized up to date. This

is partly because of high pressures of the HDO process and corrosive environment of the hydrothermal media that require special designs of the reactor and other equipment employed.

There are also a few problems that require more research to be done before the process can be scaled up. One of the problems is high consumption of hydrogen that has to be minimized in order to make the process more economically viable. The amount of hydrogen used for the conversion of lipids through the dehydration route is significantly higher than that through decarbonylation/decarboxylation routes. However, the decarboxylation route can theoretically consume more hydrogen than the dehydration route due to the secondary reactions such as water-gas shift and methanation (Donnis, Egeberg et al. 2009). The amount of hydrogen consumed in those processes is known to be sensitive to the process conditions and catalysts used. Therefore, more research needed to understand the optimal pathways resulting in minimization of unnecessary hydrogen consumption.

The conventional HDO of lipid-based feedstocks, irrespective of the reaction mechanisms involved, mainly leads to formation of straight-chain alkanes. They are highly attractive compound of renewable diesel as they provide high cetane numbers. However, they can also cause cold flow problems of the diesel. Therefore, more research on catalytic isomerization and/or dewaxing of the linear saturated hydrocarbons is required in order to optimize the renewable diesel properties (Crossley, Faria et al. 2010). In this area, two broad sections have to be further investigated: (1) process optimization and (2) improved isomerization catalysts.

The most important research area of the HDO process is developing an optimal catalytic system able to provide adequate activity and stability at the HDO conditions. Despite the problem of catalyst stability is well known, few studies have been carried out in the area. Conventional hydrotreating catalysts used in the most of HDO studies have shorter catalyst lives due to the poor quality of lipid-based feedstocks in comparison with petroleum-based feedstocks. Therefore, it is critical to develop catalysts specifically for the HDO of lipid-based feedstocks.

From a commercial applications point of view, an ideal HDO catalyst should possess the following qualities:

1. High activity for deoxygenation.
2. Ability to minimize coke formation and/or withstand large amounts of coke.
3. High tolerance to poisons (phosphorus, nitrogen, and metals (magnesium)). It is critical from the point of view of increasing the overall life of the catalyst load to optimize both the level of purification of lipid-based feedstocks and the tolerance of the catalysts for the contaminants.
4. High tolerance to water. As it was determined in the previous studies, presence of water in the HDO media may have a deactivation effect on the performance of catalysts used in the process (Laurent and Delmon 1994, Şenol, Viljava et al. 2005). The specific of the HDO process, especially in hydrothermal media, is that the catalysts are exposed to large amounts of water. Therefore, high tolerance to water is essential for HDO catalysts. The research by Crossley and co-workers showed that nanocatalysts are able to adsorb on the surface of emulsified oil particles, thus stabilizing water-oil emulsions and catalyze reactions at the water-oil interphase (Crossley, Faria et al. 2010).

5. Ability to be readily recovered via simple processes (e.g., hot air burn) and reused.

## **2.6. Executive summary**

### **Hydrodeoxygenation**

- The paper is first of its kind that reviews the state-of-the-art studies related to the catalytic HDO of lipid-based feedstocks for the last decade.
- HDO of lipid-based feedstocks is a very important research area and an attractive process to upgrade oil-based feedstocks to liquid transportation fuels.
- The paper reviews the different chemical reactions and reaction mechanisms involved in the process.
- The process parameters and the optimized process conditions have been discussed.
- The economic and environmental importance of HDO process will continue being the motive power of overcoming the technological challenges and the future research in the area of renewable fuels.

### **Heterogeneous catalysts**

- A number of various heterogeneous catalytic used in HDO process has been reviewed.
- Bimetallic catalysts are found to be more active than monometallic catalysts.

- The enhanced performance of bimetallic catalytic systems was attributed to the effect of synergy when two or more compounds functioning together provide an effect not independently obtainable.
- Nanomaterials have also attracted a great interest in catalyst application as they help catalysts to become active, efficient, reusable, stable, and pollutant-free.

### **Algal lipids**

- The application of aqueous HDO has been discussed for the first time which can be more suitable for the HDO of algal based lipids.
- Advantages of using aqueous HDO for the wet feedstocks such as microalgae have been reviewed.

### **2.7. Acknowledgments**

The authors would like acknowledge the encouragements and supports of colleagues at Department of Civil and Environmental Engineering at Old Dominion University in the preparation of this article. Our special appreciation is to the Dean of Batten College of Engineering and Technology (BCET) and the Research Foundation at Old Dominion University (ODURF) for providing the financial support.



## CHAPTER 3

### HYDROTHERMAL CATALYTIC LIQUEFACTION OF UNHYDROLYZED SOLIDS

*Note: the contents of this chapter have been published in Biofuels. Popov, S., Ruhl, I., Uppugundla, N., da Costa Sousa, L., Balan, V., Hatcher P.G., Kumar, S. Bio-oil via catalytic liquefaction of unhydrolyzed solids in aqueous medium. Biofuels, 5 (4), 431-446, (2014). DOI:10.1080/17597269.2014.987099.*

Bioethanol can be produced from lignocellulosic feedstock using a biochemical route involving enzymatic hydrolysis followed by microbial fermentation. During these processes, about 30 to 40% of the biomass is left behind as wet unhydrolyzed solids (UHS), depending on the type of biomass, enzyme loading, and duration of enzymatic hydrolysis. The UHS is mostly composed of lignin, bound enzymes, undigested recalcitrant carbohydrates and ash. The efficient conversion of UHS into bio-oil will increase overall conversion efficiency of biomass to liquid fuels (bioethanol and bio-oil) and has potential to reduce the cost of biofuel production from lignocellulosic biomass. In this paper we report the results of bio-oils production from UHS via hydrothermal liquefaction (HTL) under varying temperatures (280-350°C) and subcritical water conditions. The effects of  $K_2CO_3$  and supported bimetallic  $CoMo/Al_2O_3$  catalysts during HTL process were investigated. The UHS used in this study was produced after enzymatic hydrolysis of pretreated by Ammonia Fiber Expansion (AFEX<sup>TM</sup>) method corn stover (ACS). Bio-oil yields at different HTL temperatures were quantified and characterized using  $^1H$ -NMR,  $^{13}C$ -NMR, GC-MS, and elemental analysis. The yield of

bio-oil was higher in the presence of 5 wt% of  $K_2CO_3$  during HTL in comparison to  $CoMo/Al_2O_3$  catalyst. The highest degree of liquefaction and bio-oil yield were respectively 43.4% and 30.1 wt% at 350 °C in the presence of  $K_2CO_3$  while the highest ECR was 57.1% at 320 °C in the presence of  $K_2CO_3$ . The study is one of the first of its kind where unhydrolyzed solids left behind after bioethanol production were used for making bio-oils with traditional and reduced bimetallic  $CoMo/Al_2O_3$  catalysts in aqueous medium. The results of the study can contribute to development of lignocellulosic biomass-based biorefinery concept.

### **3.1. Introduction**

The U.S. Energy Independence and Security Act of 2007 (EISA) mandates 36 billion gallons per year (BGY) of biofuels production by 2022, of which 16 BGY of advanced biofuels are to be produced from lignocellulosic biomass. In order to meet these requirements, a number of biochemical and thermochemical methods are being developed and evaluated to efficiently produce biofuels from lignocellulosic biomass. The bioethanol production from lignocellulosic biomass has been successfully demonstrated at pilot/demo scale but a cost-effective commercial production is still significantly below the EISA envisioned target of 2 BGY lignocellulosic biofuels by year 2014 (Balan, Chiaramonti et al. 2013). At present, the majority of biofuel production technologies in the U.S. are aimed at producing cellulosic ethanol using biochemical routes (Balan, Chiaramonti et al. 2013, Kumar 2013) that use enzymes to decompose complex carbohydrates into sugars, which can then be fermented into ethanol molecules by yeasts and other microorganisms. Due to recalcitrance of lignocellulosic biomass, a

pretreatment step is required prior to enzymatic hydrolysis in order to improve enzyme accessibility to the carbohydrate substrates. Ammonia fiber expansion (AFEX) pretreatment is one of the leading alkaline pretreatment processes that employ liquid or gaseous ammonia as a pretreatment agent to produce highly digestible biomass, which can be used as an animal feed or a biofuel feedstock (Balan, Bals et al. 2009). In an AFEX-based biochemical refinery, about 30-40% of the biomass remains unconverted into ethanol, resulting in a residue called unhydrolyzed solids (UHS) (Jin, Gunawan et al. 2012). A typical commercial biorefinery would use about 2000 metric tons (MT) of biomass per day (Tao, Aden et al. 2011), generating 600-800 MT of UHS per day. It is widely accepted that the energy requirements for the biorefinery can be satisfied by combusting the UHS to generate heat and power (Kumar and Murthy 2011). However, a large amount of energy is required for drying wet biomass (moisture content >150% on a dry weight basis) before it can be used for combustion and producing heat and electricity. Heat and electricity can be obtained from less costly renewable energy sources (e.g. wind, solar, geothermal, etc.) while the fixed carbon present in UHS could be better applied to produce value-added products in a future biorefinery. UHS composition from AFEX pretreated corn stover included lignin, bound enzymes, undigested recalcitrant carbohydrates, and ash. To improve the overall carbon and energy utilization in a biochemical biorefinery, it is important to evaluate the technologies that are capable of efficiently converting wet UHS into value-added products such as fuels and chemicals.

The conversion of biomass under subcritical water medium is considered an efficient and environmentally benign method for advanced biofuel production that can utilize wet biomass (Savage 2009). Hydrothermal liquefaction (HTL) is one of the viable

processing strategies to convert wet biomass into bio-oil or liquid hydrocarbons (Delrue, Li-Beisson et al. 2013). HTL technology capitalizes on the extraordinary properties of water as a solvent and reaction medium to convert biomass components with high oxygen content into petroleum-like products (bio-oil) that contain significantly lower amount of oxygen heteroatoms. HTL is especially suitable for converting wet biomass into high energy density bio-oil and biochar without drying of the feedstock at relatively low temperatures when compared to other thermal processes such as pyrolysis (Jena and Das 2011, Vardon, Sharma et al. 2012). HTL technology was first suggested by Berl in 1944 as a method to readily convert biomass into bio-oil in aqueous medium (Berl 1944). In his studies, Berl treated alkaline solutions of biomass under hydrothermal conditions at about 230°C to produce bio-oils containing up to 60% of the feedstock's carbon content and 75% of its heating value. HTL studies continued during the second half of the 20<sup>th</sup> century focusing mainly on improving the carbon conversion efficiency and reducing the oxygen content of bio-oils, which typically accounts for 10-20 wt% of the bio-oil (Kruse, Funke et al. 2013). Several thermochemical biomass conversion technologies and mechanisms have been reported over the recent years (Peterson, Vogel et al. 2008) and a number of different approaches for HTL of biomass have been reported up to date (Kruse, Funke et al. 2013). HTL conditions cover a range of temperatures 280-380 °C, pressures 7-30 MPa, and reaction times 10-60 min. (Peterson, Vogel et al. 2008). Most of the HTL processes involve various catalysts, reducing gases, and other additives (Hicks 2011) attempting to improve deoxygenation reaction and reduce the oxygen content of the bio-oil. HTL of a typical lignocellulosic biomass (forest products and residues, agricultural residues, and dedicated energy crops) with an oxygen content of 30-50% and higher heating values (HHV) of 10-20 MJ/kg is capable of producing bio-oils containing

10-20 wt% oxygen with HHV of 30-36 MJ/kg (Peterson, Vogel et al. 2008). Although significant deoxygenation occurs during the liquefaction process, HTL alone is not able to produce typical hydrocarbon fuels because of the presence of residual oxygen heteroatoms. Therefore, further deoxygenation of bio-oils is required for this purpose (Li, Garedew et al. 2012).

Most of the studies related to catalytic HTL of lignocellulosic biomass employed alkali catalysts to increase bio-oil yields and suppress biochar formation (Minowa, Zhen et al. 1998, Karagoz, Bhaskar et al. 2004). In some studies, heterogeneous catalysts (noble metals, mono-, and bimetallic oxides on different supports) were used for direct liquefaction of algal biomass in hydrothermal media (Duan and Savage 2011). However, these catalysts seem to be more efficient for deoxygenation of resulting bio-oils (Furimsky 2000). Presence of transition metal oxides increases yields of gaseous products and reduces oxygen and nitrogen contents of bio-oil. However, these catalysts provide lower bio-oil yields and recover less energy in the form of bio-oil compared to the homogeneous ones (Jena, Das et al. 2012).

CoMo/Al<sub>2</sub>O<sub>3</sub> and NiMo/Al<sub>2</sub>O<sub>3</sub> catalysts are commonly used for removal of N and S heteroatoms from crude oil and therefore can also be efficient for removal of N, S, and O from bio-oils. Those catalysts have received an increased attention for upgrading bio-oils (Furimsky 2000, Elliott 2007) but a number of alternative catalysts have also been reported for upgrading bio-oils and lignin-derived compounds (Choudhary and Phillips 2011, Hicks 2011). Bimetallic catalysts are more active in the reduced form for some types of reactions while the sulfided counterparts are more active for others. Typically, the CoMo or NiMo catalysts are used in a sulfided form in the presence of H<sub>2</sub>S. It is

believed that sulfiding is necessary to protect the metal oxides species from being reduced to the metal form, which are more active for hydrogenolysis reactions and can lead to coke deposition and deactivation of the catalyst. However, there are some disadvantages of using sulfided catalysts for processing biomass such as (1) additional cost of the sulfiding agent, storage tank, pumps, and additional equipment; (2) formation of mercaptans that may lead to the presence of sulfur in the product streams; (3) sulfiding agent ( $H_2S$ ) must be removed from the products and the sulfur must be recovered from the  $H_2S$ ; (4) corrosive effects of  $H_2S$  (Krár, Kovács et al. 2010). To prevent these problems, the reduced form of the catalysts (also in the presence of  $H_2$ ) would be a more attractive option for hydrothermal processing/deoxygenation of biomass. It was proposed that reduced Mo-based catalysts might exhibit behavior similar to that of sulfided forms (Vogelzang, Li et al. 1983, Wang and Ozkan 2005). The active sites of both reduced and sulfided CoMo catalysts were the same for hydrotreating reactions, however, reaction mechanisms were different (Wang and Cai 2013). A reduced form of CoMo/ $Al_2O_3$  and other bimetallic catalysts have been widely used for hydrothermal treatment of biomass (Roberts, Daage et al. 2013), upgrading products of fast pyrolysis (Fivga 2011), upgrading lipids to alkanes (Krár, Kovács et al. 2010, Hancsók, Kasza et al. 2012), hydrodeoxygenation of model compounds (Bunch, Wang et al. 2007), water-gas shift- and hydrotreating reactions (Wang and Cai 2013). Similarly, homogeneous (water-soluble) catalysts such as  $Na_2CO_3$ ,  $K_2CO_3$ ,  $Ni(NO_3)_2$  were used for increasing bio-oil yield at lower temperatures (Tungal and Shende 2013).

The objectives of this research were to: (i) study the HTL of ACS-UHS with homogeneous ( $K_2CO_3$ ) and heterogeneous (CoMo/ $Al_2O_3$ ) catalysts (without adding sulfur

to the reaction media) and understand the effect of the reduced bimetallic catalyst as a function of temperature and reaction time on the HTL process; (ii) maximize the overall bio-oil and energy yields by optimizing the process conditions and develop the mass balance for the integrated bioethanol and bio-oil production from corn stover. To the best of our knowledge, there are no reported studies on HTL of ACS-UHS. The integration of biochemical and thermochemical conversion of lignocellulosic biomass could be important for the future of the biorefinery concept in terms of maximizing the carbon utilization to produce fuels and chemicals in an economically viable way.

### **3.2. Experimental part**

In the current study, ACS-UHS was subjected to HTL in a 500 mL batch reactor equipped with Parr 4848 controller at three different temperatures (280, 320, and 350 °C) in the absence and at the presence of  $K_2CO_3$  and reduced  $CoMo/Al_2O_3$  catalysts for 30 min. The preheating time ranged between 30 to 40 min depending on the required reaction temperature. Reaction temperatures were selected based on the typical HTL conditions reported elsewhere for the similar applications (Karagoz, Bhaskar et al. 2005, Choudhary and Phillips 2011). The homogeneous catalyst was dissolved in the reaction medium. The pelletized heterogeneous catalyst was suspended in a stainless steel cage installed in the reactor. The liquid and solid phases were separated after the completion of an experiment and bio-oils were extracted from the both phases.

Extraction of bio-oils from the liquid and solid phases was performed with diethyl ether and acetone, respectively, as described by Karagoz et al. (Karagoz, Bhaskar et al. 2004, Karagoz, Bhaskar et al. 2005, Karagoz, Bhaskar et al. 2005). Diethyl ether and

dichloromethane are the two non-polar solvents most commonly used for extractions of organic substances from aqueous solutions. However, diethyl ether has the highest dielectric constant from all non-polar solvents (4.3) and is therefore capable of extracting a wider range of HTL products (both non-polar and slightly polar) from the aqueous phase. It also has the lowest boiling point from all non-polar solvents (34.6 °C) and so can be easily removed after the separation of the ether and water phases.

The gaseous products were collected after cooling the reactor down to the ambient temperature and analyzed using GC. The aqueous phase was analyzed for pH using a probe and for total organic carbon (TOC) using Shimadzu TOC-V<sub>CPH</sub> analyzer. Biomass, bio-oils, and biochar were subjected to elemental analysis (C, H, and N) and higher heating values (HHV) of the products were calculated using Dulong's formula (Akdeniz and Gündoğdua 2007). The composition of bio-oils was studied using GC-MS, <sup>1</sup>H NMR and <sup>13</sup>C NMR spectroscopy. All the analyses were done in triplicate.

### **3.2.1. Materials**

The biomass degrading enzymes (Cellic CTec2 and Htec2) used in the preparation of the ACS-UHS were a generous gift from Novozymes (Franklinton, NC, USA) while the Multifect Pectinase (MP) enzymes were a generous gift from Genencor (currently DuPont, Palo Alto, CA, USA). The solvents (diethyl ether, acetone), chemicals (K<sub>2</sub>CO<sub>3</sub> (lab grade, > 99%) and anhydrous Na<sub>2</sub>SO<sub>4</sub>) were purchased from Fischer Scientific Inc., USA, and used as received. SCOTTY gas calibration standard containing 50 wt% H<sub>2</sub>, 10 wt% CH<sub>4</sub>, 10 wt% CO, 20 wt% CO<sub>2</sub>, 5 wt% ethylene, and 5 wt% propane was purchased from Air Liquid America Specialty Gases LLC, USA, for calibrating GC.



Pelletized (1/8" extrusions) CoMo/Al<sub>2</sub>O<sub>3</sub> catalyst (3.5% CoO, 14% MoO<sub>3</sub>, surface area ~244 m<sup>2</sup>/g) was purchased from Strem Chemicals, Inc., USA and reduced under the flow hydrogen atmosphere (1 L/min) at 500 ± 5 °C for 2 h before being used.

### 3.2.2. Feedstock

ACS-UHS was produced using a high pressure stainless steel vessel (Parr company, IL) using the following pretreatment conditions: anhydrous ammonia to biomass loading - 1:1, moisture - 60%, temperature - 100°C, reaction time - 30 min as described in (Balan, Bals et al. 2009). Residual ammonia present in the pretreated biomass was removed by keeping the biomass in the hood overnight. The ACS-UHS with < 10% moisture content was stored in a Ziploc bag at 4°C until further use. High solid loading (18%) enzymatic hydrolysis was performed under sterile conditions in a 2 L baffled shake flask. Commercial enzymes (Ctec2, Htec2, and Multifect Pectinase) at 15 mg/g of glucan and autoclaved water were added to ACS-UHS in a baffled flask. This addition was performed in a laminar flow chamber to avoid microbial contamination during the enzymatic hydrolysis, which was carried out at 50 °C, pH 5.0 (adjusted with 6 M HCl), for 24 h. The hydrolyzed biomass was then transferred to a centrifuge tube and centrifuged at 10,000 rpm using a Beckman Coulter (Brea, CA, USA) centrifuge for a period of 30 min. The supernatant (hydrolysate) was transferred to another vessel and the residual sugars bound to the ACS-UHS were removed by washing two times with water (10 time v/w) followed by repeated centrifugation and supernatant removal. Most of the wet ACS-UHS (~70.5% moisture) was transferred into a Ziploc bag and stored at -20 °C

until further use. Some amount of this ACS-UHS was dried in an oven at  $45 \pm 2^\circ\text{C}$  for 72 h, ground, and used as a feedstock in the study.

### 3.2.3. ACS-UHS composition analysis

Extractive-based compositional analyses of the ACS-UHS were performed according to NREL Laboratory Analytical Procedures (LAPs): “*Preparation of samples for compositional analysis*” and “*Determination of structural carbohydrates and lignin in biomass*” (NREL/TP-510-42618). The biomass was subjected to extraction with water and ethanol prior to the acid hydrolysis step. The sugar concentrations of the extracts were included in the composition. Monomeric sugars were quantified using Shimadzu HPLC system equipped with an Aminex HPX-87P carbohydrate analysis column (Biorad, Hercules, CA) and Waters 410 refractive index detector (RID). Degassed HPLC grade water with 5 mM  $\text{H}_2\text{SO}_4$  was used as a mobile phase at 0.6 mL/min. Injection volume was 20  $\mu\text{L}$  with a run time of 20 min. The products after microbial fermentation of ACS hydrolysate were analyzed for ethanol and residual sugars with the above mentioned HPLC system equipped with an Aminex HPX-87H column (Biorad, Hercules, CA). The elemental analysis of ACS-UHS was done using Thermo-Finnigan Flash EA 1112 elemental analyzer. The composition and results of the elemental analysis of ACS-UHS used in this study are provided in Table 10.

**Table 10.** Composition, elemental analysis, and HHV of ACS-UHS

Sample	Carbohydrates composition			Lignin, wt%	Ash, wt%	Elemental analysis, wt%				HHV** MJ/kg
	Glucan, wt%	Xylan, wt%	Arabinan, wt%			C	H	N	O*	
ACS-UHS	13.90	5.79	1.05	52.49	12.32	44.64	4.92	2.94	47.50	14.21
RSD, %	<1.5	<1.2	<1.0	<2.0	<2.0	<1.9	<1.9	<1.9	<1.9	-

\*O percentage was calculated based on the difference assuming that biomass contains only C, H, O, and N elements

\*\*HHV was calculated using Dulong's formula:  $\text{HHV (MJ/kg)} = 33.5 (\text{C}\%) + 142.3 (\text{H}\%) - 15.4 (\text{O}\%) - 14.5 (\text{N}\%)$  (Akdeniz and Gündoğdua 2007)

### 3.2.4. Apparatus and experimental procedure

HTL experiments were carried out in a 500 mL batch reactor equipped with a Parr 4848 controller (Parr Instrument, Moline, IL, USA) at  $280 \pm 1$  °C,  $320 \pm 1$  °C, and  $350 \pm 1$  °C for 30 min, both in the absence and at the presence of the catalysts. The heating rate was 10-15 °C/min depending on the required reaction temperature. The reaction time did not include the preheating and cooling time. The autogenously obtained pressures were  $950 \pm 5$  psi,  $1640 \pm 5$  psi, and  $2400 \pm 5$  psi, respectively. In a typical experiment, 50 g of UHS (dry basis) and 200 mL of deionized water were loaded into the reactor. For the catalytic runs, 5 wt% (2.5 g) of  $\text{K}_2\text{CO}_3$  or 5 g of reduced  $\text{CoMo}/\text{Al}_2\text{O}_3$  were added to the reaction media. After loading, the reactor was purged with helium for 5 min. The reaction medium was continuously stirred at 100 rpm. After completing an experiment, the reactor was rapidly cooled down to the room temperature. The experimental conditions used for HTL experiments are shown in Table 11.

**Table 11.** Experimental conditions used in the study

<b>Exp. No.</b>	<b>Temperature, °C</b>	<b>Catalyst</b>
1	280	No catalyst
2	320	No catalyst
3	350	No catalyst
4	280	K <sub>2</sub> CO <sub>3</sub>
5	320	K <sub>2</sub> CO <sub>3</sub>
6*	350	K <sub>2</sub> CO <sub>3</sub>
7	280	CoMo/Al <sub>2</sub> O <sub>3</sub>
8	320	CoMo/Al <sub>2</sub> O <sub>3</sub>
9*	350	CoMo/Al <sub>2</sub> O <sub>3</sub>

\*Experiments conducted in duplicate

### 3.2.5. Bio-oil separation protocol

The overall procedure for the separation of the HTL products is shown in Fig. 13. In the current study, bio-oils from the liquid and solid phases were extracted with diethyl ether and acetone, respectively. After cooling the reactor down to the ambient temperature, the temperature and pressure were recorded and used for quantifying the gaseous products. The gaseous products from runs 6 and 9 (the catalytic HTL with maximum bio-oil yields) were collected and analyzed using SRI 8610C GC equipped with a 10' x 1/8" SS Hayesep-D packed column and a thermal conductivity detector.

Helium at 10 mL/min was used as the carrier gas. The temperature program was set up as follows: initial temperature 40 °C, hold for 5 min, ramp at 10°C/min, final temperature 120 °C.

The stainless steel cage with the heterogeneous catalyst pellets was removed from the reactor. The homogeneous catalyst was not recovered from the aqueous phase. The solid and liquid products were rinsed from the reactor to a flask using 100 mL of deionized water, acidified with 1 M HCL to obtain pH of approximately 1-2, kept overnight at 4 °C (12 h), and separated by vacuum filtration. Acidification was used for precipitating of organic acids and soluble lignin and, therefore, for better separation of the solid and liquid phases (Radoykova, Nenkova et al. 2013). Before acidification, the total organic carbon (TOC) and pH of the aqueous phase were measured for all the experiments. The solid products were dried in an oven at  $65 \pm 2$  °C for 24 h and quantified.

After that, 200 mL of diethyl ether was added to the aqueous portion, and the mixture was shaken vigorously for about 10 min. The water-ether mixture was then separated using a separating funnel. The ether phase was dried over anhydrous  $\text{Na}_2\text{SO}_4$ , filtered, and evaporated in a vacuum rotary evaporator at room temperature. After removal of the ether, the remaining fraction was quantified and labeled as light bio-oil (LBO). The oven-dried solid portion was washed several times with 300 mL of acetone, after which the solids were separated from the extract by vacuum filtration. After removal of acetone from the extract in a vacuum rotary evaporator at 40 °C, the obtained product was quantified and labeled as heavy bio-oil (HBO). The sum of LBO and HBO was labeled as total bio-oil (TBO). The remaining solids were dried in an oven at  $105 \pm 2$  °C for 4 h, quantified, and labeled as biochar.

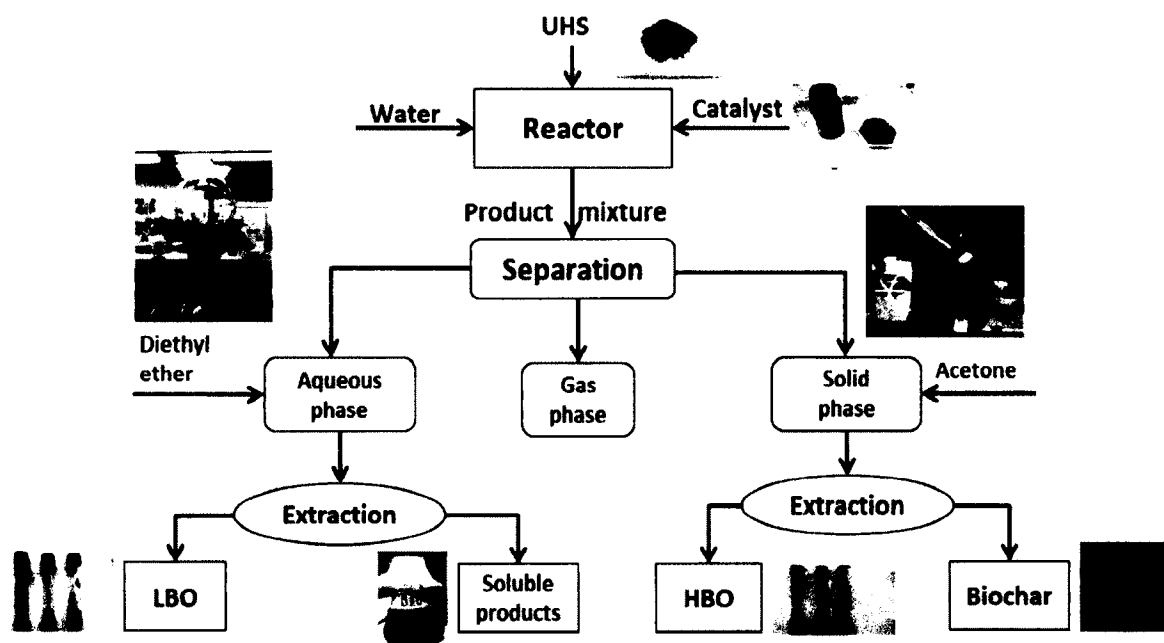


**Figure 13.** Products separation procedure that was followed to produce light bio-oil (LBO), heavy bio-oil (HBO), biochar, and aqueous-soluble products from ACS-UHS.

After deactivation,  $\text{CoMo}/\text{Al}_2\text{O}_3$  catalyst can be regenerated by burning out the coke in a muffle furnace at  $575\text{ }^\circ\text{C}$  for 4 h, reduced by hydrogen as described above, and reused in the HTL process.

### 3.2.6. Bio-oil characterization

One dimensional  $^1\text{H}$  and 2D hetero nuclear  $^1\text{H}$ - $^{13}\text{C}$  single quantum coherence (HSQC) experiments of liquid bio-oils from experiments 6 and 9 were obtained using a Bruker AVANCE III NMR spectrometer. Solid-state  $^{13}\text{C}$  NMR of biochar was obtained with a Bruker AVANCE II 400 MHz NMR spectrometer with a 4 mm cross polarization

(CP) magic angle spinning (MAS) probe (spin=12kHz). Bio-oils were dissolved in methanol and analyzed with a Hewlett Packard 6890 gas chromatography system with a Restek Rtx-5 column (30 m x 0.25 mm x 0.25  $\mu$ m) and a Pegasus III time-of-flight mass spectrometer (LECO Corporation). The oven was held at 50  $^{\circ}$ C for 2 min, ramped up to 200  $^{\circ}$ C at a rate of 5  $^{\circ}$ C/min, and then ramped to 300  $^{\circ}$ C at a rate of 20 $^{\circ}$ C/min. Samples were injected in the split mode at 250  $^{\circ}$ C with helium as the carrier gas. The compounds were identified using the NIST library of mass spectra.

### 3.3. Results and discussion

#### 3.3.1. Product distribution

The pH and TOC of the aqueous products produced immediately after HTL process are shown in Fig. 14 a, b.

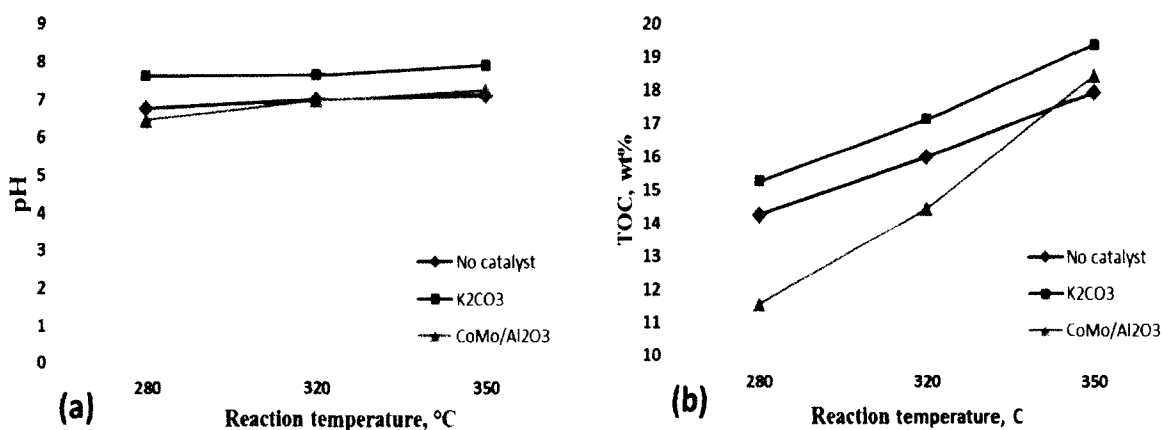


**Figure 14.** (a) pH and (b) TOC of the aqueous phase as functions of temperature. RSD (a) < 2.8%, RSD (b) < 2.2%.

A slight increase in pH was observed for all the experiments with  $K_2CO_3$  in this study. The TOC of the aqueous phase was also higher for all the runs in the presence of  $K_2CO_3$  for all the temperatures studied. These observations can be explained by the known effect of alkali solutions that inhibit the formation of char while favoring the formation of bio-oil (Minowa, Zhen et al. 1998). The TOC content of the aqueous phase most likely included glucopyranose, benzenediol, and other glucan-and lignin-derived compounds (3-methyl-1,2-benzenediol, 4-methyl-1,2-benzenediol, 4-ethyl-1,2-benzenediol, etc.) that are soluble in water at the ambient conditions (Ba, Chaala et al. 2004).

The gas composition from runs 6 and 9 (350 °C with  $K_2CO_3$  and  $CoMo/Al_2O_3$ , respectively) is shown in Table 12. As can be seen from the table,  $CO_2$  yield in the experiment with  $CoMo/Al_2O_3$  catalyst was higher than in the one with  $K_2CO_3$ . This effect can be explained by the high deoxygenation activity of this catalyst that can promote decarboxylation at the reaction temperatures above 300 °C (Laurent and Delmon 1994). The gaseous phase consisted of  $CO_2$  (major component),  $CO$ ,  $CH_4$ , and trace amount of  $C_2H_4$ . The highest amounts of gaseous products was also observed when  $CoMo/Al_2O_3$  was used as a catalyst, which can be explained by the high deoxygenation/decarboxylation activity of this catalyst as well as by the steam reforming of the aqueous product intermediates, lower-temperature water-gas shift reaction, and methanation reaction (Demirbas 2011).



**Table 12.** Composition of gaseous products obtained after catalytic runs at 350 °C

Run	Temperature, °C	Catalyst	Gaseous products		
			CH <sub>4</sub> , wt%	CO, wt%	CO <sub>2</sub> , wt%
6*	350	K <sub>2</sub> CO <sub>3</sub>	1.5 ± 0.5	9.6 ± 0.8	88.9 ± 1.2
9*	350	CoMo/Al <sub>2</sub> O <sub>3</sub>	1.8 ± 0.5	4.2 ± 0.8	94.0 ± 1.2

\* Experiments conducted in duplicate

**Bio-oils:** Visually, LBO was dark viscous liquid and HBO was dark tarry substance under the ambient conditions. Bio-oils (LBO and HBO) yields obtained during all the liquefaction experiments are shown in Fig. 15. The increase of the reaction temperature from 280 to 350 °C resulted in higher LBO yields and lower HBO yields for all the runs. Maximum TBO yield was observed at 350 °C (30.1 wt%) in the presence of homogenous catalyst. The further increase of the reaction temperature might lead to a degradation of bio-oils and increase in producing gaseous products for all the experimental conditions. These results were similar to the results of HTL of biomass discussed by Aktar and Amin in a recent review paper (Akhtar and Amin 2011).

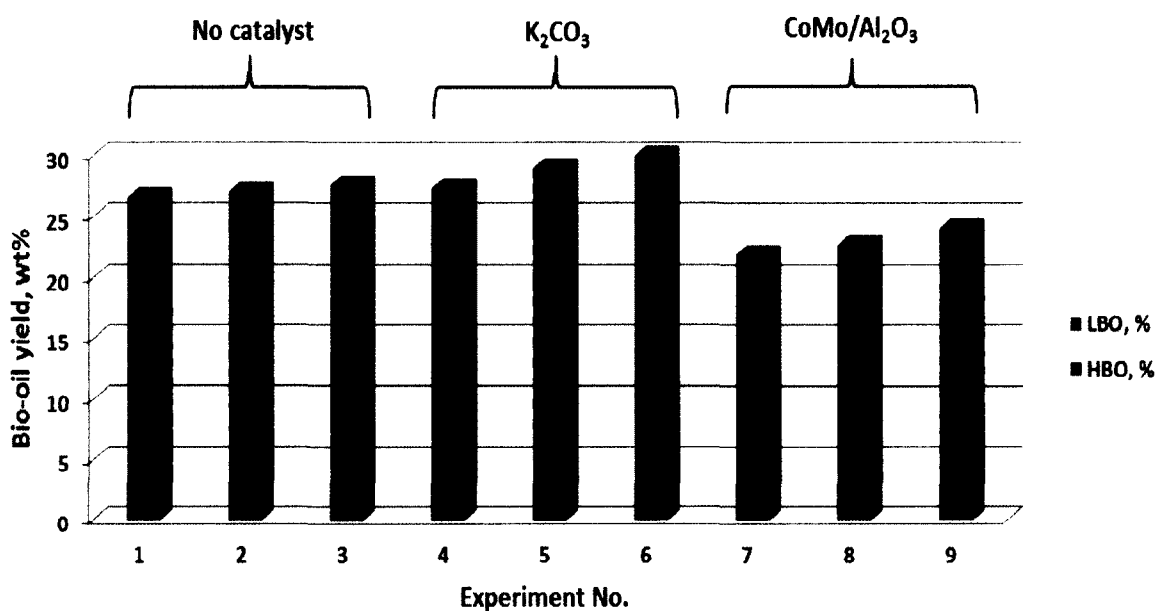


**Figure 15.** Bio-oil yields for all the HTL experiments (RSD < 2.5%).

Table 13 provides the distribution of all the products obtained during the HTL of ACS-UHS.

**Table 13.** HTL products obtained under different experimental conditions

Run	Catalyst	Temp., °C	Conversion, wt%	LBO <sup>1</sup> , wt%	HBO <sup>2</sup> , wt%	TBO, wt%	Biochar <sup>3</sup> , wt%	Gas <sup>4</sup> , wt%	WSP*, wt%	DL, %
1	No catalyst	280	50.6	8.8	17.8	26.6	31.6	0.8	41.0	31.9
2	No catalyst	320	54.6	11.7	15.4	27.1	30	8.1	34.8	35.8
3	No catalyst	350	60.0	13.9	13.7	27.6	26.2	11.4	34.8	40.1
4	K <sub>2</sub> CO <sub>3</sub>	280	57.7	11.9	15.5	27.4	26.8	3.9	41.9	34.2

5	K <sub>2</sub> CO <sub>3</sub>	320	64.6	16	13	29	22.4	5.9	42.7	38.3
6	K <sub>2</sub> CO <sub>3</sub>	350	68.7	18.8	11.3	30.1	20.1	11.4	38.4	43.4
7	CoMo/Al <sub>2</sub> O <sub>3</sub>	280	60.6	10.3	11.6	21.9	27.9	0.1	50.1	25.9
8	CoMo/Al <sub>2</sub> O <sub>3</sub>	320	66.4	12.0	10.7	22.7	23	11.9	42.4	32.4
9	CoMo/Al <sub>2</sub> O <sub>3</sub>	350	73.7	15.6	8.5	24.1	17.8	21.6	36.5	41.3

RSD < <sup>1</sup>1.5, <sup>2</sup>1.5, <sup>3</sup>2.0, <sup>4</sup>2.3%

\*Water-soluble products

Conversion was calculated using Eq. (32)

Degree of liquefaction was calculated using Eq. (33)

It can be seen from the table that the biochar formation in the catalytic runs was lower than that in the thermal (non-catalytic) runs. The homogeneous catalyst inhibited the formation of biochar more efficiently and favored the formation of bio-oils. Minowa et al. studied the liquefaction of cellulose in hot compressed water using Na<sub>2</sub>CO<sub>3</sub> as a catalyst. They observed that the alkali catalyst inhibited the formation of char and favored the formation of bio-oils (Minowa, Zhen et al. 1998). Our results are in good agreement with their observations. The conversion and degree of liquefaction shown in Table 13 were calculated according to the formulae:

$$\text{Conversion} = \frac{m_{\text{UHS}} - m_{\text{Biochar}}}{m_{\text{UHS}}} \times 100\% \quad (32)$$

$$\text{Degree of Liquefaction} = \frac{\text{TOC}}{C_{\text{UHS}}} 100\% \quad (33)$$

Where  $m_{\text{UHS}}$  – mass of unhydrolyzed solids (dry basis),  $m_{\text{Biochar}}$  – mass of biochar (dry basis), TOC – mass of total organic carbon in the aqueous phase,  $C_{\text{UHS}}$  – mass of elemental carbon in unhydrolyzed solids, g.

As can be seen from Table 13, the maximum degree of liquefaction (DL) was 43.4 wt% at 350 °C with the use of  $\text{K}_2\text{CO}_3$  catalyst, which is similar to what was reported for an alkali catalyzed HTL of biomass (Karagoz, Bhaskar et al. 2004).  $\text{CoMo}/\text{Al}_2\text{O}_3$  catalyst turned out to be relatively less efficient for HTL of this type of biomass. This might be due to the high decarboxylation activity of the heterogeneous catalyst that resulted in extensive gas formation and removal of carbon from the biomass mainly in the form of  $\text{CO}_2$  (Laurent and Delmon 1994).

The optimal conditions for ACS-UHS liquefaction were in the range of reaction temperatures from 320 to 350°C with the use of the homogeneous ( $\text{K}_2\text{CO}_3$ ) catalyst. Although TBO yield was higher at 350°C, the TBO produced at 320°C had higher carbon and hydrogen contents. This phenomenon is consistent with the higher heating values and the energy conversion ratios discussed below. TBO yield for run 6 (350°C with  $\text{K}_2\text{CO}_3$  catalyst) was 30.1 wt%, which was the highest bio-oil yield obtained in the study.

The highest conversion of ACS-UHS (73.7 wt%) was observed for the run 9 (350 °C with  $\text{CoMo}/\text{Al}_2\text{O}_3$  catalyst) vs. 60.0 and 68.7 wt%. for runs 3 and 6 (350 °C with no catalyst and with  $\text{K}_2\text{CO}_3$  catalyst). However, this was mainly due to the higher gas formation than in the respective runs 3 and 6 while bio-oil formation in run 9 was lower.

### 3.3.2. Energy contents of bio-oils and biochar

The elemental analysis, H/C and O/C ratios, and higher heating values (HHV) of the raw biomass as well as bio-oils and biochar produced at 280, 320, and 350 °C in the absence and at the presence of both the homogeneous and heterogeneous catalysts are provided in Table 14.

**Table 14.** Elemental analysis, H/C and O/C ratios, and HHV of bio-oils and biochar (RSD <1.8%)

Run	Sample	Catalyst	Temperature, °C	C, wt%	H, wt%	N, wt%	O*, wt%	H/C (molar basis)	O/C (molar basis)	HHV**, MJ/kg
-	ACS-UHS	-	-	44.6	4.9	2.9	47.5	1.32	0.80	14.2
1	Biochar	No catalyst	280	46.7	3.4	3.1	46.8	0.88	0.75	12.9
2	Biochar	No catalyst	320	45.5	2.9	3.2	48.3	0.77	0.80	11.5
3	Biochar	No catalyst	350	48.9	3.0	3.3	44.9	0.73	0.69	13.2
4	Biochar	K <sub>2</sub> CO <sub>3</sub>	280	48.6	3.7	3.2	44.4	0.92	0.68	14.3
5	Biochar	K <sub>2</sub> CO <sub>3</sub>	320	48.5	3.4	3.2	44.9	0.85	0.69	13.7
6	Biochar	K <sub>2</sub> CO <sub>3</sub>	350	49.5	3.3	3.0	44.2	0.80	0.67	14.0
7	Biochar	CoMo/Al <sub>2</sub> O <sub>3</sub>	280	51.0	3.9	3.4	41.7	0.91	0.61	15.7
8	Biochar	CoMo/Al <sub>2</sub> O <sub>3</sub>	320	49.7	3.4	3.5	43.4	0.81	0.65	14.2
9	Biochar	CoMo/Al <sub>2</sub> O <sub>3</sub>	350	47.4	2.8	3.4	46.4	0.72	0.73	12.3

1	LBO	No catalyst	280	63.3	7.2	1.2	28.3	1.37	0.34	26.9
2	LBO	No catalyst	320	54.7	6.7	0.8	37.8	1.47	0.52	21.9
3	LBO	No catalyst	350	54.6	6.7	0.7	38.0	1.47	0.52	21.9
4	LBO	K <sub>2</sub> CO <sub>3</sub>	280	56.3	7.0	1.1	35.7	1.48	0.48	23.1
5	LBO	K <sub>2</sub> CO <sub>3</sub>	320	62.5	6.9	0.9	29.6	1.33	0.35	26.1
6	LBO	K <sub>2</sub> CO <sub>3</sub>	350	54.1	6.9	0.9	38.1	1.53	0.53	21.9
7	LBO	CoMo/Al <sub>2</sub> O <sub>3</sub>	280	59.7	6.2	1.2	32.9	1.24	0.41	23.5
8	LBO	CoMo/Al <sub>2</sub> O <sub>3</sub>	320	60.7	6.6	1.0	31.7	1.30	0.39	24.7
9	LBO	CoMo/Al <sub>2</sub> O <sub>3</sub>	350	54.8	6.0	0.8	38.5	1.32	0.53	20.9
1	HBO	No catalyst	280	67.1	7.7	1.9	23.3	1.37	0.26	29.5
2	HBO	No catalyst	320	70.7	7.6	2.0	19.8	1.28	0.21	31.1
3	HBO	No catalyst	350	72.3	8.3	2.2	17.2	1.38	0.18	33.0
4	HBO	K <sub>2</sub> CO <sub>3</sub>	280	67.0	7.7	2.0	23.4	1.37	0.26	29.4
5	HBO	K <sub>2</sub> CO <sub>3</sub>	320	69.1	7.5	2.1	21.3	1.31	0.23	30.3
6	HBO	K <sub>2</sub> CO <sub>3</sub>	350	72.4	7.9	2.1	17.6	1.31	0.18	32.5
7	HBO	CoMo/Al <sub>2</sub> O <sub>3</sub>	280	66.1	7.7	1.6	24.6	1.40	0.28	29.1
8	HBO	CoMo/Al <sub>2</sub> O <sub>3</sub>	320	69.0	7.6	1.7	21.7	1.33	0.24	30.4
9	HBO	CoMo/Al <sub>2</sub> O <sub>3</sub>	350	69.9	8.1	1.8	20.1	1.40	0.22	31.6

\*Oxygen percentage was calculated based on the difference assuming that the biomass contains only C, H, O, and N elements

\*\*Higher Heating Value (HHV) was calculated using Dulong's formula:  $HHV (MJ/kg) = 33.5 (C\%) + 142.3 (H\%) - 15.4 (O\%) - 14.5 (N\%)$  (Akdeniz and Gündoğdua 2007)

It can be seen from Table 14 that HHVs of both LBO and HBO were higher for all the runs, H/C ratios of LBOs were higher for the thermal and homogeneous catalytic runs, and O/C ratios of both LBO and HBO were lower for all the runs than the respective values of the raw biomass. The HHVs of the extracted biochar did not show a significant difference in comparison to the raw biomass. This might be due to the prior extraction of HBO, which reduced the HHVs of the solid residue to the reported values. The HHV of 26.1 MJ/kg and 30.3 MJ/kg were respectively observed for LBO and HBO obtained at 320°C in the presence of the homogeneous catalyst (run 5). For comparison, Fig. 16 a, b shows the energy distribution of the products obtained from runs 6 and 9 (350 °C with K<sub>2</sub>CO<sub>3</sub> and CoMo/Al<sub>2</sub>O<sub>3</sub>, respectively). HHVs of the water-soluble products were calculated based on the difference.

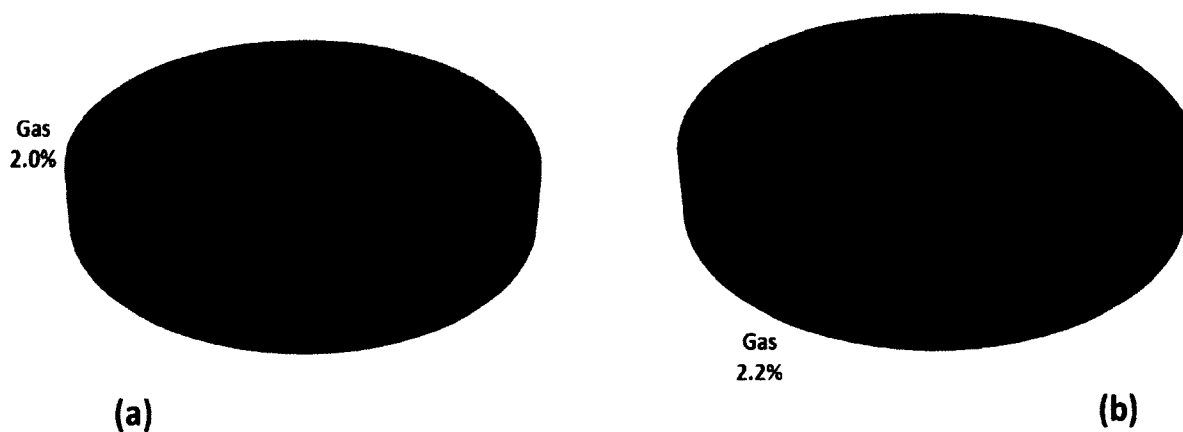


**Figure 16.** (a) Energy (HHV) distribution of the products from runs 6 (350 °C with K<sub>2</sub>CO<sub>3</sub>) and (b) – from run 9 (350 °C with CoMo/Al<sub>2</sub>O<sub>3</sub>).

Energy conversion ratio is defined as a ratio between the useful output of an energy produced during the HTL process of biomass and the input, in energy terms. ECRs of ACS-UHS for bio-oils were calculated for all the runs using the following of formula (Ramsurn and Gupta 2012):

$$\text{ECR} = \frac{m_{\text{LBO}} * \text{HHV}_{\text{LBO}} + m_{\text{HBO}} * \text{HHV}_{\text{HBO}}}{m_{\text{UHS}} * \text{HHV}_{\text{UHS}}} 100\% \quad (34)$$

where  $m_{\text{LBO}}$ ,  $m_{\text{HBO}}$ ,  $m_{\text{UHS}}$  – masses of LBO, HBO, and UHS, g, respectively;  $\text{HHV}_{\text{LBO}}$ ,  $\text{HHV}_{\text{HBO}}$ ,  $\text{HHV}_{\text{UHS}}$  – higher heating values of LBO, HBO, UHS, kJ/g, respectively.

The distribution of ECRs for all the runs is compared in Fig. 17.

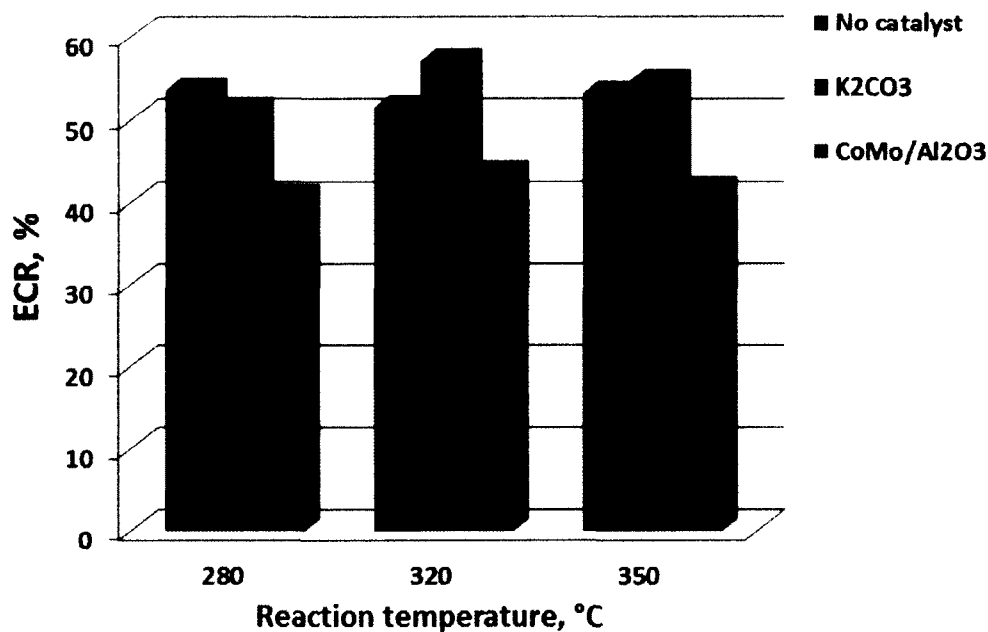


**Figure 17.** Energy conversion ratios for all the HTL experiments.



The highest ECR of 57.1% was observed for the bio-oils obtained at 320 °C in the presence of the homogeneous catalyst. Ramsurn and Gupta reported 66.6% of ECR for switchgrass to biocrude via a two-stage process and compared their results with various feedstock including microalgae using the same equation (3) (Ramsurn and Gupta 2012). The majority of lignocellulosic biomass had less than 53% of ECR whereas one of the studies on microalgae (*Nannochloropsis* sp.) reported 85.8% of ECR. The particularly high conversion of the microalgae may be attributed to the application of higher pressure (350 bar) and the fact that the feedstock contained only 25.1 wt% of oxygen as compared to ACS-UHS having 47.5 wt% of oxygen (Brown, Duan et al. 2010). Generally, herbaceous lignocellulosic biomasses (switchgrass, rice husk, and corn stover) have been reported to have low ECRs to bio-oils irrespective of the different thermochemical liquefaction methods. However, in this study, we demonstrated ECR of bio-oils produced from ACS-UHS can be 57.1%, which is significantly higher than 45% of ECR obtained from pyrolysis of similar feedstock (switchgrass). The highest TBO yield with slightly lower HHV (21.9 MJ/kg for LBO and 32.5 MJ/kg for HBO) was observed for run 6 (350 °C with  $K_2CO_3$ ) and these process conditions were considered as the optimal for ACS-UHS liquefaction.

### 3.3.3. Composition of bio-oils and biochar

Runs 6 and 9 were selected for compositional analyses of the products because they provided the highest bio-oil yields for the catalytic runs. Even though  $CoMo/Al_2O_3$  did not demonstrate the high liquefaction activity, it provided an opportunity to observe the difference in bio-oil compositions produced in the presence of homogeneous and

heterogeneous catalysts. Table 15 shows the composition of the LBOs from run 6 and 9 as identified by GC-MS.

**Table 15.** Identification of compounds in LBO from runs 6 (350 °C, Na<sub>2</sub>CO<sub>3</sub>) and run 9 (350 °C, CoMo/Al<sub>2</sub>O<sub>3</sub>) by GC-MS (RSD <2%)

Peak No.	RT, min	Compound	Peak area, %	
			Run 6	Run 9
1	6.94	2-Methyl-2-cyclopenten-1-one	1.79	2.59
2	9.09	Phenol	52.20	40.99
3	11.83	4-Methyl-phenol	1.90	3.95
4	12.31	2-Methoxy-phenol	16.53	15.17
5	14.54	4-Ethyl phenol	9.78	14.02
6	15.48	1,2-Benzenediol	14.83	9.45
7	17.27	3-Methoxy-1,2-benzenediol	-	3.46
8	17.75	4-Ethyl-2-methoxy phenol	2.98	3.96
9	19.72	2,6-Dimethoxy-phenol	0.00	5.17
10	20.50	4-Ethyl-1,3-benzenediol	-	1.25
Total			100.00	100.00

It can be seen from the table that LBO is a complex mixture of phenol and benzenediol derivatives with phenol, 2-methoxy-phenol, 4-ethyl phenol, 1,2-benzenediol, and 4-ethyl-2-methoxy phenol being the major compounds. Dominance of phenol and benzenediol derivatives can be explained by breaking  $\beta$ -aryl and benzoyl-ether bonds of lignin resulting in production of phenolic compounds that might further decompose to benzenediol derivatives. The recent study by Singh et al. also reported the presence of substituted phenols and aromatic ethers present in bio-oils due to the breakage of various C-C and C-O-C ether bonds ( $\beta$ -O-4 or/and  $\alpha$ -O-4) present in lignin (Singh, Prakash et al. 2014). The results of the chromatographic analysis of LBO are similar to the results reported by other researchers for hydrothermal or pyrolytic treatments of lignocellulosic biomass (Kruse and Gawlik 2003, Karagoz, Bhaskar et al. 2005).

The compounds were clearly derived from the lignin-rich starting material that was partially depolymerized. Phenolic compounds dominated the LBO fractions by over 98% of the total peak area. This is consistent with the composition of the liquefaction products observed by Karagoz et al. (Karagoz, Bhaskar et al. 2005). Furthermore, these researchers described a likely pyrolytic mechanism of formation of phenol, 2-methoxy-phenol, and 1,2-benzenediol from lignin monomers (Filley, Hatcher et al. 2000, Karagoz, Bhaskar et al. 2004, Pandey and Kim 2011, Kibet, Khachatryan et al. 2012). Based on the results from Table 15 and the results of non-catalytic runs reported by Karagoz et al. for the similar application (Karagoz, Bhaskar et al. 2005), the main difference between non-catalytic and catalytic runs was the presence of variety of benzenediol derivatives in the products from the catalytic runs. However, in non-catalytic runs, only 1,2-benzenediol in was observed. The use of catalysts increased the amount of 2-methoxy-phenol and

significantly reduced the amounts of 4-methyl-phenol and 1,2-benzenediol in LBO compared to the non-catalytic runs. The heavy bio-oil fractions were not readily ionized with GC-MS and, therefore, NMR analysis was employed to broaden our molecular understanding of the bio-oils' composition.

Bio-oils obtained in this study can be further upgraded into drop-in fuels. LBO contained 25-35 wt% of oxygen and HBO – 20-25 wt% of oxygen (HBO) (Table 14) while conventional fuels have less than 1 wt%. The main objective of upgrading bio-oils into fuels is removal of oxygen heteroatoms by hydrogenation, dehydration (removal oxygen in form of water), decarboxylation (removal of oxygen in form of CO<sub>2</sub>), and decarbonylation (removal of oxygen in form of CO). These reactions occur at 250-350°C and 10-18 MPa in the presence of various catalysts such as CoMo, NiMo, NiW, Ni, Co, Pd, and CuCrO on different supports such as Al<sub>2</sub>O<sub>3</sub>,  $\gamma$ - Al<sub>2</sub>O<sub>3</sub>, SiO<sub>2</sub>-Al<sub>2</sub>O<sub>3</sub>, zeolite Y/ Al<sub>2</sub>O<sub>3</sub>, C under the hydrogen atmosphere. In a catalytic hydrodeoxygenation (HDO) of bio-oils, oxygen content can be reduced to 0.1 wt% with hydrogen consumption of 4 wt% (Goudriaan and Peferoen 1990, Peterson, Vogel et al. 2008, Demirbas 2011). HDO allows obtaining liquid products similar to diesel and jet fuel with a cetane numbers of > 50.

#### **3.3.3.1. <sup>1</sup>H NMR analysis**

The proton NMR spectra of LBO from run 6 and 9 indicated no major differences in chemical composition between these bio-oils (Fig. 18).

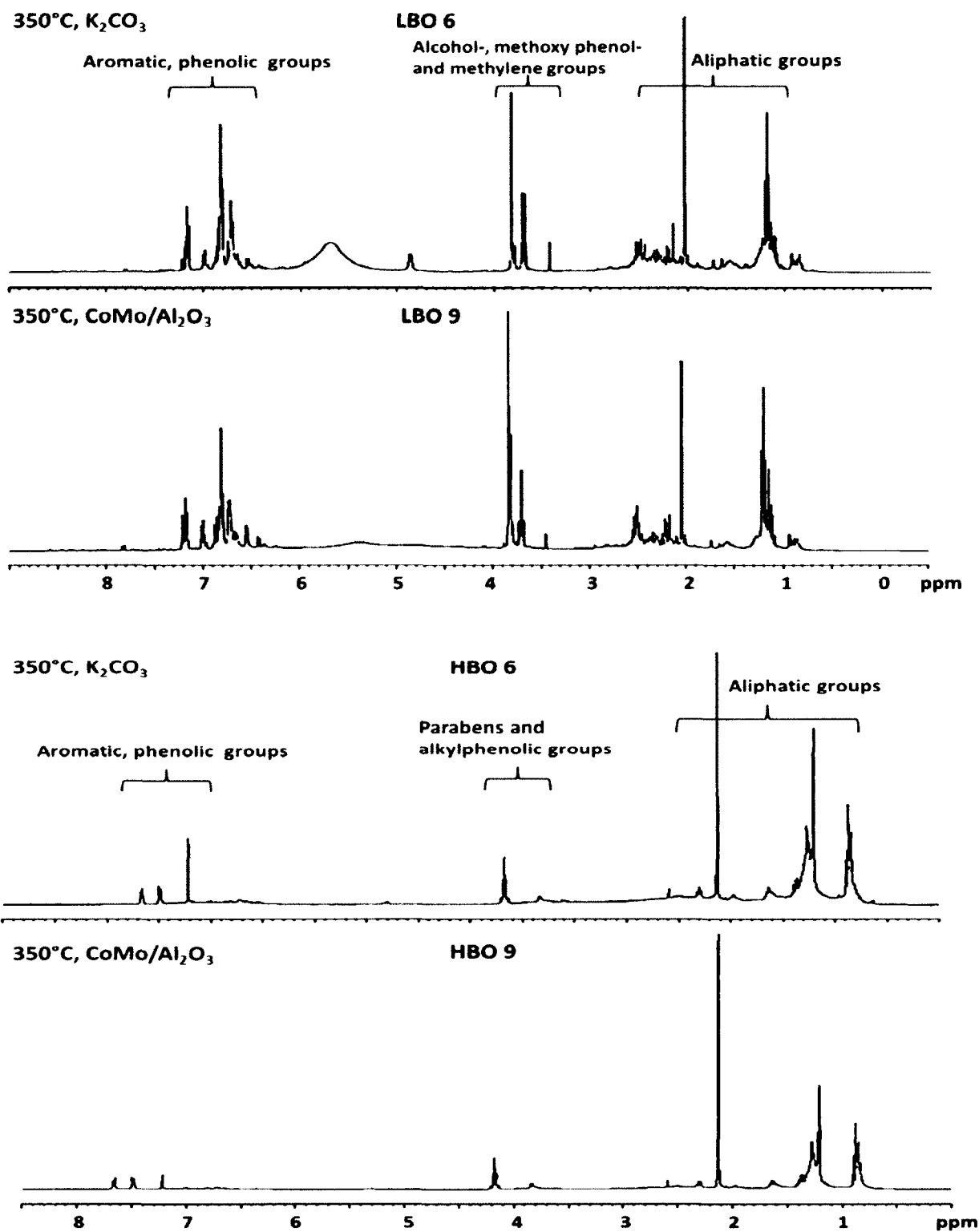


Figure 18. 1D  $^1\text{H}$  NMR spectra of LBO and HBO from runs 6 and 9 in  $\text{CDCl}_3$ .

The chemical shift region from 0.5 to 1.5 ppm represent aliphatic protons attached to carbon atoms at least two bonds removed from a C=C double bond or a heteroatom (O or N). The normalized integrated area from 0.5 to 1.5 ppm for Runs 6 and 9 are 41% and 43%, respectively, of the entire spectrum area. Contrastingly, the proton spectra of HBO of run 6 and 9 contain more aliphatic protons (77% and 81%, respectively when normalized to 100%) than the LBO. The chemical shift region from 1.5 to 3.0 ppm represents protons on aliphatic carbon atoms that are bonded to an aromatic or olefinic (C=C) bond or two bonds away from a heteroatom. LBO spectra contain more protons in this region relative to the entire integrated signal than the HBO spectra.

The chemical shift region from 3.0 to 4.5 ppm is representative of hydrocarbons adjacent to alcohols, methoxy phenols and methylene groups attached to a benzene-carboxylic ester. The chemical shift region from 4.5 to 6.1 ppm is typical for side-chain carbons in lignin molecules. The region of spectra from 6.1 to 8.5 ppm contains aromatic protons and possibly hetero-aromatics (O and N). LBO contains more resonances in this region suggesting that the aromatic diversity is much greater than HBO. However, the proton spectra contain many overlapping signals that make interpretation difficult and limit it to general functional group descriptions. A two dimensional experiment, such as Heteronuclear Single Quantum Coherence (HSQC), acquires significant resolution improvement by correlating  $^1\text{H}$  directly bonded to  $^{13}\text{C}$  (Koenig, Sleighter et al. 2010).

### 3.3.3.2. $^1\text{H}$ - $^{13}\text{C}$ two dimensional NMR analyses

The  $^1\text{H}$ - $^{13}\text{C}$  HSQC NMR demonstrates the superior resolution of two-dimensional spectra of LBO of run 6. This resolution of the two-dimensional spectra allows observing

four distinct peaks at 1.2, 8.8 ppm ( $^1\text{H}$ ,  $^{13}\text{C}$ ), 1.2, 16 ppm, 1.2, 16 ppm, 1.2, 22 ppm, and 1.2, 30 ppm respectively. In the  $^1\text{H}$  spectra (Fig. 18) at 1.2 ppm, the 4 peaks all overlap, but in the 2D spectrum, the cross peaks are clearly resolved.

Both LBO and HBO contain common moieties assigned to phenols (6.8, 115 ppm, 6.7, 121 ppm, 6.8, 121 ppm), methoxy phenols (3.8, 56 ppm, 6.8, 112 ppm, 6.8, 120 ppm) and alkyl-substituted benzenes. Contrastingly to LBO, HBO does not exhibit signals from a diversity of aromatic compounds. Cross peaks indicate parabens and alkylphenolic compounds and are consistent with *p*-hydroxybenzoate (3.8, 56 ppm; 4.2, 68 ppm; 7.7, 129 ppm; 7.5, 131 ppm) and benzene-di-carboxylic acid, di-isooctyl ester with a  $\text{C}_6$  branched chain substituent (1.7, 39 ppm; 4.2, 68 ppm; 7.7, 129 ppm; 7.5, 131 ppm).

LBO contains much more oxygenated aromatic compounds including hydroxyphenyls, benzene-diols, phenols, methoxy phenols and alkyl-substituted benzenes. Not only is this clearly seen in the number of cross peaks in the aromatic region (Fig. 18) from 6 to 8 ppm in the  $^1\text{H}$  dimension and 100 to 145 in the  $^{13}\text{C}$  dimension, but it is also evident in the number of cross peaks from 2.0 to 3.0 ppm ( $^1\text{H}$  dimension) and 15 to 50 ppm ( $^{13}\text{C}$  dimension) resulting from methyl- and ethyl-phenols and cyclic ketones. The cross peaks at 3.8, 56 ppm and 3.7, 58 ppm are assigned to methoxyl and di-methoxyl groups attached to lignin-like aromatic structures such as guaiacyl, syringyl, *p*-coumarate, and ferulate (Koenig, Sleighter et al. 2010).

### 3.4. HTL mechanism

HTL of biomass using subcritical water is potentially more advantageous over other thermochemical processes such as pyrolysis. It allows utilizing a wide variety of

wet biomass feedstocks without the need of its energy intensive drying. Under the reaction conditions (temperature 280-400 °C, pressure 20-25 MPa, time from few minutes to few hours, water-to-biomass ratio from 2 to 50), water serves as a reactant and reaction medium with a low viscosity and high solubility of organic substances. These conditions provide fast, homogeneous, and efficient reactions. The high concentration of  $H^+$  and  $OH^-$  accelerates many acid- or base-catalyzed reactions, such as hydrolysis (Hunter and Savage 2004). Due to these advantages, feedstock macromolecules are decomposed into fragments that are reactive, unstable, and tend to repolymerize into oily compounds with heavier molecular weights.

ACS-UHS used as a feedstock in this study, contains mainly lignin (53 wt%) and undigested recalcitrant carbohydrates. Hydrothermal treatment of lignin was investigated by many authors in in the late 80's. HTL reactions result in formation of a liquid product that can be easily stored, transported, and used for hydrogenation/deoxygenation upgrading. During HTL of lignin-based feedstock, a variety of soluble phenols, catechol-, guaiacol-, and other methoxy phenols are produced by hydrolysis of the feedstock's ether bonds. These products can further degrade by hydrolysis of methoxy groups while their benzene rings remain stable. It was also reported that repolymerization of these products occurred leading to formation of heavier insoluble products such as condensed phenols and phenolic biochar deposits (Barbier, Charon et al. 2012).

Catalysts play an important role in reducing biochar formation and increasing bio-oil yield. The presence of alkali catalysts (Na-, K-, and  $Ca^{2+}$  hydroxides and carbonates) facilitates solubility of lignin and suppresses condensation/repolymerization reactions (Ramsurn and Gupta 2012). Metallic and bimetallic oxide or sulfide- or noble metal-



based catalysts (often under the hydrogen atmosphere) may assist in depolymerization of lignin-based feedstock by cracking, hydrogenolysis, and hydrodeoxygenation reactions and improve bio-oil yield (Oasmaa, Alén et al. 1993, Zakzeski, Bruijninx et al. 2010). They seem to be an attractive option since they allow producing hydrocarbon-like products with lower oxygen content. However, heterogeneous catalysts typically provide lower bio-oil yields than homogeneous (alkali) catalysts. It seems to be more promising to depolymerize lignin-based feedstock by basic catalysts in the first stage followed by hydroprocessing with the objective to produce alkylbenzenes on sulfided hydrotreating or hydrocracking catalysts in the second stage (Shabtai, Zmierczak et al. 2003).

We assume that unlike alkali catalysts, the reduced CoMo/Al<sub>2</sub>O<sub>3</sub> used in our study does not significantly contribute to stabilization of bio-oil and inhibiting the formation of biochar from bio-oil, which results in lower bio-oil yield. Instead, it promotes decarboxylation of the aqueous products and probably their steam reforming as well as the methanation reaction, which leads to an extensive gas formation.

### **3.5. Overall mass balance for a conceptual biorefinery**

To determine the process yields, mass balance around pretreatment, enzyme hydrolysis, fermentation, and HTL and was developed and summarized in Fig. 19.

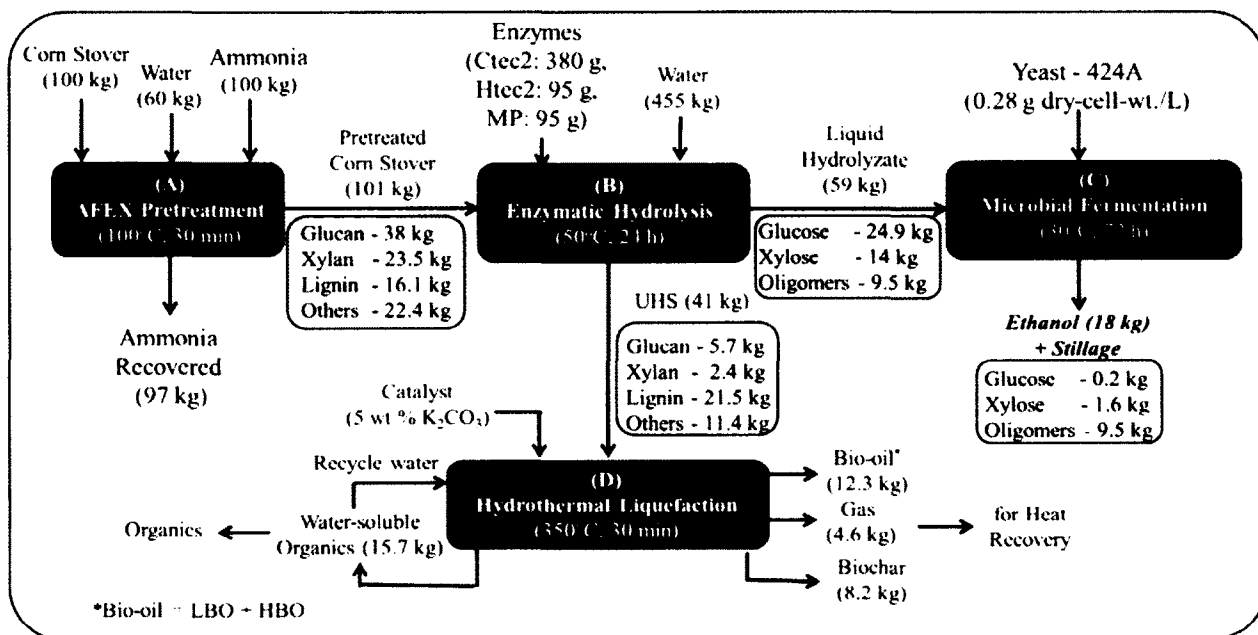


**Figure 19.** The overall mass balance for four different unit operations of a conceptual biorefinery to produce bioethanol and bio-oil from ACS-UHS. All the weights are reported on a dry basis.

Corn stover subjected to AFEX pretreatment (dry to dry process) was not altered in terms of carbohydrate composition. The ammonia released after AFEX pretreatment can be recycled and reused in a biorefinery. After 24 h of enzymatic hydrolysis of the ACS at 18% solid loading using the best combination of commercial enzymes (Ctec2, Htec2, and Multifect pectinase) approximately 70% glucan and 80% xylan were converted into soluble sugars. The rate of enzyme hydrolysis was fast during the first 24 h but after that slowed down considerably due to the substrate crystallinity, accessibility of unhydrolyzed polysaccharides, product inhibition, enzyme deactivation etc. (Hall, Bansal et al. 2010, Qing, Yang et al. 2010). For this reason, 24 h enzymatic hydrolysis was preferred to increase the efficiency of the whole process.

The residual UHS composed of 20.7% carbohydrates, 52.5% lignin and 5% protein was catalytically converted into bio-oil (30.1%), biochar (20.1%), gas (11.4%) and water-soluble organics (38.4%) through the HTL process, adding further value to the biorefinery. *Saccharomyces cerevisiae* (424A) produced 18 kg of ethanol with 95% metabolic yield consuming 99% of glucose and 88% of xylose without the addition of nutrients during the microbial fermentation of ACS hydrolysate. Since 424A strain can consume only monomeric sugars, about 9.5 kg of oligomeric sugars were left behind after the fermentation. The low carbohydrate conversion of ACS was compensated by the high metabolic yields during fermentation. The viability of the biorefinery ultimately depends on the cost of pretreatment, carbohydrate conversion, and ultimately ethanol yields and value added product streams (bio-oil, biochar, etc). About 41 kg of UHS was produced after 24 h of hydrolysis of 100 kg of ACS-UHS. Subjecting the 41 kg of UHS to the HTL process may conceptually result in the formation of 12.3 kg bio-oil, 4.6 kg gaseous products, 8.2 kg biochar, and 15.7 kg water-soluble organics. ECR for bio-oil produced at 320°C with K<sub>2</sub>CO<sub>3</sub> catalyst was 57.1%. Bio-oil can be further upgraded to obtain stable liquid compounds that can be used as transportation fuels or fuel additives through zeolite upgrading or catalytic hydrodeoxygenation (Hicks 2011). Biochar can be used as a solid fuel or a soil amendment additive. It is interesting to note that ECR for just bioethanol production from corn stover by AFEX pretreatment, enzymatic hydrolysis, and fermentation was 32.7%. Therefore, when HTL of ACS-UHS is integrated with bioethanol production from corn stover, the overall ECR can be increased up to 89.8%.

### 3.5.1. Energy requirements for HTL process

Estimation of energy requirements for HTL process was done by calculation the energy return on energy invested (ERoEI) by dividing the amount of energy in the produced bio-oils with the amount of energy required to bring the ACS-UHS suspension from 20°C and 1 atm to the best liquefaction conditions (320°C and 1640 psi (112 atm)) as described by (Valdez, Nelson et al. 2012). In order to determine the enthalpy of the reaction medium, the tables of thermodynamic properties of water were used assuming that the ACS-UHS-water mixture had the same enthalpy as the subcritical water under the above conditions. The enthalpy of the reaction medium was 1.46 MJ/kg. The bio-oil energy content was 57.1% of ACS-UHS that had HHV 14.21 MJ/kg. In a typical experiment, 0.2 kg of water and 0.05 kg of biomass were used. Therefore, the energy invested in HTL process was  $1.46 \text{ MJ/kg} * 0.2 \text{ kg} = 0.29 \text{ MJ}$ . The energy return with the produced bio-oils was  $14.21 \text{ MJ/kg} * 0.05 \text{ kg} * 0.571 = 0.406 \text{ MJ}$ . Therefore, ERoEI for the optimal HTL conditions was 1.40 (energy positive HTL). This calculation was based only on the liquefaction reactor. The ERoEI for the entire process would be higher because biochar with the energy content of 21.7% of ACS-UHS was also produced. In this case, ERoEI would be 1.93. In a properly designed HTL process, heat recovery should be incorporated so that the hot reactor effluents would be used to heat the feed stream. In this way, up to 80% of the heat can be recovered (Valdez, Nelson et al. 2012).

### 3.6. Future perspective and potential research areas

The study of catalytic liquefaction of ACS-UHS showed that this feedstock can be efficiently utilized for producing bio-oils with high energy density that can be further

upgraded to renewable transportation fuels. However, production of bio-oils through hydrothermal liquefaction and their upgrading to liquid fuels have not been commercialized up to date. Those processes require robust and selective catalysts developed specifically for liquefaction and conversion of bio-oils into liquid fuels. A number of studies have been done in this area that include C-O bonds cleavage through zeolite upgrading, hydrodeoxygenation, multi-step upgrading, unsupported organometallic catalysts upgrading (Hicks 2011), electrocatalytic hydrogenation and hydrodeoxygenation (Singh, Prakash et al. 2014), etc. The results of these studies show a good progress toward the potential commercialization of the liquid fuel production from bio-oils. However, further research is required to determine the optimal conditions and catalysts for bio-oil production/ upgrading.

Another area that can be further investigated is increasing degree of liquefaction and ECR of bio-oil production from lignin-based feedstock. A number of efficient liquefaction technologies exist up to day (Peterson, Vogel et al. 2008). However, further research is required to maximize the liquid product yield for the transportation fuels production. In this respect, using alcohols for HTL of lignin-based feedstock seems to be a promising way of maximizing bio-oil yield (Singh, Prakash et al. 2014).

The efficiency of different solvents for extraction of bio-oil from the aqueous phase might be a research area of interest. To our knowledge, no systematic information on solvent selectivity toward LBO was reported. Diethyl ether was used for LBO extraction in our study. However, a number of other non-polar solvents might be used for this extraction providing the higher bio-oil yield and/or lower oxygen content.

### 3.7. Executive summary

- Hydrothermal processing of ACS-UHS can provide an efficient method of bio-oil production. It is advantageous over pyrolysis as it allows converting biomass into bio-oils with higher energy and separation efficiency.
- Subcritical water technologies require less energy consumption since no phase change occurs (water remains in the liquid state). HTL allows producing liquid, solid, and gaseous products from wet and mixed feedstock with reduced mass transfer resistance.
- The use of 5 wt%  $K_2CO_3$  during HTL provided the higher degree of liquefaction (43.4%), higher total bio-oil yield (30.1 wt%), and higher ECR (57.1%) compared to HTL with no catalyst and CoMo/ $Al_2O_3$  catalyst.
- The formation of gaseous products was favored when CoMo/ $Al_2O_3$  was used. GC-MS and NMR results showed that the bio-oil contained mainly lignin-derived phenolic compounds.
- LBO contained a more diverse suite of phenolic compounds derived from lignin monomers while HBO contained a less complex mixture of compounds such as parabens and alkylphenols.
- Integration of bio-oil production from wet unhydrolyzed solids with bioethanol production in a second generation lignocellulosic-based biorefinery can increase the overall ECR from 57.1% to 89.8%.

### **3.8. Acknowledgments**

The authors would like to acknowledge the encouragement and support of our colleagues from the Department of Civil and Environmental Engineering at Old Dominion University in the preparation of this article. Our special appreciation is to the Research Foundation at Old Dominion University (ODURF) for providing the financial support for this research. We thank Prof. Bruce Dale (Michigan State University) for providing his laboratory space and equipment to process the ACS-UHS used in this study. We would also like to thank Prof. Nancy Ho (Purdue University) for providing yeast strain 424A and commercial enzymes Novozymes (Ctec2 and Htec2) and Genencor (Multifect Pectinase) for this research project.

## CHAPTER 4

### HYDROTHERMAL TREATMENT FOR ENHANCING OIL EXTRACTION AND BIOCHAR PRODUCTION FROM OILSEEDS

*Note: the contents of this chapter have been submitted for publication in the journal Renewable Energy in August 2014 and included into the international patent application.*

Popov, S., Abdel-Fattah, T., Kumar, S. Hydrothermally assisted oil extraction and hydrochar production from oilseeds. Submitted to *Renewable Energy*, ref. # RENE-D-14-01661R3. *The status of the manuscript at the time is under revision.*

Kumar, S., Popov, S., Majeranowski, P.J., Kostenyuk, I. Subcritical water assisted oil extraction and green coal production from oilseeds. International patent application PCT/US2013/064966, October 23, 2012.

A novel integrated oil extraction process that includes hydrothermal pretreatment and oil extraction (HPOE) from whole oilseeds followed by hydrothermal carbonization (HTC) of the extracted seedcake to biochar was developed. Five different types of oilseeds including cotton-, flax-, mustard-, canola-, and jatropha seeds were used in the study. The seeds were subjected to hydrothermal pretreatment in the range of temperatures from 120 to 210 °C for 30 min. Oils were extracted from the pretreated seeds using *n*-hexane in a Soxhlet apparatus for 120 min. The crude oil yields from the pretreated seeds at 180 °C and 210 °C were significantly higher (up to 30 wt%) than those from the respective untreated ground seeds. The seedcake after oil extraction was



subjected to HTC at 300 °C with the recycled aqueous phase collected from the pretreatment step. The produced biochar had higher heating value of 26.5 kJ/g comparable to that of bituminous coal. BET surface area and pore volume analysis showed that the pretreated seeds had larger surface area and pore volume/size than the respective raw seeds, which resulted in better extractability of oil, shorter extraction time, and overall efficiency of HPOE process. Analyses of the crude oil did not show significant signs of degradation after the hydrothermal pretreatment of oilseeds. The study is the first of its kind where integrated oil extraction and biochar production from oilseeds have been studied with the objective of minimizing feedstock preparation and maximizing oil extraction and overall energy conversion using environmentally benign hydrothermal processes.

#### **4.1. Introduction**

Oilseeds are a valuable source of oil that can be readily extracted and used in a number of applications. The oil content of various oilseeds typically accounts for 15-50 wt% the total seed mass. Oilseeds are primarily used for the production of vegetable oil and oilseed meal for food and animal feed. Oils of non-food quality are being envisioned as a valuable renewable feedstock for producing biodiesel or other alternative fuels that provide national energy security, reduce impact on the environment, and stimulate rural economic growth without affecting the food market (Demirbas and Demirbas 2007). The advantages of using oils from non-food-based resources for biofuel production include their availability, high energy density, biodegradability, near-zero aromatic and sulfur

content, and non-toxicity. The liquid nature of the oils makes them a convenient feedstock for transportation and processing.

One of the most costly stages in the production of fuels from oil-based feedstock is the extraction and purification of oils derived from the biomass (Naik, Goud et al. 2010). Therefore, developing efficient and robust oil extraction methods is a major challenge facing biofuels industries. A variety of methods of extracting oils from oilseeds exist to date. The oils are typically extracted using either mechanical pressing or different organic solvents. Mechanical extraction is simple but leaves behind up to 5-6 wt% unextracted oil (O'Brien, Farr et al. 2000). Solvent extraction provides better oil recovery but requires thorough preparation of the feedstock including drying, cleaning, dehulling, conditioning, flaking, cooking/tempering, and pre-pressing (Dunford 2012). A number of solvents can be used for oil extraction from oilseeds. However, *n*-hexane is the only solvent that has been used on a commercial scale and has demonstrated high efficiency for extraction of neutral lipids (triglycerides) from various oil crops (Safari 2011). For these reasons, *n*-hexane was employed as a solvent for extraction of oils in this study.

Hydrothermal pretreatment of oilseeds might be a promising way of increasing the extractability of oils without prior grinding and/or dehulling oilseeds (Go, Liu et al. 2013). Processing biomass under hydrothermal (subcritical water) conditions is considered an efficient and environmentally benign method that capitalizes on the extraordinary properties of water as a solvent and reaction medium. In subcritical water-based processes, water is kept in a liquid phase by applying pressure greater than the vapor pressure of water. In this way, the latent heat required for phase change of water is avoided, which requires less energy than steam generation (Kumar 2013).

A few types of oilseeds with different morphologies were used in this study. The hydrothermal pretreatment of the oilseeds was performed in a wide range of subcritical temperatures in order to determine the optimal conditions of the HPOE process. The process was aimed at maximizing extractability of oils mostly from inedible/non-food quality crops for biodiesel production. HPOE can also be used for extraction of oils from edible crops under milder conditions in order to minimize changes of the oil quality. In this case, carbonization of the extracted seedcake is not necessary; instead, it can be used as an animal feed. However, additional research is required for using HPOE for food applications.

Biochar is a valuable co-product that can be used as solid fuel, co-fired with coal, or as a soil amendment agent for growing oil crops. After a simple activation step, it can also be used for industrial wastewater treatment (Regmi, Garcia Moscoso et al. 2012). For some types of oilseeds like jatropha, which are highly toxic, utilization of the seedcake poses a challenge. Therefore, biochar production can be a feasible option that adds value to the overall process. Shackley et al. estimate the cost of biochar produced from green waste from \$91 to \$329 per ton depending on the type of storage and production facility (Shackley, Hammond et al. 2011).

The focus of this study was to develop and investigate an integrated oil extraction process that employs HPOE of the whole oilseeds followed by HTC of the extracted seedcake. The schematic of the integrated process is shown in Fig. 20. To the best of our knowledge, no research has been done on oil extraction and biochar production from hydrothermally pretreated seeds up to date (Kumar, Popov et al. 2014).

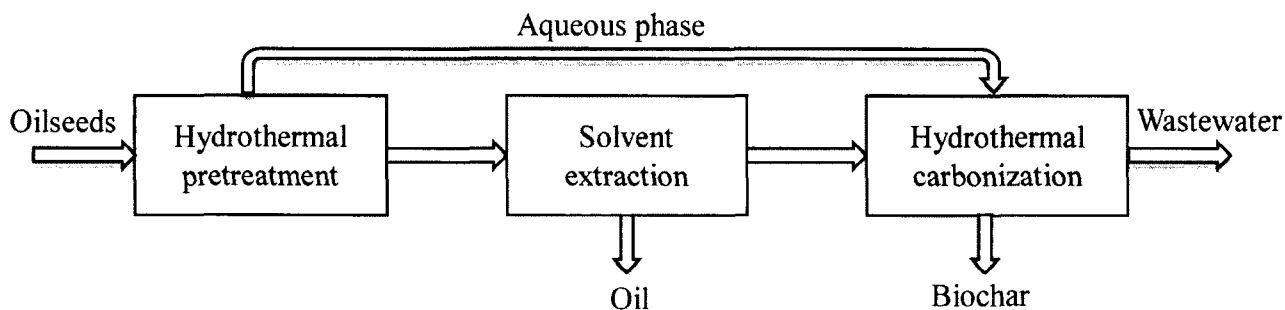


**Figure 20.** Schematic of the integrated HPOE process.

The novelty of the proposed process are: (i) using environmentally benign hydrothermal processes for maximizing oil yield without feedstock preparation, (ii) studying the effect of hydrothermal pretreatment on the oil yield from oilseeds with different morphologies and in a wide range of temperatures (120-210 °C), (iii) integrating oil extraction with biochar production, which increases the overall energy conversion of the feedstock.

The objectives of this study were as follows: (i) to evaluate the effect of hydrothermal pretreatment of oilseeds on the crude oil yields in the range of temperatures from 120 to 210 °C, (ii) to study the kinetics of Soxhlet extraction from both ground raw and whole pretreated seeds, (iii) to compare the composition and quality of the extracted crude oils, (iv) to utilize the extracted seedcake for biochar production using the aqueous phase obtained after the pretreatment step, and (v) to develop the overall mass balance of the HPOE process and evaluate its energy requirements.

The integrated process provides several major advantages over conventional processes including better extractability of oil, shorter extraction time, tolerance to high moisture content of the feedstock, avoidance of preparation stages, and utilization of

extracted seedcake for biochar production. The proposed HPOE process can potentially be integrated with biodiesel productions.

## 4.2. Materials and methods

### 4.2.1. Materials

Five types of oilseeds including cotton-, flax-, yellow mustard-, canola-, and *Jatropha curcas* seeds were purchased and used as received. The cottonseeds were obtained from a local farm in Virginia (white fuzzy seeds), the flax-, mustard-, and canola seeds were purchased from Superior Nut Company, Cambridge, MA, Penzeys Spices, Wauwatosa, WI, and Seedland, Wellborn, FL, respectively. *Jatropha curcas* seeds were purchased from Tree Seeds Plus eBay store. *n*-hexane 95% (Optima), methanol 99.9% (Optima LC/MC), ethanol 190 proof (95%), sodium hydroxide  $\geq 97\%$  (Pellets/Certified ACS), potassium hydroxide  $\geq 95\%$  (Pellets/Certified ACS), dichloromethane 99.5% (Pfaltz & Bauer Inc.), 2,2-diphenyl-1-picrylhydrazyl (95%), gallic acid (Powder/Certified), toluene  $\geq 99.5\%$  (Certified ACS) were purchased from Fischer Scientific USA and used as received.

For oil quality analysis, MXT-WAX capillary column (30 m x 0.53 mm x 1  $\mu\text{m}$ ) and FAME standards #1 and #3 containing 20 wt% methyl esters of caprylic (8:0), capric (10:0), lauric (12:0), myristic (14:0), palmitic (16:0), stearic (18:0), oleic (18:1), linoleic (18:2), and linolenic (18:3) acids (20 wt% each) were purchased from Restek, Bellefonte, PA. Rtx-65TG capillary column (30 m x 0.25 mm x 0.1  $\mu\text{m}$ ) was purchased from Restek, Bellefonte, PA. SCOTTY gas calibration standard containing 50 wt% H<sub>2</sub>, 10 wt% CH<sub>4</sub>,

10 wt% CO, 20 wt% CO<sub>2</sub>, 5 wt% ethylene, and 5 wt% propane was purchased from Sigma-Aldrich.

#### **4.2.2. Experimental part**

##### **4.2.2.1. Hydrothermal pretreatment of oilseeds**

The seeds for hydrothermal pretreatment experiments were used as received (without dehulling and grinding). All the oilseeds were dried for 24 h in an oven at  $65 \pm 3$  °C, packed in plastic bags, and stored in a dark and dry place at room temperature before being used. The moisture content of the seeds was determined with a moisture meter Denver Instrument IR 35 by drying them at 105 °C to constant weight. The moisture of oilseeds was  $\leq 1 \pm 0.2$  wt%.

The temperatures between 150 and 200 °C are typically used for hydrolysis of different types of biomass. Subcritical water treatment at the above temperatures was successfully employed for improving lipid extraction from yeast, activated sludge, and some oilseeds (Go, Liu et al. 2013). We used a broader range of pretreatment temperatures and longer times because oilseeds with very different morphologies were used as a feedstock in the study.

Hydrothermal pretreatment of the seeds was carried out in a 500 mL batch reactor equipped with a Parr 4848 controller at  $120 \pm 1$ ,  $150 \pm 1$ ,  $180 \pm 1$ , and  $210 \pm 1$  °C (the respective autogenous pressures were 205, 690, 1725, and  $3500 \pm 10$  kPa) for 30 min with continuous stirring at 300 rpm. In a typical experiment, the reactor was loaded with 30 g of seeds and 300 mL of deionized water, sealed, and kept under the above

conditions. The preheating time ranged between 10 min to 20 min ( $\sim 10$  °C/min) depending on the required reaction temperature.

After cooling the reactor down to the ambient temperature, the solid and liquid phases were separated by vacuum filtration. The pretreated seeds were dried in an oven at  $65 \pm 3$  °C for 24 h until the moisture content was below 1 wt%. After that, these pretreated seeds were gravimetrically quantified and stored at 4 °C for further analyses and solvent extraction. The aqueous product was stored at 4°C for further analyses and use in HTC experiments for biochar production. At least two replicates were done for each type of seed under different experimental conditions.

#### **4.2.2.2. Oil extraction**

The next step of the study was Soxhlet extraction of all the oilseeds with *n*-hexane as described elsewhere (Lawson 2010). The seeds having undergone hydrothermal pretreatment were used for the solvent extraction without grinding. The raw (untreated) seeds were ground into a fine fraction ( $< 0.71$  mm) with a food grinder for 60 s before the extraction step. 10 g of ground raw and pretreated at 120, 150, 180, and 210 °C seeds of each type was extracted with 300 mL of *n*-hexane in a Soxhlet apparatus for 120 min (8 cycles). Here, an extraction cycle is the filling of the Soxhlet apparatus chamber (250 mL) with *n*-hexane and the emptying of the solvent into a flask. One cycle of extraction took about 15 min. After extraction, *n*-hexane was removed by vacuum evaporation, and the crude oils were kept in an oven at  $70 \pm 3$  °C for 4 h to remove the remains of the solvent. Subsequently, the oils were gravimetrically quantified and stored at 4 °C. The

extracted seedcake was dried in an oven at  $65 \pm 3$  °C for 24 h until the moisture content was below 1 wt%, gravimetrically quantified, and stored at 4 °C.

#### 4.2.2.3. Kinetics of oil extraction

Since canola seeds provided the highest oil yield, they were used for the kinetic study of oil extraction efficiency. The kinetic study on both ground raw and pretreated at 210 °C canola seeds was carried out with 1, 2, 4, 6, and 8 cycles of Soxhlet extraction with *n*-hexane.

Kinetics of oil extraction processes is most often modeled by using the film theory (Veljković and Milenović 2002), the theory of unsteady diffusion through plant material (Velickovic, Milenovic et al. 2006), and the empirical Ponomaryov's equation (Ponomaryov 1976). Derivations of the model equations can be found elsewhere (Veljković and Milenović 2002). All the models are two-parametric and are based on the two-stage extraction mechanism. One parameter characterizes the washing stage (so-called washing coefficient, *b*) and the second one characterizes the slow extraction stage (so-called slow extraction coefficient, *k*).

For the purpose of mathematical modeling of the oil extraction from the seeds, Ponomaryov's model was applied to the kinetic study. The basic equation of this kinetic model is provided below:

$$(1 - q/q_0) = kt + b \quad (35)$$

where: *q* – oil content of the seeds during the extraction, g/100 g

*q*<sub>0</sub> – oil content present in the seeds, g/100 g



$k$  – specific rate of slow extraction, i.e., slope of the dependence of  $(1 - q/q_0)$  versus time (slow extraction coefficient),  $\text{min}^{-1}$

$b$  – washing coefficient, 1

$t$  – time, min

The parameters of the kinetic model were calculated from the experimental data by means of linear regression using equation (35).

#### **4.2.2.4. HTC of the seedcake**

In order to add value to the oils, extracted canola and jatropha seedcakes pretreated at  $210^\circ\text{C}$  were subjected to HTC in a 500 mL batch reactor equipped with Parr 4848 controller. 20 g of the extracted seeds and 300 mL of the aqueous phase obtained after their pretreatment were loaded into the reactor. The reactor was sealed, purged with nitrogen for 5 min, and kept at the temperature of  $300^\circ\text{C}$  and autogenous pressure of  $8600 \pm 10$  kPa for 60 min with continuous stirring at 300 rpm. The preheating time was 30 min ( $\sim 10^\circ\text{C}/\text{min}$ ). After the reactor cooled down to the ambient temperature, the gas phase was volumetrically quantified and collected for analysis, and the solid and liquid phases were separated by vacuum filtration. The produced biochar was dried in an oven at  $65 \pm 3^\circ\text{C}$  for 24 h and gravimetrically quantified. The HTC experiments were done in duplicate.

### 4.2.3. Analytical part

#### 4.2.3.1. Aqueous phase analyses

The aqueous phase collected after the pretreatment step was volumetrically quantified and analyzed for pH, total organic carbon (TOC), and total nitrogen (TN) with Shimadzu TOC<sub>VPN</sub> analyzer. All the analyses were done in triplicate.

#### 4.2.3.2. Crude oil analyses

The oil yield (in g/100 g of dry seeds) after each extraction was determined as a ratio of the mass of the extracted crude oil to the mass of the seeds used for extraction. Evaluation of any possible degradation of canola and jatropha oils after their hydrothermal pretreatment was performed by free fatty acid (FFA) titration, gas chromatography (GC-FID), gas chromatography-mass spectrometry (GC-MS), and Fourier transform infrared spectroscopy (FTIR). The unsaponifiable matter and antioxidant activity of the crude oils extracted from the raw and pretreated at 210 °C canola and jatropha seeds were also determined. All the analyses were done in triplicate.

**FFA titration:** The oils obtained from raw and pretreated at 120, 150, 180, and 210 °C canola and jatropha seeds were dissolved in isopropanol (1:10) and titrated against 0.1 N NaOH solution with phenolphthalein indicator to determine their FFA concentrations.

**GC-FID:** The oils extracted from raw and pretreated canola and jatropha seeds were analyzed with SRI-GC8610C gas chromatograph equipped with a flame ionization detector (FID) to compare their chromatograms/FFA profiles. External calibration curves

were generated using 0.2-20 mg of pure standards dissolved in dichloromethane. Each calibration curve was generated by fitting a straight line with the y-intercept passing through zero ( $R^2 > 0.98$ ). The oils were converted into fatty acid methyl esters (FAMES) with methanol and NaOH as a catalyst (0.35% methoxide). The obtained FAMES were washed with deionized water, re-dissolved in *n*-hexane, separated from the water phase, dried over anhydrous  $\text{Na}_2\text{SO}_4$ , recovered by vacuum evaporation, and dissolved in dichloromethane. Helium at 130 kPa (10 mL/min) was used as a carrier gas. The temperature program was set up as follows: the initial oven temperature 120 °C, hold for 3 min, ramp at 20 °C/min to 220 °C, hold for 10 min; injector temperature 230 °C, detector temperature 250 °C. 1  $\mu\text{L}$  of each sample was injected into the column. FAMES were identified by comparing their retention times and peak areas with the standards.

**GC-MS:** The oils extracted from raw and pretreated canola and jatropha seeds were analyzed with Shimadzu GCMS-QP2010 gas chromatograph-mass spectrometer to compare their chromatograms/compositions. The oils were dissolved in dichloromethane and 1  $\mu\text{L}$  of each sample was injected into the column with the split ratio 1:80. Helium at 82.5 kPa (0.7 mL/min) was used as a carrier gas. The temperature program was set up as follows: the initial oven temperature 220 °C, hold for 2 min, ramp at 5 °C/min to 350 °C, hold for 37 min; injector temperature 350 °C, detector temperature 350 °C.

**FTIR:** FTIR analysis of oils extracted from the raw and pretreated at 210 °C canola and jatropha seeds was done with a Shimadzu IR Prestige-21 spectrophotometer in the range of wavenumbers of 4000-400  $\text{cm}^{-1}$  to compare the absorbance spectra of the oils and detect any changes in their functional groups.

**Unsaponifiable matter:** The amount of unsaponifiable matter in the crude oils extracted from all the raw and pretreated at 210 °C seeds was determined using an official method ISO 18609 (2000).

**Antioxidant activity:** Antioxidant activity of the crude oils extracted from the raw and pretreated at 210 °C canola and jatropha seeds was determined using the 2,2-diphenyl-1-picrylhydrazyl (DPPH) radical scavenging capacity method as described elsewhere (Karadag, Ozcelik et al. 2009). The DPPH method is widely used to test the ability of compounds to act as free radical scavengers or hydrogen donors and to evaluate the antioxidant activity of foods. The oil samples (50-400 mg/mL) were dissolved in toluene and DPPH reagent (0.8-6.4 mg/mL) was added to the samples. Absorbance of the oil samples was measured with UV-spectrophotometer at 520 nm. Gallic acid was used as a reference standard.

#### **4.2.3.3. Gaseous products analysis**

The gaseous products obtained after HTC of canola and jatropha seedcakes were volumetrically quantified, collected, and analyzed with SRI-GC8610C gas chromatograph equipped with 10' x 1/8" SS Hayesep-D packed column and a thermal conductivity detector (TCD). Helium at 145 kPa (10 mL/min) was used as a carrier gas for the analysis. The temperature program was set up as follows: initial temperature 40 °C, hold for 7 min, ramp at 10 °C/min to 120 °C. External calibration curves were generated using a SCOTTY gas calibration standard mixture. The analysis was done in triplicate.

#### 4.2.3.4. Solid phase analyses

At different stages of processing, oilseeds were subjected to Brunauer-Emmett-Teller (BET) surface area and pore volume/size analysis, scanning electron microscope (SEM) analysis, ash analysis, and elemental analysis. All the analyses were done in triplicate.

**BET:** BET analysis was carried out with a NOVA 2000e surface area and pore size analyzer (Quantachrome Instruments). Ground raw and pretreated at 210 °C canola and jatropha seeds after the Soxhlet extraction were used for the analysis. In order to avoid volatilization, the samples were subjected to degassing at 70°C with continuous flow of nitrogen and helium at 70 kPa prior to the analysis. Liquid nitrogen was used as an adsorbent during the analysis. Multi-Point BET method was used to determine the surface area and BJH method was used as the most common and accurate method to compute the pore volume and size of the samples.

**SEM:** SEM images of the samples of the ground raw and pretreated at 210 °C jatropha seeds were obtained using a JEOL JSM-6060 LV environmental electron microscope. The samples were placed on an adhesive carbon tape attached to an aluminum stub and sputtered with gold plasma. The surface morphology of the samples was studied at 450-480x magnification.

**Ash analysis:** Ash analysis of the raw, pretreated, extracted, and carbonized canola and jatropha seeds was done according to NREL/TP-5100-60956 standard method. The samples were placed in ceramic crucibles and kept in a muffle furnace at  $575 \pm 5$  °C for 4

h. After cooling the furnace down, inorganic content of the samples (ash) was determined gravimetrically.

**Elemental analysis:** Elemental analysis of the raw, pretreated, extracted, and carbonized canola and jatropha seeds was carried out with a ThermoFinnigan Flash EA 1112 automatic elemental analyzer and higher heating values (HHVs) of all the samples were calculated on ash basis using modified Dulong's formula (Basu 2013):

$$\text{HHV} = (349.1 (\%C) + 1178.3 (\%H) - 103.4 (\%O) - 15.1 (\%N) - 21.1 (\%Ash)) / 1000 \quad (36)$$

#### 4.2.4. Statistics

For all the experimental data and analyses results, mean values and relative standard deviations (RSD) were calculated and used for evaluating the variability in the data sets.

### 4.3. Results and discussion

#### 4.3.1. Hydrothermal pretreatment of oilseeds

After the hydrothermal pretreatment, the oilseeds acquired a darker color but retained their original shapes. Weights of the seeds after the pretreatment step are provided in Table 16.

**Table 16.** Weights of oilseeds after hydrothermal pretreatment (RSD < 2%).

Pretreatment temperature, °C	Cotton		Flax		Mustard		Canola		Jatropha	
	g	wt%	g	wt%	g	wt%	g	wt%	g	wt%
120	21.6	72.0	25.7	85.7	23.7	79.0	26.6	88.7	25.8	86.2
150	19.5	65.0	22.5	75.0	20.0	66.7	24.9	81.7	23.5	78.3
180	18.3	61.0	19.4	64.7	18.7	62.3	21.8	72.7	21.7	72.5
210	16.3	54.3	17.8	59.3	17.0	56.7	20.2	67.3	19.4	64.7

The results of the pH and TOC analyses of the aqueous phase collected after the hydrothermal pretreatment of the oilseeds for all the conditions studied are provided in Fig. 21 a, b.

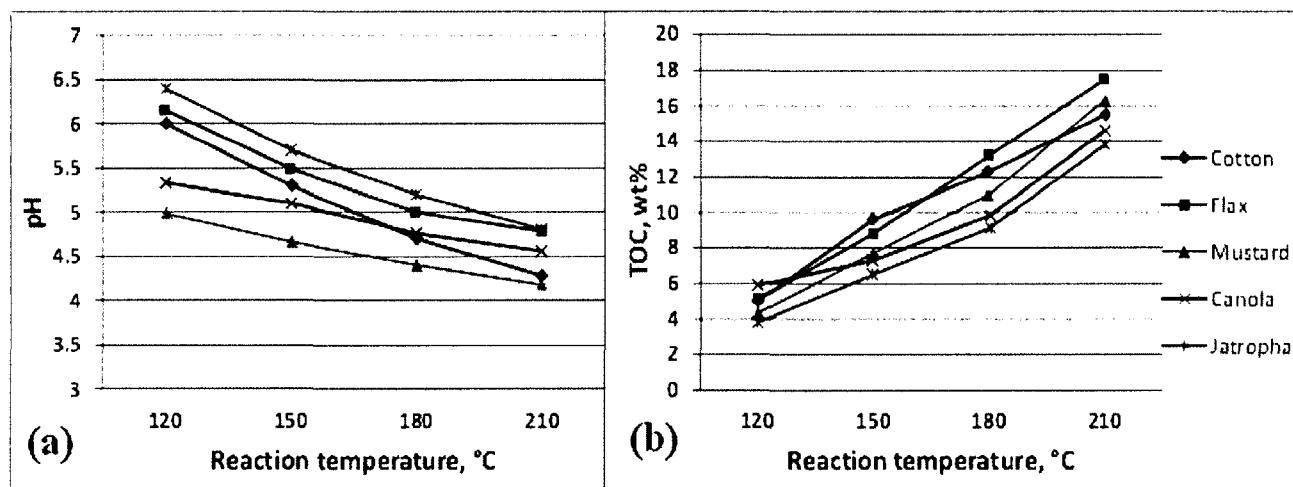


**Figure 21.** (a) Distribution of products' pH in aqueous phase (RSD < 2.8%), (b) distribution of TOC in aqueous phase (RSD < 2.2%).

TN distributions followed the similar trend with concentrations of 30-35% of the respective TOC. Quantification of the solid phase and analyses of the aqueous phase after the hydrothermal pretreatment (Table 16, Fig. 21 a, b) indicated that hydrolysis of the cellulose shells of the oilseeds as well as carbohydrates and proteins from the kernels took place in the pretreatment step. Soluble carbohydrates, peptides/amino acids, and other hydrolysis products released into the aqueous phase reduced its pH and increased the amounts of TOC and TN. Lower pH and higher TOC and TN concentrations were observed for higher pretreatment temperatures.

#### **4.3.2. Oil extraction**

The pretreated oilseeds were used for the extraction with n-hexane (without grinding) in a Soxhlet apparatus. The respective raw (untreated) seeds as controls were ground into a fine fraction ( $\leq 0.71$  mm) prior to the extraction step. The results of crude oil extraction from all the ground raw and pretreated seeds are provided in Fig. 22.



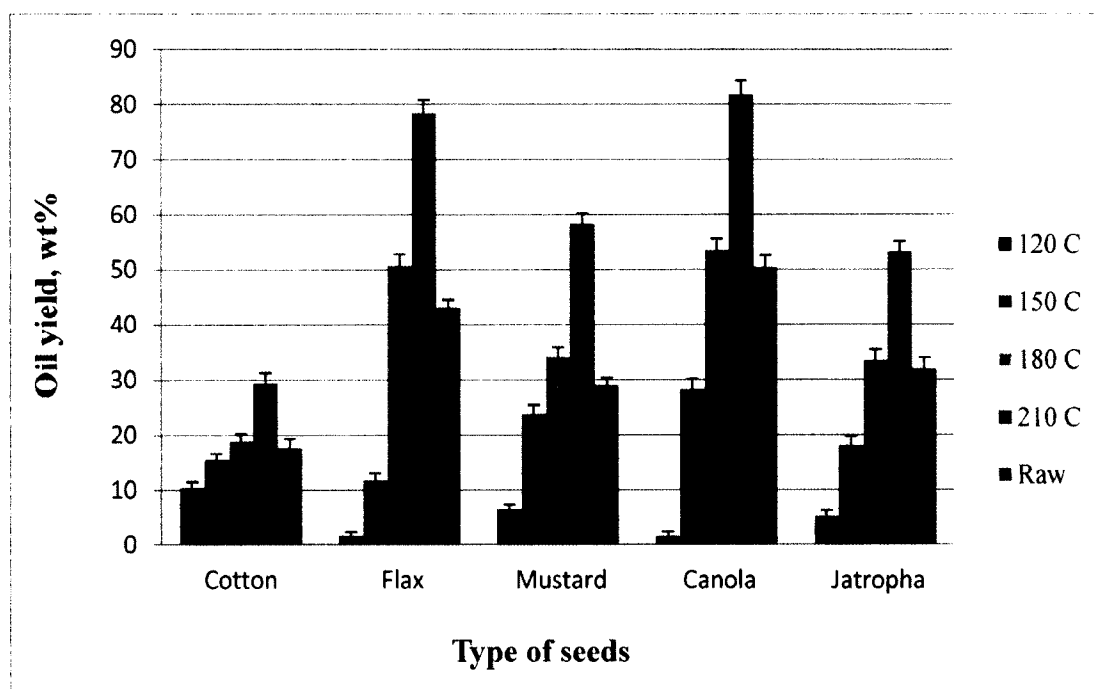


**Figure 22.** Crude oil yields from raw and hydrothermally pretreated at different temperatures oilseeds.

As can be seen in Fig. 22, the HPOE process for all the oilseeds pretreated at 180 and 210 °C resulted in higher crude oil yields compared to those from the respective ground raw seeds (controls). The crude oil yields from the cotton-, flax-, mustard-, canola-, and jatropha seeds pretreated at 210 °C were higher than those from the respective raw seeds by 11.6, 35.3, 31.3, 32.9, and 21.1 wt% and reached as much as 81.7 wt% for canola seeds (on a pretreated seed basis).

Calculations of the crude oil yields on a raw (untreated) seed basis showed that the yields from the most of seeds pretreated at 210 °C exceeded the yields from the respective ground raw seeds. The results of oil extraction from the raw and pretreated

seeds on a raw seed basis are provided in Fig. 23. Calculations were done for mean values of oil yields and seed weights.

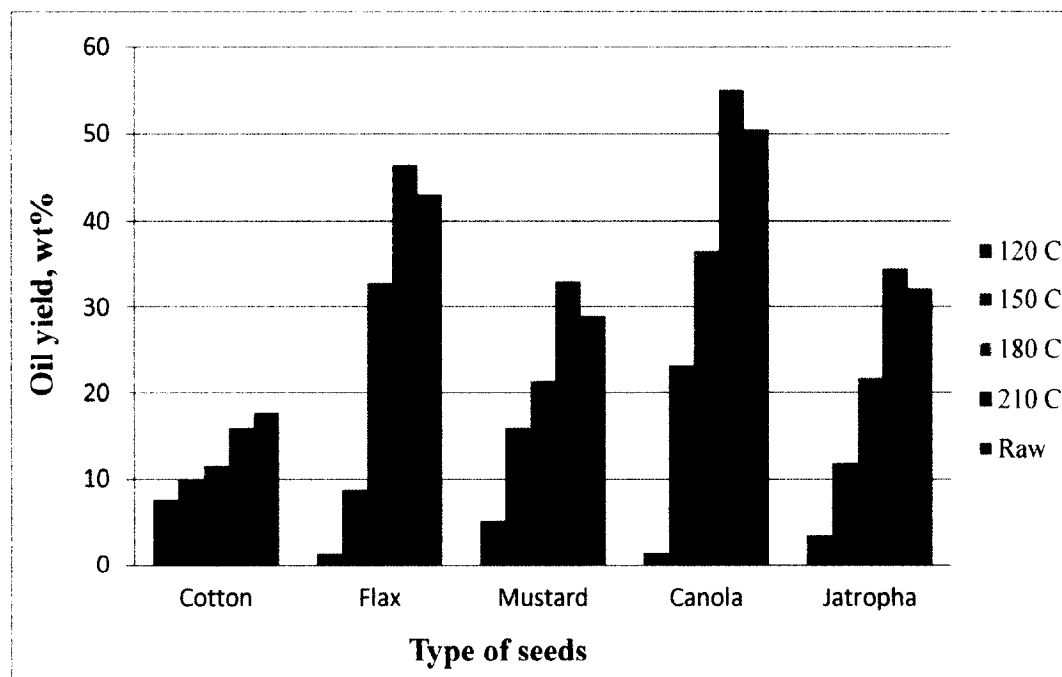


**Figure 23.** Crude oil yields from raw and hydrothermally pretreated at different temperatures seeds on a raw seed basis.

The crude oil yields from the hydrothermally pretreated flax-, mustard-, canola-, and jatropha seeds calculated on a raw seed basis were higher than those from the respective raw seeds by 3.4, 4.0, 4.5, and 2.3 wt% (Fig. 22). A part of this excess can be attributed to unsaponifiable matter present in the crude oils.

FFA concentrations in the oils obtained from the raw and pretreated at 120, 150, 180, and 210 °C canola and jatropha seeds were determined by titration (Fig. 24).

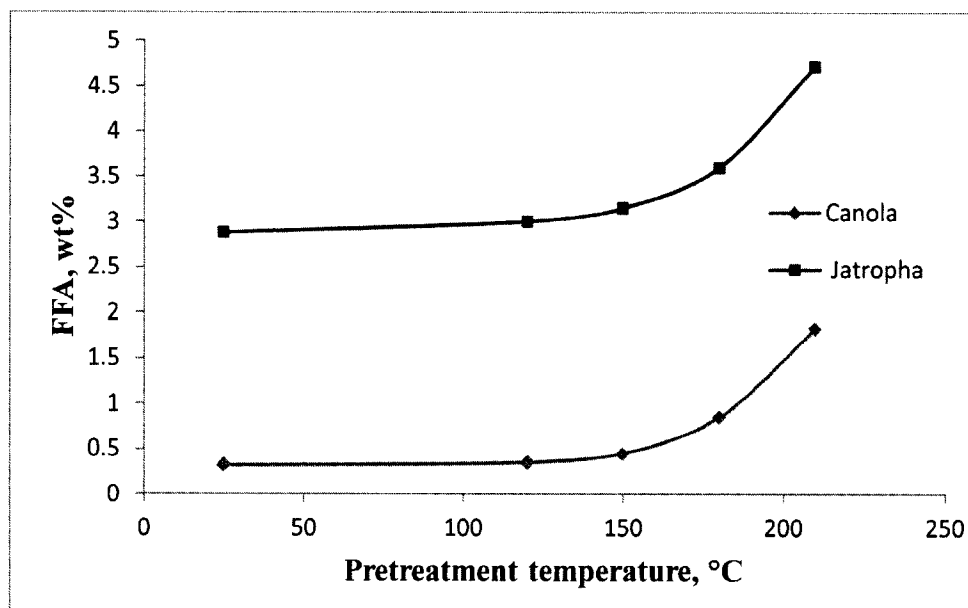


**Figure 24.** FFA concentrations in crude oils extracted from raw and pretreated at different temperatures canola and jatropha seeds (RSD < 2.1%).

As can be seen in Fig. 24, FFA concentrations increased from 0.32 to 1.82 wt% for canola- and from 2.88 to 4.72 wt% for jatropha oil with increase of the pretreatment temperature.

The oils extracted from raw and pretreated canola and jatropha seeds were also analyzed with GC-FID to compare their compositions. FFA profiles of the samples were consistent with the respective profiles of canola and jatropha oils reported elsewhere (Pitts and Thomson 2003). The compositions of the oils extracted from the raw and pretreated seeds are shown in Table 17.

**Table 17.** Fatty acid compositions of oils extracted from raw and hydrothermally pretreated canola and jatropha seeds

Sample	Fatty acid composition, wt%					
	Palmitic (16:0)	Stearic (18:0)	Oleic (18:1)	Linoleic (18:2)	Linolenic (18:3)	
Canola	Raw	8.0 ± 0.1	2.0 ± 0.1	55.3 ± 0.2	20.6 ± 0.15	13.2 ± 0.15
	Pretreated	7.6 ± 0.1	2.5 ± 0.1	59.6 ± 0.2	17.0 ± 0.15	12.3 ± 0.15
Jatropha	Raw	14.1 ± 0.15	7.0 ± 0.1	44.4 ± 0.2	32.5 ± 0.2	< 1
	Pretreated	13.6 ± 0.15	7.4 ± 0.1	47.2 ± 0.2	29.8 ± 0.2	< 1

As shown in Table 17, hydrothermal pretreatment did not significantly change FFA profiles of canola and jatropha oils. However, a noticeable increase of C18:1 and decrease of C18:2 and C18:3 FAMES concentrations in the oils extracted from pretreated seeds compared to the ones extracted from raw seeds were observed.

Hydrolysis of triglycerides typically begins at temperatures above 250 °C (Alenezi, Leeke et al. 2009). The increase of FFA concentrations and the change of FFA profiles of oils extracted from hydrothermally pretreated oilseeds at the temperatures above 180 °C can be attributed to the simultaneous hydrolysis of phospholipids and the hydrogenation of the double bonds of C18:2 and C18:3 FFAs resulting in formation of C18:1 and C18:0 FFAs. This phenomenon was reported by Shin et al. who studied the stability of FFAs under subcritical water conditions (Shin, Ryu et al. 2012) and Changi et

al. who reported the reaction pathway of phospholipids under sub- and supercritical water conditions (Changi, Matzger et al. 2012).

GC-MS analysis of oils extracted from raw and pretreated at 210 °C canola and jatropha seeds did not show any difference in their composition. In both types of oils, insignificant amounts of mono- and diglycerides ( $0.5 \pm 0.2$  wt%) were observed. Mainly triglycerides with molecular weights ranging from 780 to 860 were detected in all the samples. Mono- and diglycerides were quantified by assuming that their detector responses were similar to that of triglycerides and calculating their concentrations from peak areas.

FTIR analysis was done for the samples extracted from raw and pretreated canola and jatropha seeds. The absorbance spectra of the oils extracted from both types of the raw seeds were similar as well as the spectra of both types of the oils extracted from the pretreated seeds. Therefore, only the spectra for jatropha oils are provided (Fig. 25 a, b).

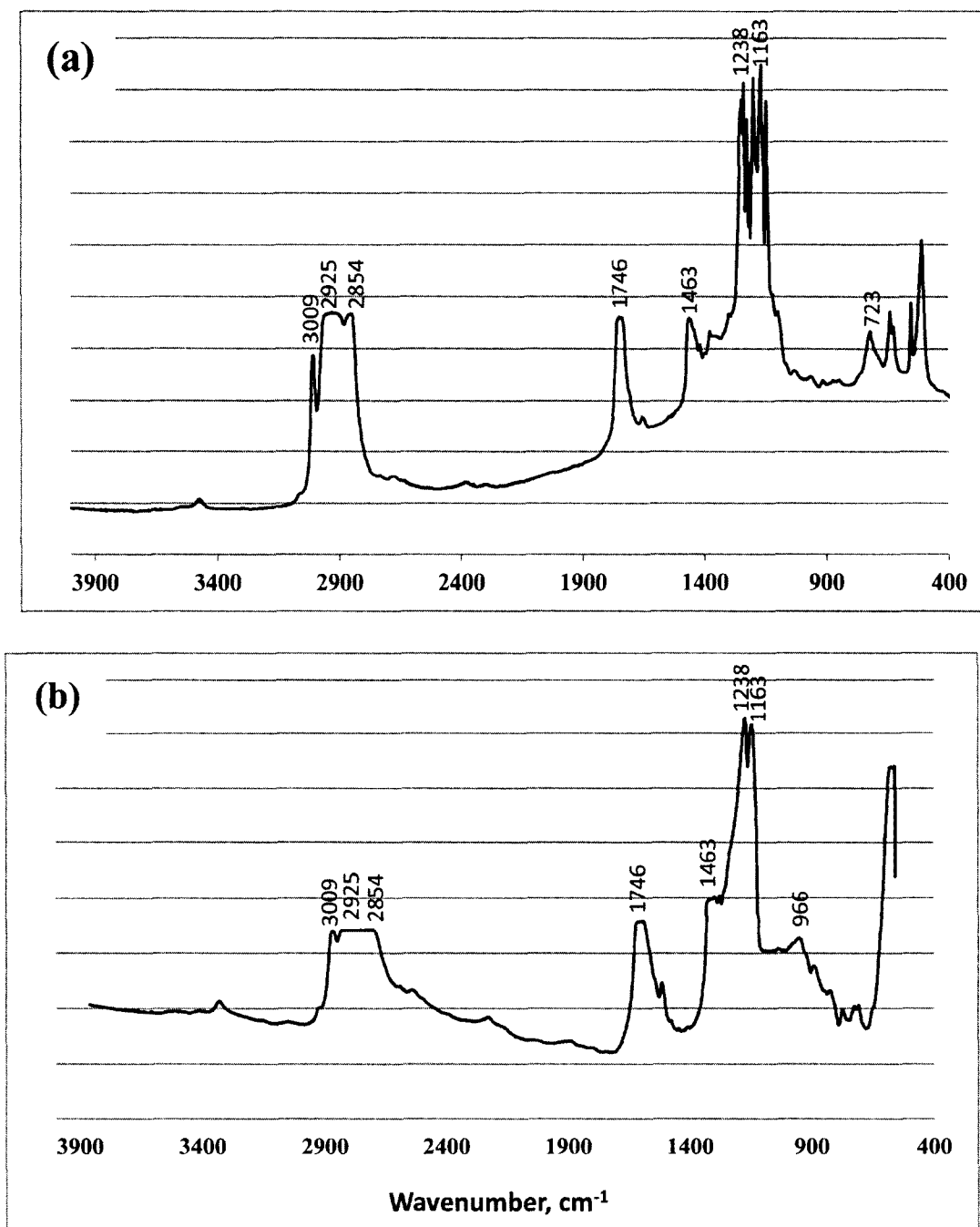


**Figure 25.** FTIR spectra of oils extracted from (a) raw and (b) pretreated at 210 °C jatropha seeds.

Table 18 provides the analytical evaluation of these spectra (Vlachos, Skopelitis et al. 2006). It can be seen in Fig. 25 that both samples do not have a significant difference in composition except for the bands around 723 and 966  $\text{cm}^{-1}$  assigned to *cis*- and *trans* -CH=CH- banding out of plane, respectively.

**Table 18.** Evaluation of FTIR spectra of jatropha oils

Wavenumber, $\text{cm}^{-1}$	Functional group
3009	C-H stretching vibration of the <i>cis</i> -double bond (=CH)
2925, 2854	Symmetric and asymmetric stretching vibration of the aliphatic $\text{CH}_2$ group
1746	Ester carbonyl functional group of the triglycerides
1463	Bending vibrations of the $\text{CH}_2$ and $\text{CH}_3$ aliphatic groups
1238, 1163	Stretching vibration of the C-O ester groups
966	<i>trans</i> -CH=CH- banding out of plane
723	<i>cis</i> -CH=CH- banding out of plane

An infrared absorbance band at 966  $\text{cm}^{-1}$  that is unique for *trans* fatty acids (Mossoba, Milosevic et al. 2007) was observed in the spectra of the oil samples extracted from the pretreated at 210 °C seeds. This is consistent with *cis-trans* isomerization studies of vegetable oils or model compounds of fatty acids reported elsewhere (Kemény, Recseg et al. 2001). It is well known that heat induced formation of *trans* fatty acids during deodorization of vegetable oils occurs when temperatures are above 200 °C and

overheated water steam is present. It can be concluded that hydrothermal pretreatment of oilseeds at 210°C promotes *trans* isomerization of the oils.

Antioxidant activity of the oils extracted from the raw and pretreated at 210 °C canola and jatropha seeds was determined using DPPH method. The samples of oils extracted from the pretreated seeds showed a more than twice higher DPPH radical scavenger activity than the samples of oils extracted from the respective raw seeds (37% and 34% vs. 16% and 10% (RSD < 3%) for 400 mg/mL samples with 6.4 mg/mL DPPH). The results of the DPPH analysis indicates that the oils extracted from the hydrothermally pretreated seeds have better antioxidant properties than the ones extracted from the respective raw seeds. It can be implied that unsaponifiable constituents of the oils (hydrocarbons, terpene alcohols, sterols, tocopherols, and other phenolic compounds as well as other hydrolysis products) may act as oxidation inhibitors under a range of conditions (Bosku 1976). This suggests that the oils extracted from hydrothermally pretreated seeds are relatively more stable than those extracted from raw seeds.

The results of analysis of unsaponifiable matter in the crude oils extracted from the raw and pretreated at 210 °C seeds are provided in Table 19.



**Table 19.** Unsaponifiable matter in crude oils extracted from raw and pretreated at 210 °C seeds, wt%

Type of seeds	Unsaponifiable matter	Unsaponifiable matter
	(raw seeds)	(pretreated seeds)
<b>Cotton</b>	1.6 ± 0.1	3.5 ± 0.2
<b>Flax</b>	1.7 ± 0.1	3.8 ± 0.22
<b>Mustard</b>	1.7 ± 0.1	4.3 ± 0.21
<b>Canola</b>	1.8 ± 0.15	4.8 ± 0.23
<b>Jatropha</b>	3.3 ± 0.15	4.7 ± 0.2

As shown in Table 19, the amount of unsaponifiable matter in the pretreated cotton-, flax-, mustard-, canola-, and jatropha seeds was higher than that in the respective raw seeds by 1.9, 2.1, 2.6, 3.0, and 1.4 wt%, respectively.

The comparative analyses of the oils extracted from the raw and pretreated oilseeds showed that the latter had higher FFA content, different FFA profiles of the extracted oils (increase of C18:0 and C18:1 and decrease of C18:2 and C18:3 FFAs), appearance of *trans* isomers, and better antioxidant properties.

It can be concluded that hydrothermal pretreatment of oilseeds under the conditions studied resulted in a noticeable increase of extractability of oilseeds without significant changes of the composition and quality of the extracted oils. A part of this

increase can be attributed to unsaponifiable matter present in the crude oils extracted from the pretreated seeds in higher concentrations than in the oils obtained from the raw seeds. However, the HPOE process provided better extractability of oils from the pretreated seeds compared to the ground raw ones (up to 1-1.5 wt% on an unsaponifiable matter-free basis). The process does not require grinding or other preparation of oilseeds prior to extraction, which makes hydrothermal pretreatment an attractive option.

#### 4.3.3. Kinetics of oil extraction

The crude oil yield extracted from the pretreated at 210 °C canola seeds on a raw seed basis was adopted as the oil content initially present in the seeds ( $q_0 = 55 \text{ g}/100 \text{ g}$ ).

The results of the study are shown in Table 20.

**Table 20.** Crude oil yield from ground raw and hydrothermally pretreated at 210 °C canola seeds at different number of extraction cycles (RSD < 2%)

Number of cycles	Raw canola, wt%	Pretreated canola, wt%
1	34.9	36.7
2	39.7	43.3
4	44.8	50.3
6	46.4	53.7
8	50.5	55.0

The parameters of the kinetic model were calculated from the experimental data provided in Table 20 by means of linear regression using equation (1).  $(1 - q/q_0)$  vs.  $t$  values were plotted on the graph (Fig. 26) and the equations for the linear parts of the curves were obtained.

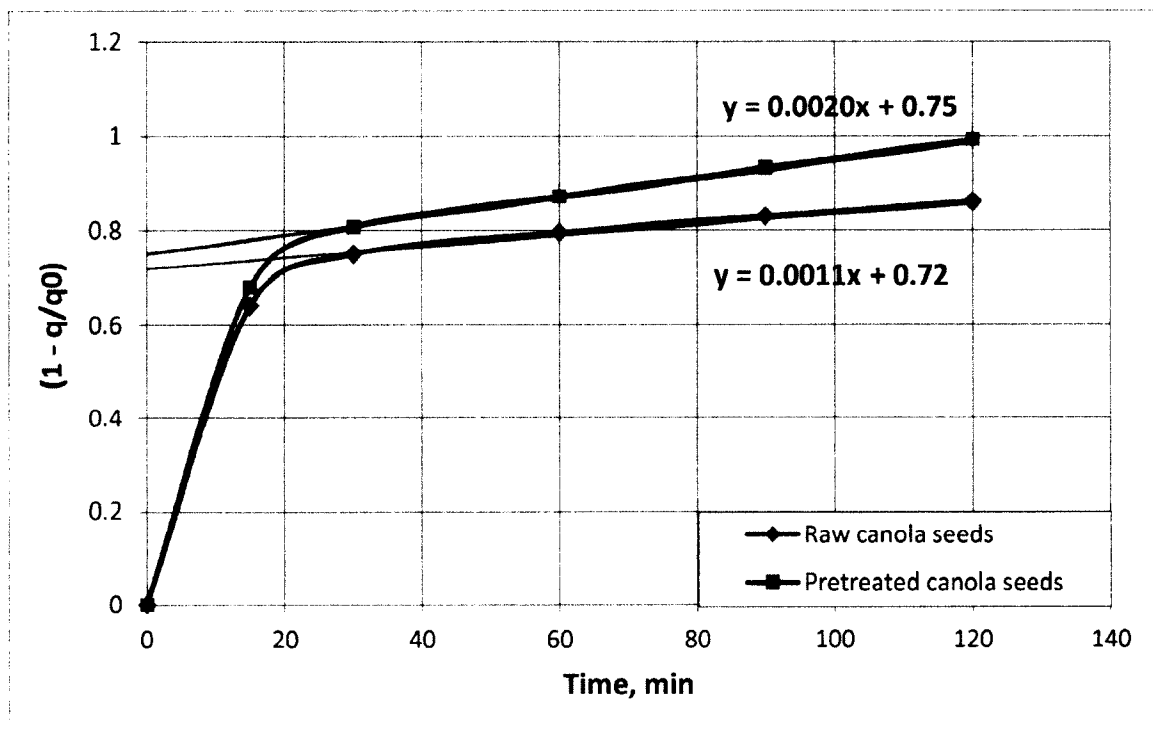


**Figure 26.** Progress of oil extraction from ground raw and hydrothermally pretreated canola seeds.

The obtained equations for the ground raw and pretreated canola seeds, respectively, can be expressed as follows:

$$(1 - q/q_0) = 0.0011t + 0.72 \quad (37)$$

$$(1 - q/q_0) = 0.0020t + 0.75 \quad (38)$$

Therefore, in the case of extraction of the raw seeds, the coefficients are:  $k_g = 0.0011 \text{ min}^{-1}$ ,  $b_g = 0.72$ ; in the case of extraction of the pretreated seeds, the coefficients are:  $k_p = 0.0020 \text{ min}^{-1}$ ,  $b_p = 0.75$  (the coefficient of linear correlation  $R^2$  for linear parts of the curves was higher than 0.98 for both cases).

As can be seen in the above equations (37) and (38), both the washing coefficient  $b$  and the specific rate of slow extraction  $k$  were higher in the case of the Soxhlet extraction of the hydrothermally pretreated canola seeds.

The plotted curves were of the same shape as those of classical extractions from plant materials reported elsewhere (Veličković, Milenović et al. 2008). Two periods of extraction can be observed for both raw and pretreated seeds: washing, characterized by a rapid increase in the concentration of the oil in the beginning of the process, and slow extraction (approximately after the first 20 min), characterized by a slow increase in the concentration of the oil. The washing period had almost the same rate for both cases ( $b_p = 0.75 \approx b_g = 0.72$ ) while the slow extraction period rate was noticeably faster for the hydrothermally pretreated seeds ( $k_p = 0.0020 > k_g = 0.0011$ ).

Based on the kinetic study, the faster extraction of hydrothermally pretreated seeds can be explained by the shorter distance that oil has to diffuse from the seed body in order to reach the solvent. This phenomenon can be due to the higher porosity and greater surface area of the pretreated seeds, which enables more oil to come into direct contact with the solvent, thus enhancing the slow extraction period rate.

#### 4.3.4. HTC of the seedcake

The gaseous products after HTC of the extracted canola seeds consisted of CH<sub>4</sub> (1.4 ± 0.2 wt%), CO (9.6 ± 0.2 wt%), and CO<sub>2</sub> (89.0 ± 0.2 wt%). The analyses of the gas products obtained after the carbonization of extracted jatropha seeds showed the presence of CH<sub>4</sub> (1.2 ± 0.2 wt%), CO (10.2 ± 0.2 wt%), CO<sub>2</sub> (88.5 ± 0.2 wt%), and traces of C<sub>2</sub>H<sub>2</sub>. The calculated masses of the gaseous products were 4.3 ± 0.3 g (21.6 wt%) for canola and 2.4 ± 0.3 g (12.1 wt%) for jatropha seeds. The gas formation can be attributed mainly to the soluble organic matter contained in the aqueous phase that was used for the carbonization of the extracted seedcakes.

After opening the reactor, solid and liquid phases were separated and quantified. 12.0 ± 0.1 and 12.3 ± 0.1 g (yield 60.0 and 61.5 wt%) of biochar were produced from the extracted canola and jatropha seeds, respectively.

The results of the BET surface area and pore volume/size analysis for raw and pretreated canola and jatropha seeds are provided in Table 21.

**Table 21.** BET surface area and pore size/volume analysis results for raw and pretreated canola and jatropha seeds (RSD < 2.5%).

Sample	Surface area, m <sup>2</sup> /g	Pore volume, cc/g	Pore diameter, nm
	(Multi-Point BET)	(BJH method)	(BJH method)
Canola	Raw	1.81	7.10 * 10 <sup>-4</sup>
	Pretreated	24.67	7.77 * 10 <sup>-3</sup>

<b>Jatropha</b>	<b>Raw</b>	1.30	$7.22 * 10^{-4}$	20.60
	<b>Pretreated</b>	24.70	$8.40 * 10^{-3}$	54.20

As we can see in Table 21, the surface area, pore volume, and pore size of the hydrothermally pretreated oilseeds were greater than those of the raw seeds, which provided their better extractability and shorter extraction time (Table 20, Fig. 26). This phenomenon can be attributed to the partial hydrolysis of the oilseeds with degradation of the cellulose hulls, swelling of the kernel matrix, and removal of carbohydrates and proteins from the kernels to the aqueous phase in the pretreatment step. This retains lipids in the solid phase and thus increases their concentration in the pretreated seeds. Hydrothermal pretreatment changes the oilseeds morphology and makes their structure more porous with a greater surface area, which reduces the mass transfer resistance and makes the oils more accessible to the solvent.

SEM images of the samples of the ground raw and pretreated at 210 °C jatropha seeds are shown in Fig. 27.

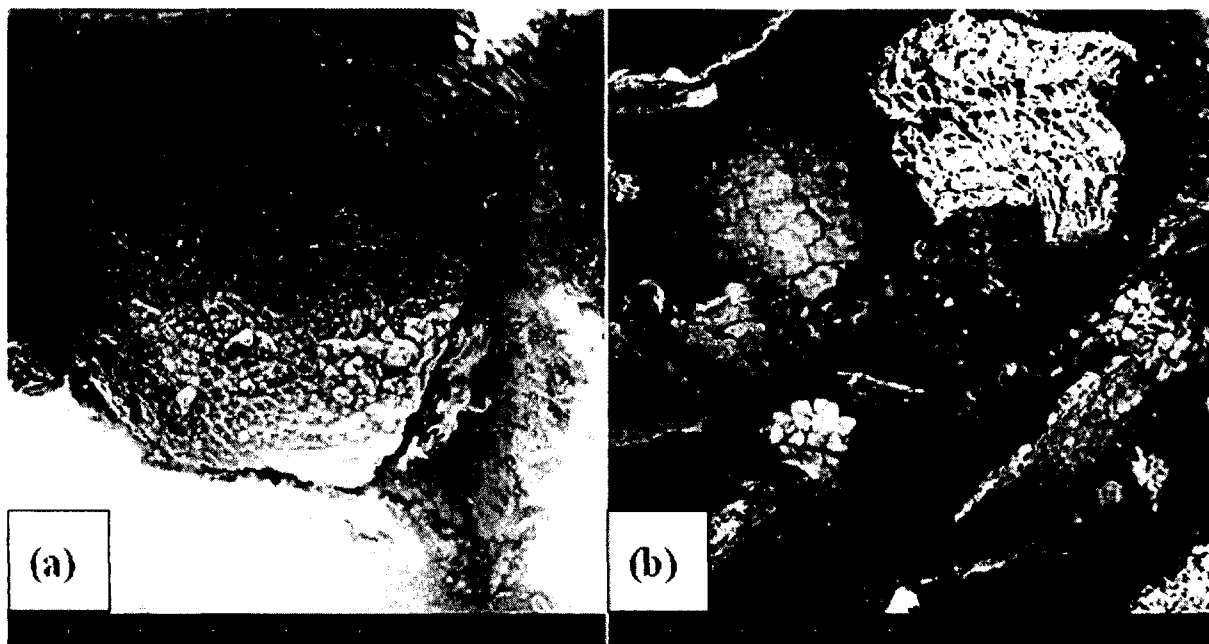


**Figure 27.** SEM images of raw (a) and hydrothermally pretreated (b) jatropha seeds.

SEM images showed that the pretreated seeds have smaller particles and a more porous structure compared to the raw ones. The more porous structure of the seed matrix favors the better oil extraction.

The results of ash analysis of the raw canola and jatropha seeds, their intermediate products, and the biochar are provided in Table 22 (RSD < 3%). The results of elemental analyses of the raw, pretreated, extracted canola and jatropha seeds, and biochar are shown in Table 22.

**Table 22.** Elemental and ash analyses of raw, pretreated, extracted, and hydrothermally carbonized canola and jatropha seeds (RSD < 1.9%, R<sup>2</sup> for N, C, and H > 0.99)

Sample	N, wt%	C, wt%	H, wt%	O*, wt%	Ash, wt%	HHV**, kJ/g	
<b>Raw seeds</b>	<b>Canola</b>	3.23	58.39	9.29	29.09	3.8	27.84
	<b>Jatropha</b>	2.69	57.36	9.36	30.59	4.2	27.76
<b>Pretreated seeds</b>	<b>Canola</b>	1.27	67.44	10.65	20.64	3.5	34.38
	<b>Jatropha</b>	1.34	65.65	10.40	22.61	4.0	32.73
<b>Extracted seeds</b>	<b>Canola</b>	5.15	50.22	6.15	38.48	3.0	18.90
	<b>Jatropha</b>	7.40	44.1	6.8	41.8	3.5	18.83
<b>Biochar</b>	<b>Canola</b>	4.87	64.22	6.61	24.30	2.8	26.47
	<b>Jatropha</b>	4.0	64.7	5.7	25.6	3.0	26.58

\*O percentage was calculated based on the difference assuming that biomass contains only N, C, H, and O

\*\*HHV was calculated using the modified Dulong's formula on an ash basis (Eq. 36)

As can be seen in Table 22, the extracted oilseeds contain a high amount of nitrogen (5.15 and 7.40 wt%). The extracted seedcake yielded biochar of a good quality (26.5-26.6 kJ/g) comparable to that of high-volatile bituminous coal, which can be used



as solid fuel or for co-firing with coal. Biochar can also be used for soil amendment (e.g., for growing oil crops) or, after a simple activation process, for industrial wastewater treatment (Regmi, Garcia Moscoso et al. 2012).

#### 4.3.5. Mass and energy distribution of the products

Table 23 provides the mass and energy distribution of all the products obtained during the hydrothermal pretreatment at 210 °C, extraction, and carbonization of canola and jatropha seeds. Energy conversion ratios (ECRs) were calculated for both oil and biochar using the data from Tables 16 and 22 and the following formulae (Ramsurn and Gupta 2012):

$$ECR_o = \frac{m_o \times HHV_o}{m_s \times HHV_s} 100\% \quad (39)$$

$$ECR_c = \frac{m_c \times HHV_c}{m_s \times HHV_s} 100\% \quad (40)$$

where:  $m_o$  – mass of the extracted oil, g

$HHV_o$  – higher heating value of the oil, kJ/g

$m_s$  – mass of the seeds, g

$HHV_s$  – higher heating value of the seeds, kJ/g

$m_c$  – mass of the biochar, g

$HHV_c$  – higher heating value of the biochar, kJ/g

**Table 23.** Mass and energy distribution of the products obtained during HPOE processing and carbonization of canola and jatropha seeds

Sample		Mass, g	Mass, wt%	HHV, kJ/g	Energy content, kJ	ECR, %
Raw seeds	Canola	30.0	100.0	27.8	835.2	-
	Jatropha	30.0	100.0	27.8	834.0	-
Oil	Canola	16.5	55.0	36.0	594.0	71.2
	Jatropha	10.3	34.4	45.0	463.5	55.6
Biochar	Canola	2.2	7.3	26.5	58.2	7.0
	Jatropha	5.6	18.7	26.6	148.8	17.8
Soluble organics	Canola	10.5	35.0	17.4	182.9	21.8
	Jatropha	13.0	43.3	17.1	221.6	26.6
Gas	Canola	0.8	2.7	0.03	0.02	0.0
	Jatropha	1.1	3.6	0.03	0.03	0.0

As shown in Table 23, the integrated HPOE process allowed obtaining 55 wt% crude oil and 7.3 wt% biochar from the canola seeds, which energy content accounted for 71.2 and 7.0%, respectively (the overall ECR was 78.2%). Jatropha seeds provided 34.4 wt% crude oil and 18.7 wt% biochar with the energy content accounted for 55.6 and 17.8%, respectively (the overall ECR was 73.4%).

#### 4.4. Overall mass balance and energy requirements for HPOE process

In order to determine the process yields, the mass balance (100 kg, on a dry basis) around the hydrothermal pretreatment of canola and jatropha seeds, their solvent extraction, and the HTC of the seedcake was developed and summarized in Fig 28. The aqueous phase containing soluble organics can be further recycled for the next hydrothermal carbonization step or/and used as a source of nutrients for growing oil crops. The integrated HPOE process allowed producing 55 and 34.4 wt% crude oils, which can be used for biodiesel production, and 7.3 and 18.7 wt% biochar, thus utilizing 62.3 and 53.1 wt% of the oilseed mass for producing valuable products with an overall ECR of 78.2 and 73.4%.

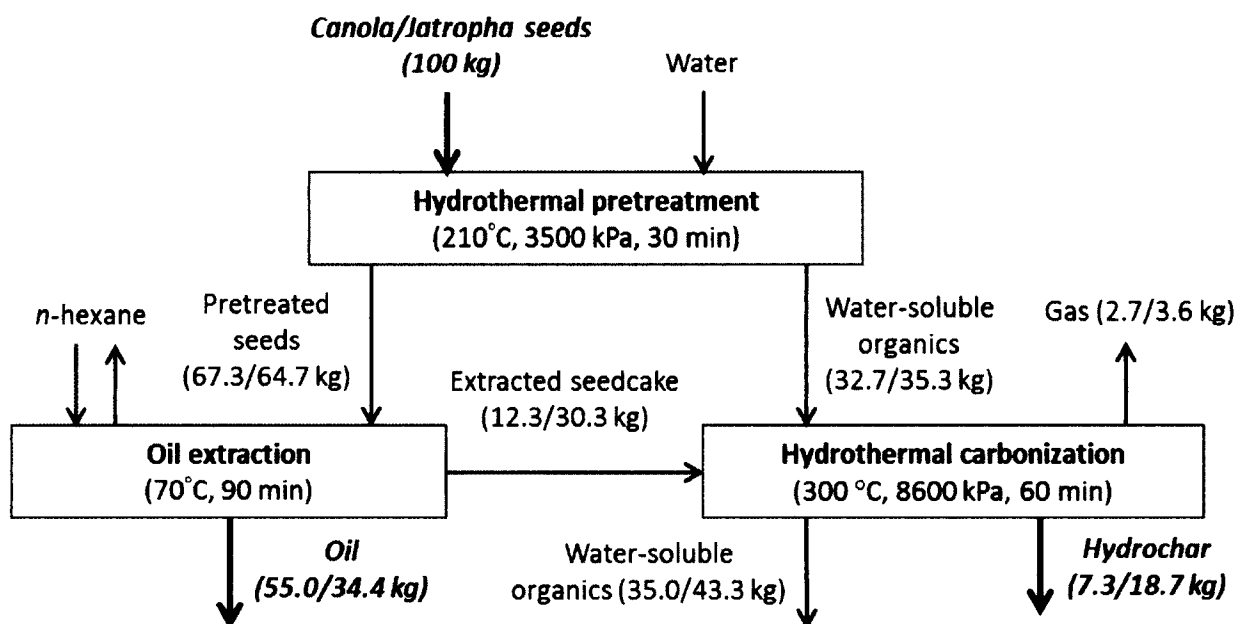


**Figure 28.** Overall mass balance for three different unit operations of HPOE process to produce oil and biochar from canola and jatropha seeds.

Subcritical water (hydrothermal) processes employ hot compressed water that is kept in a liquid state by applying pressure greater than the pressure of steam. In this way, the latent heat required for the phase change of water is avoided, which requires less energy than steam generation. The energy required for the vaporization of water (2260 kJ/kg) is much higher than the energy required for the subcritical water processes. In order to bring water from 25 °C to the subcritical state at 210 °C and 3500 kPa (the conditions required for hydrothermal pretreatment), 898.3 kJ/kg of energy is required. The subcritical water carbonization at 300 °C and 8600 kPa requires 1344.7 kJ/kg of energy. In the integrated process, the aqueous phase after hydrothermal pretreatment is used for the carbonization of the extracted seedcake. In order to bring water from 210 °C to 300 °C, 446.4 kJ/kg of additional energy is required.

The average energy content of oilseeds was 27.8 kJ/g (27,800 kJ/kg). The pretreated jatropha seeds after vacuum filtration contained about 10 wt% moisture and could be extracted without drying. Since our goal was to maximize the oil yield, the oilseeds were dried for the clarity of the experiments. Therefore, in a properly designed HPOE process, the total energy requirements should not exceed 1600 kJ/kg including the drying of oilseeds. This energy is equivalent to 5.8% of energy content of the seeds. Further, it is possible to recover and recycle most of the heat from the subcritical water.

#### **4.5. Conclusions**

HPOE is an integrated process that employs hydrothermal pretreatment of whole oilseeds and oil extraction steps followed by HTC of the extracted seedcake. The integrated process provides several major advantages over conventional processes: better

extractability of oil, shorter extraction time, tolerance to high moisture content of the feedstock, avoiding preparation stages, and utilization of the extracted seedcake for biochar production. Hydrothermal pretreatment of oilseeds in subcritical water at 180-210 °C for 30 min is an efficient step that changes the oilseeds morphology and enhances extractability of oilseeds during the following solvent extraction step even without prior grinding and dehulling the oilseeds. For five types of the seeds used in the study, the oil yields obtained from the whole pretreated seeds was slightly higher (1-1.5 wt%) than that obtained from the ground raw ones on unsaponifiable matter-free basis. Hydrothermal pretreatment at the conditions studied did not significantly change the composition and quality of the extracted oils, which makes them suitable for biofuel production.

The oils extracted from pretreated seeds had a higher antioxidant activity, which implies better resistance to autoxidation. The results of this study suggest that the proposed integrated process can be an economical and efficient way of oil extraction and biochar (co-product) production from different oilseeds.

#### **4.6. Acknowledgments**

The authors would like to acknowledge the encouragement and support of our colleagues at the Department of Chemistry and Biochemistry at Old Dominion University in the preparation of this article. We also acknowledge Dr. Florin Barla from Old Dominion University for his help with the oil analyses. Our special appreciation goes to the Research Foundation at Old Dominion University (ODURF) for providing the financial support for this research.

## CHAPTER 5

### HYDROTHERMAL LIQUEFACTION OF *SCENEDESMUS SP.* AND CATALYTIC GASIFICATION OF THE AQUEOUS PHASE IN NEAR- AND SUPERCRITICAL WATER

*Scenedesmus sp.* was liquefied in a batch reactor at 300 °C for 30 min. Under these conditions, 75 wt% of the energy initially present in the microalga remained in a lipid-rich solid product that could be used for liquid fuel production. The liquefaction degree was 32-33 wt% on a carbon basis. The liquid phase consisting mainly of partially hydrolyzed carbohydrates and proteins contained 25 wt% of the energy initially present in the microalga and were rich in nutrients required for growing the fresh algae. In this study, we attempted to maximize the overall energy yield by producing gas from the extracted aqueous phase. The liquid phase was extracted with dichloromethane yielding 4.5 wt% of bio-oil that contained 6.9 % energy. After that, the extracted aqueous phase was subjected to gasification in a continuous flow reactor over activated carbon catalyst at the temperatures from 350 to 400 °C with a weight hourly space velocity (WHSV) of 3.3 h<sup>-1</sup>. The highest gasification efficiency of 10.2% was observed at 400 °C, which is 5.7 times greater than that in the control experiments without catalyst. The gas produced with catalyst contained mostly H<sub>2</sub> and light hydrocarbons while the gas produced without catalyst consisted mainly of H<sub>2</sub> and CO<sub>2</sub>. The results of the study show that considerable amount of H<sub>2</sub> and gaseous hydrocarbons can be produced at relatively low temperature of 400 °C using activated carbon as catalyst.

## 5.1. Introduction

At present, scientists all over the world conduct active research on alternative fuels that could replace traditional sources of energy in the near future. To date, renewable biofuels are mainly produced by hydrolysis and fermentation of starch/sugar crops and transesterification of plant oils. However, replacing the world demand for petroleum products by the above technologies is not a sustainable alternative because the productivity of terrestrial crops is not sufficient for a large scale production. In order to replace petroleum products in the US, over 60% of the agricultural land would have to be used for biofuel production. This would lead to a shortage of land for agriculture and directly compete with the production of food and fodder.

Microalgae production rates are much higher than land-based crops; the calculation of the area required for the microalgae cultivation shows that only 3% of the territory would be sufficient for the biofuel production and replacement of the petroleum products in the US (Carlozzi 2003). Moreover, algal biomass can be produced on lands that are not suitable for higher plants as well as in a wide variety of water sources and so does not compete with the production of food for the growing population.

At present, microalgae industry specializes on producing high value products such as specific proteins, pigments, or fatty acids, and only small amounts of biodiesel are produced from microalgae. If those technologies were combined with the biofuel production, the economic issue could be successfully resolved.

Biofuels derived from microalgae are currently considered to be the most economical and technically viable route that is able to compete with petroleum-derived

fuels (Chisti 2010). This is due to a number of important advantages they have in comparison with land-based energy crops:

1. Higher annual growth rates, e.g., rates of up to 37 tons per ha per annum have been recorded, primarily due to higher photosynthetic efficiencies (up to 10% of the solar energy) when compared with terrestrial plants (Weissman and Tillett 1992);
2. Higher lipid productivity (up to 75% dry weight for some algae species), with higher proportion of triacylglycerols (TAG) that are essential for efficient biodiesel production (Schenk, Thomas-Hall et al. 2008);
3. Microalgae production can effect biofixation of CO<sub>2</sub> (production utilizes about 1.83 kg of CO<sub>2</sub> per kg of dry algal biomass yield) thus making a contribution to air quality improvement (Chisti 2008);
4. Capability of growing in wastewater, which offers the potential for integrating the treatment of organic effluent with biofuel production (Cantrell, Ducey et al. 2008);
5. Capability to thrive in saline/brackish water/coastal seawater and tolerate marginal lands (e.g. desert, arid- and semi-arid lands) that are not suitable for conventional agriculture;
6. Inherent yield of valuable co-products such as proteins, polyunsaturated fatty acids (PUFAs), pigments, biopolymers may be used to enhance the economics of production systems (Spolaore, Joannis-Cassan et al. 2006).

Therefore, microalgal feedstock is the only viable alternative for a large scale biofuel production seen today.



Due to microalgae's extensive use in the mariculture and the food supplement industry, their biochemical composition has been thoroughly investigated (Dunstan, Volkman et al. 1993). In spite of the wide variety of classes and species, microalgae and cyanobacteria generally consist of 4-64wt% of carbohydrates, 6-71wt% protein, and 2-40wt% lipids (up to 75wt% for some algae species) on the dry biomass basis (Cantrell, Ducey et al. 2008). The high lipid content facilitates its potential use as a biodiesel or renewable diesel feedstock because the lipids can be readily extracted and converted into fatty acid esters or upgraded via catalytic deoxygenation.

The composition and the fatty acid profile of microalgal lipids substantially vary with the species, its life cycle, and its cultivation conditions. Thus, microalgal cells harvested during stationary phase have higher acylglycerol contents and lower polar lipid contents than those harvested during logarithmic phase (Dunstan, Volkman et al. 1993). It should be taken into consideration that acylglycerols are the only lipid fractions that can be used for transesterification at the current industrial-scale refineries. Also, microalgal fractions that contain high levels of polar lipids and non-acylglycerol neutral impurities have to be purified before converting into usable biodiesel (Spolaore, Joannis-Cassan et al. 2006).

The suitability of microalgal biomass for biofuel production has to be examined on a case-by-case basis. In order to achieve the highest possible production rate, oil content has to be balanced against growth kinetics. Furthermore, there are many advantages in having a robust species of alga since the system will be less sensitive to variations in parameters like temperature, pH, and salinity. As it was said above, oil composition and size are also important in order to achieve a simple separation and post

processing. Last but not least, it is important that an alga strain is well known and sufficient research and information about it is available.

Many potential pathways are currently under consideration for production of biofuels and bioproducts from the biomass. These pathways can be classified into the following three general categories:

1. Those that focus on the direct algal production of recoverable fuel molecules (e.g. ethanol, hydrogen, methane, and alkanes) from algae without the need for extraction;
2. Those that process the whole algal biomass to yield fuel molecules; and
3. Those that process algal extracts (e.g. lipids, carbohydrates) to yield fuel molecules.

These technologies are primarily based on similar methods developed for the conversion of terrestrial plant-based oils and products into biofuels. However, output streams from algae have very complex compositions that have to be taken into consideration before the above technologies can be applied effectively.

The conversion of lipid extracts derived from algal sources is the typical mode of biofuel production from algae. This technology is relatively mature and has been demonstrated to be the “gold standard” in the conversion of vegetable oils into biodiesel. This is why this technology seems to be most feasible for a large-scale production of biofuels.

In recent year, there is a considerable interest in research and development of methods for converting plant oils via catalytic deoxygenation into hydrocarbons that are fully fungible with petroleum-derived transportation fuels (Popov and Kumar 2013).

It is also important to consider production of valuable co-products in order to enhance the economics of the process. A number of different commercial products can be derived from microalgae and cyanobacteria. They include products for human and animal nutrition, polyunsaturated fatty acids, antioxidants, coloring substances, fertilizers, and a variety of specialty products such as bioflocculants, biodegradable polymers, cosmetics, pharmaceuticals, and stable isotopes for research purposes (Cherubini 2010).

One of the critical aspects in developing a conversion technology that derives benefit from every potential input is the processing of algal remnants after extraction of algal lipids for biofuel production. This includes anaerobic digestion of algal remnants to produce gas, fermentation of any recoverable polysaccharides into biofuels, and gasification of extracted biomass to produce hydrogen and light hydrocarbons.

In order to reduce costs and accelerate commercialization of microalgae-derived biofuels, the following strategies must be taken into consideration:

1. Identification of fast growing algae with high lipid content;
2. Development of low cost harvesting, dewatering, extraction, and conversion technologies;
3. Concurrent extraction of valuable co-products.

The concept of biorefinery for utilization of every component of the algal biomass raw material must be considered as a means to enhance the economics of the process. This concept must also include integration of the microalgae cultivation in carbon capture, wastewater treatment in order to enhance the viability and sustainability of microalgae as a biofuel resource, and nutrient recycle.

The problem with microalgae production is the economics. The cost of algal biomass production is still higher than the costs of other biomass sources (Acién, Fernández et al. 2012). A significant part of these costs are due to the costs of nutrients (nitrogen, phosphorus, potassium and others) that algae require for their growth. Sustainability also plays an important role in the commercial microalgae production. The shortage of phosphorus as a key nutrient is expected to be an urgent problem in coming years (Cordell, Drangert et al. 2009). Therefore, nutrient recycling is becoming a key factor for the large scale cultivation of microalgae.

Hydrothermal liquefaction (HTL) is considered as an efficient and environmentally benign method for direct conversion of biomass into liquid products in a closed oxygen-free reactor at a certain temperature (200–380 °C), pressure (5–28 MPa), and reaction time (5–60 min) (Behrendt, Neubauer et al. 2008). In this process, the hot compressed water serves as a reactant, reaction medium, and catalyst (Kumar 2013).

In the last years, HTL of biomass for biofuel production has received an increasing attention due to a number of advantages compared to other thermochemical processes. It can utilize wet feedstock, thus avoiding the energy-costly process of drying algal biomass, is not dependent on the type of biomass processed, is able to convert biomass resistant to other thermochemical methods to liquid and solid products with high energy density, and provides easier product separation.

Liquid phase, which is a mixture of oxygenated hydrocarbons and other O/N-containing compounds, is the most important product of HTL that can be upgraded to liquid fuels and chemicals (Zhu, Albrecht et al. 2013). Among the rest, the liquid phase contains most of the nutrients initially present in the feedstock that can be recovered and

recycled for microalgae cultivation. A number of studies on nutrient recovery through the aqueous by-product after HTL, which can be used for growing algae, were conducted in recent years (Tsukahara, Kimura et al. 2001, Jena, Vaidyanathan et al. 2011).

Hydrothermal gasification (HTG) is a process that typically involves high temperatures (500-700 °C), pressures (5-50 MPa), transitional or noble metal catalysts on a heat-resistant support (i.e., TiO<sub>2</sub>, Al<sub>2</sub>O<sub>3</sub>), a source of carbon to yield a gas product that contains H<sub>2</sub>, CH<sub>4</sub>, C<sub>2</sub>H<sub>6</sub>, CO, CO<sub>2</sub>, and other gases in various proportions (Navarro, Peña et al. 2007). Hydrogen is a valuable energy carrier, which is currently produced from via thermos-catalytic processes from methane, naphtha, and coal (Balat and Kırtay 2010). However, depletion of fossil fuel reserves and carbon emission concerns has led to studying technologies for hydrogen production from carbon neutral biomass and biomass-derived materials (Matsumura, Minowa et al. 2005). Among the different methods, HTG is a most promising way of hydrogen production from biomass feedstock. It does not require drying and grinding of biomass, is not subject to tarring of equipment, and has a high reaction efficiency and hydrogen selectivity (Akiya and Savage 2002). It was reported that hydrogen production from biomass has lower cost than that produced with other technologies (Bartels, Pate et al. 2010).

HTG process has received a lot of attention since it provides safe, non-toxic, readily available, inexpensive, and environmentally benign medium and flexible conditions for biomass processing. However, this technology requires high temperature and pressure to achieve good hydrogen yields. These drawbacks cause high operating cost, which is the biggest obstacle in developing and commercializing HTG. In order to overcome this obstacle, many researchers conduct intensive research on the catalytic

HTL that allows reducing the reaction temperature and pressure. Our work also aimed at reduction of reaction temperature using a low-cost activated carbon catalyst. Many researchers believe that from many other hydrogen production methods HTG has the greatest potential (Kruse, Krupka et al. 2005, Matsumura, Minowa et al. 2005).

In this study, we attempted to maximize the amount of energy derived from *Scenedesmus sp.* by gasification of the extracted aqueous phase obtained after HTL at relatively low temperatures (350-400 °C). We used a continuous flow reactor packed with low-cost activated charcoal as catalyst assuming that it is sufficiently active under the conditions studied. The processed aqueous phase was intended to be used as a source of nutrients for microalgae growth in the followed up research. The schematic of the proposed process is shown in Fig. 29.

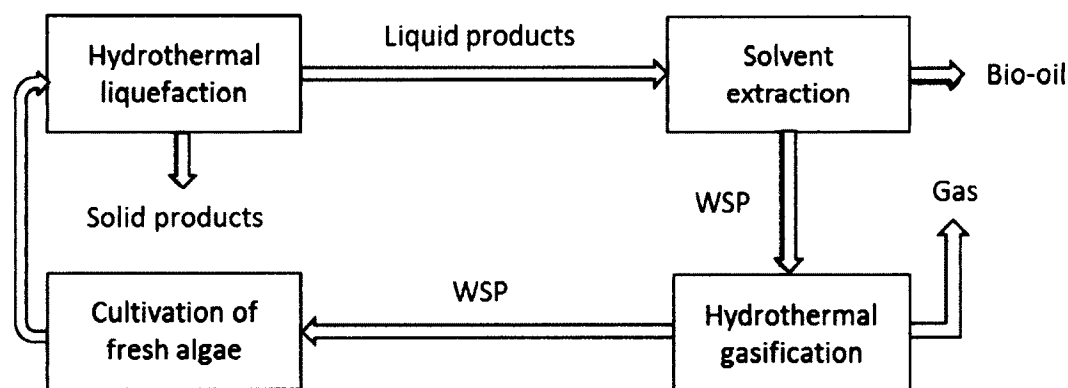


**Figure 29.** Schematic of HTL of microalgae followed by HTG of the extracted aqueous phase.

The objectives of this research were to (i) maximize the overall energy yield from algal biomass; (ii) study HTG of the aqueous phase after bio-oil extraction in order to

produce hydrogen and gaseous hydrocarbons; (iii) compare the effects of activated carbon catalyst on HTG with non-catalytic runs; (iv) develop the mass balance of the process. To our knowledge, there were no reported studies on HTG of the liquefied *Scenedesmus sp.* over activated carbon.

The integration of HTL and HTG of the algal biomass with the following nutrient recycle could be an important approach to the biorefinery concept in terms of maximizing the carbon utilization in an economically viable way.

## **5.2. Experimental section**

### **5.2.1. Materials and methods**

Microalga *Scenedesmus sp.* was produced at the ODU Algae Production Facility near Hopewell, Virginia. The alga was dried in an oven at  $65 \pm 3$  °C for 24 h and stored in a plastic bottle in a dark place at room temperature before being used. The moisture content of the alga was determined with a moisture meter Denver Instrument IR 35 by drying them at 105 °C to constant weight. The moisture of the algal biomass was  $\leq 1.9 \pm 0.1$  wt%. Granulated activated charcoal Darco and dichloromethane (99.5%) for analysis were purchased from Fischer Scientific USA and used as received. The granulated activated charcoal was sieved to remove particle sizes  $<500$   $\mu\text{m}$  before being used.

In this study, algal biomass was subjected to HTL in a 500 mL batch reactor equipped with Parr 4848 controller at  $300 \pm 2$  °C (the autogenous pressure was  $1500 \pm 5$  psi (10.3 MPa)) for 30 min with continuous stirring at 300 rpm. The preheating time was about 30 min (10 °C/min). The reaction temperatures were selected based on the typical

HTL conditions reported elsewhere for the similar applications (Vardon, Sharma et al. 2012). In a typical experiment, the reactor was loaded with 50 g of the dry algal biomass and 300 mL of deionized water, sealed, and kept under the above conditions. Prior to the HTL, the reactor was purged with helium for 5 min to remove oxygen. After cooling down the reactor to the ambient temperature, the reaction products were separated, quantified, and analyzed as described below in the respective section. HTL of algal biomass was conducted five times to obtain the sufficient amount of the aqueous phase for the HTG experiments.

The gasification experiments were carried out in a 65 mL HiP tubular reactor MS-18 with the overall length of 19" and inside diameter of 9/16". The reactor was packed with the granulated activated charcoal (18.2 g) that occupied 30% of the reactor volume and installed inside of a horizontal electric furnace that allowed precise temperature control. The experimental setup is shown in Fig. 30.

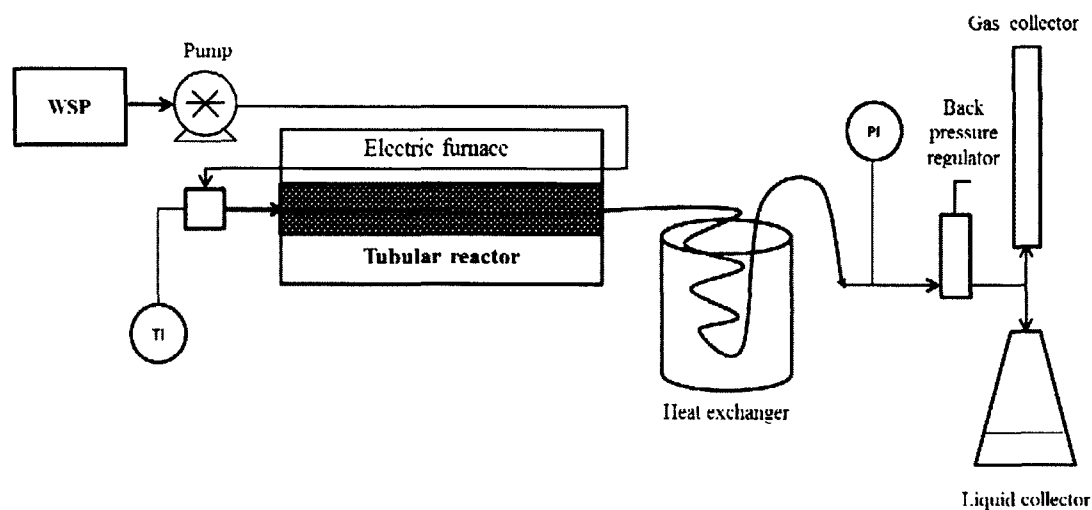


**Figure 30.** Experimental setup for hydrothermal gasification of the aqueous phase.



A high pressure and high precision dual piston pump Shimadzu LC-10AD was used to deliver the extracted aqueous phase containing water-soluble products (WSP) into the reactor. Gasification products were cooled down in a water heat exchanger. The flowrate of the gaseous products was measured periodically with a volumetric burette filled with water and a stopwatch. Samples of the gas were taken from the burette with a syringe and analyzed as described below. The liquid reaction products were collected in a 500 mL flask. and analyzed as described below. The pressure inside the reactor was regulated with the back pressure regulator and kept close to  $3500 \pm 10$  psi (24.1 MPa) for all the experiments. The WSP flowrate was kept at 1 mL/min for all the experiments. The temperature inside the reactor was measured with two thermocouples equipped with controllers; one thermocouple was installed in the middle of the reactor, the other – immediately after the reactor. The experiments were conducted at the three different temperatures:  $350 \pm 2$  °C,  $375 \pm 2$  °C, and  $400 \pm 2$  °C. The pressure in the system was measured with the pump controller before the reactor and with PGS-35B-5000 general service pressure gauge (Omega, USA) after the reactor. The residence time in the reactor was adjusted to 24 min.

Weight hourly space velocity (WHSV) was  $3.3 \text{ h}^{-1}$  for all the experiments and was calculated using Eq. 41:

$$\text{WHSV} = \frac{\text{Feed mass flow, g/h}}{\text{Catalyst mass, g}} \quad (41)$$

The experiments started with pumping into the reactor 1 mL/min of deionized water until the desired temperature and pressure were reached and stabilized. After that, the pump was switched to pumping the WSP. A typical experiment was conducted for 5 h

until 300 mL of the aqueous phase was used for better accuracy. After each experiment, the system was flushed with deionized water at 10 mL/min for at least 1 h.

Before the main experimental part, two series of control experiments were conducted. The first series was carried out with deionized water only to determine whether the gas formation other than from the WSP occurs during the HTG process at different reaction temperatures (350-400 °C). The second series was carried out with the WSP but without the catalyst that was substituted with glass beads to determine whether the gas formation occurs without a catalyst at different reaction temperatures (350-400 °C). The volume of the glass beads loaded into the reactor was adjusted to keep the residence time at the same value (24 min).

## **5.2.2. Product separation and analyses**

### **5.2.2.1. Product separation**

The products obtained after HTL of algae were separated using different techniques. After cooling down the batch reactor, the temperature and pressure of the gaseous phase was recorded and used for calculations of moles of gas in the mixture using the universal gas law. A sample of the gas mixture was taken with a syringe and analyzed using a gas chromatograph (GC) equipped with a thermal conductivity detector (TCD). After that, the gas was vented, and the reactor was opened.

The solid and liquid products were transferred from the reactor to a 500 mL beaker, and the reactor was washed with 50 mL of deionized water to remove any residual products. The solid and liquid products were separated by vacuum filtration. The

solid products (lipid-rich residue) were dried in an oven at  $65 \pm 3$  °C for 24 h until the moisture content was below 1 wt%, quantified, and stored at 4 °C for the elemental analysis. The liquid phase was quantified, analyzed for TC/TN and pH, and extracted with dichloromethane to recover bio-oil as described by (Vardon, Sharma et al. 2012). 200 mL of dichloromethane was added to the aqueous phase and shaken vigorously for 10 min. After that, the organic and aqueous phases were separated in a separating funnel, and dichloromethane from the organic phase was evaporated in a vacuum rotary evaporator. The obtained bio-oil was quantified and stored at 4 °C for the elemental analysis. The extracted aqueous phase containing WSP was stored at 4 °C for TC/TN and pH analyses and using in HTG experiments.

The liquid products after HTG were collected and stored at 4 °C for TC/TN and pH analyses. The samples of the gaseous products were taken from the burette with a syringe and analyzed with GC-TCD for identification of the compounds, quantification of the individual gases in the mixture, and HHV calculations.

#### **5.2.2.2. Analysis of the catalyst**

Brunauer-Emmett-Teller (BET) surface area and pore volume/size analysis of the catalyst was carried out with a NOVA 2000e surface area and pore size analyzer (Quantachrome Instruments). The samples were degassed at 120 °C with continuous flow of nitrogen and helium at 10 psi overnight prior to the analysis. Liquid nitrogen was used as an adsorbent during the measurements. Multi-Point BET method was used to determine the surface area and BJH method was used as the most common and accurate method to compute the average pore volume and pore size of the samples.

### 5.2.2.3. Analyses of the products

The gaseous products after HTL and HTG were identified and quantified with SRI 8610C GC equipped with a 6' molecular sieve MS-13X connected to a 10' × 1/8" HayeSep D packed column and a TCD. Helium at 20 mL/min was used as carrier gas. The temperature program was set up as follows: initial temperature 40 °C, hold for 20 min, final temperature 40 °C. For analysis of a gas mixture for hydrogen, argon was used as carrier gas. The temperature program for hydrogen analysis was set up as follows: initial temperature 200 °C, hold for 20 min, final temperature 200 °C. SCOTTY gas calibration standard containing 50 mol% H<sub>2</sub>, 10 mol% CH<sub>4</sub>, 10 mol% CO, 20 mol% CO<sub>2</sub>, 5 mol% ethylene, and 5 mol% propane was purchased from Air Liquide America Specialty Gases LLC, USA. The amount of each gas in the mixture was determined in mol%. After that the mass of each gas in the mixture and the total mass of the gas was calculated. All the analyses have been done in triplicate.

The aqueous phase collected after HTL, bio-oil extraction, and HTG was volumetrically quantified and analyzed for pH, total carbon (TC), and total nitrogen (TN) with Shimadzu TOC<sub>VPN</sub> analyzer. All the analyses have been done in triplicate.

Elemental analysis (C, H, and N) of algal biomass, solid products, and extracted bio-oil was carried out with ThermoFinnigan Flash EA 1112 automatic elemental analyzer. Higher heating values (HHVs) of all the samples on ash basis were evaluated using modified Dulong's formula (Basu 2013):

$$\text{HHV} = \frac{(349.1 (\%C) + 1178.3 (\%H) - 103.4 (\%O) - 15.1 (\%N) - 21.1 (\%Ash))}{1000} \quad (42)$$

Ash analysis of algal biomass and solid products after HTL was done according to NREL/TP-5100-60956 standard method. The samples were placed in ceramic crucibles and kept in a muffle furnace at  $575 \pm 5$  °C for 4 h. After cooling down the furnace, inorganic content of the samples (ash) was determined gravimetrically.

All the analyses have been done in triplicate. For all the analyses results, mean values and relative standard deviations (RSD) were calculated and used for evaluation of variability in the data sets.

### 5.3. Results and discussion

#### 5.3.1. HTL of algal biomass

After each HTL run and separation of the gaseous, liquid, and solid phases, the obtained products were quantified and analyzed with different methods. The gaseous products were analyzed with GC-TCD to determine their composition and amount of each gas in the mixture. The results of GC-TCD analysis is provided in Table 24.

**Table 24.** Composition and amount of the gas produced during HTL of algae (RSD < 3%)

H <sub>2</sub> , mol%	CH <sub>4</sub> , mol%	CO, mol%	CO <sub>2</sub> , mol%	C <sub>2</sub> C <sub>4</sub> , mol%	C <sub>2</sub> C <sub>6</sub> , mol%	V of gas, L	Moles of gas, mol	Mass of gas, g
0.3	0.0	1.7	94.7	0.6	0.0	2.0	0.083	3.5

As we can see from Table 24,  $3.5 \pm 0.2$  g or 7.1 wt% of gas was produced from 50 g of algae and the gaseous products from the HTG of the algal biomass consisted mostly from  $\text{CO}_2$ .

The liquid phase was analyzed for TC/TN and pH immediately after the separation process. The average TC was  $27.2 \pm 0.5$  g/L, TN –  $13.3 \pm 0.3$  g/L, pH –  $8.4 \pm 0.1$ .

Degree of liquefaction was calculated using the formula (43) and yielded  $32.6 \pm 0.2$  %.

$$\text{Degree of liquefaction} = \frac{\text{TC}_{\text{liq.}}}{C_{\text{algae}}} 100\% \quad (43)$$

where  $\text{TC}_{\text{liq.}}$  – mass of total carbon in the liquid phase, g

$C_{\text{algae}}$  – mass of elemental carbon in the algal biomass, g

After the analyses, the liquid phase was extracted with dichloromethane and yielded  $2.1 \pm 0.1$  g or  $4.5 \pm 0.3$  wt% of bio-oil. TC, TN, and pH of the extracted aqueous phase was  $16.0 \pm 0.3$  g/L,  $6.9 \pm 0.2$  g/L, and  $8.2 \pm 0.1$ , accordingly.

The mass of the solid phase after drying was  $25.5 \pm 0.5$  g or 51.5 wt%.

The elemental analysis of the microalgae and the HTL products (solid phase, extracted bio-oil, and gaseous products and their HHVs are provided in Table 25. The percentage of C, H, and O in the gaseous phase was calculated from its compositional analysis with GC-TCD.

**Table 25.** Elemental analyses of microalgae, solid phase, bio-oil, and gaseous products after HTL at 300 °C (RSD < 1.9%, R<sup>2</sup> for N, C, and H > 0.99)

Sample	Mass, g	% N	%C	%H	%O*	Ash, wt%	HHV**, kJ/g	HHV, kJ	HHV, %
Algae	49.40	8.91	50.80	7.46	32.83	8.40	22.81	1126.93	100.00
Solids	25.46	4.92	62.94	9.84	22.30	8.23	31.02	789.55	75.11
Bio-oil	2.21	9.46	63.94	10.32	16.29	0.00	32.65	72.16	6.86
Gas	3.49	-	25.56	0.00	74.44	0.00	0.00	0.00	0.00

\*O percentage was calculated based on the difference assuming that biomass contains only N, C, H, and O

\*\*HHVs were evaluated using modified Dulong's formula (Eq. 42):  $HHV \text{ (kJ/g)} = (349.1 (\%C) + 1178.3 (\%H) - 103.4 (\%O) - 15.1 (\%N) - 21.1 (\%Ash))/1000$

The distribution of the products and energy (HHV) after the HTL is shown in Fig. 31.

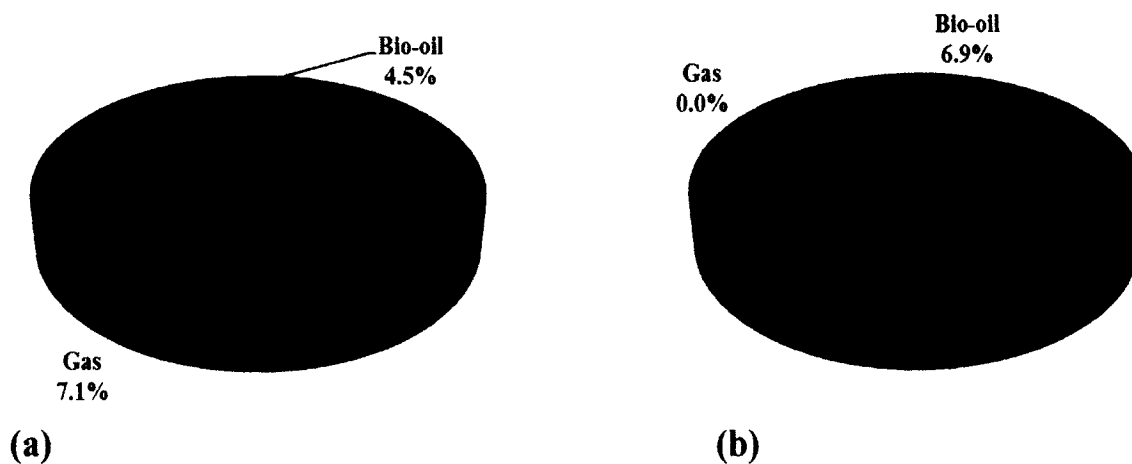


**Figure 31.** (a) Products and (b) energy (HHV) distribution from HTL of algae at 300 °C.

As we can see from Table 25 and Fig. 31, the solid products had HHV of 31.02 kJ/g and contained most of the energy initially present in the microalgae (75.1%). The bio-oil had higher HHV than the solids (32.65 kJ/g) and accounted for 6.9% of the energy initially present in the algal biomass. This can be explained by the high lipid content of those products that were partially deoxygenated during the HTL (22.3 wt% and 16.3 wt% oxygen versus 32.8 wt% in the algal biomass) by releasing 7.1 wt% of the gas consisting mostly from CO<sub>2</sub>. The most abundant HTL product was the solid phase that accounted for 51.5 wt% of the total products. Along with bio-oil that accounted for 4.5 wt%, they can be used for biofuel production. Since nonpolar compounds were extracted from the aqueous phase, it contained mostly polar products of hydrolysis of carbohydrates and proteins. It was reported that the main WSPs of HTL of microalga *Nannochloropsis sp.* and flash hydrolysis of *Scenedesmus sp.* were carbohydrates/oligosaccharides, carboxylic acids, amino acids, oligopeptides, phenols/polyphenols, alcohols, ketones, aldehydes, amides, indoles, and other heterocyclic N-containing compounds (Brown, Duan et al. 2010, Zhou, Zhang et al. 2010, Garcia-Moscoso, Obeid et al. 2013).

The extracted aqueous phases from all the HTL runs were mixed together and used in the HTG experiments.

### **5.3.2. HTG of the aqueous phase**

The extracted aqueous phase was subjected to HTG in a continuous flow reactor loaded with granulated activated carbon at 350, 375, and 400 °C. The BET surface area and pore volume/size analysis of the fresh granulated activated carbon used as a catalyst in the study showed that its surface area was  $600 \pm 20 \text{ m}^2/\text{g}$ , average pore volume was



$0.95 \pm 0.05 \text{ cm}^3/\text{g}$ , and average pore size was  $60 \pm 5 \text{ nm}$ . After a series of three experiments, the surface area of the catalyst was  $175 \pm 5 \text{ m}^2/\text{g}$ , average pore volume was  $0.60 \pm 0.02 \text{ cm}^3/\text{g}$ , and the average pore size did not significantly change. The formation of solid deposits on the catalyst surface was not observed under the conditions studied.

The first series of control experiments with deionized water only (blank runs) at different reaction temperatures (350-400 °C) did not show the formation of detectable amounts of gas produced from the reaction of water with the carbon catalyst. This is consistent with the studies by (Xu, Matsumura et al. 1996, Matsumura, Xu et al. 1997) who showed that carbon can promote H<sub>2</sub> and CO formation at much higher reaction temperatures and pressures (600–650°C, 25.5–34.5 MPa). We do not exclude the possibility of water-gas shift, reverse water-gas shift, and/or methanation reactions. However, carbon gasification, if it occurs, is much slower than gasification of the liquefied biomass (Xu, Matsumura et al. 1996).

The second series of control experiments with the aqueous phase obtained after the HTL of algae but without the carbon catalyst that was substituted with glass beads was carried out at the reaction conditions studied (350-400 °C, 3500 psi (24.1 MPa), residence time 24 min). The gas formation was observed at all the reaction temperatures. The flowrate of the gas formation was measured and its composition was analyzed with GC-TCD. The aqueous phase before and after the HTG process was analyzed for TC/TN and pH. Based on these data, the gasification efficiency, gas yields, elemental composition, and HHVs were calculated and compared with the results obtained in the main series of experiments. The maximum gas flowrate in non-catalytic runs was 0.96 mL/min versus 4.62 mL/min in catalytic runs at 400 °C, gasification efficiency was 5.7

times lower, composition of the gas produced was different (the gas contained mainly H<sub>2</sub> and CO<sub>2</sub>). The detailed results of the control experiments are provided below in comparison with the main series of experiments (catalytic runs).

The aqueous phase before and after the HTG process was analyzed for TC/TN and pH. pH of the effluent aqueous phase in some experiments reached 9.0-9.25, which can be explained by the presence of the high concentration of ammonium. No increase in the pressure drop was observed during all the HTG experiments.

The gasification efficiency is defined as moles of carbon in the gas divide by moles of carbon in the aqueous phase. Gas yields were calculated by dividing moles of gas produced by moles of carbon reacted. The reacted carbon was calculated from the difference between TC in the feed and reactor effluent. The unreacted carbon was determined as carbon content in the effluent divided by carbon content in the feed. The carbon balance was calculated by dividing the sum of carbon in the effluent and gaseous phase by the carbon in the feed.

The compositions of the gaseous phases for all the catalytic and non-catalytic runs are provided in Table 26.

**Table 26.** Composition of gaseous products from the catalytic and non-catalytic runs (RSD < 5%)

Exp. No.	Reaction temperature, °C	H <sub>2</sub> , mol %	CH <sub>4</sub> , mol %	CO, mol %	CO <sub>2</sub> , mol %	C <sub>2</sub> H <sub>4</sub> , mol %	C <sub>2</sub> H <sub>6</sub> , mol %
<b>Catalyst</b>							
1	350	45.8	13.1	2.1	18.5	2.5	7.3
2	375	39.0	20.7	6.7	13.2	1.9	9.2
3	400	33.0	29.8	9.5	7.0	0.9	11.3
<b>No catalyst</b>							
4	350	45.4	7.0	1.4	27.9	3.7	3.1
5	375	42.4	9.1	7.2	23.0	3.3	4.8
6	400	37.5	12.8	10.4	18.8	2.9	5.8

As we can see from Table 26, the major gases produced were hydrogen, methane, carbon mono- and dioxides, and ethane with a small amount of ethylene present in the mixture. It is possible that ammonia was also present in the gaseous phase, but it was not detected by GC-TCD probably because the methane peak overlapped the one of ammonia. The gas yields for both catalytic and non-catalytic runs are shown in Fig. 32.

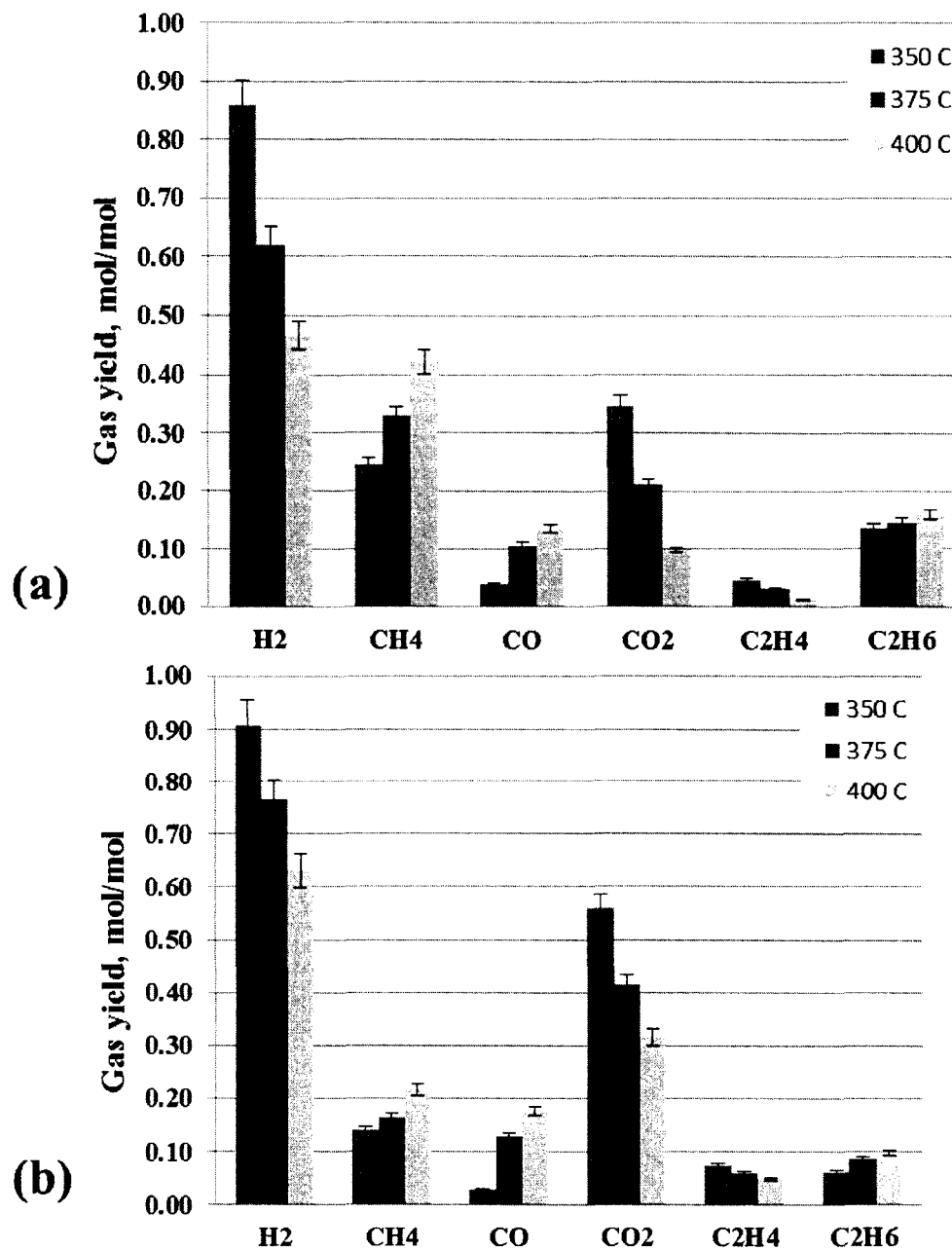


Figure 32. Product gas yields for (a) catalytic and (b) non-catalytic runs.

As we can see from Fig. 32, in the catalytic runs, the major product gases were hydrogen, methane, carbon dioxide, and ethane while in the non-catalytic runs hydrogen

and carbon dioxide prevailed. At 400 °C, the amount of hydrogen and carbon dioxide in the catalytic run reduced while the amount of methane and ethane increased. The same trend was observed for the non-catalytic runs, however, the amounts of methane and ethane were much lower.

The elemental composition and HHVs of the gases produced under all the conditions studied is provided in Table 27.

**Table 27.** Elemental compositions and HHV gaseous products from the catalytic and non-catalytic runs (RSD < 5%)

Exp. No.	Reaction temperature, °C	Mass, g	%C	%H	%O	HHV*, kJ/g	HHV, kJ	HHV, %
<b>Catalyst</b>								
1	350	0.07	43.70	13.61	56.30	25.47	1.81	0.17
2	375	0.18	57.48	16.49	42.52	33.27	5.99	0.57
3	400	0.85	63.66	19.02	36.34	35.74	30.55	2.91
<b>No catalyst</b>								
4	350	0.05	35.93	9.20	64.07	16.76	0.87	0.08
5	375	0.09	39.63	9.78	60.37	19.11	1.76	0.17
6	400	0.20	43.10	10.51	56.90	21.55	4.27	0.41

\*HHV was evaluated using simplified Dulong's formula:  $HHV \text{ (kJ/g)} = (349.1 \text{ (\%C)} + 1178.3 \text{ (\%H)} - 103.4 \text{ (\%O)})/1000$

As can be seen from Table 27, the gas produced in the catalytic run at 400 °C had the highest HHV 35.7 kJ/g due to the presence of greater amounts of carbon and hydrogen and lesser amount of oxygen than in the gases produced in all other runs.

Fig. 33 shows the gasification efficiencies for all the experimental conditions.

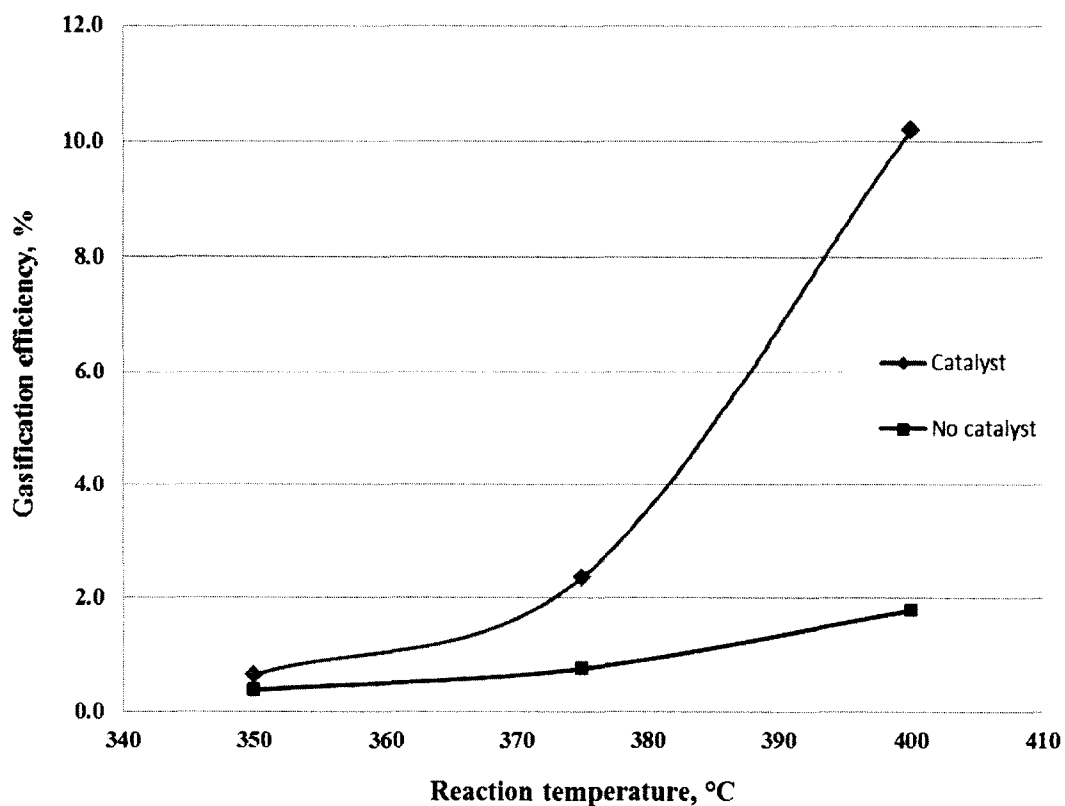


**Figure 33.** Gasification efficiencies for catalytic and non-catalytic HTG of the aqueous phase (RSD < 5%).

As we can see from Fig. 33, the highest gasification efficiency 10.2% was achieved for the HTL of the aqueous phase with activated carbon as catalyst at 400 °C. The relatively low gasification efficiency under these conditions can be explained by (1)

insufficient reaction temperature required for HTG of the aqueous phase derived from the algae, (2) insufficient activity of the activated carbon as catalyst, (3) recalcitrant nature of the compounds present in the extracted aqueous phase (peptides, polyphenols, indoles, and other heterocyclic N-containing compounds), (4) low concentration of carbohydrates and carboxylic acids in the aqueous phase that are readily gasified under the mild conditions (*Scenedesmus obliquus* contains only 10-17 wt% of carbohydrates while the amount of proteins is 50-56 wt%) (Becker 2007). In order to provide the better HTG of the aqueous phase, higher reaction temperatures, lower feed flowrates, more active noble metal catalysts could be employed. Ruthenium catalysts are seem to be the best option for HTG of the aqueous phase after HTL of biomass at relatively low reaction temperature (400 °C) (Stucki, Vogel et al. 2009).

The summary of the HTG of the extracted aqueous phase after the HTL of microalga *Scenedesmus sp.* is shown in Table 28.

**Table 28.** Gasification efficiencies, unreacted aqueous carbon, and carbon balance closure (RSD < 5%)

	Catalyst			No catalyst		
	350	375	400	350	375	400
<b>Reaction temperature, °C</b>	350	375	400	350	375	400
<b>Gasification efficiency, %</b>	0.6	2.4	10.2	0.4	0.8	1.8
<b>Unreacted carbon in effluent, %</b>	94.1	88.1	80.4	99.0	96.2	87.5
<b>Carbon balance, %</b>	94.8	90.5	90.6	99.3	97.0	89.2

As can be seen from Table 28, the highest gasification efficiency of 10.2% was observed for the HTG of the aqueous phase with activated carbon as catalyst at 400 °C. The deficit of the unreacted carbon in the effluent aqueous phase and pure closure of the carbon balance can be explained by an extensive tar formation in the cold parts of the experimental setup (inside and after the heat exchanger).

Products and energy distribution of all the products obtained in the HTL and catalytic HTG at 400 °C is provided in Fig. 34. Products distribution is presented in wt% on a dry basis.

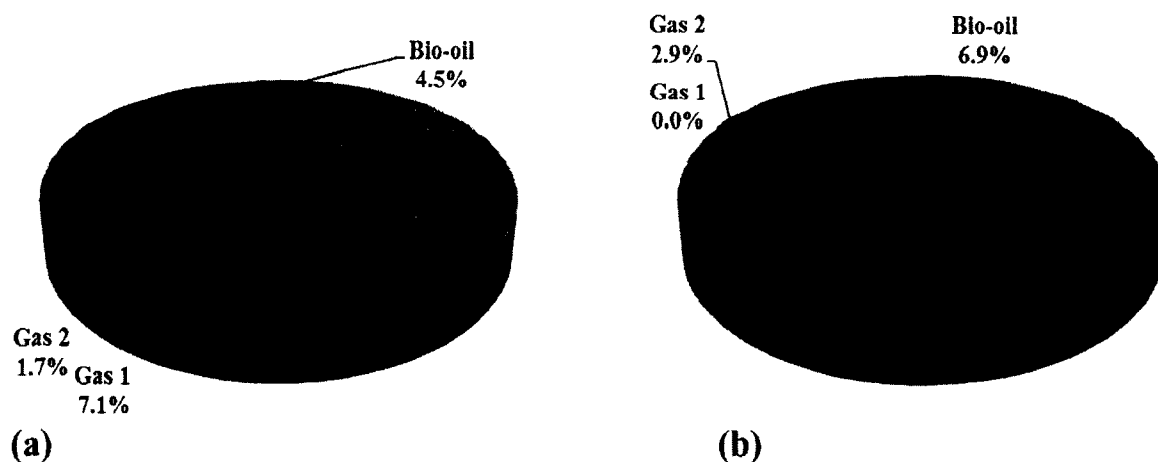


**Figure 34.** (a) Products and (b) energies (HHV) distribution from the HTL and catalytic HTG at 400 °C.

Gas 1 was produced during the HTL of alga in the batch reactor, Gas 2 was formed during the HTG of the extracted aqueous phase. The energy-rich solids, bio-oil,



and Gas 2 contributed 57.7 wt% to the total mass and 84.9% to the total energy (HHV) of the algal biomass.

The WSP from the aqueous phase after its HTG can be a good source of nutrients for growing fresh algae. HTG reduces the organic matter and increases the amount of nitrogen bioavailable as ammonium in the aqueous phase. As it was reported by Barreiro et al., HTG of the aqueous phase provides a way to recover nutrients with simultaneous production of energy in form of gas. They showed that some strains of microalgae (i.e., *Chlorella vulgaris* and *Nannochloropsis gaditana*) can grow as well as in the standard medium even when 75% of the nutrients were substituted by the addition of WSP after HTG. The nutrients recycling can significantly reduce the demand of fresh nutrients for algae cultivation, strongly impact the algae production industry, and lead to a nutrient-neutral process (López Barreiro, Bauer et al. 2015).

#### **5.4. Overall mass balance**

In order to determine the process yields, mass balance around the HTL of microalgal biomass, solvent extraction of the liquid phase, and HTG of the extracted aqueous phase was developed and summarized in Fig 35. 100 kg of dry algal biomass (moisture content 1.9 wt%) were subjected to HTL at 300 °C for 30 min yielding 51.6 kg of energy-rich solid residue, 41.3 kg of liquid products, and 7.1 kg (4.1 m<sup>3</sup>) of gas. The liquid phase was extracted with dichloromethane yielding 4.5 kg of energy-rich bio-oil and 36.8 kg of WSP in the aqueous phase. The latter was subjected to continuous HTG over activated carbon as catalyst at 400 °C and resulted in producing 1.6. kg (2.6 m<sup>3</sup>) of

energy-rich gas and 35.3 kg of WSP. The WSP can be recycled as a source of nutrient for growing fresh algae.

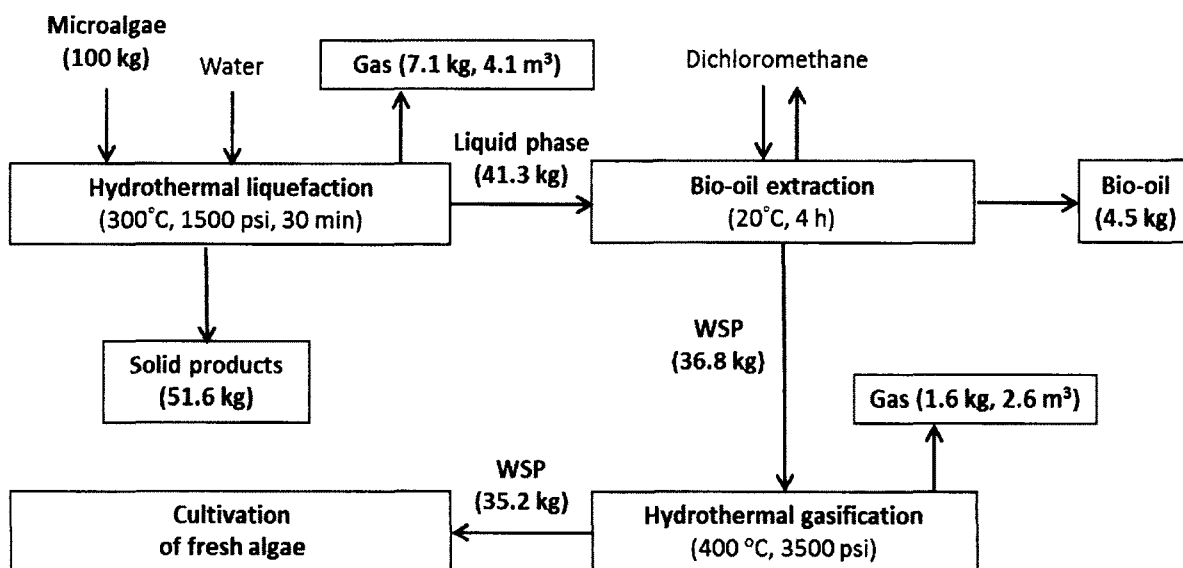


**Figure 35.** Overall mass balance for HTL of microalgae followed by HTG of the extracted aqueous phase.

## 5.5. Conclusions

Microalga *Scenedesmus sp.* was liquefied in a batch reactor at 300 °C and 1500 psi (10.3 MPa) for 30 min. The liquefaction degree under these conditions was 32-33 wt% on a carbon basis. The obtained liquid phase was extracted with dichloromethane yielding 4.5 wt% of bio-oil that contained 6.9 % energy. The solid products and bio-oil that contain 82% of the microalgae energy can be used for renewable fuel production. The extracted aqueous phase was gasified over a low-cost activated carbon as catalyst in a continuous flow process at 350-400 °C and 3500 psi (24.1 MPa) with WHSV of 3.3 h<sup>-1</sup>.

The highest gasification efficiency of 10.2% was observed at 400 °C, which is 5.7 times greater than that in the control experiments without catalyst, providing 2.9% of additional energy. The gas produced with catalyst contained mostly H<sub>2</sub> and light hydrocarbons while the gas produced without catalyst consisted mainly of H<sub>2</sub> and CO<sub>2</sub>. The results of the study show that considerable amount of H<sub>2</sub> and gaseous hydrocarbons can be produced at relatively low temperature of 400 °C using a low-cost activated carbon as catalyst. The processed aqueous phase can be used as a source of nutrients for growing fresh algae. In this study, we proved the concept that utilization of the aqueous phase can be performed via the low-temperature gasification over the low-cost catalyst and obtained promising results. The processed aqueous phase can significantly reduce the demand of fresh nutrients for algae cultivation and lead to a nutrient-neutral process. The relatively low gasification efficiency can be due to the recalcitrant nature of the compounds present in the extracted aqueous phase. It can be increased by increasing the reaction temperature of the HTG process. Further research is required to determine the optimal process conditions and to study the impact of the WSP present in the effluent aqueous phase on the microalgae growth.

## **5.6. Acknowledgments**

The authors acknowledge our colleagues from the Department of Chemistry and Biochemistry at Old Dominion University for their help with the analyses. Our special appreciation is to the National Science Foundation (Grant NSF-CBET-CAREER: 1351413) for providing the financial support for this research.

## CHAPTER 6

### RAPID HYDROTHERMAL DEOXYGENATION OF OLEIC ACID IN A CONTINUOUS FLOW PROCESS

*Note: the contents of this chapter have been published in the journal Energy & Fuels.*

Popov, S., Kumar, S. Rapid hydrothermal deoxygenation of oleic acid over activated carbon in a continuous flow process. *Energy & Fuels*, **29** (5), 3377–3384 (2015). DOI: 10.1021/acs.energyfuels.5b00308.

In this study, a novel approach to converting fatty acids into *n*-alkanes was investigated. Fuel range hydrocarbons were obtained in a continuous flow process from oleic acid using near- and supercritical water as reaction media, granulated activated carbon as a catalyst, and 1% formic acid as an in situ source of hydrogen. Experiments were conducted in a packed tubular reactor with the weight hourly space velocity of 4 h<sup>-1</sup> at the temperatures from 350 to 400 °C and pressure 3500 psi (24.1 MPa). The oil to water to formic acid ratio was 1:5:0.05 by volume. The main reaction pathways were hydrogenation of oleic acid and decarboxylation/decarbonylation of stearic acid to form heptadecane. The yield of heptadecane 67% with the selectivity greater than 80% was observed at 370 °C. The results of the study show that efficient hydrothermal deoxygenation of fatty acids can be achieved with activated carbon as a catalyst and formic acid as an in situ source of hydrogen within minutes. Kinetics study showed that the rates of oleic acid conversion displayed Arrhenius behavior with the activation energy of 100 kJ/mol.

## 6.1. Introduction

Biomass with high lipid content (e.g., jatropha seeds, microalgae) is an attractive feedstock for renewable fuel production. There is a considerable interest in research and development of methods for converting triglycerides and fatty acids into hydrocarbons that are fully fungible with petroleum-derived transportation fuels (Popov and Kumar 2013). Significant efforts were made to adapt petroleum hydrotreating technology to producing hydrocarbons from plant oils (Smith, Greenwell et al. 2009). These efforts included providing respective reaction conditions (250-400°C, 10-20 MPa), using conventional hydrotreating catalysts (e.g., CoMo/Al<sub>2</sub>O<sub>3</sub>, NiMo/Al<sub>2</sub>O<sub>3</sub>) or noble metal catalysts (e.g., Pt/C, Pd/C), and supplying H<sub>2</sub> with high feed rates (100-700 L/L) for removal of oxygen from oils in form of H<sub>2</sub>O.

The high consumption of gaseous H<sub>2</sub> makes the hydrodeoxygenation process costly. In order to reduce the production costs, consumption of H<sub>2</sub> has to be minimized or eliminated. In this respect, decarboxylation process that removes oxygen from fatty acids in form of CO<sub>2</sub> appears to be more advantageous than hydrodeoxygenation that removes oxygen in form of H<sub>2</sub>O (Mäki-Arvela, Kubickova et al. 2006, Bernas, Eränen et al. 2010, Immer and Lamb 2010, Rozmysłowicz, Mäki-Arvela et al. 2011).

Almost all the decarboxylation studies were done using fatty acids without solvent or dissolved in hydrocarbon solvent, and the best results were achieved using noble metals (e.g., Pt/C, Pd/C) as catalysts (Kubickova, Snare et al. 2005, Snare, Kubičková et al. 2006, Snare, Kubičková et al. 2008, Fisk, Morgan et al. 2009, Vam 2013).

Using sub- and supercritical water for processing biomass-derived products is considered an efficient and environmentally benign method that capitalizes on the extraordinary properties of water as a reactant and reaction medium and provides the ideal conditions for ionic/free-radical reactions. In subcritical water-based processes, water is kept in a liquid state by applying pressure greater than the pressure of vapor at the reaction temperature. In this way, the energy consumed for the water to steam phase change (the latent heat of water vaporization is 2.26 MJ/kg) is avoided, which significantly reduces the energy requirements for hydrothermal processes (Kumar 2013).

There is a growing potential for using hot compressed water as a reaction medium for catalytic decarboxylation of fatty acids (Watanabe, Iida et al. 2006, Fu, Lu et al. 2010, Fu, Lu et al. 2011, Fu, Shi et al. 2011, Santillan-Jimenez and Crocker 2012, Yang, Nie et al. 2013). Subcritical water was proven to be a favorable environment for hydrolysis of triglycerides without using alkali or acid catalysts (Patil, Butala et al. 1988, Patil, Raghunathan et al. 1988, King, Holliday et al. 1999, Alenezi, Baig et al. 2009). Decarboxylation of the produced fatty acids into hydrocarbons can ideally be accomplished in the same aqueous medium without prior separation. Watanabe et al. demonstrated that stearic acid can be converted into alkanes in supercritical water at 400°C for 30 min using NaOH and KOH as catalysts (Watanabe, Iida et al. 2006). However, the selectivity to hydrocarbons reported for this process was low (<15%). Savage and co-workers reported the results of their studies on hydrothermal hydrogenation and decarboxylation of fatty acids in hot compressed water over Pt/C and Pd/C catalysts without H<sub>2</sub> added (Fu, Lu et al. 2010, Fu, Lu et al. 2011). They showed that deoxygenation of saturated (lauric, palmitic, and stearic) and unsaturated (oleic and

linoleic) fatty acids can be done in near- and supercritical water with high selectivity (>90%) toward the respective decarboxylation products for saturated fatty acids.

Savage et al. also demonstrated that activated carbon alone possesses catalytic activity for hydrothermal decarboxylation of palmitic and oleic acids (Fu, Shi et al. 2011). The experiments for the above studies were conducted in batch reactors for 3 h without H<sub>2</sub> added, and deoxygenation products from oleic acid contained both alkanes and alkenes. This indicates that an in situ formation of H<sub>2</sub> occurs during the deoxygenation process, most likely from gasification of oleic acid itself, yielding H<sub>2</sub> and aromatic/cyclic compounds. The amount of H<sub>2</sub> produced is insufficient for complete hydrogenation of oleic acid and the resulting hydrocarbons. The use of batch reactors takes a considerable amount of time to complete the conversions and makes it problematic to scale the process up.

We attempted to develop and investigate a rapid and inexpensive continuous flow process that could be readily scaled up and used for renewable fuel production via hydrothermal deoxygenation of biomass with high lipid content. We used activated carbon as a catalyst in our process because it could be an attractive low-cost option for this type of conversions provided that it is sufficiently active under the conditions studied. The novelties of the proposed process are: i) using hydrothermal medium for deoxygenation of fatty acids; ii) using continuous flow process that significantly reduces reaction time and makes the process scalable; iii) using activated carbon as a low-cost decarboxylation catalyst; iv) using formic acid as an in situ source of H<sub>2</sub> for hydrogenation of the intermediate products.

To the best of our knowledge, there has been no report on hydrothermal deoxygenation of fatty acids using activated carbon as a catalyst and formic acid as an in situ source of H<sub>2</sub> in a continuous flow process. In this article, we report on the rapid hydrothermal catalytic deoxygenation of oleic acid in a continuous flow reactor loaded with low-cost granulated activated charcoal.

## **6.2. Experimental section**

### **6.2.1. Materials and methods**

Oleic acid lab grade >97%, formic acid reagent grade 88%, and granulated activated charcoal Darco were purchased from Fischer Scientific USA. All the chemicals were used as received. The oleic acid was loaded into the piston feeder and used as a feedstock in the study. 1% v/v formic acid was added to deionized water and served as an additional source of H<sub>2</sub> during the hydrothermal hydrogenation process. The granulated activated charcoal was sieved to remove particle sizes <500 μm before being loaded into the reactor.

The deoxygenation experiments were conducted in a 65 mL HiP tubular reactor MS-18 with the overall length of 19" and inside diameter of 9/16". The reactor was packed with the granulated activated charcoal (18.2 g) and installed inside of a horizontal electric furnace that allowed precise temperature control. The catalyst occupied 30% of the reactor volume. The experimental setup is shown in Fig. 36.



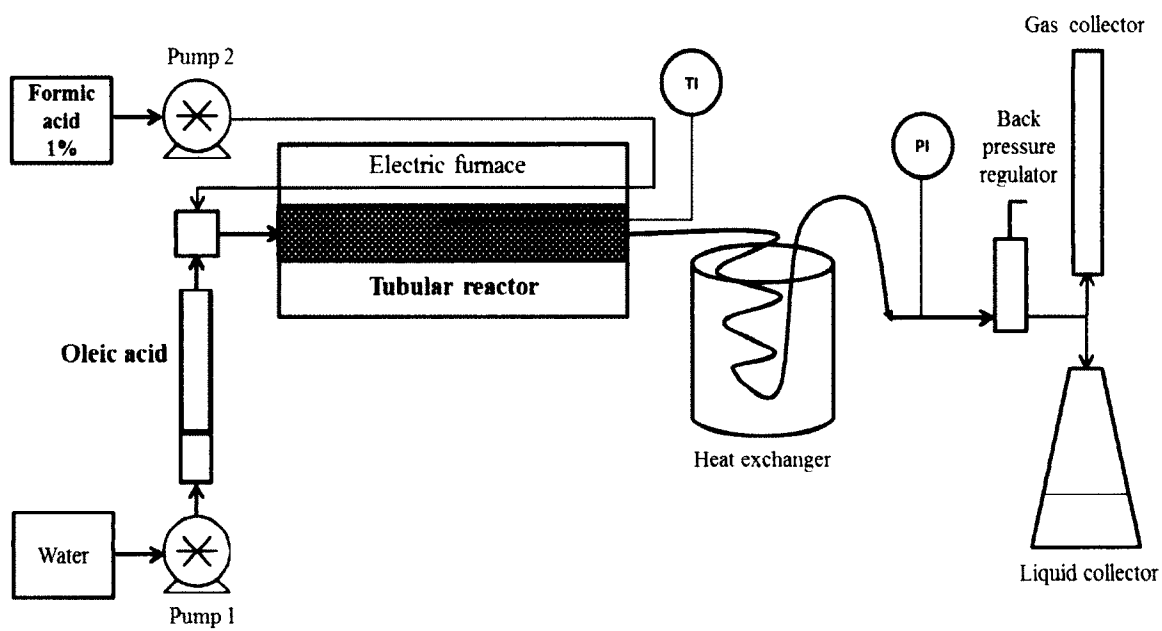


**Figure 36.** Experimental setup for rapid hydrothermal deoxygenation of oleic acid.

Two high pressure and high precision dual piston pumps Shimadzu LC-10AD were used to deliver both oleic acid and 1% v/v formic acid into the reactor with independently adjusted flowrates. Oleic acid was loaded into a 81 mL vertical piston feeder and delivered into the reactor by applying pressure from Pump 1. A HiP tubular reactor MS-19 with the overall length of 23" and inside diameter of 9/16" equipped with a piston separator was used as a feeder. 1% v/v formic acid was preheated in the furnace, mixed with oleic acid, and delivered into the reactor with Pump 2. Reaction products were cooled down in a water heat exchanger. The liquid products were collected for mass balance calculations and further analyses. The volume flowrate of the gaseous products was measured periodically with a volumetric burette filled with water and a stopwatch. The samples of the gaseous products were taken from the burette with a syringe and analyzed with a gas chromatograph.

The pressure inside the reactor was regulated with the back pressure regulator and kept close to  $3500 \pm 10$  psi (24.1 MPa) for all the experiments. The ratio of oleic acid to 1% v/v formic acid was kept at 0.2:1 mL/min for all the experiments, i.e., oleic acid entered the system at  $6.34 \times 10^{-4}$  mol/min. The temperature inside the reactor was measured with two thermocouples equipped with controllers; one thermocouple was installed in the middle of the reactor, the other – immediately after the reactor. The experiments were conducted at six different temperatures:  $350 \pm 2^\circ\text{C}$ ,  $360 \pm 2^\circ\text{C}$ ,  $370 \pm 2^\circ\text{C}$ ,  $380 \pm 2^\circ\text{C}$ ,  $390 \pm 2^\circ\text{C}$ , and  $400 \pm 2^\circ\text{C}$ . The pressure in the system was measured with the pump controllers before the reactor and with PGS-35B-5000 general service pressure gauge (Omega, USA) before the back pressure regulator. The residence time in the reactor was adjusted to 21 min.

Weight hourly space velocity (WHSV) was  $4 \text{ h}^{-1}$  for all the experiments and was calculated using Eq. 44:

$$\text{WHSV} = \frac{\text{Feed mass flow, g/h}}{\text{Catalyst mass, g}} \quad (44)$$

The experiments started with pumping 1% v/v formic acid into the reactor until the desired temperature and pressure were reached and stabilized. After that, the other pump started delivering oleic acid into the reactor through the piston feeder. A typical experiment was conducted for 6 h 40 min until the 81 mL piston feeder was empty. The liquid reaction products and water were collected in a 500 mL flask. The obtained products were separated from water, quantified, and analyzed with a gas chromatograph-mass spectrometer (GC-MS). After each experiment, the system was flushed with pure deionized water at 10 mL/min for at least 1 h.

Two series of control experiments were conducted before the main experimental part. The first series was carried out with deionized water only to determine whether the gas formation other than from formic or oleic acids occurs during the deoxygenation process at different reaction temperatures (350-400 °C). The second series was carried out with oleic acid and water but without formic acid added to water to determine whether hydrogenation of oleic acid occurs without a donor of H<sub>2</sub> at different reaction temperatures (350-400 °C).

## **6.2.2. Product separation and analyses**

### **6.2.2.1. Analyses of the catalyst**

Brunauer-Emmett-Teller (BET) surface area and pore volume/size analysis of the catalyst was carried out with a NOVA 2000e surface area and pore size analyzer (Quantachrome Instruments). The samples were degassed at 120 °C with continuous flow of nitrogen and helium at 10 psi overnight prior to the analysis. Liquid nitrogen was used as an adsorbent during the measurements. Multi-Point BET method was used to determine the surface area and BJH method was used as the most common and accurate method to compute the average pore volume and pore size of the samples.

X-ray diffraction (XRD) pattern of the catalyst was obtained with a Rigaku MiniFlex II SX Desktop X-ray diffractometer between 5 and 90° (2θ) at a scan rate 3 deg/min to study its structure.

Energy dispersive spectroscopy (EDS) was carried out with a JEOL JSM-6060 LV environmental scanning electron microscope (SEM) to determine the presence of

metals on the activated carbon that might contribute to the hydrogenation/deoxygenation catalysis.

The results of Fourier transform infrared spectroscopy (FTIR) for commercial granulated activated carbons were taken from the related studies (Jung, Ahn et al. 2001, Barkauskas and Dervinyte 2004, Marsh and Rodríguez-Reinoso 2006). FTIR was employed to determine the surface functional groups that can catalyze the hydrogenation/deoxygenation reactions.

#### **6.2.2.2.Product separation**

Under the conditions studied, oleic acid and water formed stable (milk-like) emulsions that were difficult to separate by physical means alone. The reaction products containing mostly hydrocarbons did not form emulsions with water, however, an organic solvent was employed to efficiently separate the organic and water phases for all the experiments. 100 mL of diethyl ether was added to the flask containing the reaction products and water. The mixture was shaken vigorously for 10 min and placed into a separation funnel for a few hours. After that, the organic and water phases were separated and diethyl ether from the organic phase was removed with a vacuum evaporator.

#### **6.2.2.3.Analyses of the products**

The gaseous products were identified with SRI 8610C GC equipped with a 6' molecular sieve MS-13X connected to a 10' × 1/8" HayeSep D packed column and a thermal conductivity detector (TCD). Helium at 20 mL/min was used as carrier gas. The

temperature program was set up as follows: initial temperature 40 °C, hold for 20 min, final temperature 40 °C. SCOTTY gas calibration standard containing 50 mol% H<sub>2</sub>, 10 mol% CH<sub>4</sub>, 10 mol% CO, 20 mol% CO<sub>2</sub>, 5 mol% ethylene, and 5 mol% propane was purchased from Air Liquide America Specialty Gases LLC, USA.

The liquid products were analyzed with an Agilent 6890 GC and a LECO Pegasus III TOF-MS system equipped with an Rtx-5 (30 m × 0.25 mm × 0.25 μm) and an Rxi-17 (0.79 m × 0.1 mm × 0.1 μm) capillary columns and a flame ionization detector (FID). The oven temperature was held at 50 °C for 2 minutes, ramped up to 200 °C at a rate of 5 °C/min, and then ramped to 300 °C at a rate of 20 °C/min. Samples were injected in a split mode (50:1) at 250 °C and helium was used as carrier gas. All the compounds were identified using the NIST library of mass spectra. For the major compounds, quantitative analysis was done by generating and using calibration curves. The minor compounds, for which we did not have standards, were quantified by making a reasonable assumption that the detector response was proportional to the mass of carbon atoms in the identified molecules.

Conversion was calculated as the amount of oleic and steric acids that had reacted (Eq. 45):

$$X = \frac{\text{Products yield, wt\%}}{\text{Feed, wt\%}} \times 100\% \quad (45)$$

Product yields were calculated as the amounts of products of interest divided by the initial amount of oleic acid delivered into the reactor. Selectivity was calculated as the amount of a product of interest (heptadecane) divided by the amount of oleic and stearic acids that had reacted (Eq. 46):

$$S = \frac{\text{Heptadecane yield, wt\%}}{X, \text{ wt\%}} \times 100\% \quad (46)$$

An average formation of a solid deposit on the catalyst from a series of six experiments was determined gravimetrically. The weight of the catalyst was recorded before and after each series, and the difference was divided by the number of experiments and the amount of oleic acid used in an experiment.

All the experiments and analyses were carried out in triplicate, and the reported values are the mean results from at least three independent experiments/analyses. The reported uncertainties are the relative standard deviations (RSD) from those experiments/analyses' results.

### 6.3. Results and discussion

#### 6.3.1. Structural and compositional properties of the catalyst

The BET surface area and pore volume/size analysis of the granulated activated carbon used as a catalyst in our study showed that its surface area was  $600 \pm 20 \text{ m}^2/\text{g}$ , average pore volume was  $0.95 \pm 0.05 \text{ cm}^3/\text{g}$ , and average pore size was  $60 \pm 5 \text{ nm}$ . After a series of six experiments, the surface area of the catalyst was  $25 \pm 5 \text{ m}^2/\text{g}$ , average pore volume was  $0.30 \pm 0.02 \text{ cm}^3/\text{g}$ , and the average pore size did not significantly change over time.

XRD pattern for the activated carbon used in the study (Fig. S1) indicated that the sample was amorphous, but a detectable amount of  $\text{SiO}_2$  was present in the catalyst. However, it was reported that  $\text{SiO}_2$  alone does not possess any catalytic activity toward the hydrothermal decarboxylation of fatty acids (Fu, Shi et al. 2011). Savage et al. did a

control experiment with palmitic acid and silica instead of activated carbon in a batch reactor (370°C, 3 h) in order to determine whether SiO<sub>2</sub> was able to influence the hydrothermal decarboxylation reaction. No measurable amount of pentadecane was produced. Thus it was concluded that the inert material has no measurable activity for hydrothermal decarboxylation at the reaction conditions studied (Fu, Shi et al. 2011).

EDS spectrum of the activated carbon used as a catalyst in the study showed no evidence for the presence of significant amounts of metals in the sample (Fig. S2, Table S1). The overall amount of the most abundant Ca<sup>2+</sup> and Mg<sup>2+</sup> ions that do not possess deoxygenation activity was < 0.5 atom%. Savage et al. who studied hydrothermal decarboxylation of fatty acids over similar activated carbon (Darco) did not find evidence that its catalytic activity could be attributed to the presence of metals or their oxides either (Fu, Shi et al. 2011).

FTIR spectra of commercial granulated activated carbons can be found elsewhere (Jung, Ahn et al. 2001, Barkauskas and Dervinyte 2004, Marsh and Rodríguez-Reinoso 2006). The main surface functional groups present in the commercial activated carbons that determine their properties and activities are shown in supplementary Table S2.

To our knowledge, the catalytic mechanism of activated carbons toward fatty acid deoxygenation was not studied up to date. However, it was observed that its activity depends on the surface area and the number of oxygenated functional groups on the surface (Medina, Larsen et al. 2003). Snåre et al. observed higher deoxygenation rates when metal catalysts with carbonaceous supports were used (Snåre, Kubičková et al. 2006). This was attributed to the ability of carbon to promote the reaction through its amphoteric properties and surface functionalities. Also, Pd/C catalysts of varying acidity

were screened for decarboxylation of ethyl stearate (Mäki-Arvela, Kubickova et al. 2006). It was found that the most alkaline catalysts afforded highest yields of *n*-heptadecane.

### 6.3.2. Hydrothermal deoxygenation products

Two series of control experiments were conducted before the main experimental part. The first series was carried out with deionized water only (blank runs) at different reaction temperatures (350-400°C) to determine whether gas formation occurs from the reaction of water with the carbon catalyst. No detectable amount of gaseous products was observed at the conditions studied. This is consistent with the studies on carbon-catalyzed gasification of organic feedstocks in supercritical water by Antal et al. (Xu, Matsumura et al. 1996, Matsumura, Xu et al. 1997). Their studies show that carbon is able to promote formation of H<sub>2</sub> and CO at much higher temperatures (600–650 °C, 25.5–34.5 MPa). Even though we did not observe gas formation during the blank experiments, we think it is possible that water reacted with the carbon forming a small amount of H<sub>2</sub> and CO with further reacting of CO to form more H<sub>2</sub> under the reaction conditions studied. This gas might be dissolved in water or form very small suspended bubbles. However, carbon gasification, if it occurs, is much slower than gasification of formic and oleic acids (Xu, Matsumura et al. 1996).

The second series of control experiments on rapid hydrothermal deoxygenation of oleic acid over activated carbon in a continuous flow process under near- and subcritical conditions without a source of H<sub>2</sub> (formic acid) was also carried out. The experiments led to formation of alkenes rather than alkanes, and the reaction products tended to isomerize



even at relatively low temperatures (350 °C). Formation of a noticeable amount of stearic acid was not observed in the process either (Table 29). This could be due to the short residence time (21 min) and high WHSV of the continuous process (4 h<sup>-1</sup>) that did not provide the conditions for the sufficient in situ generation of H<sub>2</sub> and hydrogenation of oleic acid and the reaction products. The control experiments and analyses of liquid and gas phases showed that deoxygenation of oleic acid and the products of its cracking occurred easily through decarboxylation pathway mostly. However, hydrogenation of their double bonds could not be achieved without an additional source of H<sub>2</sub>. The control experiments at higher temperatures yielded mostly aromatic/cyclic compounds and large amounts of gaseous products.

**Table 29.** Products from hydrothermal deoxygenation of oleic acid at 350 °C without formic acid added

Product	Yield, wt%
2-Methyl-1,4-hexadiene	0.8 ± 0.1
3-Octene	1.5 ± 0.1
3-Nonene	1.2 ± 0.1
3,5-Dimethyl-1-hexene	0.6 ± 0.1
3-Decene	0.8 ± 0.1
2-Undecene	1.2 ± 0.1
3-Dodecene	0.8 ± 0.1
5-Hexadecene	1.0 ± 0.1

2-Methyl-1-pentadecene	1.5 ± 0.1
5-Heptadecene	10.2 ± 0.5
Oleic acid	78.7 ± 1

Hydrothermal decarboxylation of fatty acids for a much longer time without H<sub>2</sub> added led to production of both alkanes and alkenes (Fu, Lu et al. 2010, Fu, Lu et al. 2011, Fu, Shi et al. 2011). H<sub>2</sub> that was produced in situ during those experiments and contributed to the products' hydrogenation most likely originated from hydrothermal gasification of the fatty acid feedstock. It is unlikely that gasification of the activated carbon would occur at the conditions studied to produce the sufficient amount of H<sub>2</sub> (Matsumura, Xu et al. 1997). Therefore, in order to obtain alkanes only and reduce the reaction time, an inexpensive donor of ionic/free-radical H<sup>+</sup> is required.

Formic acid is known to readily decompose under hydrothermal conditions (above 320 °C) yielding H<sub>2</sub> and CO<sub>2</sub> (Yu and Savage 1998). Therefore, a small amount of formic acid (≤1%) was added to the aqueous medium to serve as a donor of H<sub>2</sub> in this study. This made it possible to produce *n*-alkanes with good yield and selectivity to heptadecane in a continuous flow process within a short residence time of 21 min and WHSV of 4 h<sup>-1</sup>. The main results of the hydrothermal deoxygenation of oleic acid over granulated activated carbon at all the conditions studied are provided in Table 30.

**Table 30.** Conversion, deoxygenation product yield, and selectivity to heptadecane at different reaction temperatures

Temperature, °C	Conversion of oleic acid, %	Conversion of stearic acid, %	Heptadecane yield, wt%	Selectivity, %
350 ± 2	77.9 ± 2	23.4 ± 1	11.7 ± 0.5	49.9 ± 2
360 ± 2	92.4 ± 1.5	56.0 ± 1.5	44.0 ± 1	78.6 ± 3
370 ± 2	99.4 ± 0.5	83.2 ± 2	67.1 ± 1.5	80.6 ± 4
380 ± 2	99.7 ± 0.3	96.2 ± 1.5	69.7 ± 1.5	72.5 ± 3
390 ± 2	≈ 100	98.4 ± 1	31.2 ± 1	31.7 ± 2
400 ± 2	≈ 100	98.8 ± 0.2	9.7 ± 0.5	9.8 ± 1

As can be seen from Table 30, the highest heptadecane yields of 67.1% and 69.7% were produced at 370 °C and 380 °C and the highest selectivity of 80.6% was observed at 370 °C. The latter was considered the optimal temperature for the hydrothermal deoxygenation process.

The main characteristics of the hydrothermal deoxygenation of oleic acid over activated carbon in a continuous flow process are shown in Fig. 37. As we can see from Fig. 37, the stearic acid was almost completely converted into hydrocarbons at 380 °C and higher. The yield of heptadecane, the main deoxygenation product, reached its maximum (about 72%) between 370 °C and 380 °C. The maximum selectivity of the deoxygenation process to heptadecane (80.6%) was observed at 370°C.

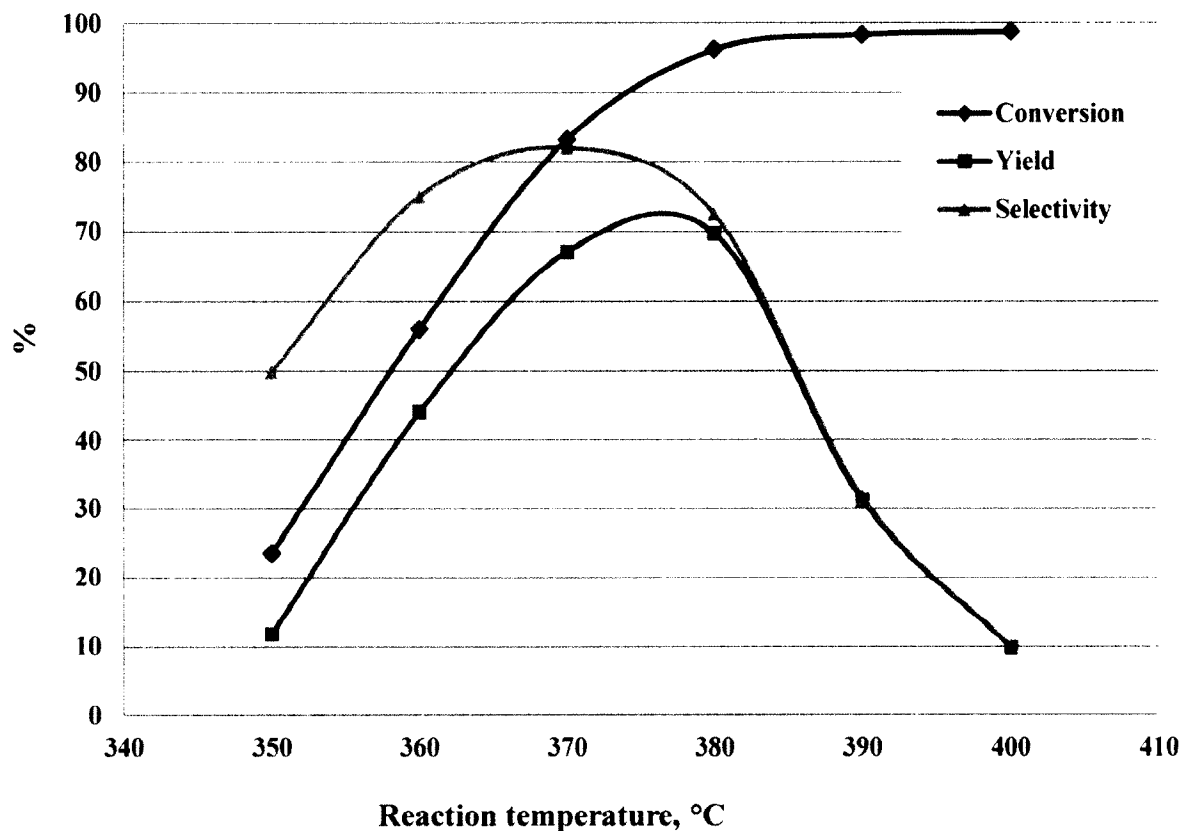


**Figure 37.** Conversion of stearic acid, heptadecane yield, and selectivity to heptadecane at different reaction temperatures (RSD<4%).

Fig. 38 shows the chromatograms of the deoxygenation products obtained at 360°C, 370 °C, and 380 °C. It is clearly seen that conversion of oleic acid into stearic acid, disappearance of stearic acid, and arising *n*-alkanes increases with increasing the reaction temperature.

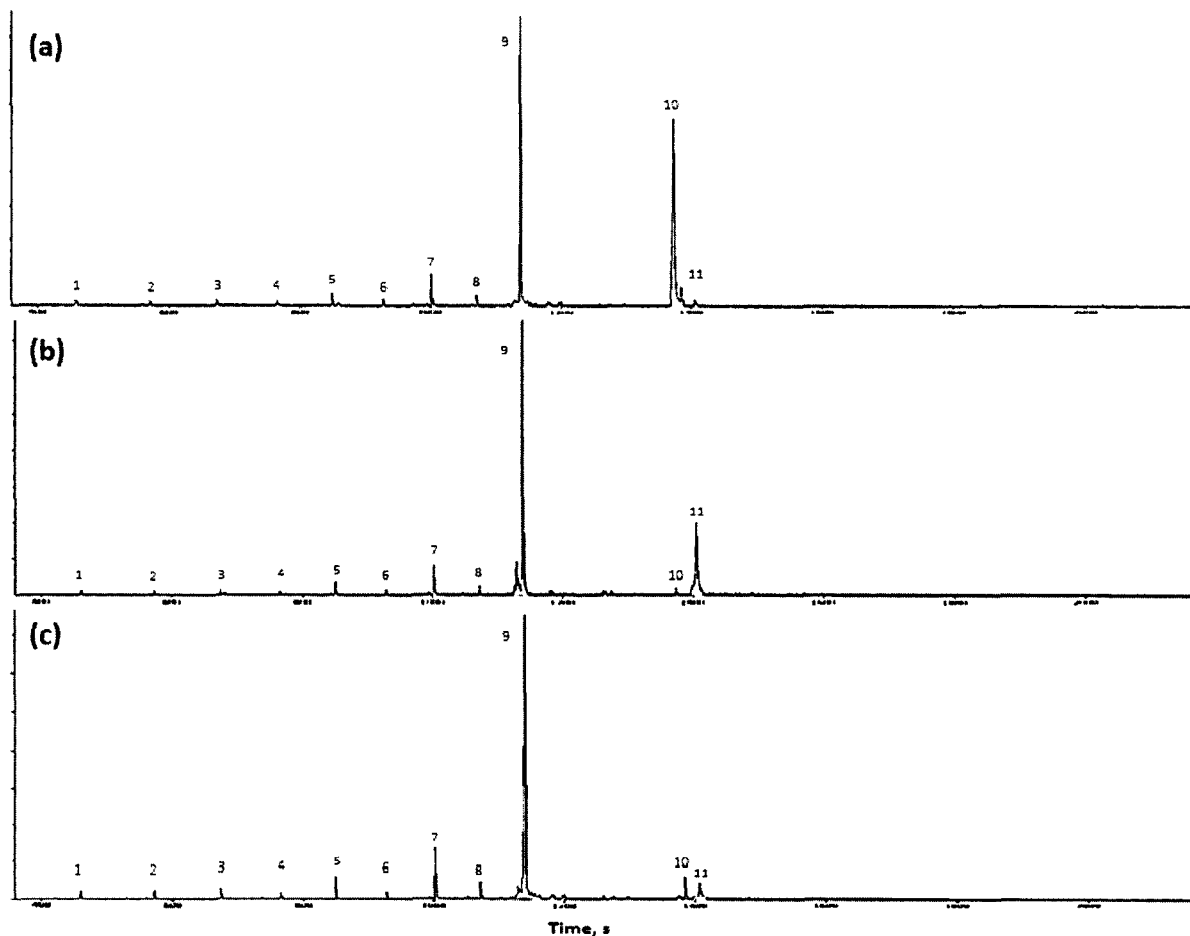


**Figure 38.** GC-FID of the products from hydrothermal deoxygenation of oleic acid at: **(a)** 360 °C, **(b)** 370°C, and **(c)** 380 °C. Peak 1: nonane, 2: decane, 3: undecane, 4: dodecane, 5: tridecane, 6: tetradecane, 7: pentadecane, 8: hexadecane, 9: heptadecane, 10: oleic acid, 11: stearic acid.

The results of GC-MS analysis of all the products obtained in the study are provided in Table 31.

**Table 31.** Products from hydrothermal deoxygenation of oleic acid over activated carbon at different reaction temperatures

Product	Yield, wt%, at					
	350 °C	360 °C	370 °C	380 °C	390 °C	400 °C
Ethylbenzene	-	-	-	-	2.9 ± 0.5	4.6 ± 0.5
p-Xylene	-	-	-	-	5.5 ± 0.5	7.0 ± 0.5
Nonane	0.3 ± 0.05	0.4 ± 0.05	0.5 ± 0.05	0.6 ± 0.05	3.2 ± 0.5	0.6 ± 0.05
Decane	0.3 ± 0.05	0.4 ± 0.05	0.5 ± 0.05	0.6 ± 0.05	3.5 ± 0.5	3.2 ± 0.5
Undecane	0.5 ± 0.05	0.7 ± 0.05	0.9 ± 0.05	1.1 ± 0.1	5.8 ± 0.5	2.5 ± 0.5
Dodecane	0.3 ± 0.05	0.4 ± 0.05	0.5 ± 0.05	0.7 ± 0.05	3.2 ± 0.5	1.2 ± 0.1
Tridecane	0.6 ± 0.05	1.0 ± 0.1	1.3 ± 0.1	1.5 ± 0.1	4.9 ± 0.5	1.7 ± 0.1
Tetradecane	0.5 ± 0.05	0.7 ± 0.05	1.0 ± 0.05	1.2 ± 0.1	1.4 ± 0.1	0.7 ± 0.05
Pentadecane	1.8 ± 0.1	4.0 ± 0.5	4.5 ± 0.5	5.2 ± 0.5	2.8 ± 0.5	1.4 ± 0.1
Hexadecane	0.8 ± 0.1	1.5 ± 0.1	1.7 ± 0.1	1.8 ± 0.1	1.2 ± 0.1	0.4 ± 0.05
Heptadecane	11.7 ± 1	44.0 ± 1	67.1 ± 1	69.7 ± 1	31.2 ± 1	9.7 ± 1
Oleic acid	7.6 ± 1	7.5 ± 1	7.8 ± 1	0.6 ± 0.05	0.2 ± 0.005	-
Stearic acid	68.9 ± 1	36.5 ± 1	9.0 ± 1	3.3 ± 0.5	1.5 ± 0.1	-

As we can see from Table 31, activated carbon has a good catalytic activity for deoxygenation of oleic and stearic acids. The main deoxygenation product was heptadecane, C<sub>17</sub>H<sub>36</sub> *n*-alkane, originating from direct decarboxylation/decarbonylation of stearic acid. The maximum yields of heptadecane (67.1% and 69.7%) were observed at 370°C and 380 °C. The deoxygenation products obtained under those conditions were yellow or light brown liquids with diesel-like smell. All the minor deoxygenation products were shorter *n*-alkanes, which indicated that activated carbon also possessed an activity for cracking of fatty acids and their intermediates. The products obtained at 350°C and 360 °C were white or yellowish solids under the normal conditions. This can be explained by the presence of significant amounts of stearic acid in the reaction products. The products obtained at 390 °C and 400 °C were dark brown liquids with strong benzene-like smell.

Table 32 provides the distribution of liquid and gaseous deoxygenation products from oleic acid at all the temperatures studied.

**Table 32.** Product distribution of liquid and gaseous products from hydrothermal deoxygenation of oleic acid at different temperatures (RSD < 5%)

Reaction temperature, °C	Liquid products, wt%	Gaseous products, wt%
350	98.8	1.0
360	98.4	1.2
370	97.3	1.8
380	94.6	4.3

390	88.7	9.7
400	76.6	21.5

As we can see from Table 32, considerable gas formation from oleic acid occurred at the temperatures above 390 °C, thus reducing liquid product yields. Yields of gaseous products were calculated from oleic acid only (the difference between total gas yields and gas yields from formic acid). For this purpose, the blank experiments with formic acid solution only were conducted at the same experimental conditions and gas formation rates were measured for all the runs. The average formation of a solid deposit on the catalyst surface was  $0.67 \pm 0.02$  wt% per an experiment (or 0.1 wt%/h). At the reaction temperatures studied, no noticeable signs of catalyst deactivation were observed for at least six experimental runs. Composition of the gaseous product obtained at 380 °C is shown in Table 33.

**Table 33.** Yields of gaseous products from hydrothermal deoxygenation of oleic acid at 380 °C

Compound	Yield, wt%
Hydrogen	$25.0 \pm 3$
Methane	$8.3 \pm 2$
Carbon monoxide	$3.5 \pm 1$
Carbon dioxide	$37.5 \pm 3$



Ethane	4.0 ± 1
Propane	21.7 ± 2

As we can see from Table 33, two groups of gaseous products arose from the hydrothermal deoxygenation of oleic acid. One group (H<sub>2</sub>, CO<sub>2</sub>, CO) arose from decomposition/deoxygenation of formic and oleic acids. The other group (CH<sub>4</sub>, C<sub>2</sub>H<sub>6</sub>, C<sub>3</sub>H<sub>8</sub>) arose from cracking of fatty acids and *n*-alkanes. H<sub>2</sub> was a major product that originated from formic acid decomposition and participated in hydrogenation of oleic acid. CO<sub>2</sub> and CO are the two main by-products, which show that deoxygenation occurred through both decarboxylation and decarbonylation of oleic and stearic acids. CO yield was always about an order of magnitude lower than CO<sub>2</sub> yield. Therefore, decarboxylation was the main reaction pathway leading to hydrocarbon production from fatty acids.

Equations 47-49 show the main reaction pathways for hydrothermal hydrogenation and deoxygenation of oleic acid:

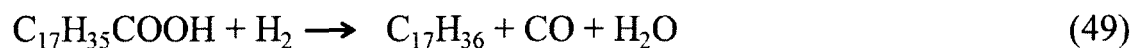
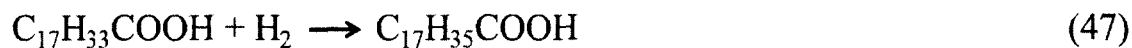


Table 31 shows the yields of products from hydrothermal deoxygenation of oleic acid at the reaction temperatures studied. The major reaction products were stearic acid

and heptadecane. Stearic acid was formed from oleic acid through hydrogenation reaction (47). Hydrogenation of the double bond in oleic acid appears to be faster than its decarboxylation to form C<sub>17</sub> alkane (Immer, Kelly et al. 2010, Fu, Lu et al. 2011, Fu, Shi et al. 2011). The reported rate of palm stearin hydrogenation was four orders of magnitude faster than the observed rate of stearic acid deoxygenation; it was not limited by intraparticle mass transfer resistance and did not depend on the catalyst particle and pore size (Tike and Mahajani 2006). Heptadecane was formed mainly through decarboxylation (48) and decarbonylation (49) reactions. The minor reaction products (C<sub>9</sub>-C<sub>16</sub> alkanes) were produced due to C-C bond cracking. At the reaction temperatures above 390°C, aromatization and cyclization began to prevail over other reactions.

The rate of stearic acid deoxygenation is not limited by intraparticle mass transfer resistance either. In heterogeneous catalytic fluid–solid reaction systems, the rate of intraparticle diffusion is in steady state and equal to the rate of the reaction. Therefore, under these conditions, the mass transferring steps do not affect the reaction rate. The rate of reaction can be calculated from the reaction mechanism assuming that the concentration at the catalyst site is the same as that of the bulk (Klaewkla, Arend et al. 2011).

The reaction mechanisms of fatty acid deoxygenation largely depend on the reaction conditions (Santillan-Jimenez and Crocker 2012) (Gosselink, Hollak et al. 2013). At high partial pressures of H<sub>2</sub>, decarbonylation is favored (Boda, Onyestyák et al. 2010). At low partial pressure of H<sub>2</sub>, deoxygenation proceeds mostly via decarboxylation (Immer and Lamb 2010, Berenblyum, Podoplelova et al. 2011), which was observed in the process studied here. Berenblyum et al. (Berenblyum, Podoplelova et al. 2011)

studied the deoxygenation pathways of propionic acid over a Pd catalyst using density functionality theory calculations. They found that the rate determining step for both decarboxylation and decarbonylation is C-C bond cleavage in the coordinated carboxylic acid moiety. Decarboxylation seems to be more favorable than decarbonylation because Gibb's free energy and the heat required for the reaction are lower. (Snåre, Kubičková et al. 2006)

### **6.3.3. Kinetics of stearic acid deoxygenation**

Kinetics of stearic acid deoxygenation in hydrothermal medium over an activated carbon catalyst was investigated over the following experimental conditions: temperatures from 350 °C to 380 °C, reaction pressure of 3500 psi (24.1 MPa), oil to water to formic acid ratio (1:5:0.05), catalyst load 18.2 g. 16.7% oleic acid in water (1% v/v formic acid) entered the system at 1.2 mL/min delivering  $6.34 \times 10^{-4}$  mol/min of oleic acid, WHSV 4 h<sup>-1</sup>.

Kinetics analysis was based on the reactant's disappearance. The activation energy is a parameter that indicates the sensitivity of a chemical reaction rate to temperature. Since the observed rate of oleic acid deoxygenation is a combined rate of two reactions (hydrogenation of oleic acid and deoxygenation of stearic acid), the "apparent" activation energy was estimated by using the observed overall rate of stearic acid disappearance as a function of temperature. The activation energy was determined from linear regression of  $\ln r$  versus  $1000/T$  for the reaction temperatures between 350 and 380 °C where the reaction rate was linearly proportional to the change in stearic acid

conversion (Fig. 37). The rate ( $r$ ) of stearic acid disappearance was calculated for each reaction temperature and provided in Table 34.

**Table 34.** Effect of temperature on the stearic acid conversion and the rate of its deoxygenation

Temperature, °C	Conversion of stearic acid, %	Rate of stearic acid disappearance, mol/g <sub>cat</sub> × min
350	23.44	$8.16 \times 10^{-6}$
360	56.02	$1.95 \times 10^{-5}$
370	83.18	$2.89 \times 10^{-5}$
380	96.16	$3.35 \times 10^{-5}$

In order to estimate the “apparent” activation energy of the process, the following equation was used (Vam 2013):

$$\ln r = -\frac{E_a}{RT} + \text{constant} \quad (50)$$

where  $r$  is the rate of stearic acid disappearance, mol/g<sub>cat</sub> × min;

$E_a$  is activation energy of the process, kJ/mol;

$R$  is the universal gas constant =  $8.314 \times 10^{-3}$  kJ/mol × °K;

$T$  is the reaction temperature, °K.

The natural logarithm of the rate of stearic acid disappearance shown in Table 34 ( $\ln r$ ) was plotted versus  $1000/T$  in Figure 39.

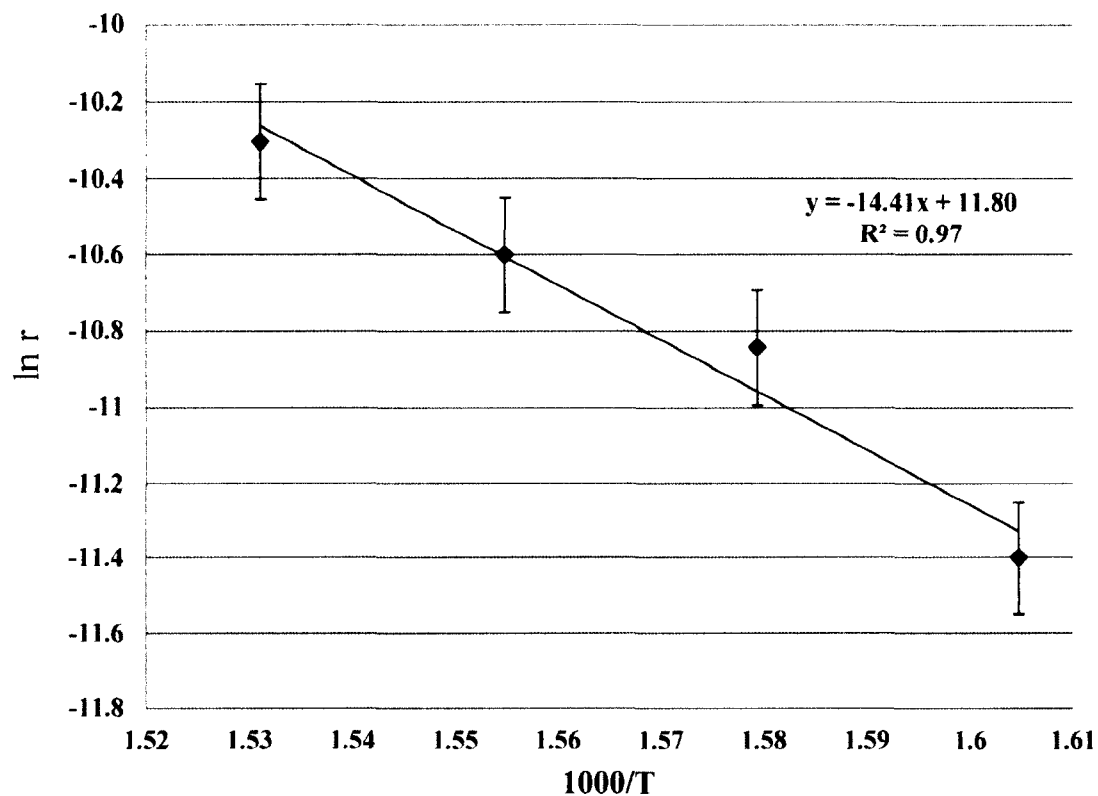


**Figure 39.** Effect of temperature on the rate of stearic acid disappearance in Arrhenius form.

Plotting  $\ln r$  vs  $1000/T$  yields a straight line with a slope of  $-E_a/R$ , as shown in Fig. 4. The slope of the line was -14.41. Multiplying the slope by  $(-R)$  yields  $E_a = 120 \pm 5$  kJ/ mol.

This value is consistent with the activation energy determined by Savage et al. ( $125 \pm 3$  kJ/mol) for a similar application (hydrothermal decarboxylation of palmitic acid

over activated carbon in a batch reactor) (Fu, Shi et al. 2011). The same research group evaluated the activation energy for hydrothermal decarboxylation of palmitic acid over Pt/C catalyst, which was about  $79 \pm 5$  kJ/mol (Fu, Lu et al. 2010). This is expectable since Pt/C is a more active decarboxylation catalyst than the carbon support alone. At the same time, Vam who studied continuous deoxygenation of stearic acid diluted in  $C_{24}$  solvent in a fixed-bed reactor over Pd/C catalyst with  $H_2$  added evaluated the activation energy of the process to be 148 kJ/mol (Vam 2013). The lower activation energy required for performing decarboxylation in hydrothermal medium over activated carbon (120 kJ/mol) can be explained by the lesser sensitivity of the process to temperature as well as by an extraordinary transport and solvent properties of sub- and supercritical water that can act as a reactant, reaction medium, and catalyst for different ionic/free-radical reactions on deoxygenation of biomass-derived products (Kumar 2013).

#### **6.4. Conclusions**

The rapid hydrothermal continuous flow deoxygenation process was developed and investigated. The study demonstrates that conversion of unsaturated and saturated fatty acids into straight-chain alkanes is possible over activated carbon in hydrothermal media within minutes. No supplying of gaseous  $H_2$  with high feed rates and no noble metals are required. Formic acid in low concentrations can serve as an active donor of free-radical hydrogen and provide the complete hydrogenation of unsaturated fatty acids/hydrocarbons within a short residence time. The study shows that activated carbon can be a promising and inexpensive alternative to the costly noble metal catalysts for renewable fuel production in hydrothermal medium. The products obtained in this

process were saturated *n*-alkanes produced through hydrogenation of oleic acid and decarboxylation or decarbonylation of stearic acid. No hydrodeoxygenation was observed under the conditions studied. Heptadecane was the major deoxygenation product. At 370-380 °C, the yield of heptadecane was about 70% with the selectivity 80% within 21 min of residence time and WHSV of 4 h<sup>-1</sup>. Kinetics study showed that the reaction rate of stearic acid disappearance displayed Arrhenius behavior with the activation energy of 120 kJ/mol.

The proposed process is readily scalable and offers a green approach to renewable fuel production. The processing of biomass in sub- and supercritical water media is an efficient and environmentally benign method that can utilize wet biomass. The feedstock for this process can be derived from terrestrial plants or microalgae. Activated carbon used as a catalyst in the process can be produced from woody biomass and other renewable resources. Formic acid used as a donor of hydrogen in the study is available at low cost in bulk quantities and considered a carbon neutral, renewable product that can be obtained by catalytic partial oxidation of wet biomass in aqueous media (OxFA process) (Albert, Wolfel et al. 2012).

## **6.5. Acknowledgments**

The authors would like to acknowledge our colleagues from the Department of Chemistry and Biochemistry at Old Dominion University for their assistance with GC-MS analyses. We are also grateful for the financial support from the National Science Foundation (Grant NSF-CBET-CAREER: 1351413).

## Supplementary Data

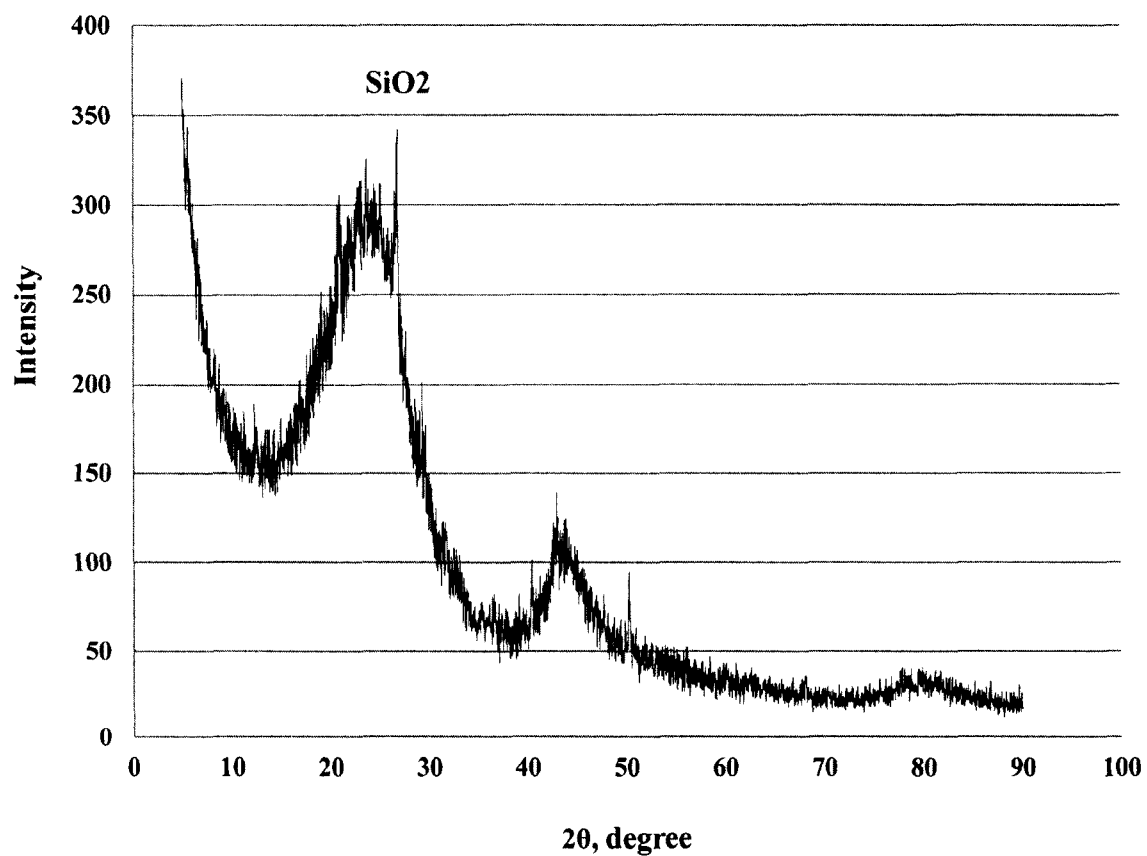


**Figure S1.** XRD pattern for fresh granulated activated carbon used as a catalyst in the study.



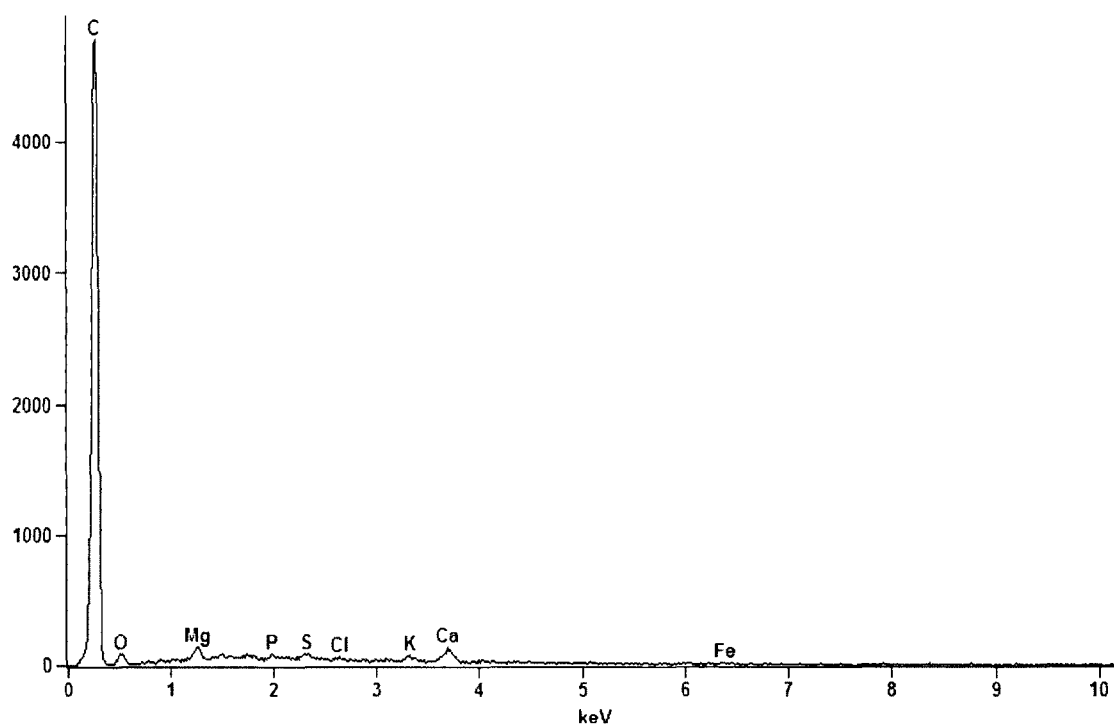


**Figure S2.** EDS spectrum of the activated carbon used as a catalyst in the study.

**Table S1.** Quantitative results of EDS analysis of the activated carbon catalyst

<b>Element</b>	<b>Atom %</b>
<b>C</b>	$94.95 \pm 0.54$
<b>O</b>	$4.32 \pm 0.32$
<b>Mg</b>	$0.29 \pm 0.02$
<b>P</b>	$0.04 \pm 0.01$
<b>S</b>	$0.07 \pm 0.01$
<b>Cl</b>	$0.03 \pm 0.01$
<b>K</b>	$0.06 \pm 0.01$
<b>Ca</b>	$0.20 \pm 0.01$
<b>Fe</b>	$0.04 \pm 0.01$

**Table S2.** Wavenumbers and principal bonds in FTIR spectra of commercial granulated activated carbons

Wavenumber, $\text{cm}^{-1}$	Assignments
3500-3300	O-H stretching (intermolecular hydrogen bonded)
2930-2900	C-H asym. stretching
2720	C-H (aldehydes)
1740	C=O stretching in esters
1625-1610	C=C aromatic skeletal stretching
1580-1570	C=C stretching band
1450-1420	C-H asym. bending
1375-1317	C-H asym. and sym. bending
1284-1240	C-O asym. stretching of aromatic ethers, esters, and phenols
1260-1000	C-O in carboxylic acids, alcohols, phenols, and esters
700-400	C-C stretching

## CHAPTER 7

### CONCLUSIONS AND RECOMMENDATIONS

In this work, a few major hydrothermal processing techniques of conversion of biomass into biofuels and valuable byproducts were investigated. In Chapter 2, the state-of-the-art studies related to the catalytic HDO of lipid-based feedstocks for the last decade was reviewed. It was shown that HDO of lipids is an important research area and attractive process to upgrade oils to liquid transportation fuels. Different chemical reactions (hydrogenation, dehydration, decarboxylation, and reaction mechanisms involved in the process were studied. The process parameters and the optimized process conditions have been discussed. A number of various heterogeneous catalytic used in HDO process has been reviewed. It was shown that bimetallic catalysts are more active than monometallic catalysts due to the effect of synergy when two or more compounds functioning together provide an effect not independently obtainable. The application of aqueous HDO to upgrading algal lipids has been discussed and advantages of using aqueous HDO for the processing wet feedstocks such as microalgae have been reviewed.

In producing renewable fuels from lipid-based feedstocks in hydrothermal media, the main objective is to remove oxygen, which can be readily performed by dehydration and decarboxylation. Despite the presence of a large amount of water, dehydration is a typical thermochemical reaction that occurs in hydrothermal media at elevated temperatures and pressures in the presence of an Arrhenius acid such as  $\text{H}_2\text{SO}_4$ . Decarboxylation is another major route of oxygen removal, which is more attractive because it also increases H/C ratio. The latter allows producing biofuels with increased HHVs.

TAGs can be readily split to form FFAs and glycerol via Colgate-Emery process (Barneby and Brown 1948). The process has been conducted at the conditions similar to that of hydrothermal processing (250 °C and 5 MPa) without a catalyst and with oil-to-water ratio of 2:1. These conditions make the process more steam-based hydrolysis than subcritical one. King and co-workers found that fast hydrolysis of TAGs can be conducted at the temperatures of 330 to 340 °C and oil-to-water ratios of 1:2.5 to 5.0. At these conditions, the yield of FFAs can be 90 to 100% (King, Holliday et al. 1999). It was observed that the phase behavior of components is crucial for the process and determined that the reaction quickly went to completion with almost 100% yield of FFAs when the mixture became a single phase at 339 °C.

In recent years, a few studies on fatty acid decarboxylation in hydrothermal media without adding hydrogen were carried out. The advantage of hydrothermal medium is not only the use of water as an environmentally benign solvent but also the avoidance of a separation step after TAGs hydrolysis and generation of FFAs (Idem, Katikaneni et al. 1996, Huber and Dumesic 2006). FFAs have been shown to degrade in hydrothermal media producing long-chain hydrocarbons. Watanabe and co-workers investigated the decomposition of stearic acid ( $C_{17}H_{35}COOH$ ) in a fixed bed batch reactor to the maximum temperature of 400 °C (Watanabe, Iida et al. 2006). Two major products,  $C_{17}H_{36}$  and  $C_{16}H_{32}$ , were found in the reaction products. The authors compared this process to the stearic acid pyrolysis and found that stearic acid decomposition under hydrothermal conditions was suppressed and resulted in prevailing alkenes over alkanes. The formation of shorter-chain hydrocarbons was also suppressed under the hydrothermal

conditions. However, when NaOH or KOH was added, decomposition of stearic acid enhanced significantly producing more alkanes than alkenes.

Fu et al. conducted a series of research projects on hydrothermal deoxygenation of fatty acids. It was reported that Pd/C and Pt/C catalysts possess catalytic activity in near critical water at 370 °C for decarboxylation of a saturated fatty acid (palmitic acid) with 76% molar yield of pentadecane (Fu, Lu et al. 2010). It was found that Pt/C catalyst is more active in water than Pd/C catalyst. However, the catalyst metal dispersion exhibited a significant reduction (from 38.9% to 0.8% for Pt and from 21.1 to 1.5% for Pd) after the reaction for 1-3 h.

Fu et al. (Fu, Lu et al. 2011) studied the effect of degree of fatty acid unsaturation on the decarboxylation over Pt/C catalyst in subcritical water at 330 °C. It was reported that unsaturated fatty acids provided much lower heptadecane yield (< 20%) and selectivity than saturated fatty acids (> 80%) after the reaction for 2.5 h.

Fu et al. also demonstrated that activated carbon itself possesses catalytic activity for decarboxylation of both saturated and unsaturated fatty acids, which can be a low-cost alternative to the expensive noble metal catalysts (Fu, Shi et al. 2011). However, the major product from oleic acid conversion was stearic acid with 24% molar yield. The desired decarboxylation product (heptadecane) molar yield was only 6% after the reaction at 370 °C for 3 h. In all cases, complete hydrogenation was not observed, and the reaction products included both alkanes and alkenes.

Further research is required in order to increase hydrogenation and deoxygenation efficiency of the hydrothermal process, increase conversion of fatty acids, molar yield of alkanes, and selectivity for the respective products in an economically viable way. Based

on the information obtained from the review of existing HDO technologies, a novel approach to hydrothermal deoxygenation of lipid-based feedstock was developed and investigated in Chapter 6.

In Chapter 3, HTL of lignin-based feedstock was studied using a conventional homogeneous ( $K_2CO_3$ ) and heterogeneous bimetallic ( $CoMo/Al_2O_3$ ) catalysts. It was shown that HTL ACS-UHS can provide an efficient method of bio-oil production. It is advantageous over pyrolysis as it allows converting biomass into bio-oils with higher energy and separation efficiency. Subcritical water technologies require less energy consumption since no phase change occurs (water remains in the liquid state). HTL allows producing liquid, solid, and gaseous products from wet and mixed feedstock with reduced mass transfer resistance. The use of 5 wt%  $K_2CO_3$  during HTL provided the higher degree of liquefaction (43.4%), higher bio-oil yield (30.1 wt%), and higher ECR (57.1%) compared to HTL with no catalyst and  $CoMo/Al_2O_3$  catalyst. The formation of gaseous products was favored when  $CoMo/Al_2O_3$  was used. GC-MS and NMR results showed that the bio-oil contained mainly lignin-derived phenolic compounds. LBO contained a more diverse suite of phenolic compounds derived from lignin monomers while HBO contained a less complex mixture of compounds such as parabens and alkylphenols. Integration of bio-oil production from wet unhydrolyzed solids with bioethanol production in a second generation lignocellulosic-based biorefinery can increase the overall ECR from 57.1% to 89.8%.

The study of catalytic liquefaction of ACS-UHS showed that this feedstock can be efficiently utilized for producing bio-oils with high energy density that can be further upgraded to renewable transportation fuels. However, production of bio-oils through

hydrothermal liquefaction and their upgrading to liquid fuels have not been commercialized up to date. Those processes require robust and selective catalysts developed specifically for liquefaction and conversion of bio-oils into liquid fuels. A number of studies have been done in this area that include C-O bonds cleavage through zeolite upgrading, hydrodeoxygenation, multi-step upgrading, unsupported organometallic catalysts upgrading (Hicks 2011), electrocatalytic hydrogenation and hydrodeoxygenation (Singh, Prakash et al. 2014), etc. The results of these studies show a good progress toward the potential commercialization of the liquid fuel production from bio-oils. However, further research is required to determine the optimal conditions and catalysts for bio-oil production/ upgrading.

Another area that can be further investigated is increasing degree of liquefaction and ECR of bio-oil production from lignin-based feedstock. A number of efficient liquefaction technologies exist up to day (Peterson, Vogel et al. 2008). However, further research is required to maximize the liquid product yield for the transportation fuels production. In this respect, using alcohols for HTL of lignin-based feedstock seems to be a promising way of maximizing bio-oil yield (Singh, Prakash et al. 2014).

The efficiency of different solvents for extraction of bio-oil from the aqueous phase might be a research area of interest. To our knowledge, no systematic information on solvent selectivity toward LBO was reported. Diethyl ether was used for LBO extraction in our study. However, a number of other non-polar solvents might be used for this extraction providing the higher bio-oil yield and/or lower oxygen content.

Finally, the systematic research on the catalytic upgrading the obtained bio-oil to hydrocarbons is required.



In Chapter 4, a novel integrated oil extraction process (HPOE) that employs the hydrothermal pretreatment of oilseeds with different morphologies and solvent extraction of oils followed by the hydrothermal carbonization of the extracted seedcake was developed and studied. The integrated oil extraction process can provide a more economically viable way to producing valuable feedstock for biodiesel and renewable diesel production.

HPOE employs hydrothermal pretreatment of whole oilseeds and oil extraction steps followed by HTC of the extracted seedcake. The integrated process provides several major advantages over conventional processes: better extractability of oil, shorter extraction time, tolerance to high moisture content of the feedstock, avoiding preparation stages, and utilization of the extracted seedcake for biochar production. Hydrothermal pretreatment of oilseeds in subcritical water at 180-210 °C for 30 min is an efficient step that changes the oilseeds morphology and allows maximizing oil extraction during the following solvent extraction step even without prior grinding and dehulling the oilseeds. For five types of the seeds used in the study, the oil yields obtained from the whole pretreated seeds was slightly higher (1-1.5 wt%) than obtained from the ground raw ones on unsaponifiable matter-free basis. Hydrothermal pretreatment at the conditions studied did not significantly change the composition and quality of the extracted oils, which makes them suitable for biofuel production.

The oils extracted from pretreated seeds had a higher antioxidant activity, which implies better resistance to autoxidation. The results of this study suggest that the proposed integrated process can be an economical and efficient way of oil extraction and biochar (co-product) production from different oilseeds.

The integrated process can be further optimized for the HPOE of a wider range of oilseeds, especially the ones of non-food quality, and microalgae in order to provide the feedstock for renewable fuel production.

In Chapter 5, the HTL of microalga *Scenedesmus sp.* followed by the catalytic hydrothermal gasification of the aqueous phase in a continuous flow process in order to produce hydrogen and gaseous hydrocarbons before the nutrient recycling of the eluent was investigated. Microalga *Scenedesmus sp.* was liquefied in a batch reactor at 300 °C and 1500 psi (10.3 MPa) for 30 min. The liquefaction degree under these conditions was 32-33 wt% on a carbon basis. The obtained liquid phase was extracted with dichloromethane yielding 4.5 wt% of bio-oil that contained 6.9 % energy. The solid products and bio-oil that contain 82% of the microalgae energy can be used for renewable fuel production. The extracted aqueous phase was gasified over a low-cost activated carbon as catalyst in a continuous flow process at 350-400 °C and 3500 psi (24.1 MPa) with WHSV of 3.3 h<sup>-1</sup>. The highest gasification efficiency of 10.2% was observed at 400 °C, which is 5.7 times greater than that in the control experiments without catalyst, providing 2.9% of additional energy. The gas produced with catalyst contained mostly H<sub>2</sub> and light hydrocarbons while the gas produced without catalyst consisted mainly of H<sub>2</sub> and CO<sub>2</sub>. The results of the study show that considerable amount of H<sub>2</sub> and gaseous hydrocarbons can be produced at relatively low temperature of 400 °C using a low-cost activated carbon as catalyst. The processed aqueous phase can be used as a source of nutrients for growing fresh algae. In this study, we proved the concept that utilization of the aqueous phase can be performed via the low-temperature gasification over the low-cost catalyst and obtained promising results. The processed aqueous phase can

significantly reduce the demand of fresh nutrients for algae cultivation and lead to a nutrient-neutral process. The relatively low gasification efficiency can be due to the recalcitrant nature of the compounds present in the extracted aqueous phase. It can be increased by increasing the reaction temperature of the HTG process. Further research is required to determine the optimal process conditions and to study the impact of the WSP present in the effluent aqueous phase on the microalgae growth.

One of the main goals of this work was to find an efficient way of the renewable fuel production from algal oil, which mainly contains unsaturated fatty acids. Oleic acid was employed as a model compound in the study. In this research project, a novel approach to converting fatty acids into *n*-alkanes was investigated (Chapter 6).

The rapid hydrothermal continuous flow deoxygenation process was developed and investigated. The study demonstrates that conversion of unsaturated and saturated fatty acids into straight-chain alkanes is possible over activated carbon in hydrothermal media within minutes. No supplying of gaseous H<sub>2</sub> with high feed rates and no noble metals are required. Formic acid in low concentrations can serve as an active donor of free-radical hydrogen and provide the complete hydrogenation of unsaturated fatty acids/hydrocarbons within a short residence time. The study shows that activated carbon can be a promising and inexpensive alternative to the costly noble metal catalysts for renewable fuel production in hydrothermal medium. The products obtained in this process were saturated *n*-alkanes produced through hydrogenation of oleic acid and decarboxylation or decarbonylation of stearic acid. No hydrodeoxygenation was observed under the conditions studied. Heptadecane was the major deoxygenation products. At 370-380 °C, the yield of heptadecane was about 70% with the selectivity 80% within 21

min of residence time and WHSV of  $4 \text{ h}^{-1}$ . Kinetics study showed that the reaction rate of stearic acid disappearance displayed Arrhenius behavior with the activation energy of 120 kJ/mol.

The proposed process is readily scalable and offers a green approach to renewable fuel production. The processing of biomass in sub- and supercritical water media is an efficient and environmentally benign method that can utilize wet biomass. The feedstock for this process can be derived from terrestrial plants or microalgae. Activated carbon used as a catalyst in the process can be produced from woody biomass and other renewable resources. Formic acid used as a donor of hydrogen in the study is available at low cost in bulk quantities and considered a carbon neutral, renewable product that can be obtained by catalytic partial oxidation of wet biomass in aqueous media (OxFA process) (Albert, Wolfel et al. 2012).

Further research is required on hydrothermal catalytic deoxygenation of algal and other non-food oils with the objective of maximizing alkanes yield and minimizing production costs including energy. Different low-cost catalysts, oil-to-water ratios, and flowrates can be investigated. An efficient method of extraction of algal lipids to provide the feedstock for renewable fuel production can be developed and studied. Hydrothermal extraction of oils from hydrothermally pretreated oilseeds (Chapter 4) can also be investigated. Although partial hydrolysis of the extracted oils into FFAs can occur during this process, it is beneficial for the following deoxygenation process. Scaling up the continuous flow process of algal lipids deoxygenation can be an important followed up research project.

## REFERENCES

- Aatola, H., Larmi, M., Sarjovaara, T., & Mikkonen, S. (2009). Hydrotreated vegetable oil (HVO) as a renewable diesel fuel: Trade-off between NO<sub>x</sub>, particulate emission, and fuel consumption of a heavy duty engine. *SAE Int. J. Engines* 1(1), 1251-1262.
- Acién, F. G., Fernández, J. M., Magán, J. J., & Molina, E. (2012). Production cost of a real microalgae production plant and strategies to reduce it. *Biotechnology Advances*, 30(6), 1344-1353.
- Akdeniz, F. & Gündoğdua, M. (2007). Direct and alkali medium liquefaction of *Laurocerasus officinalis* Roem. *Energy Conversion and Management*, 48(1), 189-192.
- Akhtar, J. & Amin, N. A. S. (2011). A review on process conditions for optimum bio-oil yield in hydrothermal liquefaction of biomass. *Renewable and Sustainable Energy Reviews*, 15(3), 1615-1624.
- Akhtar, J., & Amin, N. A. S. (2011). A review on process conditions for optimum bio-oil yield in hydrothermal liquefaction of biomass. *Renewable & Sustainable Energy Reviews*, 15(3), 1615-1624.
- Akiya, N. & Savage, P. E. (2002). Roles of water for chemical reactions in high-temperature water. *Chemical Reviews*, 102(8), 2725-2750.
- Albert, J., Wolfel, R., Bosmann, A., & Wasserscheid, P. (2012). Selective oxidation of complex, water-insoluble biomass to formic acid using additives as reaction accelerators. *Energy & Environmental Science*, 5(7), 7956-7962.

- Alenezi, R., Baig, M., Wang, J., Santos, R., & Leeke, G. A. (2009). Continuous flow hydrolysis of sunflower oil for biodiesel. *Energy Sources, Part A: Recovery, Utilization, and Environmental Effects*, 32(5), 460-468.
- Alenezi, R., Leeke, G. A., Santos, R. C. D., & Khan, A. R. (2009). Hydrolysis kinetics of sunflower oil under subcritical water conditions. *Chemical Engineering Research and Design*, 87(6), 867-873.
- American Society for Testing and Materials (ASTM) standard D 1655. Standard specification for aviation turbine fuels. West Conshohocken, PA.
- American Society for Testing and Materials (ASTM) standard D 6751. Standard specification for biodiesel fuel blend stock (B100) for middle distillate fuels. West Conshohocken, PA.
- American Society for Testing and Materials (ASTM) standard D 7566-11a. Standard specification for aviation turbine fuel containing synthesized hydrocarbon: Subcommittee D02.J0.06.
- American Society for Testing and Materials (ASTM) standard D 975. Standard specification for diesel fuel oils: West Conshohocken, PA.
- Antal, M. J., Brittain, A., DeAlmeida, C., Ramayya, S., & Roy, J. C. (1987). *Heterolysis and homolysis in supercritical water*. Paper presented at the ACS Symp. , Washington, DC.
- Ba, T., Chaala, A., Garcia-Perez, M., Rodrigue, D. & Roy, C. (2004). Colloidal properties of bio-oils obtained by vacuum pyrolysis of softwood bark. Characterization of water-soluble and water-insoluble fractions. *Energy & Fuels*, 18(3), 704-712.

- Balan, V., Bals, B., Chundawat, S. P., Marshall, D., & Dale, B. E. (2009). Lignocellulosic biomass pretreatment using AFEX. *Methods Mol Biol*, 581, 61-77.
- Balan, V., Chiaramonti, D. & Kumar, S. (2013). Review of US and EU initiatives toward development, demonstration, and commercialization of lignocellulosic biofuels. *Biofuels, Bioproducts and Biorefining*, 7(6), 732-759.
- Balat, H. & Kırtay, E. (2010). Hydrogen from biomass – Present scenario and future prospects. *International Journal of Hydrogen Energy*, 35(14), 7416-7426.
- Barbier, J., Charon, N., Dupassieux, N., Loppinet-Serani, A., Mahé, L., Ponthus, J. & Cansell, F. (2012). Hydrothermal conversion of lignin compounds. A detailed study of fragmentation and condensation reaction pathways. *Biomass and Bioenergy*, 46(0), 479-491.
- Barbour, R., Rickeard, D., & Elliott, N. (2000). Understanding diesel lubricity. *SAE Technical Paper 2000-01-1918*.
- Barkauskas, J. & Dervinyte, M. (2004). An investigation of the functional groups on the surface of activated carbons. *J.Serb.Chem.Soc.*, 69(5), 363-375.
- Barneby, H.L., & Brown, A.C. (1948). Continuous fat splitting plants using the colgateemery process. *J. Am. Oil Chem. Soc.*, 25(3), 95–99.
- Bartels, Jeffrey R., Pate, Michael B., & Olson, Norman K. (2010). An economic survey of hydrogen production from conventional and alternative energy sources. *International Journal of Hydrogen Energy*, 35(16), 8371-8384.
- Basu, P. (2013). *Biomass gasification, pyrolysis, and torrefaction : practical design and theory*. Amsterdam: Academic Press.

- Becker, E. W. (1994). *Microalgae: biotechnology and microbiology* (1 edition ed.): Cambridge University Press.
- Becker, E.W. (2007). Micro-algae as a source of protein. *Biotechnology Advances*, 25, 207–210.
- Behrendt, F., Neubauer, Y., Oevermann, M., Wilmes, B., & Zobel, N. (2008). Direct liquefaction of biomass. *Chem. Eng. Technol*, 31(5), 667-677.
- Bell, J. L. S., Palmer, D. A., Barnes, H. L., & Drummond, S. E. (1994). Thermal decomposition of acetate: III. Catalysis by mineral surfaces. *Geochimica et Cosmochimica Acta*, 58(19), 4155-4177.
- Benedict, J.H., & Daubert, B.F. (1950). The partial hydrogenation of triolein. *J. Am. Chem. Soc.*, 72, 4356-4359.
- Berenblyum, A. S., Podoplelova, T. A., Shamsiev, R. S., Katsman, E. A., & Danyushevsky, V. Ya. (2011). On the mechanism of catalytic conversion of fatty acids into hydrocarbons in the presence of palladium catalysts on alumina. *Petroleum Chemistry*, 51(5), 336-341.
- Berl, E. (1944). Production of oil from plant material. *Science*, 99(2573), 309-312.
- Bernas, H., Eränen, K., Simakova, I., Leino, A. R., Kordás, K., Myllyoja, J. & Murzin, D. Y. (2010). Deoxygenation of dodecanoic acid under inert atmosphere. *Fuel*, 89(8), 2033-2039.
- Bezergianni, S., Kalogianni, A., & Vasalos, I.A. (2009). Hydrocracking of vacuum gas oil–vegetable oil mixtures for biofuels production. *Bioresour Technol*, 100, 3036–3042.
- Bezergianni, S., Voutetakis, S, & Kalogianni, A. (2009). Catalytic hydrocracking of fresh and used cooking oil. *Ind Eng Chem Res*, 48(18), 8402-8406.



- Boda, L., Onyestyák, G., Solt, H., Lónyi, F., Valyon, J. & Thernesz, A. (2010). Catalytic hydroconversion of tricaprylin and caprylic acid as model reaction for biofuel production from triglycerides. *Applied Catalysis A: General*, 374(1–2), 158-169.
- Bosku, D., Morton, I. (1976). Effect of plant sterols on the rate of deterioration of heated oils. *J. Sci. Food Agric.*, 27, 928-932.
- Bridgwater, A. V., & Peacocke, G. V. C. (2000). Fast pyrolysis processes for biomass. *Renewable Sustainable Energy Rev.*, 4, 1-73.
- Brown, M. R., Jeffrey, S. W., Volkman, J. K., & Dunstan, G. A. (1997). Nutritional properties of microalgae for mariculture. *Aquaculture*, 151(1–4), 315-331.
- Brown, T. M., Duan, P., & Savage, P. E. (2010). Hydrothermal liquefaction and gasification of *Nannochloropsis* sp. *Energy & Fuels*, 24(6), 3639-3646.
- Bruun, S. & Luxhoi, J. (2008). Is biochar production really carbon-negative? *Environmental Science & Technology*, 1388.
- Bu, Q., Lei, H., Zacher, A.H., Wanga, L., Ren, S., Liang, J., Wei, Y., Liu, Y., Tang, J., Zhang, Q., & Ruan R. (2012). A review of catalytic hydrodeoxygenation of lignin-derived phenols from biomass pyrolysis. *Bioresourse Technology*, 124, 470-477.
- Bunch, A. Y., Wang, X. & Ozkan, U. S. (2007). Hydrodeoxygenation of benzofuran over sulfided and reduced Ni–Mo/ $\gamma$ -Al<sub>2</sub>O<sub>3</sub> catalysts: Effect of H<sub>2</sub>S. *Journal of Molecular Catalysis A: Chemical*, 270(1–2), 264-272.
- Byrd, A. J., Kumar, S., Kong, L., Ramsurn, H. & Gupta, R. B. (2011). Hydrogen production from catalytic gasification of switchgrass biocrude in supercritical water. *International Journal of Hydrogen Energy*, 36(5), 3426-3433.

- Calzavara, Y., Jousot-Dubien, C., Boissonnet, G., & Sarrade, S. (2005). Evaluation of biomass gasification in supercritical water process for hydrogen production. *Energy Conversion and Management*, 46, 615-631.
- Cantrell, K. B., Ducey, T., Ro, K. S. & Hunt, P. G. (2008). Livestock waste-to-bioenergy generation opportunities. *Bioresource Technology*, 99(17), 7941-7953.
- Carlozzi, P. (2003). Dilution of solar radiation through "culture" lamination in photobioreactor rows facing south-north: a way to improve the efficiency of light utilization by cyanobacteria (*Arthrospira platensis*). *Biotechnol Bioeng*, 81(3), 305-315.
- Centeno, A., Laurent, E., & Delmon, B. (1995). Influence of the support of CoMo sulfide catalysts and of the addition of potassium and platinum on the catalytic performances for the hydrodeoxygenation of carbonyl, carboxylic and guaiacol-type molecules. *Appl Catal A*, 154, 288-298.
- Centi, G., & Santen, R. A. van. (2007) *Catalysis for Renewables: From Feedstock to Energy Production* (pp. 413-423): Wiley-VCH Verlag GmbH & Co. KGaA.
- Chakinala, A. G., Brilman, D. W. F., van Swaaij, W. P.M. & Kersten, S. R. A. (2010). Catalytic and non-catalytic supercritical water gasification of microalgae and glycerol. *Ind. Eng. Chem. Res.*, 49(3), 1113-1122.
- Changi, S., Matzger, A. J., & Savage, P. E. (2012). Kinetics and pathways for an algal phospholipid (1,2-dioleoyl-sn-glycero-3-phosphocholine) in high-temperature (175-350 °C) water. *Green Chemistry*, 14(10), 2856-2867.
- Cherubini, F. (2010). The biorefinery concept: Using biomass instead of oil for producing energy and chemicals. *Energy Conversion and Management*, 51(7), 1412-1421.

- Chisti, Yusuf. (2007). Biodiesel from microalgae. *Biotechnology Advances*, 25(3), 294-306.
- Chisti, Yusuf. (2008). Biodiesel from microalgae beats bioethanol. *Trends in Biotechnology*, 26(3), 126-131.
- Chisti, Yusuf. (2010). Fuels from microalgae. *Biofuels*, 1(2), 233-235.
- Chornet, E. & Overend, R. P. (1985). Biomass liquefaction: An overview. In Ralph P. Overend, T. A. Milne & L. K. Mudge (Eds.), *Fundamentals of Thermochemical Biomass Conversion* (pp. 967-1002). New York: Elsevier Applied Science.
- Choudhary, T. V., & Phillips, C. B. (2011). Renewable fuels via catalytic hydrodeoxygenation. *Applied Catalysis A: General*, 397(1-2), 1-12.
- Clothier, P. Q. E., Aguda, B. D., Moise, A., & Pritchard, H. O. (1993). How do diesel-fuel ignition improvers work? *Chemical Society Reviews*, 22(2), 101-108.
- Cordell, D., Drangert, J. O., & White, S. (2009). The story of phosphorus: Global food security and food for thought. *Global Environmental Change*, 19(2), 292-305.
- Corma, A., Iborra, S. & Velty, A. (2007). Chemical routes for the transformation of biomass into chemicals. *Chemical Reviews*, 107(6), 2411-2502.
- Cortright, R. D., Davda, R. R., & Dumesic, J. A. (2002). Hydrogen from catalytic reforming of biomass-derived hydrocarbons in liquid water. *Nature*, 418(6901), 964-967.
- Crossley, S., Faria, J., Shen, M., & Resasco, D. E. (2010). Solid nanoparticles that catalyze biofuel upgrade reactions at the water/oil interface. *Science* 327(5961), 68-72.

- Da Rocha Filho, G.N., Brodzki, D. & Djega-Mariadassou, G. (1993). Formation of alkanes, alkylcycloalkanes and alkylbenzenes during the catalytic hydrocracking of vegetable oils. *Fuel*, 72(4), 543-549.
- Davda, R.R. & Dumesic, J. A. (2004). Renewable hydrogen by aqueous-phase reforming of glucose. *Chemical Communications*(1), 36-37.
- Davda, Rupali R., & Dumesic, James A. (2003). Catalytic reforming of oxygenated hydrocarbons for hydrogen with low levels of carbon monoxide. *Angewandte Chemie International Edition*, 42(34), 4068-4071.
- Davis, J.L., & Barteau, M.A. (1990). Spectroscopic identification of alkoxide, aldehyde, and acyl intermediates in alcohol decomposition on Pd(111). *Surface Science*, 235(2-3), 235-248.
- De Angelis, L., Risé, P., Giavarini, F., Galli, C., Bolis, C. L., & Colombo, M. L. (2005). Marine macroalgae analyzed by mass spectrometry are rich sources of polyunsaturated fatty acids. *Journal of Mass Spectrometry*, 40(12), 1605-1608.
- Delrue, F., Li-Beisson, Y., Setier, P. A., Sahut, C., Roubaud, A., Froment, A. K., & Peltier, G. (2013). Comparison of various microalgae liquid biofuel production pathways based on energetic, economic and environmental criteria. *Bioresour Technol*, 136, 205-212.
- Demirbas, A. (2000). Mechanisms of liquefaction and pyrolysis reactions of biomass. *Energy Conversion and Management* 41, 633-646.
- Demirbas, A. (2006). Oily products from mosses and algae via pyrolysis. *Energy Sources, Part A: Recovery, Utilization, and Environmental Effects*, 28, 933-940.
- Demirbas, A. (2011). Competitive liquid biofuels from biomass. *Applied Energy*, 88(1), 17-28.

- Demirbas, A. H., & Demirbas, I. (2007). Importance of rural bioenergy for developing countries. *Energy Conversion and Management*, 48(8), 2386-2398.
- DOE, U.S. (2010). National Algal Biofuels Technology Roadmap: U.S. Department of Energy, Office of Energy Efficiency and Renewable Energy, Biomass Program.
- Donnis, B., Egeberg, R., Blom, P., & Knudsen, K. (2009). Hydroprocessing of bio-oils and oxygenates to hydrocarbons. Understanding the reaction routes. *Topics in Catalysis*, 52(3), 229-240.
- Duan, P. & Savage, P. E. (2011). Hydrothermal liquefaction of a microalga with heterogeneous catalysts. *Industrial & Engineering Chemistry Research*, 50(1), 52-61.
- Dunford, N. T. (2012). Advancements in oil and oilseed processing *Food and Industrial Bioproducts and Bioprocessing* (pp. 115-143): Wiley-Blackwell.
- Dunstan, G., Volkman, J., Barrett, S., & Garland, C. (1993). Changes in the lipid composition and maximisation of the polyunsaturated fatty acid content of three microalgae grown in mass culture. *Journal of Applied Phycology*, 5(1), 71-83.
- Elliott, D. C. (2007). Historical developments in hydroprocessing bio-oils. *Energy & Fuels*, 21(3), 1792-1815.
- Elliott, D. C. (2008). Catalytic hydrothermal gasification of biomass. *Biofuels, Bioproducts and Biorefining*, 2, 254-265.
- Elliott, D. C., Beckman, D., Bridgwater, A. V., Diebold, J. P., Gevert, S. B., & Solantausta, Y. (1991). Developments in direct thermochemical liquefaction of biomass: 1983-1990. *Energy & Fuels*, 5(3), 399-410.

- Elliott, D.C., Sealock, J.L.J., & Baker, E.G. (1993). Chemical processing in high-pressure aqueous environments. 2. Development of catalysts for gasification. *Industrial and Engineering Chemistry Research*, 32(8), 1542–1548.
- European Committee for Standardization. Standard EN 14112. Fat and oil derivatives - .ty Acid Methyl Esters (FAME) - Determination of oxidation stability (accelerated oxidation test).
- European Committee for Standardization. Standard EN 14214. Automotive fuels – fatty acid methyl esters (FAME) for diesel engines – requirements and test methods.
- European Committee for Standardization. Standard EN 590. Automotive fuels – diesel – requirements and test methods.
- Farrell, A. E., Plevin, R. J., Turner, B. T., Jones, A. D., O'Hare, M. & Kammen, D. M. (2006). Ethanol can contribute to energy and environmental goals. *Science*, 311, 506-508.
- Ferrari, M., Bosmans, S., Maggi, R., Delmon, B., & Grange, P. (2001). CoMo/carbon hydrodeoxygenation catalysts: influence of the hydrogen sulfide partial pressure and of the sulfidation temperature. *Catalysis Today*, 65(2–4), 257-264.
- Ferrari, M., Maggi, R., Delmon, B., & Grange, P. (2001). Influences of the hydrogen sulfide partial pressure and of a nitrogen compound on the hydrodeoxygenation activity of a CoMo/carbon catalyst. *Journal of Catalysis*, 198(1), 47-55.
- Filley, T. R., Hatcher, P. G., Shortle, W. C., & Praseuth, R. T. (2000). The application of <sup>13</sup>C-labeled tetramethylammonium hydroxide (<sup>13</sup>C-TMAH) thermochemolysis to the study of fungal degradation of wood. *Organic Geochemistry*, 31(2–3), 181-198.

- Fisk, C. A., Morgan, T., Ji, Y., Crocker, M., Crofcheck, C. & Lewis, S. A. (2009). Bio-oil upgrading over platinum catalysts using in situ generated hydrogen. *Applied Catalysis A: General*, 358(2), 150-156.
- Fivga, A. (2011). *Comparison of the effect of pre-treatment and catalysts on liquid quality from fast pyrolysis of biomass*. (Ph.D.), Aston University, Birmingham, UK.
- Fu, J., Lu, X. & Savage, P. E. (2010). Catalytic hydrothermal deoxygenation of palmitic acid. *Energy & Environmental Science*, 3(3), 311-317.
- Fu, J., Lu, X., & Savage, P. E. (2011). Hydrothermal decarboxylation and hydrogenation of fatty acids over Pt/C. *ChemSusChem*, 4(4), 481-486.
- Fu, J., Shi, F., Thompson, L. T., Lu, X. & Savage, P. E. (2011). Activated carbons for hydrothermal decarboxylation of fatty acids. *ACS Catalysis*, 1(3), 227-231.
- Furimsky, E. (2000). Catalytic hydrodeoxygenation. *Applied Catalysis A: General*, 199(2), 147-190.
- Garcia Moscoso, J. L., Obeid, W., Kumar, S. & Hatcher, P. G. (2013). Flash hydrolysis of microalgae (*Scenedesmus sp.*) for protein extraction and production of biofuels intermediates. *The Journal of Supercritical Fluids*, 82(0), 183-190.
- Go, A., Liu, Y-T. & Ju, Y-H. (2013). Applicability of subcritical water treatment on oil seeds to enhance extractable lipid. *BioEnergy Research*, 7(2), 711-719.
- Gosselink, R. W., Hollak, S. A. W., Chang, S-W, van Haveren, J., de Jong, K. P., Bitter, J. H. & van Es, D. S. (2013). Reaction pathways for the deoxygenation of vegetable oils and related model compounds. *ChemSusChem*, 6(9), 1576-1594.
- Goudriaan, F., & Peferoen, D. G. R. (1990). Liquid fuels from biomass via a hydrothermal process. *Chemical Engineering Science*, 45(8), 2729-2734.

- Guo, J., Ruan, R., & Zhang, Y. (2012). Hydrotreating of phenolic compounds separated from bio-oil to alcohols. *Industrial & Engineering Chemistry Research*, 51(19), 6599-6604.
- Gusmao, J., Brodzki, D., Djega-Mariadassou, G., & Frety, R. (1989). Utilization of vegetable oils as an alternative source for diesel-type fuel: hydrocracking on reduced Ni/SiO<sub>2</sub> and sulfided Ni-Mo/γ-Al<sub>2</sub>O<sub>3</sub>. *Catal Today*, 5, 533-544.
- Guzman, A., Torres, J.E., Prada, L.P., & Nunez, M. L. (2010). Hydroprocessing of crude palm oil at pilot plant scale. *Catalysis Today*, 156, 38-43.
- Halim, R., Harun, R., Webley, P. A., & Danquah, M. K. (2013). Bioprocess engineering aspects of biodiesel and bioethanol production from microalgae. In James W. Lee (Ed.), *Advanced Biofuels and Bioproducts* (pp. 601-628): Springer New York.
- Hall, M., Bansal, P., Lee, J. H., Realf, M. J., & Bommarius, A. S. (2010). Cellulose crystallinity--a key predictor of the enzymatic hydrolysis rate. *FEBS J*, 277(6), 1571-1582.
- Hancsók, J., Kasza, T., Kovács, S., Solymosi, P., & Holló, A. (2012). Production of bioparaffins by the catalytic hydrogenation of natural triglycerides. *Journal of Cleaner Production*, 34(0), 76-81.
- Herrero, M., Cifuentes, A., & Ibañez, E. (2006). Sub- and supercritical fluid extraction of functional ingredients from different natural sources: Plants, food-by-products, algae and microalgae: A review. *Food Chemistry*, 98(1), 136-148.
- Hicks, J. C. (2011). Advances in C–O bond transformations in lignin-derived compounds for biofuels production. *The Journal of Physical Chemistry Letters*, 2(18), 2280-2287.



- Holmgren, J., Gosling, C., Marinangeli, R., Marker, T., Faraci, G., & Perego, C. (2007). New developments in renewable fuels offer more choices : Vegetable oil-based diesel can offer better integration within crude-oil refineries for fuels blending. *Hydrocarbon processing* 86(9), 67-72.
- Huber, G. W., & Dumesic, J. A. (2006). An overview of aqueous-phase catalytic processes for production of hydrogen and alkanes in a biorefinery. *Catalysis Today*, 111(1-2), 119-132.
- Huber, G. W., Iborra, S., & Corma, A. (2006). Synthesis of transportation fuels from biomass: Chemistry, catalysts, and engineering. *Chem. Rev.*, 106, 4044.
- Huber, G. W., O'Connor, P., & Corma, A.. (2007). Processing biomass in conventional oil refineries: Production of high quality diesel by hydrotreating vegetable oils in heavy vacuum oil mixtures. *Applied Catalysis A: General*, 329(0), 120-129.
- Huesemann, M. H., & Benemann, J.R. (2009). Biofuels from microalgae: Review of products, processes and potential, with special focus on *Dunaliella sp.* In J.E.W. Polle A. Ben-Amotz, and D.V. Subba Rao (Ed.), *The Alga Dunaliella: Biodiversity, Physiology, Genomics, and Biotechnology* (Vol. 14, pp. 445-474). New Hampshire: Science Publishers.
- Hunter, S. E., & Savage, P. E. (2004). Recent advances in acid- and base-catalyzed organic synthesis in high-temperature liquid water. *Chemical Engineering Science*, 59(22-23), 4903-4909.
- Idem, R. O., Katikaneni, S. P. R., & Bakhshi, N. N. (1996). Thermal cracking of canola oil: reaction products in the presence and absence of steam. *Energy & Fuels*, 10(6), 1150-1162.

- Immer, J. (2010 ). *Kinetics of catalytic deoxygenation of stearic acid over Pd/C*. (Ph.D. Dissertation), North Carolina State University.
- Immer, J. G., & Lamb, H. H. (2010). Fed-batch catalytic deoxygenation of free fatty acids. *Energy & Fuels*, 24(10), 5291-5299.
- Immer, J. G., Kelly, M. J., & Lamb, H. H. (2010). Catalytic reaction pathways in liquid-phase deoxygenation of C18 free fatty acids. *Applied Catalysis A: General*, 375(1), 134-139.
- ISO 18609:2000 Animal and vegetable fats and oils - Determination of unsaponifiable matter - Method using hexane extraction (2000).
- Jena, U., & Das, K. C. (11-14 October, 2009). *Production of biocrude oil from microalgae via thermochemical liquefaction process*. Paper presented at the Bioenergy Engineering, Bellevue, Washington.
- Jena, U., & Das, K. C. (2011). Comparative evaluation of thermochemical liquefaction and pyrolysis for bio-oil production from microalgae. *Energy & Fuels*, 25(11), 5472-5482.
- Jena, U., Das, K. C., & Kastner, J. R. (2012). Comparison of the effects of  $\text{Na}_2\text{CO}_3$ ,  $\text{Ca}_3(\text{PO}_4)_2$ , and NiO catalysts on the thermochemical liquefaction of microalga *Spirulina platensis*. *Applied Energy*, 98(0), 368-375.
- Jena, U., Vaidyanathan, N., Chinnasamy, S., & Das, K. C. (2011). Evaluation of microalgae cultivation using recovered aqueous co-product from thermochemical liquefaction of algal biomass. *Bioresource Technology*, 102(3), 3380-3387.
- Jin, M., Gunawan, C., Uppugundla, N., Balan, V., & Dale, B. E. (2012). A novel integrated biological process for cellulosic ethanol production featuring high

- ethanol productivity, enzyme recycling and yeast cells reuse. *Energy & Environmental Science*, 5(5), 7168-7175.
- Jung, M-W., Ahn, K.-H., Lee, Y., Kim, K-P., Rhee, J.-S., Tae Park, J., & Paeng, K-J. (2001). Adsorption characteristics of phenol and chlorophenols on granular activated carbons (GAC). *Microchemical Journal*, 70(2), 123-131.
- Kalderis, D., Kotti, M. S., Méndez, A., & Gascó, G. (2014). Characterization of hydrochars produced by hydrothermal carbonization of rice husk. *Solid Earth*, 5(1), 477-483.
- Kalinichev, A. G., & Churakov, S. V. (1999). Size and topology of molecular clusters in supercritical water: a molecular dynamics simulation. *Chem. Phys. Letters*, 302, 411-417.
- Kalnes, T. N, Marker, T., Shonnard, D. R, & Koers, K. P. (2008). Green diesel production by hydrorefining renewable feedstocks. *Biofuels*, (4), 7-11.
- Kalnes, T.N., Marker, T., & Shonnard, D.R. (2007). Green diesel: a second generation biofuel. *Int. J. Chem. Reactor Eng.*, 5, 1-9.
- Kamm, B., Gruber, P. R., & Kamm, M. (2000). Biorefineries – Industrial Processes and Products *Ullmann's Encyclopedia of Industrial Chemistry*: Wiley-VCH Verlag GmbH & Co. KGaA.
- Karadag, A., Ozcelik, B., & Saner, S. (2009). Review of methods to determine antioxidant capacities. *Food Analytical Methods*, 2(1), 41-60.
- Karagoz, S., Bhaskar, T., Muto, A., & Sakata, Y. (2005). Catalytic hydrothermal treatment of pine wood biomass: effect of RbOH and CsOH on product distribution. *Journal of Chemical Technology and Biotechnology*, 80, 1097-1102.

- Karagoz, S., Bhaskar, T., Muto, A., Sakata, Y., & Uddin, M. A. (2004). Low temperature hydrothermal treatment of biomass: Effect of reaction parameters on products and boiling point distributions. *Energy & Fuels*, *18*, 234-241.
- Karagoz, S., Bhaskar, T., Muto, A., Sakata, Y., Oshiki, T., & Kishimoto, T. (2005). Low-temperature catalytic hydrothermal treatment of wood biomass: analysis of liquid products. *Chemical Engineering Journal*, *108*(1-2), 127-137.
- Kemény, Z., Recseg, K., Hénon, G., Kővári, K., & Zwobada, F. (2001). Deodorization of vegetable oils: Prediction of trans polyunsaturated fatty acid content. *Journal of the American Oil Chemists' Society*, *78*(9), 973-979.
- Khuwijtjaru, P., Adachi, S., & Matsuno, R. (2002). Solubility of saturated fatty acids in water at elevated temperatures. *Biosci. Biotechnol. Biochem.*, *66*(8), 1723-1726.
- Kibet, J., Khachatryan, L., & Dellinger, B. (2012). Molecular products and radicals from pyrolysis of lignin. *Environ Sci Technol*, *46*(23), 12994-13001.
- King, J., Holliday, R., & List, G. (1999). Hydrolysis of soybean oil in a subcritical water flow reactor. *Green Chemistry*, *1*(6), 261-264.
- Klaewkla, R., Arend, M., & Hoelderich, W. F. (2011). A review of mass transfer controlling the reaction rate in heterogeneous catalytic systems. In Hironori Nakajima (Ed.), *Mass Transfer - Advanced Aspects* (pp. 836): InTech.
- Knothe, G. (2009). Improving biodiesel fuel properties by modifying fatty ester composition. *Energy Environ Sci*, *2*, 759-766.
- Knothe, G. (2010). Biodiesel and renewable diesel: A comparison. *Progress in Energy and Combustion Science*, *36*, 364-373.
- Knothe, G., Krahl, J., & Gerpen, J. van (Eds.). (2005). *The biodiesel handbook*. Champaign, IL, USA.

- Koenig, A. B., Sleighter, R. L., Salmon, E., & Hatcher, P. G. (2010). NMR structural characterization of *Quercus alba* (white oak) degraded by the brown rot fungus, *Laetiporus sulphureus*. *Journal of Wood Chemistry and Technology*, 30(1), 61-85.
- Krar, M., Kovács, S., Kalló, D., & Hancsók, J. (2010). Fuel purpose hydrotreating of sunflower oil on CoMo/Al<sub>2</sub>O<sub>3</sub>. *Bioresource Technology*, 101(23), 9287-9293.
- Kritzer, P., & Dinjus, E.. (2001). An assessment of supercritical water oxidation (SCWO): Existing problems, possible solutions and new reactor concepts. *Chemical Engineering Journal*, 83, 207-214.
- Kruse, A., & Gawlik, A. (2003). Biomass conversion in water at 330-410 °C and 30-50 MPa: Identification of key compounds for indicating different chemical reaction pathways. *Ind. Eng. Chem. Res.*, 42, 267-269.
- Kruse, A., Funke, A., & Titirici, M. M. (2013). Hydrothermal conversion of biomass to fuels and energetic materials. *Curr Opin Chem Biol*, 17(3), 515-521.
- Kruse, A., Krupka, A., Schwarzkopf, V., Gamard, C., & Henningsen, T. (2005). Influence of proteins on the hydrothermal gasification and liquefaction of biomass. 1. Comparison of different feedstocks. *Industrial & Engineering Chemistry Research*, 44(9), 3013-3020.
- Kubicka, D., & Kaluza, L. (2010). Deoxygenation of vegetable oils over sulfided Ni, Mo and NiMo catalysts. *Applied Catalysis A: General*, 372(2), 199-208.
- Kubicka, D., Bejblova, M., & Vik, J. (2010). Conversion of vegetable oils into hydrocarbons over CoMo/MCM-41 catalysts. *Topics in Catalysis*, 53, 168-178.
- Kubicka, D., Simacek, S., & Zilkova, N. (2009). Transformation of vegetable oils into hydrocarbons over mesoporous-alumina-supported CoMo catalysts. *Topics in Catalysis*, 52, 161-168.

- Kubickova, I., Snare, M., Eranen, K., Maki-Arvela, P., & Murzin, D. Y. (2005). Hydrocarbons for diesel fuel via decarboxylation of vegetable oils. *Catalysis Today*, 106, 197-200.
- Kumar, D., & Murthy, G. S. (2011). Impact of pretreatment and downstream processing technologies on economics and energy in cellulosic ethanol production. *Biotechnol Biofuels*, 4, 27.
- Kumar, S. (2010). *Hydrothermal Treatment for Biofuels: Lignocellulosic Biomass to Bioethanol, Biocrude, and Biochar*. (Ph.D. Dissertation), Auburn University, Auburn. Retrieved from <http://hdl.handle.net/10415/2055>
- Kumar, S. (2013). Sub- and supercritical water technology for biofuels. In James W. Lee (Ed.), *Advanced Biofuels and Bioproducts* (pp. 147-183): Springer New York.
- Kumar, S., Hablot, E., Garcia Moscoso, J. L., Obeid, W., Hatcher, P., Duquette, B., Balan, V. (2014). Polyurethanes preparation using proteins obtained from microalgae. *Journal of Materials Science*, 49(22), 7824-7833.
- Kumar, S., Popov, S., Majeranowski, P.J., & Kostenyuk, I. (2012). Subcritical water assisted oil extraction and green coal production from oilseeds. International patent application PCT/US2013/064966.
- Kuronen, M., Mikkonen, S., Aakko, P., & Murtonen, T. (2007). Hydrotreated vegetable oil as fuel for heavy duty diesel engines. *SAE Technical Paper 2007-01-4031*.
- Lamprecht, D. (2007). Fischer-Tropsch fuel for use by the U.S. Military as battlefield-use fuel of the future. *Energy & Fuels*, 21, 1448-1453.
- Lang, X., Dalai, A. K., Bakhshi, N. N., Reaney, M. J., & Hertz, P. B. (2001). Preparation and characterization of bio-diesels from various bio-oils. *Bioresource Technology*, 80(1), 53-62.

- Laurent, E., & Delmon, B. (1994). Influence of water in the deactivation of a sulfided NiMo $\gamma$ -Al<sub>2</sub>O<sub>3</sub> catalyst during hydrodeoxygenation. *Journal of Catalysis*, 146(1), 281-291.
- Laurent, E., & Delmon, B. (1994). Study of the hydrodeoxygenation of carbonyl, carboxylic and guaiacyl groups over sulfided CoMo/ $\gamma$ -Al<sub>2</sub>O<sub>3</sub> and NiMo/ $\gamma$ -Al<sub>2</sub>O<sub>3</sub> catalysts: II. Influence of water, ammonia, and hydrogen sulfide. *Appl Catal A*, 109, 97-115.
- Laurent, E., & Delmon, B. (1994). Study of the hydrodeoxygenation of carbonyl, carboxylic and guaiacyl groups over sulfided CoMo/ $\gamma$ -Al<sub>2</sub>O<sub>3</sub> and NiMo/ $\gamma$ -Al<sub>2</sub>O<sub>3</sub> catalysts: I. Catalytic reaction schemes. *Applied Catalysis A: General*, 109(1), 77-96.
- Lawson, O.S., Oyewumi, A., Ologunagba, F.O., Ojomo, A.O. (2010). Evaluation of the parameters affecting the solvent extraction of soybean oil. *Journal of Engineering & Applied Sciences*, 5(10), 51-55.
- Leckel, D., & Liwanga-Ehumbu, M. (2006). Diesel-selective hydrocracking of an iron-based Fischer-Tropsch wax fraction C15-C45 using a MoO<sub>3</sub>-modified noble metal catalyst. *Energy & Fuels*, 20, 2330-2336.
- Leliveld, R. G., & Eijsbouts, S. E. (2008). How a 70-year-old catalytic refinery process is still ever dependent on innovation. *Catalysis Today*, 130(1), 183-189.
- Leung, A, Boocock, D G B, & Konar, S K. (1995). Pathways for the deoxygenation of triglycerides to aliphatic hydrocarbons over activated alumina. *Energy & Fuels* 9(5), 913-920.
- Li, Y., Horsman, M., Wu, N., Lan, C. Q., & Dubois-Calero, N. (2008). Biofuels from Microalgae. *Biotechnol. Prog.*, 24(4), 815-820.

- Li, Z., Garedew, M., Lam, C. H., Jackson, J. E., Miller, D. J., & Saffron, C. M. (2012). Mild electrocatalytic hydrogenation and hydrodeoxygenation of bio-oil derived phenolic compounds using ruthenium supported on activated carbon cloth. *Green Chemistry*, *14*(9), 2540-2549.
- López Barreiro, D., Bauer, M., Hornung, U., Posten, C., Kruse, A., & Prins, W. (2015). Cultivation of microalgae with recovered nutrients after hydrothermal liquefaction. *Algal Research*, *9*(0), 99-106.
- Maher, K. D., Kirkwood, K. M., Gray, M. R., & Bressler, D. C. (2008). Pyrolytic decarboxylation and cracking of stearic acid. *Industrial & Engineering Chemistry Research*, *47*(15), 5328-5336.
- Maiella, P., & Brill, T. (1998). Spectroscopy of hydrothermal reactions. 10. Evidence of wall effects in decarboxylation kinetics of 1.00 m HCO<sub>2</sub>X (X ¼ H, Na) at 280–330 C and 275 bar. *J. Phys. Chem. A* *102*(29), 5886–5891.
- Maier, W. F., Roth, W., Thies, I., & Ragué Schleyer, P. V. (1982). Hydrogenolysis, IV. Gas phase decarboxylation of carboxylic acids. *Chemische Berichte*, *115*(2), 808-812.
- Mäki-Arvela, P., Kubickova, I., Snåre, M., Eränen, K., & Murzin, D. Y. (2006). Catalytic deoxygenation of fatty acids and their derivatives. *Energy & Fuels*, *21*(1), 30-41.
- Marcus, Y. (1999). On transport properties of hot liquid and supercritical water and their relationship to the hydrogen bonding. *Fluid Phase Equilibr.*, *164*, 131-142.
- Marinangeli, R., Marker, T., Petri, J., Kalnes, T., McCall, M., Mackowiak, D., Shonnard, D. (2005). Opportunities for Biorenewables in Oil Refineries. Des Plaines: U.S. Department of Energy.



- Marsh, H., & Rodríguez-Reinoso, F. (2006). Chapter 4 - Characterization of Activated Carbon. In Harry Marsh, Francisco Rodríguez-Reinoso (Ed.), *Activated Carbon* (pp. 143-242). Oxford: Elsevier Science Ltd.
- Masaru, W., Takafumi, S., & Hiroshi, I. (2004). Chemical reactions of Cl compounds in near-critical and supercritical water. *Chemical Reviews*, *104*, 5803-5821.
- Matsumura, Y., Minowa, T., Potic, B., Kersten, S. R. A., Prins, W., van Swaij, W. P. M., Antal, M. J. (2005). Biomass gasification in near- and super-critical water: Status and prospects. *Biomass and Bioenergy*, *29*(4), 269-292.
- Matsumura, Y., Xu, X., & Antal, M. J. (1997). Gasification characteristics of an activated carbon in supercritical water. *Carbon*, *35*(6), 819-824.
- Medina, A.R., Grima, E.M., Gimenez, A.G., & Ibanez, M.J. (1998). Downstream processing of algal polyunsaturated fatty acids. *Biotechnology Advances*, *16*(3), 517-580.
- Medina, F. A, Larsen, J. W, & Schobert, H. H. (2003). Carbon as catalyst for organic electron-transfer reactions. *Fuel Chemistry Division Preprints*, *48*(1), 28.
- Meher, L. C., Vidya Sagar, D., & Naik, S. N. (2006). Technical aspects of biodiesel production by transesterification—a review. *Renewable and Sustainable Energy Reviews*, *10*(3), 248-268.
- Meyer, J. C., Marrone, P. A., & Tester, J. W. (1995). Acetic acid oxidation and hydrolysis in supercritical water. *AIChE Journal*, *41*(9), 2108-2121.
- Mills, V., & McClain, H. (1949). Fat hydrolysis. *Ind. Eng. Chem*, *41*, 1982–1985.
- Minowa, T., & Sawayama, S. (1999). A novel microalgal system for energy production with nitrogen cycling. *Fuel*, *78*(10), 1213-1215.

- Minowa, T., Zhen, F., & Ogi, T. (1998). Cellulose decomposition in hot-compressed water with alkali or nickel catalyst. *The Journal of Supercritical Fluids*, 13(1), 253-259.
- Minowa, T., Zhen, F., Ogi, T., & Varhegyi, G. (1998). Decomposition of cellulose and glucose in hot-compressed water under catalyst-free conditions. *J Chem. Eng. Japan*, 31, 131-134.
- Mittelbach, M., & Remschmidt, C. (2004). *Biodiesel – the comprehensive handbook*.
- Mossoba, M. M., Milosevic, V., Milosevic, M., Kramer, J. K., & Azizian, H. (2007). Determination of total trans fats and oils by infrared spectroscopy for regulatory compliance. *Anal Bioanal Chem*, 389(1), 87-92.
- Murata, K., Liu, Y., Inaba, M., & Takahara, I. (2010). Production of synthetic diesel by hydrotreatment of jatropha oils using Pt–Re/H-ZSM-5 catalyst. *Energy & Fuels*, 24(4), 2404-2409.
- Murtonen, T., Aakko-Saksa, P., Kuronen, M., Mikkonen, S., & Lehtoranta, K. (2010). Emissions with heavy-duty diesel engines and vehicles using FAME, HVO and GTL fuels with and without DOC + POC aftertreatment. *SAE Int. J. Fuels Lubr.*, 2(2), 147-166.
- Nagamori, M., & Funazukuri, T. (2004). Glucose production by hydrolysis of starch under hydrothermal conditions. *Journal of Chemical Technology & Biotechnology*, 79(3), 229-233.
- Naik, S. N., Goud, V. V., Rout, P. K., & Dalai, A. K. (2010). Production of first and second generation biofuels: A comprehensive review. *Renewable and Sustainable Energy Reviews*, 14(2), 578-597.

- Nava, R., Pawelec, B., Castaño, P., Álvarez-Galván, M. C., Loricera, C. V., & Fierro, J. L. G. (2009). Upgrading of bio-liquids on different mesoporous silica-supported CoMo catalysts. *Applied Catalysis B: Environmental*, 92(1–2), 154-167.
- Navarro, R. M., Peña, M. A., & Fierro, J. L. G. (2007). Hydrogen production reactions from carbon feedstocks: Fossil fuels and biomass. *Chemical Reviews*, 107(10), 3952-3991.
- Nunes, P.P., Brodzki, D., Bugli, G., & Djéga-Mariadassou, G. (1986). Hydrocracking of soybean oil under pressure: Research procedure and general aspects of the reaction. *Rev Inst Fr Pet*, 41(421-431).
- Oasmaa, A., Alén, R., & Meier, D. (1993). Catalytic hydrotreatment of some technical lignins. *Bioresource Technology*, 45(3), 189-194.
- O'Brien, R. D., Farr, W. E., & Wan, P. J. (2000). *Introduction to Fats and Oils Technology (2nd Edition)*: AOCS Press.
- Oja, S. (2008). *NExBTL – Next Generation Renewable Diesel*. Paper presented at the New Biofuels, Berlin.
- Pandey, M. P., & Kim, C. S. (2011). Lignin depolymerization and conversion: A review of thermochemical methods. *Chemical Engineering & Technology*, 34(1), 29-41.
- Patil, T. A., Butala, D. N., Raghunathan, T. S., & Shankar, H. S. (1988). Thermal hydrolysis of vegetable oils and fats. 1. Reaction kinetics. *Industrial & Engineering Chemistry Research*, 27(5), 727-735.
- Patil, T. A., Raghunathan, T. S., & Shankar, H. S. (1988). Thermal hydrolysis of vegetable oils and fats. 2. Hydrolysis in continuous stirred tank reactor. *Industrial & Engineering Chemistry Research*, 27(5), 735-739.

- Perlack, R. D., Wright, L.L., Turhollow, A. F., Graham, R. L., Strokes, B. J., & Erbach, D. C. (2005). Biomass as a feedstock for a bioenergy and bioproducts industry: The technical feasibility of a billion-ton annual supply. *A Joint report sponsored by US department of energy and US department of agriculture*, 78.
- Peterson, A. A., Vogel, F, Lachance, R. P., Froling, M., Antal, M. J., & Tester, J. W. (2008). Thermochemical biofuel production in hydrothermal media: A review of sub- and supercritical water technologies. *Energy and Environmental Science*, 1, 32-65.
- Pinzi, S., Garcia, I. L., Lopez-Gimenez, F. J., Castro, M. D. Luque de, Dorado, G., & Dorado, M. P. (2009). The ideal vegetable oil-based biodiesel composition: A review of social, economical and technical implications. *Energy Fuels*, 23(5), 2325-2341.
- Pitts, S. J., & Thomson, C. I. (2003). Analysis and classification of common vegetable oils. *J Forensic Sci*, 48(6), 1293-1297.
- Ponomaryov, V.D. (1976). Medicinal Herbs Extraction. *Medicina, Moscow*.
- Popov, S., & Kumar, S.. (2013). Renewable fuels via catalytic hydrodeoxygenation of lipid-based feedstocks. *Biofuels*, 4(2), 219-239.
- Qing, Q., Yang, B., & Wyman, C. E. (2010). Xylooligomers are strong inhibitors of cellulose hydrolysis by enzymes. *Bioresour Technol*, 101(24), 9624-9630.
- Radoykova, T, Nenkova, S, & Valchev, I. (2013). Black liquor lignin products, isolation and characterization. *Journal of Chemical Technology & Metallurgy*, 48(5).
- Ramadan, M.F., Asker, M.H.S., & Ibrahim, Z.K. (2008). Functional bioactive compounds and biological activities of *Spirulina platensis* lipids. *Czech Journal of Food Science*, 26, 211-222.

- Ramsurn, H., & Gupta, R. B. (2012). Production of biocrude from biomass by acidic subcritical water followed by alkaline supercritical water two-step liquefaction. *Energy & Fuels*, 26(4), 2365-2375.
- Rantanen, L., Linnaila, R., Aakko, P., & Harju, T. (2005). NExBTL - Biodiesel fuel of the second generation. *SAE Technical Paper 2005-01-3771*.
- Regmi, P., Garcia Moscoso, J. L., Kumar, S., Cao, X., Mao, J., & Schafran, G. (2012). Removal of copper and cadmium from aqueous solution using switchgrass biochar produced via hydrothermal carbonization process. *Journal of Environmental Management*, 109(0), 61-69.
- Roberts, V. M., Daage, M., Oldenburg, P. D., Bielenberg, J. R., Berlowitz, P. J., Long, D. C., & Oumar-Mahamat, H. (2013). Hydrothermal treatment of biomass with heterogeneous catalyst. USA Patent No. 8487148.
- Rozmysłowicz, B., Mäki-Arvela, P., Tokarev, A., Leino, A-R., Eränen, K., & Murzin, D. Y. (2011). Influence of hydrogen in catalytic deoxygenation of fatty acids and their derivatives over Pd/C. *Industrial & Engineering Chemistry Research*.
- Safari, Z., Ashrafizadeh, A., Hedayat, N. (2011). Thermodynamic study of seed oil extraction by organic solvents *Engineering and Technology*, 57, 997-1000.
- Sajilata, M. G., Singhal, Rekha S., & Kamat, Madhusudan Y. (2008). Supercritical CO<sub>2</sub> extraction of  $\gamma$ -linolenic acid (GLA) from *Spirulina platensis* ARM 740 using response surface methodology. *Journal of Food Engineering*, 84(2), 321-326.
- Santillan-Jimenez, E., & Crocker, M.. (2012). Catalytic deoxygenation of fatty acids and their derivatives to hydrocarbon fuels via decarboxylation/decarbonylation. *Journal of Chemical Technology & Biotechnology*, 87(8), 1041-1050.

- Savage, P. E. (1999). Organic chemical reactions in supercritical water. *Chemical Reviews*, 99, 603-621.
- Savage, P. E. (2009). A perspective on catalysis in sub- and supercritical water. *The Journal of Supercritical Fluids*, 47(3), 407-414.
- Schenk, P. M., Thomas-Hall, S. R., Stephens, E., Marx, U.C., Mussnug, J. H., Posten, C., & Hankamer, B. (2008). Second generation biofuels: high-efficiency microalgae for biodiesel production. *Bioenerg. Res.*, 1, 20-43.
- Sebos, I., Matsoukas, A., Apostolopoulos, V., & Papayannakos, N. (2009). Catalytic hydroprocessing of cottonseed oil in petroleum diesel mixtures for production of renewable diesel. *Fuel*, 88(1), 145-149.
- Şenol, O. İ, Ryymin, E. M., Viljava, T. R., & Krause, A. O. I. (2007). Reactions of methyl heptanoate hydrodeoxygenation on sulphided catalysts. *Journal of Molecular Catalysis A: Chemical*, 268(1-2), 1-8.
- Şenol, O. İ, Viljava, T. R., & Krause, A. O. I. (2005a). Hydrodeoxygenation of aliphatic esters on sulphided NiMo/ $\gamma$ -Al<sub>2</sub>O<sub>3</sub> and CoMo/ $\gamma$ -Al<sub>2</sub>O<sub>3</sub> catalyst: The effect of water. *Catalysis Today*, 106(1-4), 186-189.
- Şenol, O. İ, Viljava, T. R., & Krause, A. O. I. (2005b). Hydrodeoxygenation of methyl esters on sulphided NiMo/ $\gamma$ -Al<sub>2</sub>O<sub>3</sub> and CoMo/ $\gamma$ -Al<sub>2</sub>O<sub>3</sub> catalysts. *Catalysis Today*, 100(3-4), 331-335.
- Şenol, O. İ, Viljava, T. R., & Krause, A. O. I. (2007). Effect of sulphiding agents on the hydrodeoxygenation of aliphatic esters on sulphided catalysts. *Applied Catalysis A: General*, 326(2), 236-244.

- Senol, O.I., Ryymin, E.-M., Viljava, T.-R., & Krause, A.O.I. (2007). Effect of hydrogen sulphide on the hydrodeoxygenation of aromatic and aliphatic oxygenates on sulphided catalysts. *Journal of Molecular Catalysis A: Chemical*, 277, 107–112.
- Shabtai, J., Zmierczak, W., Chornet, E., & Johnson, D. (2003). Process for converting lignins into a high octane additive. US patent application US 09/972,461.
- Shackley, S., Hammond, J., Gaunt, J., & Ibarrola, R. (2011). The feasibility and costs of biochar deployment in the UK. *Carbon Management*, 2(3), 335-356.
- Sheehan, J., Dunahay, T., Benemann, J. and Roessler, P. (1998). A Look Back at the U.S. Department of Energy's Aquatic Species Program-Biodiesel from Algae: U.S. Department of Energy's Office of Fuels Development.
- Shin, H-Y., Ryu, J-H., Park, S-Y., & Bae, S-Y. (2012). Thermal stability of fatty acids in subcritical water. *Journal of Analytical and Applied Pyrolysis*, 98(0), 250-253.
- Simacek, P., Kubicka, D., Sebor, G., & Pospisil, M. (2010). Fuel properties of hydroprocessed rapeseed oil. *Fuel*, 89, 611-615.
- Simacek, S., Kubicka, D., Sebor, G., & Pospisil, M. (2009). Hydroprocessed rapeseed oil as a source of hydrocarbon-based biodiesel. *Fuel*, 88, 456–460.
- Singh, D., Rezac, M. E., & Pfromm, P. H. (2010). Partial hydrogenation of soybean oil using metal-decorated integral-asymmetric polymer membranes: Effects of morphology and membrane properties. *Journal of Membrane Science*, 348(1–2), 99-108.
- Singh, R., Prakash, A., Dhiman, S. K., Balagurumurthy, B., Arora, A. K., Puri, S. K., & Bhaskar, T. (2014). Hydrothermal conversion of lignin to substituted phenols and aromatic ethers. *Bioresource Technology*, 165(0), 319-322.

- Smith, B., Greenwell, H. C., & Whiting, A. (2009). Catalytic upgrading of tri-glycerides and fatty acids to transport biofuels. *Energy & Environmental Science*, 2(3), 262-271.
- Snåre, M., Kubičková, I., Mäki-Arvela, P., Chichova, D., Eränen, K., & Murzin, D. Yu. (2008). Catalytic deoxygenation of unsaturated renewable feedstocks for production of diesel fuel hydrocarbons. *Fuel*, 87(6), 933-945.
- Snåre, M., Kubičková, I., Mäki-Arvela, P., Eränen, K., & Murzin, D. Yu. (2006). Heterogeneous catalytic deoxygenation of stearic acid for production of biodiesel. *Industrial & Engineering Chemistry Research*, 45(16), 5708-5715.
- Spolaore, P., Joannis-Cassan, C., Duran, E., & Isambert, A. (2006). Commercial applications of microalgae. *Journal of Bioscience and Bioengineering*, 101(2), 87-96.
- Stucki, S., Vogel, F., Ludwig, C., Haiduc, A. G., & Brandenberger, M. (2009). Catalytic gasification of algae in supercritical water for biofuel production and carbon capture. *Energy & Environmental Science*, 2(5), 535-541.
- Stumborg, M., Wong, A., & Hogan, E. (1996). Hydroprocessed vegetable oils for diesel fuel improvement. *Bioresource Technology*, 56(1), 13-18.
- Tao, L., Aden, A., Elander, R. T., Pallapolu, V. R., Lee, Y. Y., Garlock, R. J., Warner, R. E. (2011). Process and technoeconomic analysis of leading pretreatment technologies for lignocellulosic ethanol production using switchgrass. *Bioresource Technol*, 102(24), 11105-11114.
- The Energy Independence & Security Act 2007 (EISA)*. (2007).
- Thigpen, P. L., & Berry, W. L. (1982). In Energy from Biomass and Wastes VI. In D. L. Klass (Ed.), (pp. 1057). Chicago: Institute of Gas Technology.



- Tike, M. A., & Mahajani, V. V. (2006). Kinetics of hydrogenation of palm stearin fatty acid over Ru/Al<sub>2</sub>O<sub>3</sub> catalyst in presence of small quantity of water. *Indian Journal of Chemical Technology*, 14, 52-63.
- Titirici, M-M., Thomas, A., & Antonietti, M. (2007). Back in the black: hydrothermal carbonization of plant material as an efficient chemical process to treat the CO<sub>2</sub> problem. *New J. Chem.*, 31, 787-789.
- Toor, S. S., Reddy, H., Deng, S., Hoffmann, J., Spangsmark, D., Madsen, L. B., Rosendahl, L. A. (2013). Hydrothermal liquefaction of Spirulina and Nannochloropsis salina under subcritical and supercritical water conditions. *Bioresource Technology*, 131(0), 413-419.
- Tsukahara, K., Kimura, T., Minowa, T., Sawayama, S., Yagishita, T., Inoue, S., & Ogi, T. (2001). Microalgal cultivation in a solution recovered from the low-temperature catalytic gasification of the microalga. *Journal of Bioscience and Bioengineering*, 91(3), 311-313.
- Tungal, R., & Shende, R. (2013). Subcritical aqueous phase reforming of wastepaper for biocrude and H<sub>2</sub> generation. *Energy & Fuels*, 27(6), 3194-3203.
- Valdez, P. J., Nelson, M. C., Wang, H. Y., Lin, X. N., & Savage, P. E. (2012). Hydrothermal liquefaction of Nannochloropsis sp.: Systematic study of process variables and analysis of the product fractions. *Biomass and Bioenergy*, 46(0), 317-331.
- Vam, A. (2013). *Kinetics of the hydro-deoxygenation of stearic acid over palladium on carbon catalyst in fixed-bed reactor for the production of renewable diesel*. (M. S. Thesis), University of Dayton, Dayton. Retrieved from [http://rave.ohiolink.edu/etdc/view?acc\\_num=dayton1373313020](http://rave.ohiolink.edu/etdc/view?acc_num=dayton1373313020)

- Vardon, Derek R., Sharma, Brajendra K., Blazina, Grant V., Rajagopalan, Kishore, & Strathmann, Timothy J. (2012). Thermochemical conversion of raw and defatted algal biomass via hydrothermal liquefaction and slow pyrolysis. *Bioresource Technology*, 109(0), 178-187.
- Veldsink, J. W., Bouma, M. J., Schöön, N. H., & Beenackers, A. A. C. M. (1997). Heterogeneous hydrogenation of vegetable oils: A literature review. *Catalysis Reviews*, 39(3), 253-318.
- Velickovic, D. T., Milenovic, D. M., Ristic, M. S., & Veljkovic, V. B. (2006). Kinetics of ultrasonic extraction of extractive substances from garden (Salvia officinalis L.) and glutinous (Salvia glutinosa L.) sage. *Ultrason Sonochem*, 13(2), 150-156.
- Veličković, Dragan T., Milenović, Dragan M., Ristić, Mihailo S., & Veljković, Vlada B. (2008). Ultrasonic extraction of waste solid residues from the Salvia sp. essential oil hydrodistillation. *Biochemical Engineering Journal*, 42(1), 97-104.
- Veljković, V., & Milenović, D. (2002). Extraction of resinoids from St. John's worth (Hypericum perforatum L.) II. Modelling of extraction kinetics. *Chem. Ind. (Belgrade)*, 56(2), 60-67.
- Viljava, T. R., Komulainen, R. S., & Krause, A. O. I. (2000). Effect of H<sub>2</sub>S on the stability of CoMo/Al<sub>2</sub>O<sub>3</sub> catalysts during hydrodeoxygenation. *Catalysis Today*, 60(1-2), 83-92.
- Viljava, T. R., Saari, E. R. M., & Krause, A. O. I. (2001). Simultaneous hydrodesulfurization and hydrodeoxygenation: Interactions between mercapto and methoxy groups present in the same or in separate molecules. *Appl. Catal. A: General*, 209, 33-43.

- Vlachos, N., Skopelitis, Y., Psaroudaki, M., Konstantinidou, V., Chatzilazarou, A., & Tegou, E. (2006). Applications of Fourier transform-infrared spectroscopy to edible oils. *Anal Chim Acta*, 573-574, 459-465.
- Vogelzang, M.W., Li, C.L., Schnit, G.C.A., Gates, B.C., & Petrakis, L. J. (1983). Hydrogenation of 1-naphthol: activities and stabilities of molybdena and related catalysts. *Journal of Catalysis*, 84, 170-177.
- Volkman, J. K., Jeffrey, S. W., Nichols, P. D., Rogers, G. I., & Garland, C. D. (1989). Fatty acid and lipid composition of 10 species of microalgae used in mariculture. *Journal of Experimental Marine Biology and Ecology*, 128(3), 219-240.
- Vonghia, E., Boocock, D. G. B., Konar, S. K., & Leung, A. (1995). Pathways for the deoxygenation of triglycerides to aliphatic hydrocarbons over activated alumina. *Energy & Fuels*, 9(6), 1090-1096.
- Wang, J. X., & Cai, Y. (2013). *The Insight of Active Sites: Reduced and Sulfided CoMo Catalysts*. Paper presented at the 23rd North American Catalysis Society Meeting, Louisville, Kentucky.
- Wang, W-C., Thapaliya, N., Campos, A., Stikeleather, L. F., & Roberts, W. L. (2012). Hydrocarbon fuels from vegetable oils via hydrolysis and thermo-catalytic decarboxylation. *Fuel*, 95, 622-629.
- Wang, X.Q., & Ozkan, U.S. (2005). Characterization of active sites over reduced Ni-Mo/Al<sub>2</sub>O<sub>3</sub> catalysts for hydrogenation of linear aldehydes. *Journal of Physical Chemistry B*, 109(5), 1882-1890.
- Watanabe, M., Iida, T., & Inomata, H. (2006). Decomposition of a long chain saturated fatty acid with some additives in hot compressed water. *Energy Conversion and Management*, 47(18-19), 3344-3350.

- Watanabe, M., Inomata, H., Osada, M., Sato, T., Adschiri, T., & Arai, K. (2003). Catalytic effects of NaOH and ZrO<sub>2</sub> for partial oxidative gasification of n-hexadecane and lignin in supercritical water[small star, filled]. *Fuel*, 82(5), 545-552.
- Weissman, J. C., & Tillett, D. M. (1992a). Design and operation of an outdoor microalgae test facility: large-scale system results. In L.M. Brown & S. Sprague (Eds.), *Aquatic Species Project Report* (pp. 32-56). Golden, Colorado: National Renewable Energy Laboratory.
- Weissman, J. C., & Tillett, D. M. (1992b). Design and operation of outdoor microalgae test facility. In Lewis M. Brown & S. Sprague (Eds.), *Aquatic Species Report* (pp. 32-57): National Renewable Energy Laboratory.
- Widjaja, A., Chien, C-C., & Ju, Y-H. (2009). Study of increasing lipid production from fresh water microalgae *Chlorella vulgaris*. *Journal of the Taiwan Institute of Chemical Engineers*, 40(1), 13-20.
- Xu, X., Matsumura, Y., Stenberg, J., & Antal, M. J. (1996). Carbon-catalyzed gasification of organic feedstocks in supercritical water. *Industrial & Engineering Chemistry Research*, 35(8), 2522-2530.
- Yakovlev, V. A., Khromova, S. A., Sherstyuk, O. V., Dundich, V. O., Ermakov, D. Yu, Novopashina, V. M., Parmon, V. N. (2009). Development of new catalytic systems for upgraded bio-fuels production from bio-crude-oil and biodiesel. *Catalysis Today*, 144(3-4), 362-366.
- Yang, C., Nie, R., Fu, J., Hou, Z., & Lu, X. (2013). Production of aviation fuel via catalytic hydrothermal decarboxylation of fatty acids in microalgae oil. *Bioresour Technol*, 146, 569-573.

- Yu, J., & Savage, P. E. (1998). Decomposition of formic acid under hydrothermal conditions. *Industrial & Engineering Chemistry Research*, 37(1), 2-10.
- Zakzeski, J., Bruijninx, P.C.A., Jongerius, A.L., & Weckhuysen, B.M. (2010). Catalytic volarization of lignin for the production of renewable chemicals. *Chem. Rev.*, 110, 3552-3599.
- Zhao, C., He, J., Lemonidou, A. A., Li, X., & Lercher, J. A. (2011). Aqueous-phase hydrodeoxygenation of bio-derived phenols to cycloalkanes. *Journal of Catalysis*, 280(1), 8-16.
- Zhao, C., Kou, Y., Lemonidou, A. A, Li, X., & Lercher, J. A. (2009). Highly selective catalytic conversion of phenolic bio-oil to alkanes. *Angewandte Chemie International Edition*, 48(22), 3987-3990.
- Zhou, D., Zhang, L., Zhang, S., Fu, H., & Chen, J. (2010). Hydrothermal liquefaction of macroalgae *Enteromorpha prolifera* to bio-oil. *Energy & Fuels*, 24(7), 4054-4061.
- Zhu, Y., Albrecht, K. O., Elliott, D. C., Hallen, R. T., & Jones, S. B. (2013). Development of hydrothermal liquefaction and upgrading technologies for lipid-extracted algae conversion to liquid fuels. *Algal Research*, 2(4), 455-464.

## APPENDIX A

### Environmental Protection Agency (EPA) P3 (People, Prosperity and the Planet)

#### Competition, Phase I and II

EPA's P3 (People, Prosperity, and the Planet) Program is a college competition program aimed at designing solutions for a sustainable future. EPA P3 offers students the quality hands-on experience that allows them to apply their knowledge to practical solutions.

A group of students was organized in order to generate ideas and submit a proposal for EPA P3 Phase I competition in the end of 2012. The students team was formed by Jose Garcia (Student Leader), Sergyi Popov, Ali Teymouri, Caleb Talbot, Hannah Drake, Jonathan Ricci, Paul Wilson, Kwamena Mfrase-Ewur, and Victor Collins under the supervision of Dr. Sandeep Kumar. The Phase I grant proposal (the portable plant for flash hydrolysis of algal biomass) was developed from May 2013 to May 2014.

The EPA P3 team had weekly meetings where the activities were planned as the research activities discussed. The following activities were part of the required work to participate in the competition:

- Preparation of a Phase I report detailing the activities and findings for the one year project;
- Preparation of a Phase II proposal with objectives and detailed activities for a two year project;
- Preparation of a poster that was displayed during the competition;

- A short 1 min video (elevator pitch) summarizing the objectives and findings of the project.

The team developed the design for the National Sustainable Design Expo in Washington, DC in April 2014 to complete the proposal for the EPA P3 Phase II Award. The 2014 EPA P3 Competition and National Sustainable Design Expo took place from April 25<sup>th</sup> to April 27<sup>th</sup> 2014) at the 3<sup>rd</sup> USA Science and Engineering Festival located at the Washington Convention Center in Washington, DC. ODU team received an Honorable Mention during the competition. The elevator pitch video won the second place.

## APPENDIX B

### 1. Standard operation procedures for SRI 8610C gas chromatograph

The standard operation procedures for SRI 8610C gas chromatograph (gas installation and connection, column installation, software installation, detector activation, sample injection, PeakSimple calibration, printing chromatograms, etc. are available at SRI Instruments website: <http://www.srigc.com/documents.htm>



## **2. Analysis of gas samples using SRI 8610C gas chromatograph with the thermal conductivity detector (TCD)**

This method was used for gas analysis in the studies reported in Chapter 3, 5, and 6.

The SRI 8610C gas chromatograph includes a TCD (Thermal Conductivity Detector), two FIDs (Flame Ionization Detector), methanizer, internal air compressor, 10-port gas sampling valve, 6' molecular sieve MS-13X connected to a 10' × 1/8" HayeSep D packed column, MXT-WAX capillary column, ambient-to-400 °C temperature-programmable column oven, PeakSimple Data System software.

The current SRI GC configuration for gas analysis includes the TCD detector, which is most common, simple, and universal. The principle of its work are described below. An eluent from the column flows over a hot tungsten-rhenium filament. When analyte emerges from the column, the conductivity of gas stream decreases, the filament gets hotter, its electrical resistance increases, and the voltage across the filament changes. The detector measures the change in voltage. Depending on the compound, the TCD responds with a detection range of 0.01% to 100% (100-1,000,000 ppm).

Quantitative analysis is based on the area of a chromatographic peak. In the linear response concentration range, the area of a peak is proportional to the quantity of that component.

The SRI 8610C was set up and calibrated for analyzing the gas mixture that contains oxygen, nitrogen, carbon oxides, methane, and ethylene as well as hydrogen (the first reversed peak on the chromatogram) with helium as carrier gas. For quantitative analysis of hydrogen it is necessary to use argon or nitrogen as carrier gas.

## General operating procedures

### Startup

1. Check to make sure that the TCD filament current is switched off.
2. Open the regulator on the helium (carrier gas) cylinder.
3. Plug in and turn on the GC. Allow the TCD detector oven to reach the required temperature (150 °C) and stabilize. It usually takes about 30 minutes.
4. Check the carrier gas pressure by pressing a button labeled Carrier 1 on the front panel of the GC. It should be 22 psi (20 mL/min).
5. Turn on the computer and run PeakSimple Data System by clicking on the respective icon.
6. Switch the TCD filaments to LOW.
7. Check the temperature program. Click on Edit, Channels, Channel 3, Temperature. In the pop-up window, the temperature program should look as follows: initial temp 40 °C, hold for 20 min, ramp 0 °C, final temp 40 °C. For most of gas analyses, the temperature of 40 °C is sufficient. Using this option, the temperature program can be changed as needed.
8. Check the event program. Click on Edit, Channels, Channel 3, Events. In the pop-up window, it should look as follows:

Time	Event
0	ZERO
0	SOUND

0.05	G ON (Valve Rotate)
2.5	A ON (Stop Flow)
7.5	A OFF (Stop Flow)
7.5	G OFF (Valve Rotate)

In this window, the event program can be edited as needed.

9. Sample is injected into the bulkhead fitting labeled "SAMPLE IN" on the front of the valve oven. The fitting is equipped with a 1/8" Swagelok nut for easy connection of the sample streams. Make sure the sample gas line is connected to the valve.
10. Open the gas stream or inject the gas sample into the gas line connected to the valve with a syringe. Typically, 1 mL of the gas sample is enough for the analysis.
11. Press the computer keyboard spacebar to initiate the run. The valve will automatically rotate to the INJECT position at 0.05 minutes.
12. The GC starts analyzing the gas sample and plotting the chromatogram curve on the monitor. After the analysis has been finished, view the results by right-clicking on the chromatogram and choosing Results from the drop-down menu. The chromatogram can be saved on the computer and/or printed.

### **Shutdown**

Shutdown is the reverse of startup:

1. Close the sample gas stream.
2. Switch the TCD filaments OFF.
3. Close PeakSimple Data System and turn the computer off.

4. Turn the GC off.
5. Close the regulator on the helium cylinder.

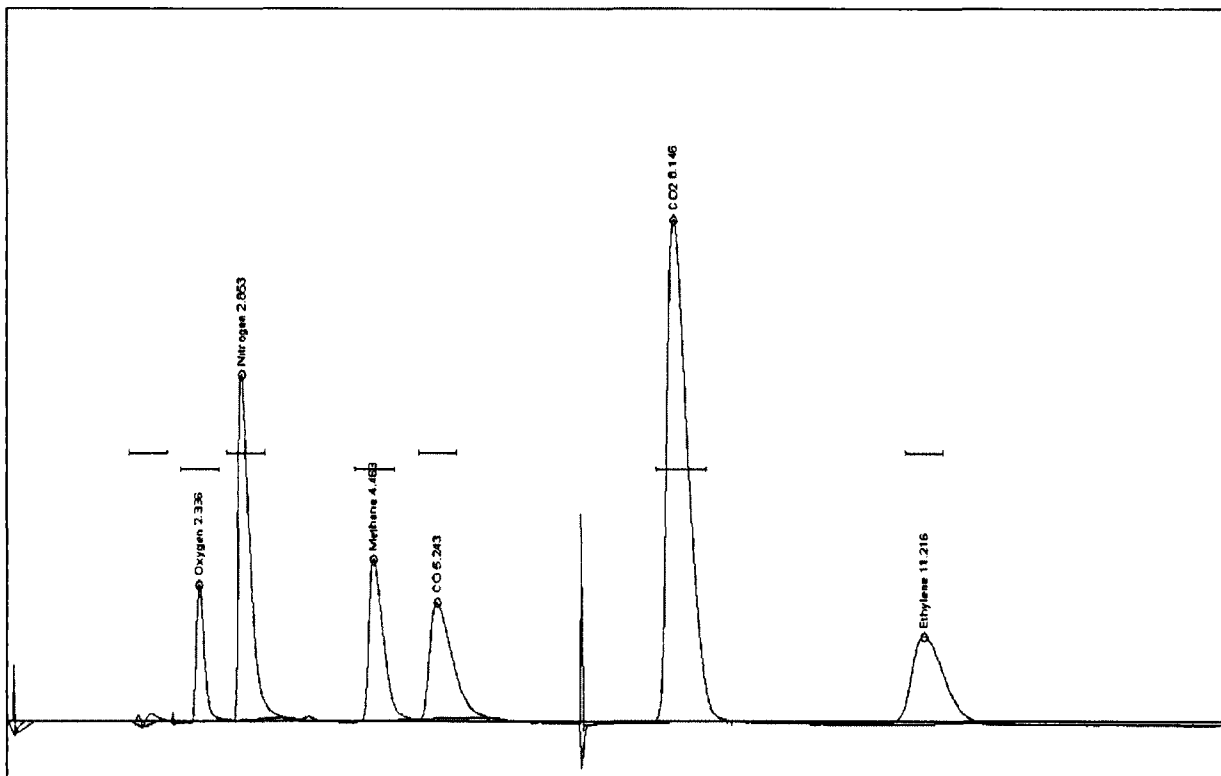


**Figure 40.** Sample chromatogram of a gas mixture analyzed with GC-TCD.

### **3. Analysis of liquid samples using SRI 8610C gas chromatograph with the flame ionization detector (FID)**

This method was used for FAMES analysis in the studies reported in Chapter 4 and 6.

The FID responds to any molecule with a carbon-hydrogen bond, but its response is either poor or nonexistent to compounds such as H<sub>2</sub>S, CCl<sub>4</sub>, or NH<sub>3</sub>. Since the FID is mass sensitive, not concentration sensitive, changes in carrier gas flow rate have little effect on the detector response. It is preferred for general hydrocarbon analysis, with a detection range from 0.1 ppm to almost 100%. The FID's response is stable from day to day, and is not susceptible to contamination from dirty samples or column bleed. It is generally robust and easy to operate, but because it uses a hydrogen diffusion flame to ionize compounds for analysis, it destroys the sample in the process.

In the FID, the carrier gas effluent from the GC column is mixed with hydrogen, then routed through an unbreakable stainless steel jet. The hydrogen mix supports a diffusion flame at the jet's tip which ionizes the analyte molecules. Positive and negative ions are produced as each sample component is eluted into the flame. A collector electrode attracts the negative ions to the electrometer amplifier, producing an analog signal for the data system input. An electrostatic field is generated by the difference in potential between the positively charged collector electrode and the grounded FID jet. Because of the electrostatic field, the negative ions have to flow in the direction of the collector electrode.

The SRI 8610C was set up and calibrated for analyzing fatty acid methyl esters (FAMES) with MXT-WAX capillary column, FID1, and helium as carrier gas.

#### **General operating procedures**

**Startup**

1. Open the regulator on the He (carrier gas) cylinder.
2. Plug in and turn on the GC. Allow the FID detector oven to reach the required temperature (250 °C) and stabilize. It usually takes about 30 minutes.
3. Check the carrier gas pressure by pressing a button labeled Carrier 2 on the front panel of the GC. It should be 19 psi (20 mL/min).
4. Open the regulator on the hydrogen cylinder.
5. Check the FID hydrogen pressure by pressing a button labeled Hydrogen 1 on the front panel of the GC. It should be 20 psi (25 mL/min).
6. Check the air pressure by pressing a button labeled Air 1 on the front panel of the GC. It should be 5 psi (250 mL/min). The approximate pressures required are printed in the gas flow chart on the right-hand side of the GC.
7. Ignite the FID by turning on the Internal Air Compressor switch located on the front panel of the GC. You must hear a small POP.
8. Verify that the FID flame is lit by holding the shiny side of a chromed wrench directly in front of the collector outlet/FID exhaust vent. If condensation becomes visible on the wrench surface, the flame is lit.
9. Set the FID amplifier gain switch to HIGH for most hydrocarbon applications. If peaks of interest go off the scale (greater than 5000 mV), set the gain to MEDIUM. When peaks of interest are 20 seconds wide or more at the base and extra noise immunity is desired, set the gain switch to HIGH (filtered).

10. Turn on the computer and run PeakSimple Data System by clicking on the respective icon.
11. Check the temperature program. Click on Edit, Channels, Channel 1, Temperature. In the pop-up window, the temperature program should look as follows: initial temp 120 °C, hold for 3 min, ramp 10 °C/min, hold for 5 min, final temp 240 °C. Using this option, the temperature program can be changed as needed.
12. Check the event program. Click on Edit, Channels, Channel 3, Events. In the pop-up window, it should look as follows:

<b>Time</b>	<b>Event</b>
0	ZERO
0	SOUND

In this window, the event program can be edited as needed.

13. Check the FID1 temperature by pressing the button labeled Detector 1 on the front panel of the GC. It should be 250 °C (it should always be higher than the oven temperature).
14. Press the computer keyboard spacebar to initiate the run.
15. Inject the FAMEs sample into the injector located on the front panel of the GC oven with a 10 µL syringe. Typically, 1 µL of the liquid sample is enough for the analysis.
16. The GC starts analyzing the liquid sample and plotting the chromatogram curve on the monitor. After the analysis has been finished, view the results by right-clicking on

the chromatogram and choosing Results from the drop-down menu. The chromatogram can be saved on the computer and/or printed.

### **Shutdown**

1. Close the regulator on the hydrogen cylinder.
2. Turn off the Internal Air Compressor.
3. Close PeakSimple Data System and turn the computer off.
4. Turn the GC off.
5. Close the regulator on the helium cylinder.



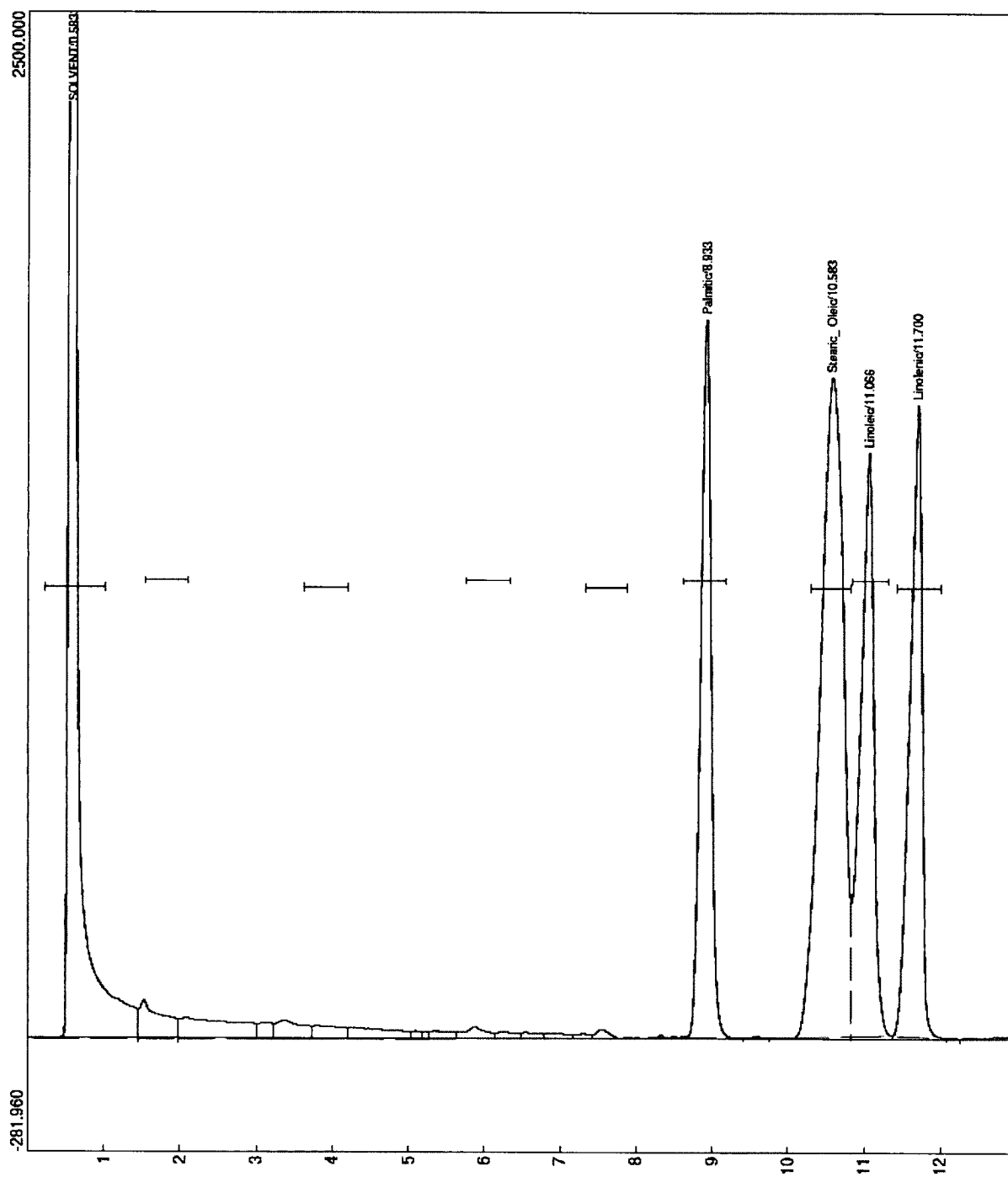


**Figure 41.** Sample chromatogram of a FAME mixture analyzed with GC-FID.

**VITA****Sergiy Popov**[spopo003@odu.edu](mailto:spopo003@odu.edu)**EDUCATION****Old Dominion University, Norfolk, Virginia**

August 2015

Ph.D. in Environmental Engineering (GPA 3.9/4.0)

Dissertation title: "Hydrothermal catalytic liquefaction and deoxygenation of biomass for renewable fuel production"

Advisor: Dr. Sandeep Kumar

**South-Russian State Technical University, Novocherkassk, Russia**

June 1981

B.S./M.S. in Chemical Engineering (GPA 4.7/5.0)

**RESEARCH EXPERIENCE**

Old Dominion University, Norfolk, Virginia

**Graduate Research Assistant**

2011-2015

- Proposed the process for rapid continuous deoxygenation of oils/fats in near- and supercritical water, designed and assembled the experimental setup, obtained fuel range hydrocarbons with high yield and selectivity, and studied the optimal conditions and kinetics of the process

- Developed a process for hydrothermal liquefaction of microalgae, low-temperature gasification of the aqueous phase with obtaining hydrogen and other light hydrocarbons, and recycling the processed medium as a fertilizer for microalgae growth
- Conducted hydrothermal pretreatment of oilseeds with different morphologies and their following solvent extraction that allowed better extractability than conventional oil extraction techniques, determined the optimal conditions of the process, and compared kinetics of oil extraction from pretreated and raw (ground) oilseeds
- Studied hydrothermal pretreatment of unhydrolyzed solid residue left behind after bioethanol production, obtained bio-oil with high heating value that can be upgraded to biofuels, determined the optimal conditions, and computed the mass and energy balances of the process
- Researched the area of catalytic deoxygenation of lipid-rich feedstock and wrote a review article on the subject
- Mastered a number of experimental and analytical skills for biomass processing, characterization, product separations, and analyses

## **TEACHING EXPERIENCE**

Old Dominion University, Norfolk, Virginia

### **Graduate Teaching Assistant**

- CEE 350 Environmental Pollution and Control Fall 2014
- CEE 495/595 Analytical Techniques in Environ. Engineering (lab sessions)  
Fall 2014, Fall 2013

- CEE 459/559 Biofuels Engineering (lab sessions) Spring 2014, Spring 2013
- ENGN 110 Exploring Engineering and Technology (lab sessions) Fall 2013, Fall 2012

## HONORS AND AWARDS

Department of Civil and Environmental Engineering Award for Excellence in Research 2015

Honorable Mention, The U.S. Environmental Protection Agency P3 Award Competition 2014

Sigma Xi, The Scientific Research Society, full member 2013-Present

Golden Key International Honour Society, member 2012-Present

Batten College of Engineering and Technology Dean's Fellowship 2011-2013

## PROFESSIONAL ASSOCIATIONS

American Chemical Society (ACS)

American Academy of Environmental Engineers and Scientists (AAEES)

American Institute of Chemical Engineers (AIChE)

American Water Works Association (AWWA)

## SELECTED PUBLICATIONS

- Popov, S., Kumar, S. Rapid hydrothermal deoxygenation of oleic acid over activated carbon in a continuous flow process. *Energy Fuels*, 29 (5), 3377–3384 (2015).

- Popov, S., Ruhl, I., Uppugundla, N., da Costa Sousa, L., Balan, V., Hatcher P.G., Kumar, S. Bio-oil via catalytic liquefaction of unhydrolyzed solids in aqueous medium. *Biofuels*, 5 (4), 431-446 (2014).
- Popov, S., Kumar, S. Renewable fuels via catalytic hydrodeoxygenation of lipid-based feedstocks. *Biofuels*, 4 (2), 219-239 (2013).

#### **PUBLICATIONS IN PROGRESS**

- Popov, S., Abdel-Fattah, T., Kumar, S. Hydrothermally assisted oil extraction and biochar production from oilseeds. Submitted to *Renewable Energy*, ref. # RENE-D-14-01661R3.

#### **PATENT APPLICATION**

Kumar, S., Popov, S., Majeranowski, P.J., Kostenyuk, I. Subcritical water assisted oil extraction and green coal production from oilseeds. International patent application PCT/US2013/064966, October 23, 2012.

#### **CONFERENCE PRESENTATIONS**

- Popov, S., Kumar, S. Rapid hydrothermal hydrogenation and decarboxylation of oleic acid over activated carbon using formic acid as in situ source of hydrogen. 2015 AIChE Annual Meeting, Salt Lake City, UT, November, 2015 (accepted).

- Popov, S., Kumar, S. A novel integrated process for producing oil and biochar from oilseeds. 247th ACS National Meeting and Exposition, Dallas, TX, March 16-20, 2014.
- Popov, S., Kumar, S. Hydrothermal catalytic liquefaction of unhydrolyzed solids for bio-oil production. 14<sup>th</sup> Annual Tidewater Student Research Poster Session, Newport News, VA, November, 2012 (3<sup>rd</sup> prize).
- Popov, S., Kumar, S., Ruhl, I. Balan, V., da Costa Sousa, L., Uppugundla, N., Dale, B.E. Hydrothermal processing of unhydrolyzed biomass for biocrude and biochar production. 2012 AIChE Annual Meeting, Pittsburgh, PA, October, 2012.
- Garcia Moscoso, J.L., Popov, S., Kumar, S. Microalgae as a feedstock for alternative fuels: Opportunities and challenges. The 4<sup>th</sup> International Forum on Systems and Mechatronics, Virginia Beach, VA, August, 2012.
- Balan, V., Kumar, S., Popov, S., Uppugundla, N., da Costa Sousa, L., Bokade, V., Dale, B. E. Hydrothermal processing of unhydrolyzed solids produced after enzyme hydrolysis of AFEX<sup>TM</sup> pretreated biomass to generate bio-oil and green charcoal. Society for Industrial Microbiology Meeting, New Orleans, LA, May, 2012 (poster).